Multiscale reaction-diffusion systems describing concrete corrosion : modeling and analysis

Please check the document version of this publication:

Multiscale Reaction-Diffusion Systems Describing Concrete Corrosion: Modeling and Analysis

Tasnim Fatima

Multiscale Reaction-Diffusion Systems Describing Concrete Corrosion: Modeling and Analysis

PROEFSCHRIFT

ter verkrijging van de graad van doctor aan de
Technische Universiteit Eindhoven, op gezag van de
rector magnificus, prof.dr.ir. C.J. van Duijn, voor een
commissie aangewezen door het College
voor Promoties in het openbaar te verdedigen
op donderdag 28 februari 2013 om 16.00 uur

door

Tasnim Fatima

geboren te Kasur, Pakistan

Dit proefschrift is goedgekeurd door de promotor:

prof.dr. M.A. Peletier

Copromotor:
dr.habil. A. Muntean

Abstract

Rapid deterioration of concrete has a major financial impact due to high maintenance costs. In the thesis, we apply the multiscale concept to develop a mathematical framework that can be useful in forecasting the service life of a sewer pipe made of concrete. Our research focuses on modeling and analysis of multiscale reaction-diffusion systems taking place in heterogeneous media.

At the pore level, the degradation processes are highly complex and hence it is very difficult to understand and predict their behavior on macroscopic (observable) scales. Since the microstructure highly effects the processes in porous media, we consider two different geometries that are trackable mathematically: uniformly periodic and locally-periodic arrays of microstructures. We take into account two different types of reaction-diffusion scenarios: (i) microscopic systems posed at the pore scale and (ii) distributed-microstructure systems which contain information from both scales (micro and macro). We show the well-posedness of the microscopic systems and apply both formal and rigorous homogenization techniques to derive the corresponding upscaled systems together with explicit formulae for the effective transport and reaction constants. As a next step, we prove convergence rates measuring the error contribution produced while scale bridging to assess the quality of our averaging strategy.

Besides from the homogenization context, we treat the solvability of reaction-diffusion systems in micro-macro formulation and we also perform preliminary multiscale numerical computations. We compute numerically the pH profiles and use them to detect the presence of free boundaries penetrating the uncorroded concrete. We also compare numerically the influence of a large mass-transfer Biot number Bi^M connecting in the limit $Bi^M \to \infty$ two different distributed-microstructure models.

This thesis sets up a framework which can turn out to be helpful for further investigations of more practical nature like the estimation of corrosion rate and the life span of the material.

Contents

Chapter 1

Introduction

This thesis deals with the derivation and analysis of a class of multiscale models which arises in the modeling of the chemical concrete corrosion of sewer pipes with sulfuric acid (the sulfatation problem), see Section 2.1 for a detailed statement of the engineering problem. We describe the evolution of the corrosion by means of partly-diffusive semilinear reaction-diffusion (RD) systems. We consider two different RD scenarios: (i) a microscopic model which is defined at the pore scale and (ii) a distributed-microstructure model which incorporates transport (diffusion) and reaction effects emerging from two separated spatial continuum scales (microscopic and macroscopic). For both scenarios, the concrete is seen as a composite material with complex chemistry involving multiple spatial scales. This fact urges the need of upscaled model derivation based on the relevant processes taking place at the pore scale. On the modelling level, we pay special attention to two specific features:

- non-equilibrium transfer of hydrogen sulfide (H_2S) from the air to the water phase (and vice versa);

- production of gypsum at microscopic solid-water interfaces.

We model the transfer of H_2S by means of Henry's law, while the production of gypsum is incorporated by a non-standard non-linear reaction rate. These two physico-chemical mechanisms couple our RD systems in a weak fashion.

Having as departure point a microscopic reaction-diffusion scenario, we consider two different geometries for the microstructures: uniformly-periodic and locally-periodic arrays of cells covering the macroscopic part of interest, see Section 2.2.3 for a discussion on possible choices of microstructures that can be treated by mathematical tools. After applying homogenization techniques, the next steps are: (i) obtain convergence rates for the averaging strategy and (ii) design efficient multiscale numerical approximations. Here we focus on (i) and correspondingly look for corrector estimates for concentrations and their fluxes, while we postpone the design of multiscale numerical approximations for a later stage. Here we propose a preliminary study: we use microscopic information [taken e.g. from a well-posed (distributed-)microstructure model] and use it to approximate numerically macroscopic pH profiles. The hope is that [in the region] the pH profile will decay significantly and indicate herewith the

approximate position of the propagating sharp corrosion front. We also plan to investigate numerically the effect of a large mass-transfer Biot number Bi^M connecting in the limit $Bi^M \to \infty$ two different RD scenarios: one with a *micro-macro transmission condition* and the other with *matched boundary condition*[1].

The sulfatation problem [as we consider it here] was originally proposed to the mathematical community by M. Böhm *et al.* in [23] (see also the subsequent papers [72, 73]), where the authors adopted a macroscopic moving-boundary modeling strategy to capture the macroscopic corrosion front penetrating the pipe. We adapt some of their modeling ideas to construct our microscopic models discussed in the forthcoming chapters. Essentially, we are interested in determining the evolution of the chemical species active in the following reaction mechanisms:

$$10\mathrm{H}^+ + \mathrm{SO}_4^{-2} + \text{org. matter} \quad \longrightarrow \quad \mathrm{H_2S(aq)} + 4\mathrm{H_2O} + \text{oxid. matter} \quad (1.1)$$

$$\mathrm{H_2S(aq)} + 2\mathrm{O}_2 \quad \longrightarrow \quad 2H^+ + \mathrm{SO}_4^{-2} \quad (1.2)$$

$$\mathrm{H_2S(aq)} \quad \rightleftharpoons \quad \mathrm{H_2S(g)} \quad (1.3)$$

$$2\mathrm{H_2O} + \mathrm{H}^+ + \mathrm{SO}_4^{-2} + \mathrm{CaCO_3} \quad \longrightarrow \quad \mathrm{CaSO_4 \cdot 2H_2O} + \mathrm{HCO_3^-} \quad (1.4)$$
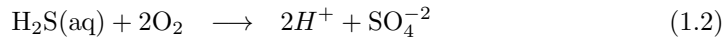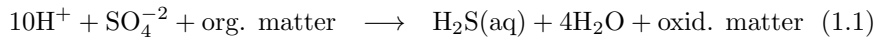
The practical (engineering) interest is in estimating the service life (the durability) of the material. Our interest lies more on the mathematical side of the problem. We wish to derive reliable well-posed and computable multiscale models for the prediction of the corrosion propagation. To this end, we take the followings steps:

1. We develop microscopic and distributed-microstructure models for (1.1) - (1.4).

2. We derive multiscale models via formal and rigorous homogenization.

3. We ensure the well-posedness of our proposed multiscale models.

4. We address the question "*How good our averaging technique is?*" and obtain corrector (error) estimates.

5. Based on microscale information, we indicate using pH profiles the approximate location of the corrosion front propagating in the uncorroded concrete.

6. We illustrate numerically the behavior of the distributed microstructure model in the large-mass transfer Biot number limit.

By achieving the above steps, we prepare a possible framework which can be helpful to explore further investigations of more practical nature like corrosion rate and life span of the material. The next natural step would be to explore intensively numerical multiscale techniques able to deal with our problem. Efficient numerical multiscale methods need to be combined with parameter identification strategies in order to bring our approach towards quantitative predictions.

---

[1]The terminology *matched boundary condition* is due to R.E. Showalter (see Chapter 9 in [67]) and *micro-macro transmission condition* is due to M. Neuss-Radu and A. Muntean [101]

1.1 Synopsis of the thesis

Each chapter deals with distinct aspects of the problem. The thesis is structured in the following fashion:

Chapter 2 is devoted to the modeling of concrete and its chemical corrosion by sulfate attack. We describe the corrosion scenario and refer to some of the related engineering and mathematical literature. We review the possible shapes of microstructures that can be treated by mathematical tools. We present the modeling of various aspects concerning sulfate corrosion needed to build microscopic and distributed-microstructure models.

In Chapter 3, we apply formal asymptotic homogenization techniques to the microscopic model proposed in Chapter 2 defined for a locally periodic array of microstructures. As a result of this, we obtain both effective and distributed-microstructure models depending on the precise scaling in ε (the geometric parameter).

Chapter 4 is devoted to the analysis of a microscopic model and the rigorous derivation of the corresponding upscaled system. The microscopic model is defined here on a uniformly periodic domain. We use the notion of two-scale convergence in the sense of Allaire and Nguestseng [8] to explore the homogenization limit and derive upscaled equations together with explicit formulae for the effective diffusion coefficients and reaction constants. Due to the nonlinear ordinary differential equation (ode) defined at the solid-water pore boundary, we need to employ periodic boundary unfolding technique to pass to the limit $\varepsilon \to 0$.

The issue regarding the quality of the upscaling is treated in Chapter 5. To ensure a correct averaging, we estimate from above the rate of the convergence for the averaging procedure. The main ingredient is the periodic unfolding procedure.

In Chapter 6, we show the solvability of the distributed-microstructure system introduced in Chapter 2. We ensure the positivity and $L^\infty-$bounds on concentrations, and then prove the global-in-time existence and uniqueness of a suitable class of positive and bounded solutions that are stable with respect to the two-scale data and model parameters.

In Chapter 7, we compute numerically the typical macroscopic pH profiles and indicate with their help the position of the corrosion front penetrating the uncorroded concrete. We also explore numerically the way in which the macroscopic Biot number Bi^M connects two reaction-diffusion scenarios with distributed microstructure.

In Chapter 8, we present the conclusions of the thesis and list possible future research directions.

The chapters begin with a brief presentation of the subject matter. There we explain how the topic relates to those in previous and subsequent chapters. The discussion on the multiscale representation of the domain and the presentation of the sulfate corrosion models are given in Chapter 2. All the chapters excepting Chapter 8 end with a section entitled "Notes and comments". This section

includes brief comments on topics that selectively complement the chapter. The choice of the topics is based on personal taste. This section is the place where we collect a few research ideas, open problems and methods of analysis in simple (often pathological) cases, rather than on pursuing each problem to its limit. Some additional references to related matters are also added. The "Notes and comments" sections are not essential for the logical understanding of the text. References to the literature are listed at the end of the thesis. The numbering of theorems, lemmata, formulae, etc. is made for each chapter separately. We explicitly state when a reference is made to the current chapter or to a different one.

Chapter 2

Modeling Concrete and its Chemical Corrosion by Sulfate Attack

This chapter is devoted to the formulation of the balance equations governing sulfate corrosion processes induced by the aggressive penetration of sulfate ions in the material and to the multiscale representation of the concrete.

This chapter is organized as follows: In Section 2.1, we describe the details of the sulfatation problem (involved chemistry, transport processes, adsorption-desorption mechanisms, Henry's law, etc.) and refer to some of the relevant civil engineering and multiscale mathematical literature. In Section 2.2, we specify the multiscale representation of the concrete material we have in mind. In Section 2.3, we present the modeling of the processes arising in the sulfatation of concrete. In Section 2.5, we present our microscopic mathematical model. We conclude the chapter with further directions and open problems concerning the modeling part. The main results in this chapter consist of the formulation of the microscopic system posed at the microscale and distributed-microstructure models modeling concrete corrosion.

2.1   Description of the problem

Before going into the actual mathematical problem we are interested in, we present the physico-chemical scenario responsible for the degradation of mechanical properties of concrete pipes. Here, we also review some of the relevant engineering literature.

2.1.1   Physical Background

Among the different chemical corrosion mechanisms of concrete sewer pipes, the most important and severe one is the biogenic sulfuric acid corrosion, a corrosion process caused by biologically produced sulfuric acid that is able to rapidly de-

stroy the concrete [115]. Hydrogen sulfide (H_2S), originates from sulfide minerals by natural acidification. It is released under certain conditions by the action of the anaerobic (non-air breathing) sulfur-reducing bacteria (e.g., Desulfovibrio) in partially saturated concrete pipes. The active micro-organisms, residing in the biofilm coating the surface of the sewer pipes, reduce the oxidized sulfur to hydrogen sulfide gas $H_2S(g)$ [108]. Hydrogen sulfide goes upwards the air, see
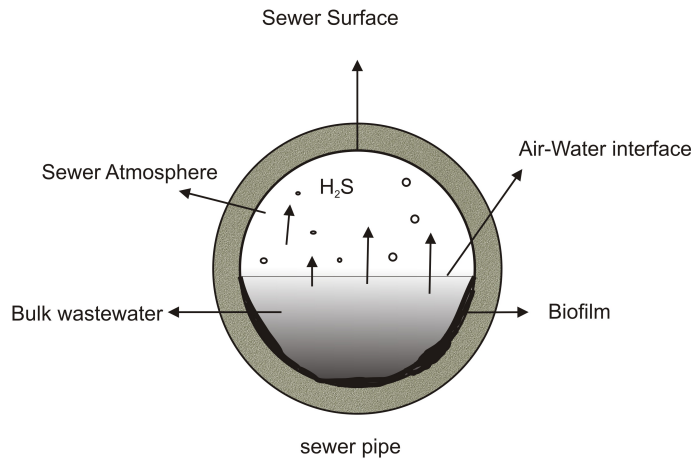
FIGURE 2.1: Cross section of a sewer pipe with dissociating H_2S from wastewater

Fig. 2.1, and enters the concrete structure where it diffuses and then dissolves in the stationary water film in the pore matrix. The back and forth transfer of hydrogen sulfide is a repeated process, see [14]. The dissolved $H_2S(aq)$ is catalyzed by many thiobacilli, (aerobic bacteria) such as Thiobacillus Thiooxidans, Thiobacillus Neapolitanus and Thiobacillus intermedius that grow on the concrete surfaces. The catalysation results in sulfuric acid H_2SO_4. Sulfuric acid is very aggressive and reacts quickly with calcium carbonate present in the concrete. The chemical mechanism gives gypsum ($CaSO_4 \cdot 2H_2O$) which has a very low structural strength. This process destroys the concrete by degrading the mechanical properties of the material. The basic chemical mechanisms are:

$$
\begin{aligned}
10H^+ + SO_4^{-2} + \text{org. matter} \quad &\longrightarrow \quad H_2S(aq) + 4H_2O + \text{oxid. matter} \\
H_2S(aq) + 2O_2 \quad &\longrightarrow \quad 2H^+ + SO_4^{-2} \\
H_2S(aq) \quad &\rightleftharpoons \quad H_2S(g) \\
2H_2O + H^+ + SO_4^{-2} + CaCO_3 \quad &\longrightarrow \quad CaSO_4 \cdot 2H_2O + HCO_3^- \, .
\end{aligned}
$$
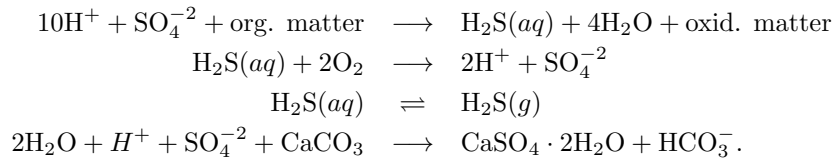
The air-water transfer process is a crucial step largely dependent on the dissociation process because of the existence of the acid-base equilibrium of H_2S. The dissociation process highly depends on the temperature, pH, and conductivity

[146]. In relatively hot environments, the biological activity is faster than usual. This causes an increased utilization of oxygen and production of sulfide [74]. The slow turbulence of the flow helps perhaps in producing the thick diffusive bound-ray layer above biofilms which stops the transportation of the organic matter and nutrients to the biofilm, see [70]. H_2S is a weak acid having a dissociation constant of 7.0 (at 20^0C). Typically the pH of the wastewater decreases, while the concentration of hydrogen sulfide increases in a sewer atmosphere.

2.1.2 A brief literature review

The problem of chemical corrosion of concrete is extensively studied since past few decades. For detailed literature studies concerning the corrosion processes in concrete, the reader is referred to the dissertation of Jensen [74] and the literature cited therein. For the description of the corrosion in concrete generated by bacteria, [23, 75, 141, 107] e.g. are key references. Our main reference sources for acid attack on concrete are [94, 17, 18, 129, 81, 133, 134]. We particularly like [17] for the clear exposition of the phenomenology [for the enumeration of the main mechanisms influencing acid corrosion]. Standard reference works concerning cement chemistry are the monographs [66, 131]. There is a lot of research done in order to estimate the service life of the concrete pipes in sewer networks, see [81, 129]. For the modeling of damages in cement materials subjected to sulfate attack; see e.g. [133, 134]. In the corrosion process, the bacteria play an importance role [114]. Parker reported for the first time the microbial analysis of the concrete corrosion product, see [113, 115, 116].

From the modeling point of view, we are very much inspired by [23] [see also the subsequent papers [72, 73]], where the authors adopted a macroscopic moving-boundary modeling strategy to capture the macroscopic corrosion front penetrating the pipe. We adapted some of their modeling ideas to construct the microscopic model discussed in this chapter.

On the mathematical side, [24, 25] are concerned with the well-posedness and uniqueness of the global weak solutions for a moving boundary problem arising in the corrosion-modeling of concrete. At the technical level, we essentially use formal asymptotics techniques for both the periodic and locally-periodic homog-enization. We refer the reader to [12] for a discussion on uniform descriptions of heterogeneous media. For the formal homogenization in uniformly periodic medium, see, for instance, [22, 35, 39, 31, 69, 117, 120, 128]. For detailed studies on the formal homogenization for uniformly period domain, we refer the reader to [79, 139, 49]. Concerning the formal homogenization in locally periodic media, we refer the reader to [19, 30, 32, 31, 84, 140].

For the rigorous passage to the homogenization limit (cf Section 4.5), there are many techniques available for the treatment of uniformly periodic setting. For studies concerning the two-scale convergence, see [8, 68, 69]. In particular, [10, 36, 104] are good references to treat the boundary terms. The paper by Marciniak *et al.* is closely related to our scenario [83] where they pass to a two-scale limit in combination with a periodic boundary unfolding technique. As

an illustration of what one can do with such a multiscale methodology, Ray *et al.* in [126] perform periodic homogenization of a non-stationary Nernst-Planck-Poisson system for various choices of scaling in ε.

It is worth noting that, since it deals with the homogenization of a linear Henry-law setting, the paper [124] is closely related to our approach. The major novelty here compared to [124] is that now we pass to the limit also in non-diffusive objects, namely in nonlinear ordinary differential equations posed at the inner water-solid interfaces - the place where corrosion localizes.

The standard references for the periodic unfolding technique are [34, 36, 38, 110]. Particularly important for us are the papers by Cioranescu and Damlamian [36, 38, 46]. Griso shows in his papers that it is possible to calculate the rate of convergence using the periodic unfolding technique requiring at the same time less regularity assumptions on the data; the important references are [59, 60]. Also, Onofrei presents error estimates for the periodic homogenization of elliptic equation with non-smooth coefficients [111].

Two-scale models have grasped a lot of attention in recent years as they approximate better physical features of scale-separated systems defined in porous media. For more information on the modeling, analysis and simulation of two-scale scenarios, we refer the reader to [88, 87, 89, 101, 105, 140, 124, 135]. For instance, in [105], the authors present the well-posedness of a two-scale model arising in the context of concrete carbonation. [136] deals with the well-posedness of a quasilinear generalization of the matched microstructure model. In [100], the authors prove the rate of convergence for a two-scale Galerkin scheme in the case when both the microstructure and macroscopic domains are two-dimensional. The proof includes two-scale interpolation-error estimates and an interpolation-trace inequality. A semi-discrete finite difference multiscale scheme is presented in [29] and authors prove two-scale energy and regularity estimates. Kouznetsova *et al.* deal with multiscale computational homogenization, see [42, 43, 76, 58] – a tool which fits well to computing distributed-microstructure models.

The work by Natalini and co-workers is related the restoration of national monuments corroded by the same reaction mechanism, see [3, 41, 61, 62]. Besides sulfatation, there are mechanisms that affect the durability of concrete based materials. A prominent example is the carbonation process. [95] deals with analysis and simulation of the free boundary problems modeling concrete carbonation. In [121], the author derives different upscaled systems describing concrete carbonation depending on the choice of the scale parameter. S. Meier not only obtains distributed-microstructure models as homogenization limits, but also emphasizes their role as stand-alone modeling technology; see [86]. For literature treating carbonation problems mathematically, see e.g. [4, 88, 97, 98].

2.2 Modeling concrete. Geometry. Multiscale representation

2.2.1 What is concrete?

Concrete, a chemically-active porous medium[1], is a composite construction material composed of aggregate, cement and water, see Fig. 2.2. The aggregate is a mixture of coarse gravel or crushed rocks such as limestone, or granite, along with a finer aggregate such as sand, see Fig. 2.3.
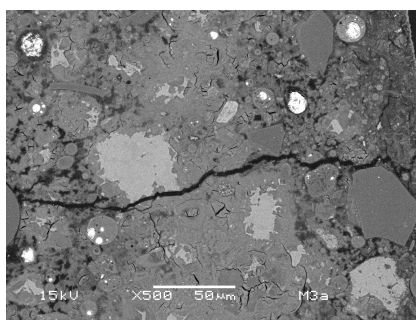
FIGURE 2.2: A zoomed in concrete surface exposed to sulfate corrosion showing the ingredients of the material (aggregates, fissures,...). Courtesy of Dr. R.E. Beddoe (TU München).
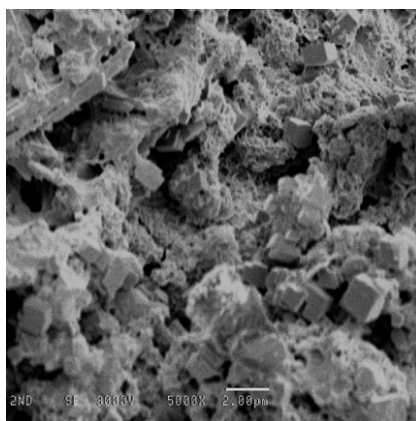
FIGURE 2.3: A magnification of inner side of concrete. Courtesy of Gordon Muir (Institute of Technology Sligo).

---

[1]A porous medium is a material containing pores. The portion of the skeleton is often called the "matrix", while the pores are holes typically filled with a fluid (liquid or gas).

Cement is a binder that sets and hardens, and is characterized as hydraulic or non-hydraulic. Hydraulic cement (e.g. Portland cement) hardens because of hydration reactions that occur independently of the mixture's water content. Non-hydraulic cements (e.g., gypsum plaster) must be kept dry in order to retain their strength [131].

In this thesis, we are focusing on cement-like materials in which hydraulic cement is used (their chemistry is simply easier). When the mixture is solidified, it forms a definite porous structure. In spite of the complex structure, concrete as well as cement paste are mechanically well-understood.

2.2.2   Basic Geometry

We consider a concrete block from a sewer pipe that is exposed to the hydrogen sulfide gas in the sewer atmosphere. We denote this macroscopic block by Ω. This is the place where corrosion processes are supposed to happen. To illustrate such a domain Ω, Fig. 2.4 points out a cross-section of sewer pipe [with hydrogen sulfide gas moving to the crown of the pipe] and a magnification of a concrete piece. Such a material has three phases, namely, water, air and concrete matrix. The diameter of a sewer pipe is in the range of $8 - 144$ inches and the wall thickness is about $\frac{1}{12}$ of the diameter. As porous material, the concrete has a
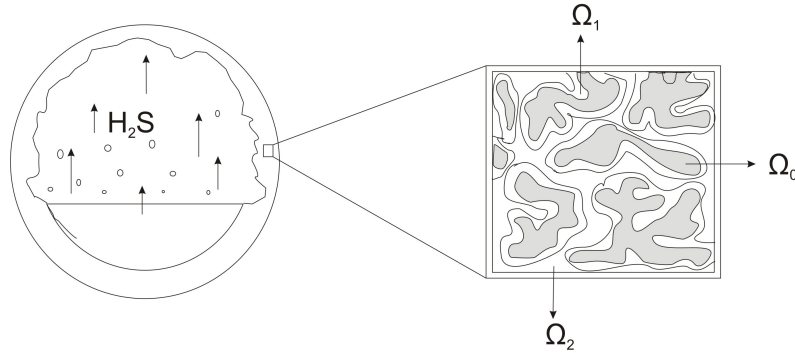
FIGURE 2.4: A cross-section of a concrete pipe linked to a zoomed in part. This zoomed in part is defined here as Ω.

solid matrix (pore skeleton) and voids (pore space). We denote the solid matrix (which is initially uncorroded) and the pore space by Ω_0 and Ω_{12}, respectively. Since the concrete in the sewer pipe is partially saturated, the void space Ω_{12} has two further non-overlapping parts Ω_1 and Ω_2. Ω_1 consists of the water-filled part of Ω_{12}, whereas Ω_2 is filled by air in the Ω. There are two interfaces among the different phases: Γ_1 represents the interface between solid matrix and water, and the interface between water-filled part and air-filled part is denoted by Γ_2. There

is no interface (i.e. no contact) between Ω_0 and Ω_2. We have

$$\Omega := \Omega_0 \cup \Omega_{12}, \qquad \Omega_{12} := \Omega_1 \cup \Omega_2, \qquad \Omega_1 \cap \Omega_2 = \emptyset, \qquad \Omega_0 \cap \Omega_{12} = \emptyset,$$

$$\Gamma_1 := \partial\Omega_0 \cap \partial\Omega_1, \qquad \Gamma_2 := \partial\Omega_1 \cap \partial\Omega_2.$$

The compounds of the aggregate have different shapes defining a *local porosity*. Due to the aggressiveness of the chemical reactions, the material ends up to deviate from a constant total porosity. The important *source of porosity* in concrete is the ratio of water to cement in the mix [143, 144]. Usually the concrete has a porosity around 5-6%. The total porosity[2] ϕ is defined as the ratio of the volume of the pore space, which we denote by $|\Omega_{12}|$, to the volume $|\Omega|$ of the whole concrete block. In the similar way, we define air-, water- and solid- fractions

$$\phi := \frac{|\Omega_{12}|}{|\Omega|}, \qquad \phi_1 := \frac{|\Omega_1|}{|\Omega_{12}|}, \qquad \phi_2 := \frac{|\Omega_2|}{|\Omega_{12}|} \quad \text{and} \quad \phi_0 := \frac{|\Omega_0|}{|\Omega|}, \qquad (2.1)$$

where $|\Omega_1|$ is the volume of the water-filled part of the pore space, $|\Omega_2|$ is the volume of the air-filled part of the pore space, while $|\Omega_0|$ denotes the volume of the solid matrix. It holds that $\phi_1 + \phi_2 = 1$ and $\phi\phi_1 + \phi\phi_2 + \phi_0 = 1$.

The initial porosity of concrete can be defined by

$$\tilde{\phi} := \frac{R_{\frac{w}{c}}\frac{\rho_c}{\rho_w}}{R_{\frac{w}{c}}\frac{\rho_c}{\rho_w} + R_{\frac{a}{c}}\frac{\rho_c}{\rho_a} + 1},$$

where $R_{\frac{w}{c}}$ and $R_{\frac{a}{c}}$ denote the water-to-cement and aggregate-to-cement ratios, whereas ρ_a, ρ_w and ρ_c are aggregate, water and cement densities, respectively; see e.g. [112]. We take the volume concentrations to be measured in unit mass per unit volume, namely ML^{-3}, and the surface concentrations in unit mass per unit area, i.e. ML^{-2}.

2.2.3 Multiscale representation of concrete

The precise structure of the concrete is far too complex (see e.g. Fig. 2.2) to be described precisely. Here, we consider two simplified microstructure models that can be handled successfully: (i) *uniformly periodic*, and (ii) *locally periodic*.

2.2.3.1 Uniformly-periodic approximations

We assume that the geometry of the porous medium Ω consists of a system of pores. The exterior boundary of Ω has of two disjoint, sufficiently smooth parts: Γ^N - the Neumann boundary and Γ^D - the Dirichlet boundary. The

---

[2]Since Ω_{12} is the total pore space, regardless of whether the pores are connected, or whether dead-end pores and fractures are present, the porosity ϕ is referred to as total porosity, see [16].

reference pore, say Y, has three pairwise disjoint connected domains Y_0, Y_1 and Y_2 with smooth boundaries Γ_1 and Γ_2, as shown in Fig. 2.5 (right). Moreover, $Y := \bar{Y}_0 \cup \bar{Y}_1 \cup \bar{Y}_2$.
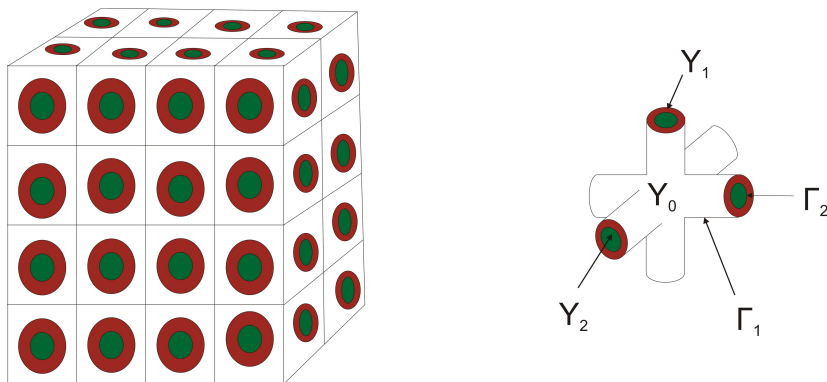
FIGURE 2.5: Left: Uniformly periodic system of pipes covering a macroscopic concrete block Ω. Right: Basic pore configuration.
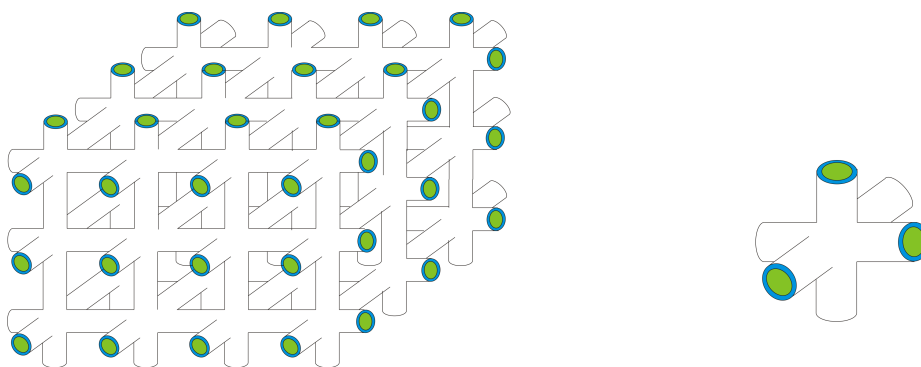
FIGURE 2.6: Left: Uniformly periodic system of micro-tube. Right: Reference pore configuration.

Let ε be a sufficiently small scaling factor denoting the ratio between the characteristic length of the pore Y and the characteristic length of the domain Ω. This is the geometric definition of the scaling factor ε (that we assume to be small). In Chapter 3, we will give another definition of ε based on reaction characteristic times.

Let χ_1 and χ_2 be the characteristic functions of the sets Y_1 and Y_2, respec-

tively. The *shifted set* Y_1^k is defined by

$$Y_1^k := Y_1 + \sum_{j=0}^{3} k_j e_j \text{ for } k := (k_1, k_2, k_3) \in \mathbb{Z}^3,$$

where e_j is the unit vector along the jth cartesian axis. By construction, Y_1^k is translation symmetric. The union of all shifted subsets of Y_1^k multiplied by ε (and confined within Ω) defines the perforated domain Ω^ε, namely

$$\Omega_1^\varepsilon := \bigcup_{k \in \mathbb{Z}^3} \{\varepsilon Y_1^k \mid \varepsilon Y_1^k \subset \Omega\}.$$

Similarly, Ω_2^ε, Γ_1^ε, and Γ_2^ε denote the union of the shifted subsets (of Ω) Y_2^k, Γ_1^k, and Γ_2^k scaled by ε. Furthermore, denote

$$Y_1^* := \bigcup \{Y_1^k : k \in \mathbb{Z}^3\}, \qquad Y_2^* := \bigcup \{Y_2^k : k \in \mathbb{Z}^3\}$$

$$\Gamma_2^* := \bigcup \{\Gamma_2^k : k \in \mathbb{Z}^3\}, \qquad \Gamma_1^* := \bigcup \{\Gamma_1^k : k \in \mathbb{Z}^3\}.$$

An example of uniformly periodic approximation of the domain Ω is given in Fig. 2.6. A few more examples of uniformly periodic approximations are given e.g. in [35, 83, 104].

2.2.3.2 Locally-periodic approximations

It is possible to stay away a bit from the periodicity assumption by considering locally periodic examples of microstructure in porous media. In other words, the "periodic" pattern is allowed to vary slightly from pore to pore. A domain having locally periodic microstructure is one whose material coefficients (e.g., diffusion coefficient and reaction constants) vary (in space) at the microscopic scale level. This variation is locally periodic in the sense that, around each point of the domain, the material coefficients vary rather fast. An example of locally periodic covering is shown in Fig. 2.7.

In the locally-periodic setting, one represents the normal vector n^ε to the "oscillating" internal boundaries of the perforations in the form suggested, for instance, in [19, 32]:

$$n^\varepsilon(x, y) := \tilde{n}(x, y) + \varepsilon n'(x, y) + \mathcal{O}(\varepsilon^2), \tag{2.2}$$

where

$$\tilde{n}(x, y) := \frac{\nabla_y P(x, y)}{|\nabla_y P(x, y)|} \tag{2.3}$$

and

$$n'(x, y) := \frac{\nabla_x P(x, y)}{|\nabla_y P(x, y)|} - \nabla_y P(x, y) \frac{\nabla_x P(x, y), \nabla_y P(x, y)}{|\nabla_y P(x, y)|^3}. \tag{2.4}$$

Here $y = \frac{x}{\varepsilon}$ and the generic surface $P(x, y)$ which describes the interfaces[3] Γ_1^ε and Γ_2^ε, respectively. is assumed to be a 1-periodic function in the variable y and sufficiently smooth with respect to both variables x, y. The function $P(x, \cdot)$ is assumed to be explicitly given for each $x \in \Omega$.

Note that in Fig. 2.7, the most inner part representing solid matrix is not connected to the outer part which is the air-filled part, whereas the air-filled part connects the neighboring pores. A 3D domain with locally-periodic covering is shown in Fig. 2.8. Now all the phases of the material are now connected.
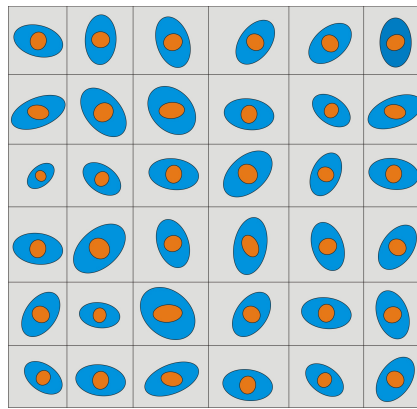
FIGURE 2.7: Locally periodic perforations with disconnected phases.
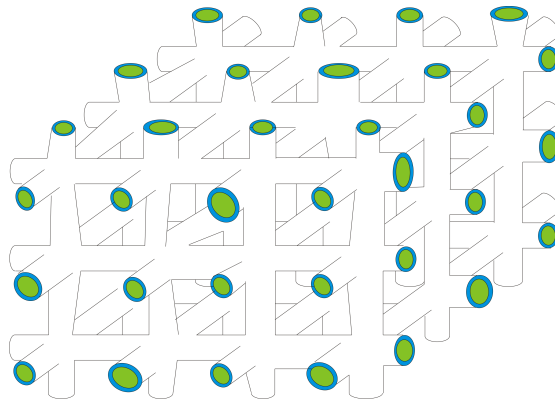
FIGURE 2.8: Locally periodic domain with varying microstructure.

---

[3]Γ_1^ε and Γ_2^ε denote the same class of objects as those defined in the periodic setting with the same name, but now the uniformly periodicity assumption is replaced by local periodicity. The same statement holds for Ω_1^ε and Ω_2^ε. This notation emphasizes the strong dependence of the geometry on the parameter x.

We define the set Y_1^{ijk} as the water-filled part in the unit pore Y^{ijk}, $i, j, k \in \mathbb{N}$. The vertices of the scaled pore Y^{ijk} are $(\frac{\varepsilon}{2}, \frac{\varepsilon}{2}, \frac{\varepsilon}{2}) + \varepsilon(i + a_1, j + a_2, k + a_3)$ with $i, j, k \in \mathbb{N}$ fixed and a_1, a_2, a_3 taking values 0 or 1. The center of the cube has coordinates $\varepsilon(i + 1, j + 1, k + 1)$, [53]. The union of all subsets of Y_1^{ijk} multiplied by ε defines the perforated domain

$$\Omega_1^\varepsilon := \bigcup_{i,j,k \in \mathbb{N}} \{\varepsilon Y_1^{ijk} \mid \varepsilon Y_1^{ijk} \subset \Omega\}.$$

Similarly, Ω_2^ε, Γ_1^ε, and Γ_2^ε denote the union of the subsets (of Ω) Γ_1^{ijk}, Y_2^{ijk}, and Γ_2^{ijk} multiplied by ε. Furthermore,

$$Y_1^* := \bigcup \{Y_1^{ijk}, i, j, k \in \mathbb{N}\}, \qquad Y_2^* := \bigcup \{Y_2^{ijk}, i, j, k \in \mathbb{N}\}$$

$$\Gamma_1^* := \bigcup \{\Gamma_{ijk}^{sw}, i, j, k \in \mathbb{N}\}, \qquad \Gamma_2^* := \bigcup \{\Gamma_{ijk}^{wa}, i, j, k \in \mathbb{N}\}.$$

Further examples of locally-periodic approximations are given, for instance, in [15, 26, 125].

2.2.3.3 Two-scale approximations

We consider a uniformly homogenous (i.e. with no apparent substructure) block, but when zoomed into a point, a certain microstructure can be seen. We introduce this way a continuous distribution of cells representing the microstructures of the medium. The precise form of the microstructure depends on the macroscopic position $x \in \Omega$. Let $Y_{0,x}$ represent the structure of the solid matrix within a local neighborhood of that point (see Fig. 2.10). Likewise, $Y_{1,x}$, $Y_{2,x}$ represent the parts of the pore space occupied by water and air. Y_x splits up into three parts

$$Y := \bar{Y}_{0,x} \cup \bar{Y}_{1,x} \cup \bar{Y}_{2,x} \quad \text{for all } x \in \Omega,$$

which are disjoint except at the boundaries. In our situation, we assume that the pore air, pore water and solid matrix are connected. Moreover, we denote by $\Gamma_{1,x} := \partial Y_{1,x} \cap \partial Y_{0,x}$ and $\Gamma_{2,x} := \partial Y_{1,x} \cap \partial Y_{2,x}$ the interfaces between the water phase and the solid matrix, and between the water and air phases, respectively. The information within each cell is described independently with respect to what happens at the macroscale. The solution of the problem posed in the cell Y_x is coupled via ∂Y_x to the macroscale Ω.

In this thesis, when talking about two-scale domain we restrict ourselves to the case when each point $x \in \Omega$ is zoomed and a fixed microstructure is seen. For further examples of two-scale models, we refer the reader to [28, 86] and the references cited therein.
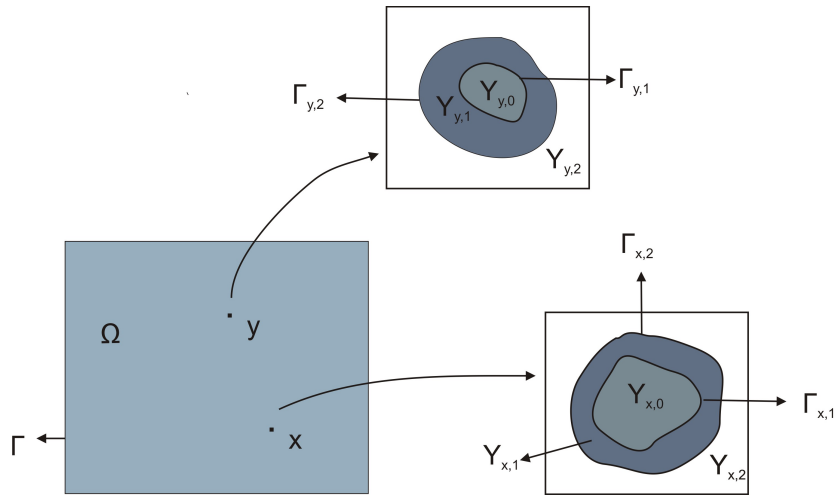
FIGURE 2.9:   Two-scale domain with distributed microstructure.
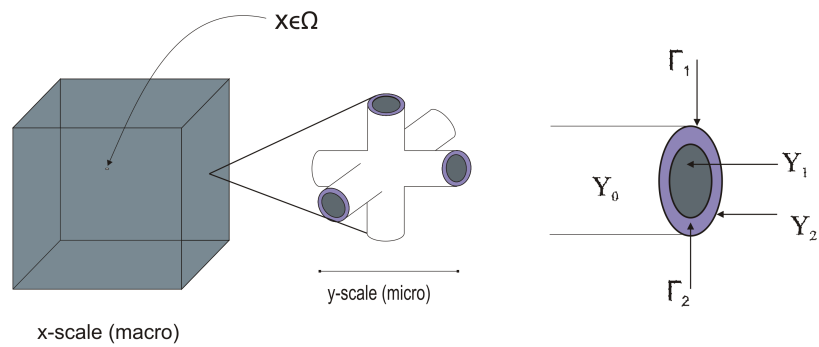
FIGURE 2.10: Left: Zoomed out cubic piece from the concrete wall. This is the scale we refer to as macroscopic. Middle: Reference pore configuration. Right: Zoomed out one end of the pore.

2.3 Specific modeling aspects arising from sulfatation of concrete

There are a few physico-chemiacl processes that are important for the actual sulfatation of concrete. We wish to introduce them in our microscopic model.

2.3.1 Production of H_2S by Henry's law

As soon as $H_2S(g)$, produced in the air space of the concrete pipe, enters the pipe wall above the waste flow, it dissolves in the water present in the concrete block. In the corrosion process, this hydrogen sulfide transfer from sewer gas to pore water is a crucial step. H_2S molecules can move between the air-filled part and the water-filled part the water-air interfaces [14]. We assume that such mass transfer takes place according to the following reversible reaction mechanism

$$H_2S(aq) \rightleftharpoons H_2S(g). \qquad (2.5)$$

In (2.5), the transfer of H_2S between air-filled parts and water-filled parts that are in contact follows a local phase equilibrium diagram of the air-water binary system at the pore level [47]. In other words, *the amount of gaseous H_2S that dissolves in a given time and volume of liquid at a constant temperature is directly proportional to the equilibrium partial pressure of gaseous H_2S in equilibrium.* This assumption at the phase equilibrium is expressed via the linear relationship

$$P_{H_2S} = \frac{1}{H}[\overline{H_2S(aq)}], \qquad (2.6)$$

where P_{H_2S} denotes the partial pressure of H_2S in the gaseous phase of the pore and $\overline{H_2S(aq)}$ represents the molar concentration of H_2S. In (2.6), the proportionality factor is known as Henry's constant on the molar concentration scale. (2.6) can be re-written in terms of mass concentrations as

$$\phi\phi_1[H_2S(aq)] = (HRT\frac{\phi_1}{\phi_2})\phi\phi_2[H_2S(g)], \qquad (2.7)$$

where R denotes the gas constant, T represents the absolute temperature and ϕ, ϕ_1, ϕ_2 are defined in (2.1). (2.7) is the so-called *phase equilibrium condition*. Based on [124], we assume that the macroscopic mass transfer at the air-water interface is proportional to the difference

$$\phi\phi_1[H_2S(aq)] - P\phi\phi_2[H_2S(g)]$$

where $P := HRT\frac{\phi_1}{\phi_2}$. The proportionality factor $Q > 0$ is referred to as the mass transfer coefficient and needs to be identified. For instance, Q can be determined by means of one-film theory of diffusion in heterogenous media [11].

We can write the net production of H_2S as

$$f_{Henry} = Q\big(\phi\phi_1[H_2S(aq)] - P\phi\phi_2[H_2S(g)]\big). \qquad (2.8)$$

We call f_{Henry} the production term by Henry's law. For related work on this subject, see [95].
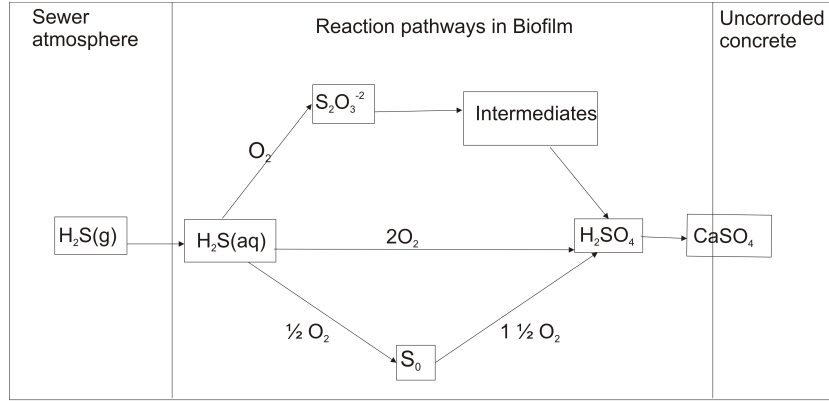
FIGURE 2.11: Reactions pathways for hydrogen sulfide, see also Fig. 4.1 in [74].

2.3.2 Modeling sulfatation reaction rate

The oxidation of hydrogen sulfide on the pipe wall surface is biologically activated after the pH of the surface drops below approximately 8-9, [115]. In corrosion products, H_2S oxidizes rapidly by the action of the bacteria to a mix of elemental sulfur and sulfuric acid [74]. We consider the sulfate corrosion process dominated by the reaction of sulfuric acid. The respective reaction is

$$2H_2O + H^+ + SO_4^{-2} + CaCO_3 \longrightarrow CaSO_4 \cdot 2H_2O + HCO_3^-. \qquad (2.9)$$
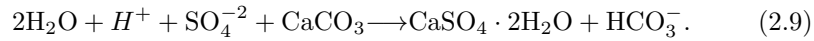
(2.9) takes place in Ω when a sufficient amount of H_2SO_4 is available and produces gypsum. We assume that (2.9) does not interfere with the mechanics of the solid parts of the domain. This is a rather strong assumption since it is known that (2.9) can actually produce local ruptures of the solid matrix [131]. From our point of view, the following scenario is relevant:

- the reaction (2.9) is very fast and it is complete in the sense that it consumes all the available calcium carbonate at the interface.

In the above situation, it is not obvious what is the correct formal expression for the reaction rate η on the interface specially if we do not stick to the assumption of elementary reaction for which mass-action kinetics would be applicable.

$$\eta(\alpha, \beta) = k_3 \bar{\alpha} \bar{\beta}, \qquad (2.10)$$

On the other hand to point out the complexity of the situation, we refer the reader to [20] for one example where the mass-action kinetics do not work. It is not at all clear how important the precise structure of η is especially if one considers this process in the fast-reaction regime. To fix ideas, we assume that

the reaction rate η takes the form

$$\eta(\alpha, \beta) = \begin{cases} k_3\alpha^p(\beta_{max} - \beta)^q & \text{if } \alpha \geq 0, \beta \geq 0 \\ 0 & \text{otherwise,} \end{cases} \tag{2.11}$$

where k_3 is a reaction constant, α is the concentration of the H_2SO_4 and β denotes the concentration of gypsum, whereas β_{max} is a known constant and $p \geq 1$ and $q \geq 1$ are the partial reaction orders. The power law structure (2.11) describing the reaction rate appears to be new in the context of sulfatation reactions. Another way to model the reaction-rate for H_2SO_4 production is

$$\eta(\alpha, \beta) = k_3 R(\overline{\alpha})Q(\overline{\beta}), \tag{2.12}$$

where R,Q are non-linear functions and the quantities with bars denote surface concentrations. For more examples of different types of reaction rates, see [78]. We consider (2.11) and (2.12) in the thesis.

We define

$$f_{Reac} := c_\Gamma\eta.$$

Remark 2.3.1. In order to understand the meaning of the reaction rate, we recall the general concept of surface chemical reactions. Consider the amount of $CaCO_4$ produced on the surface Γ_1, during an arbitrary time interval $S' \subset S := [0, \infty)$ and let $\Gamma^{sw} := \partial\Omega_s \cap \partial\Omega_{pw}$. Then

$$\mu_\Gamma(S' \times \Gamma^{sw}) = \int_{S'} \int_{\Gamma^{sw}} c_\Gamma\eta d\sigma dt := \int_{S'} \int_{\Gamma^{sw}} f_{Reac} d\sigma dt, \tag{2.13}$$

is the amount of $CaCO_4$ produced on the interface during S'. Here c_Γ stands for appropriate stoichiometric coefficient of the reaction. In (2.9), we have $c_\Gamma = 1$.

2.3.3 Mass balance of moisture in the corrosion process

The mass balance of the moisture which diffuses in concrete is given by

$$w_t + \text{div}j_w = f_w, \tag{2.14}$$

where f_w denotes all the sources and sinks that depend on w and j_w is a macroscopic flux of moisture. Adopting Bažant's model of moisture in concrete [13], we assume that the flux is of the form

$$j_w = -D\nabla w, \tag{2.15}$$

where D is the transport coefficient, see e.g. [118, 119]. For derivations of (2.14) based on different assumptions, see e.g. [13], Section 2.2.6 in [95] and Section 2.2.2 in [130].

2.3.4   Production of gypsum

We take η as in (2.11) and introduce

$$\partial_t[\text{CaSO}_4 \cdot 2\text{H}_2\text{O}] = \eta([\text{H}_2\text{SO}_4], [\text{CaSO}_4 \cdot 2\text{H}_2\text{O}]).$$

Here we consider that reaction rate η highly depends on the reaction of H_2SO_4 with the calcium carbonate and the produced gypsum does not diffuse from the surface of the solid matrix. Different choices of η have been discussed in Subsection 2.3.2. In the forthcoming chapters, we choose the form of η as it is given in (2.11) and (2.12).

2.4   Basic assumptions

Keeping in mind the 3D configuration of a typical pore (cf Section 2.2.3), we list the main geometry and modeling assumptions:

Assumption 2.4.1. (Assumptions on geometry)

1. Every pore has three distinct non-overlapping connected parts and all constituent parts connect neighboring pores to one another (see Fig. 2.5).

2. All internal (water-air and solid-water) interfaces are sufficiently smooth and do not touch each other. There are no solid-air interfaces.

These restrictions are needed not only to give a meaning to functions defined across interfaces, but also to introduce later the concept of extension as given, for instance, in [2, 39].

Assumption 2.4.2. (Modelling assumptions)

1. The reactions (1.1) – (1.4) do not interfere with the mechanics of the solid part of the pores.

2. The produced gypsum stays at the solid boundary and does not make any change in the local geometry.

3. Effect of bacteria and temperature are considered to be negligible.

2.5   Corrosion models

In this section, we introduce two concrete corrosion models incorporating the sulfatation reactions (1.1) – (1.4). First we present a microscopic model which is defined in $\varepsilon-$dependent domain. Then we give a distributive microstructure model containing information from two separated spatial scales (micro and macro).

2.5.1 Microscopic model

All physical processes take place on the microscale (pore level) but the physical phenomena that we are interested in are visible on a macroscopic level, see Fig. 2.6 for a description of the geometry we have in mind.

The unknowns $u_1^\varepsilon, u_2^\varepsilon, u_3^\varepsilon, u_4^\varepsilon, u_5^\varepsilon$ refer to the concentration of sulfuric acid (H_2SO_4), hydrogen sulfide aqueous species ($H_2S(aq)$), hydrogen sulfide gaseous species ($H_2S(g)$), moisture (H_2O) and gypsum ($CaSO_4 \cdot 2H_2O$), respectively. We consider the following system of mass-balance equations defined at the pore level:

$$\partial_t u_1^\varepsilon + \text{div}(-d_1^\varepsilon \nabla u_1^\varepsilon) = -k_1^\varepsilon u_1^\varepsilon + k_2^\varepsilon u_2^\varepsilon, \qquad x \in \Omega_1^\varepsilon,\ t \in (0, T) \quad (2.16)$$

$$\partial_t u_2^\varepsilon + \text{div}(-d_2^\varepsilon \nabla u_2^\varepsilon) = k_1^\varepsilon u_1^\varepsilon - k_2^\varepsilon u_2^\varepsilon, \qquad x \in \Omega_1^\varepsilon,\ t \in (0, T), \quad (2.17)$$

$$\partial_t u_3^\varepsilon + \text{div}(-d_3^\varepsilon \nabla u_3^\varepsilon) = 0, \qquad x \in \Omega_2^\varepsilon,\ t \in (0, T) \quad (2.18)$$

$$\partial_t u_4^\varepsilon + \text{div}(-d_4^\varepsilon \nabla u_4^\varepsilon) = k_1^\varepsilon u_1^\varepsilon, \qquad x \in \Omega_1^\varepsilon,\ t \in (0, T) \quad (2.19)$$

$$\partial_t u_5^\varepsilon = \eta^\varepsilon(u_1^\varepsilon, u_5^\varepsilon), \qquad x \in \Gamma_1^\varepsilon,\ t \in (0, T). \quad (2.20)$$

The presence of ε shows that all the functions are defined in perforated domains. We complement the system with the initial conditions

$$u_i^\varepsilon(x, 0) = u_{i0}(x), \qquad x \in \Omega_1^\varepsilon, t = 0, i \in \{1, 2, 4\} \quad (2.21a)$$

$$u_3^\varepsilon(x, 0) = u_{30}(x), \qquad x \in \Omega_2^\varepsilon, t = 0 \quad (2.21b)$$

$$u_5^\varepsilon(x, 0) = u_{50}(x), \qquad x \in \Gamma_1^\varepsilon, t = 0. \quad (2.21c)$$

The associated boundary conditions are

$$-n_1^\varepsilon \cdot d_1^\varepsilon \nabla u_1^\varepsilon = 0 \qquad x \in \Gamma_1^\varepsilon,\ t \in (0, T) \quad (2.22a)$$

$$-n_1^\varepsilon \cdot d_1^\varepsilon \nabla u_1^\varepsilon = 0 \qquad x \in \Gamma^N \cap \partial \Omega_1^\varepsilon,\ t \in (0, T) \quad (2.22b)$$

$$-n_1^\varepsilon \cdot d_1^\varepsilon \nabla u_1^\varepsilon = \varepsilon \eta^\varepsilon(u_1^\varepsilon, u_5^\varepsilon) \qquad x \in \Gamma_1^\varepsilon\ t \in (0, T) \quad (2.22c)$$

$$-n_1^\varepsilon \cdot d_2^\varepsilon \nabla u_2^\varepsilon = -\varepsilon(a^\varepsilon(x)u_3^\varepsilon - b^\varepsilon(x)u_2^\varepsilon) \qquad x \in \Gamma_2^\varepsilon,\ t \in (0, T) \quad (2.22d)$$

$$-n_1^\varepsilon \cdot d_2^\varepsilon \nabla u_2^\varepsilon = 0 \qquad x \in \Gamma_1^\varepsilon,\ t \in (0, T) \quad (2.22e)$$

$$-n_1^\varepsilon \cdot d_2^\varepsilon \nabla u_2^\varepsilon = 0 \qquad x \in \Gamma^N \cap \partial \Omega_1^\varepsilon,\ t \in (0, T) \quad (2.22f)$$

$$-n_2^\varepsilon \cdot d_3^\varepsilon \nabla u_3^\varepsilon = 0 \qquad x \in \Gamma^N \cap \partial \Omega_2^\varepsilon,\ t \in (0, T) \quad (2.22g)$$

$$u_3^\varepsilon(x, t) = u_3^D(x, t) \qquad x \in \Gamma^D \cap \partial \Omega_2^\varepsilon,\ t \in (0, T) \quad (2.22h)$$

$$-n_2^\varepsilon \cdot d_3^\varepsilon \nabla u_3^\varepsilon = \varepsilon(a^\varepsilon(x)u_3^\varepsilon - b^\varepsilon(x)u_2^\varepsilon) \qquad x \in \Gamma_2^\varepsilon,\ t \in (0, T) \quad (2.22i)$$

$$-n_1^\varepsilon \cdot d_4^\varepsilon \nabla u_4^\varepsilon = 0 \qquad x \in \partial \Omega_1^\varepsilon,\ t \in (0, T) \quad (2.22j)$$

$$u_1^\varepsilon = 0 \qquad x \in \Gamma^D \cap \partial \Omega_1^\varepsilon,\ t \in (0, T) \quad (2.22k)$$

$$u_2^\varepsilon = 0 \qquad x \in \Gamma^D \cap \partial \Omega_1^\varepsilon,\ t \in (0, T). \quad (2.22l)$$

On the right-hand side of (2.16), the first and second term appear due to the consumption and production of H_2SO_4 in (1.1) and (1.2), respectively, by mass action law. A similar argument holds for the right-hand side of (2.17) and the right hand side of (2.18) is zero due to (1.3). The right hand side of (2.20) is a

source for gypsum which is the result of fast reaction between H_2SO_4 and $CaCo_3$. Here n_i^ε denotes the outer normal to $\partial\Omega_i^\varepsilon, i \in \{1, 2\}$ ($\Omega_i^\varepsilon, \Gamma_i^\varepsilon$ are defined in Subsection 2.2.3.1). The presence of ε entering the right hand side of the boundary conditions (2.22c), (2.22d) and (2.22i) is essential to pass to the rigorous limit in the boundary terms.

In the non-dimensionalization procedure done in Section 3.2, ε appears due to the scaling of involved quantities. To get effective behaviors, we need to pass to the limit as $\varepsilon \to 0$ in (2.16)-(2.22l). The precise structure of the upscaled limit equations ($\varepsilon \to 0$) will be derived in Chapter 4 and Chapter 5. In order to do this, we restrict our attention to the micro-geometries described in Section 2.2.3 and periodic/locally periodic model parameters.

2.5.1.1   Periodic/locally periodic model parameters

We consider two different strategies.

Case 1: All functions $d_i^\varepsilon, k_j^\varepsilon, a^\varepsilon, b^\varepsilon$ defined in Ω, Γ_1^ε and Γ_2^ε are rapidly oscillating and are of one of the forms:

$$d_i^\varepsilon(x) = d_i(\tfrac{x}{\varepsilon}), i \in \{1, 2, 3, 4\}, \quad k_j^\varepsilon(x) = k_j(\tfrac{x}{\varepsilon}), j \in \{1, 2, 3\}, \qquad (2.23)$$

$$a^\varepsilon(x) = a(\tfrac{x}{\varepsilon}), \quad b^\varepsilon(x) = b(\tfrac{x}{\varepsilon}), \quad n_k^\varepsilon(x) = n_k(\tfrac{x}{\varepsilon}), k \in \{1, 2\}. \qquad (2.24)$$

where the functions d_i, k_j, a, b are $Y-$periodic and are defined on Y_1^*, Y_2^*, Γ_2^*, and on Γ_1^*, respectively.

Case 2: All functions given in (2.23) and (2.24) are locally-periodic if they depend on both slow x and fast variable $\tfrac{x}{\varepsilon}$. Here, we have

$$d_i^\varepsilon(x) = d_i(x, \tfrac{x}{\varepsilon}), i \in \{1, 2, 3, 4\}, \quad k_j^\varepsilon(x) = k_j(x, \tfrac{x}{\varepsilon}), j \in \{1, 2, 3\}, \quad (2.25)$$

$$a^\varepsilon(x) = a(x, \tfrac{x}{\varepsilon}), \quad b^\varepsilon(x) = b(x, \tfrac{x}{\varepsilon}), \quad n_k^\varepsilon(x) = n_k(\tfrac{x}{\varepsilon}), k \in \{1, 2\}. \quad (2.26)$$

We consider case 1 in uniformly periodic domains in Chapter 4 and 5, while we consider Case 1 for locally-periodic domains in Chapter 3.

2.5.2   Distributed-microstructure model

Usually distributed-microstructure models are known in the context of homogenization limits as the scale of inhomogeneity tends to zero. This system consists of the following set of partial differential equations coupled with an ordinary differential equation:

$$\partial_t w_1 - \nabla_y \cdot (d_1 \nabla_y w_1) = -k_1(y) w_1 + k_2(y) w_2 \qquad \text{in } (0, T) \times \Omega \times Y_1, \quad (2.27)$$

$$\partial_t w_2 - \nabla_y \cdot (d_2 \nabla_y w_2) = k_1(y) w_1 - k_2(y) w_2 \qquad \text{in } (0, T) \times \Omega \times Y_1, \quad (2.28)$$

$$\partial_t w_3 - \nabla \cdot (d_3 \nabla w_3) = -\alpha \int_{\Gamma_2} \big(H w_3 - w_2 \big) d\gamma_y \qquad \text{in } (0, T) \times \Omega, \qquad (2.29)$$

$$\partial_t w_4 - \nabla_y \cdot (d_4 \nabla_y w_4) = k_1(y) w_1 \qquad \text{in } (0, T) \times \Omega \times Y_1, \quad (2.30)$$

$$\partial_t w_5 = \eta(w_1, w_5) \qquad \text{on } (0, T) \times \Omega \times \Gamma_1. \quad (2.31)$$

The system (2.27)- (2.31) is equipped with the initial conditions

$$w_j(0, x, y) = w_j^0(x, y) \qquad \text{in } \Omega \times Y_1, j \in \{1, 2, 4\} \qquad (2.32\text{a})$$

$$w_3(0, x) = w_3^0(x) \qquad \text{in } \Omega \qquad (2.32\text{b})$$

$$w_5(0, x, y) = w_5^0 \qquad \text{on } \Omega \times \Gamma_1 \qquad (2.32\text{c})$$

while the boundary conditions are

$$-n(y) \cdot d_1 \nabla_y w_1 t = \eta(w_1, w_5) \qquad \text{on } (0, T) \times \Omega \times \Gamma_1 \qquad (2.33\text{a})$$

$$-n(y) \cdot d_1 \nabla_y w_1 = 0 \qquad \text{on } (0, T) \times \Omega \times (\Gamma_2 \cup (\partial Y_1 \cap \partial Y)) \qquad (2.33\text{b})$$

$$-n(y) \cdot d_2 \nabla_y w_2 = 0 \qquad \text{on } (0, T) \times \Omega \times (\Gamma_1 \cup (\partial Y_1 \cap \partial Y)) \qquad (2.33\text{c})$$

$$-n(y) \cdot d_2 \nabla_y w_2 = \alpha(H w_3 - w_2) \qquad \text{on } (0, T) \times \Omega \times \Gamma_2 \qquad (2.33\text{d})$$

$$-n(x) \cdot d_3 \nabla w_3 = 0 \qquad \text{on } (0, T) \times \Gamma_N \qquad (2.33\text{e})$$

$$w_3 = w_3^D \qquad \text{on } (0, T) \times \Gamma, \qquad (2.33\text{f})$$

$$-n(y) \cdot d_4 \nabla_y w_4 = 0 \qquad \text{on } (0, T) \times \Omega \times \Gamma_2 \qquad (2.33\text{g})$$

$$-n(y) \cdot d_4 \nabla_y w_4 = 0 \qquad \text{on } (0, T) \times \Omega \times \Gamma_1. \qquad (2.33\text{h})$$

Here w_1 denotes the concentration of H_2SO_4 in $\Omega \times Y_1$, w_2 the concentration of H_2S aqueous species in $\Omega \times Y_1$, w_3 the concentration of H_2S gaseous species in Ω, w_4 the concentration of the moisture and w_5 is the *gypsum* concentration on $\Omega \times \Gamma_1$. $\Omega, Y, Y_1, Y_2, \Gamma_1, \Gamma_2$ are shown in Fig. 2.10. ∇ without subscript denotes the differentiation with respect to macroscopic variable x, while ∇_y is the respective differential operator with respect to the micro-variable y. The parameter α is reaction constant which quantifies the resistance of the medium to the exchange and H is Henry's constant, see Section 2.3.1. The microscale and macroscale information is connected via the right-hand side of (2.29) and via the *micro-macro transmission condition* (2.33d). The information referring to the air phase Y_2 is hidden in w_3. The partial differential equation for w_3, defined on macroscopic scale, is derived by averaging over Y_2.

2.6 Notes and comments

There are many open problems and open research directions concerning the modeling of the concrete sulfatation. We mention here but a few:

1. *Role of bacteria:* Bacteria play a crucial role in the production of the hydrogen sulfate which is the main source of the degradation of the concrete. The precise role of the micro-organisms in the context of sulfate attack on concrete is quite complex and less understood. To understand their role, we may need to study enzyme kinetics, perhaps along the line of the Michaelis-Menten mechanism [103].

2. *Expansion of gypsum:* We assume that the production of the gypsum on the solid-water interface does not affect the microscopic geometry (and

therefore neither the mechanics). This is a strong assumption since it is known that sulfatation mechanism actually produces local ruptures of the solid matrix [131].

3. *Moving boundary formulations:* In practice, the macroscopic corrosion front propagates into the uncorroded concrete. To track the precise macroscopic position of the front, it is perhaps more natural to consider a free boundary formulation (as in e.g. [23]).

4. *Stochastic geometry*[4]: In stochastic representations, random microstructure can be considered. For details, see e.g. in [63, 65].

---

[4]A domain which is neither uniformly periodic nor locally periodic is closer to the actual structure.

Chapter 3

Homogenization in Locally-periodic Perforated Domains

In this chapter, we derive multiscale models via the asymptotic homogenization method for locally-periodic domains. Our goal is to obtain upscaled RD models together with explicit formulae for the effective transport and reaction coefficients using different scalings of the diffusion coefficients. We show that the averaged systems contain additional terms appearing due to the deviation of the assumed geometry from a uniformly periodic distribution of perforations. We work in two parameter regimes: (i) all diffusion coefficients are of order of $\mathcal{O}(1)$ and (ii) all diffusion coefficients are of order of $\mathcal{O}(\varepsilon^2)$ except the one for $H_2S(g)$ which is of order of $\mathcal{O}(1)$. In case (i), we obtain a set of macroscopic equations coupled with two-scale ode, while in case (ii) we are led to reaction-diffusion system with distributed-microstructure that captures the interplay between microstructural reaction effects and the macroscopic transport.

This chapter is structured as follows: In section 3.1, we present our choice of microstructure and the setting of the equations. Section 3.2 contains the non-dimensional form. In Section 3.3, we apply the homogenization procedure for two relevant parameter regimes: (a) all diffusion coefficients are of order of $\mathcal{O}(1)$ and (b) all diffusion coefficients are of order of $\mathcal{O}(\varepsilon^2)$ except the one for $H_2S(g)$ which is of order of $\mathcal{O}(1)$. In case (a), we obtain a set of upscaled equations, while in case (b) we are led to a distributed-microstructure system that captures the interplay between microstructural reaction effects and the macroscopic transport.

3.1   Geometry. Model equations

This section contains a brief discussion of the geometry and presents the model equations posed in the domain of interest.

3.1.1   Locally-periodic domains

We refer the reader to Subsection 2.2.3.2 where the concept of locally-periodic microstructure has been introduced, also see Fig. 3.1. The connectedness (see Fig. 2.8) or disconnectedness (see Fig. 2.7) of all constituent parts of the microstructure does not matter for the analysis done in this chapter.
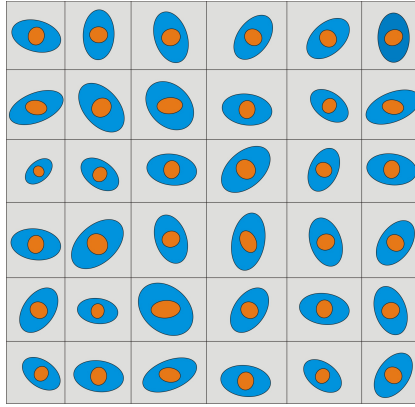
FIGURE 3.1: Locally-periodic perforations with two disconnected and one connected components.

3.1.2   Microscopic model equations

We use the microscopic model given in Subsection 2.5.1 without ε on the right hand side of the boundary conditions. In the non-dimensionalization procedure, ε will appear in the boundary conditions due to the scaling of the involved quantities.

3.2   Non-dimensionalization

Before applying formal homogenization, we want to formulate the model equations in dimensionless form with the hope to get more insight in the meaning of the parameter ε. We introduce the characteristic length L for the space variable such that $x = L\tilde{x}$, the time variable is scaled as $t = \tau s$, and for the concentrations, we use $u_i^\varepsilon = U_i v_i^\varepsilon$, $U_i = \|u_i^\varepsilon\|_\infty$ for all $i \in \{1, 2, 3, 4, 5\}$. k_j^ε are scaled as $k_j^\varepsilon = K_j \tilde{k}_j^\varepsilon$, where $K_j = \| k_j^\varepsilon \|_\infty$ for all $j \in \{1, 2, 3\}$ and $d_k^\varepsilon := D_k \tilde{d}_k^\varepsilon$ for all

$k \in \{1, 2, 3, 4\}$. We make use of two mass-transfer Biot numbers[1] for the two spatial scales in question: *micro* and *macro*. The *micro Biot number* is defined by

$$Bi^m := \frac{b_{ref}^m L}{\mathfrak{D}}, \qquad (3.1)$$

where b_{ref}^m is a reference reaction rate acting at the water solid interface within the microstructure and $\mathfrak{D}$ is a reference diffusion coefficient. The *macro Biot number* is defined by

$$Bi^M := \frac{b_{ref}^M L}{\mathfrak{D}}, \qquad (3.2)$$

where b_{ref}^M is a reference reaction rate at the water-solid interface at the macro level. The connection between the two Biot numbers is given by

$$Bi^m = \varepsilon Bi^M. \qquad (3.3)$$

In some sense, relation (3.3) defines our small scaling parameter ε with respect to which we wish to homogenize. Furthermore, we introduce two other dimensionless numbers:

$$\beta_i := \frac{U_i}{U_1} \text{ and } \gamma_i := \frac{D_i}{D_3}. \qquad (3.4)$$

β_i represents the ratio of the maximum concentration of the ith species to the maximum H_2SO_4 concentration, while γ_i denotes the ratio of the characteristic time of the ith diffusive aqueous species to the characteristic diffusion time of $H_2S(g)$. Consequently for a fixed i, the ratio γ_i is small, then the reactant gas diffuse faster through the pore than the rest of the species diffusing in the liquid phase.

We consider the RD system given in Subsection 2.5.1 without the scaling parameter ε in the boundary conditions. In terms of the newly introduced quantities, the mass-balance equation for H_2SO_4 takes the form

$$\frac{U_1}{\tau} \partial_s v_1^\varepsilon + \frac{U_1 D_1}{L^2} \operatorname{div}(-\tilde{d}_1^\varepsilon \nabla v_1^\varepsilon) = -K_1 U_1 \tilde{k}_1^\varepsilon v_1^\varepsilon + K_2 U_2 \tilde{k}_2^\varepsilon v_2^\varepsilon, \qquad (3.5)$$

and hence,

$$\beta_1 \partial_s v_1^\varepsilon + \frac{\beta_1 D_1 \tau}{L^2} \operatorname{div}(-\tilde{d}_1^\varepsilon \nabla v_1^\varepsilon) = -\frac{K_1 U_1 \tau}{U_1} \tilde{k}_1^\varepsilon v_1^\varepsilon + \frac{K_2 U_2 \tau}{U_1} \tilde{k}_2^\varepsilon v_2^\varepsilon. \qquad (3.6)$$

As reference time, we choose the characteristic time scale of the fastest species (here: $H_2S(g)$), that is $\tau := \tau_{diff} = \frac{L^2}{D_3}$. We get

$$\beta_1 \partial_s v_1^\varepsilon + \beta_1 \gamma_1 \operatorname{div}(-\tilde{d}_1^\varepsilon \nabla v_1^\varepsilon) = -\frac{\eta_{ref}^1 \tau}{U_1} \tilde{k}_1^\varepsilon v_1^\varepsilon + \frac{\eta_{ref}^2 \tau}{U_1} \tilde{k}_2^\varepsilon v_2^\varepsilon. \qquad (3.7)$$

---

[1]Biot numbers are dimensionless quantities mostly used in heat and mass transfer calculations and they quantify the resistance of a surface (thin layer) to heat and/or mass transfer.

Let us denote by $\tau_{reac}^j := \frac{U_1}{\eta_{ref}^j}$ the characteristic time scale of the jth reaction, where the quantity η_{ref}^j is a reference reaction rate for the corresponding chemical reaction. With this new notation in hand, we obtain

$$\beta_1 \partial_s v_1^\varepsilon + \beta_1 \gamma_1 \mathrm{div}(-\tilde{d}_1^\varepsilon \nabla v_1^\varepsilon) = -\Phi_1^2 \tilde{k}_1^\varepsilon v_1^\varepsilon + \Phi_2^2 \tilde{k}_2^\varepsilon v_2^\varepsilon \tag{3.8}$$

where $\Phi_j^2, j \in \{1,2,3\}$ are Thiele-like moduli. The jth Thiele modulus Φ_j^2 compares the characteristic time of the diffusion of the fastest species and the characteristic time of the jth chemical reaction. It is defined as

$$\Phi_j^2 \quad := \quad \frac{\tau_{diff}}{\tau_{reac}^j} \text{ for all } j \in \{1,2,3\}. \tag{3.9}$$

For the boundary condition involving the surface reaction, we obtain

$$\tilde{n}^\varepsilon \cdot (-\tilde{d}_1^\varepsilon \nabla v_1^\varepsilon)) = -\frac{\tau_{diff}}{\gamma_1 L \tau_{reac}^3} \tilde{\eta}(v_1^\varepsilon, v_5^\varepsilon), \tag{3.10}$$

and therefore,

$$\tilde{n}^\varepsilon \cdot (-\tilde{d}_1^\varepsilon \nabla v_1^\varepsilon)) = -\varepsilon \frac{\Phi_3^2}{\gamma_1} \tilde{\eta}(v_1^\varepsilon, v_5^\varepsilon). \tag{3.11}$$

Note that the quantity $\varepsilon\Phi_3^2$ plays the role of a Thiele modulus for a surface reaction, while Φ_1^2 and Φ_2^2 are Thiele moduli for volume reactions. Similarly, the mass-balance equation for the species $H_2S(aq)$ becomes

$$\beta_2 \partial_s v_2^\varepsilon + \beta_2 \gamma_2 \mathrm{div}(-\tilde{d}_2^\varepsilon \nabla v_2^\varepsilon) = \Phi_1^2 \tilde{k}_1 v_1^\varepsilon - \Phi_2^2 \tilde{k}_2 v_2^\varepsilon. \tag{3.12}$$

The boundary condition at the air-water interface becomes

$$\tilde{n}^\varepsilon \cdot (-\tilde{d}_2^\varepsilon \nabla v_2^\varepsilon)) = \varepsilon Bi^M\left(\frac{a^\varepsilon \beta_3}{b^\varepsilon \beta_2} v_3^\varepsilon - v_2^\varepsilon\right). \tag{3.13}$$

The mass balance equation for $H_2S(g)$ is

$$\beta_3 \partial_s v_3^\varepsilon + \beta_3 \mathrm{div}(-\tilde{d}_3^\varepsilon \nabla v_3^\varepsilon) = 0, \tag{3.14}$$

while the boundary condition at the air-water interface reads

$$\tilde{n}^\varepsilon \cdot (-\tilde{d}_3^\varepsilon \nabla v_3^\varepsilon)) = -\varepsilon Bi^M\left(\frac{a^\varepsilon}{b^\varepsilon} v_3^\varepsilon - \frac{\beta_2}{\beta_3} v_2^\varepsilon\right). \tag{3.15}$$

Finally, the mass-balance equation for moisture is

$$\beta_4 \partial_s v_4^\varepsilon + \beta_4 \gamma_4 \mathrm{div}(-\tilde{d}_4^\varepsilon \nabla v_4^\varepsilon) = \Phi_1^2 \tilde{k}_1 v_1^\varepsilon \tag{3.16}$$

and the ordinary differential equation for gypsum becomes

$$\beta_5 \partial_s v_5^\varepsilon = \Phi_3^2 \tilde{\eta}(v_1^\varepsilon, v_5^\varepsilon). \tag{3.17}$$

To simplify the notation, we drop all the tildes and keep the meaning of the unknowns and operators as mentioned in this section.

3.3 Asymptotic homogenization procedure

The key idea of this method is to guess the solution of the microscopic model using the asymptotic expansion (3.18) involving the macro (slow) variable x and the micro (fast) variable $y = \frac{x}{\varepsilon}$. In this section, we study the asymptotic behavior of the solutions to the microscopic model $\varepsilon \to 0$ for two parameter regimes reflecting two different types of diffusive-like transport of chemical species in concrete: "uniform" diffusion (see Section 3.3.1) and "structured" diffusion (see Section 3.3.2).

3.3.1 Case 1: Uniform diffusion

We consider that the diffusion speed is comparable for all concentrations, i.e. the diffusion coefficients d_k^ε are of order of $\mathcal{O}(1)$ w.r.t. ε for all $k \in \{1, 2, 3, 4\}$. To derive the limit problem in a formal way, we assume that the unknown solutions $v_i^\varepsilon(x, t), i \in \{1, 2, 3, 4, 5\}$ of the microscopic model admit the following asymptotic expansions with respect to ε

$$v_i^\varepsilon(x, t) = v_{i0}(x, y, t) + \varepsilon v_{i1}(x, y, t) + \varepsilon^2 v_{i2}(x, y, t) + \dots, \tag{3.18}$$

where $y = \frac{x}{\varepsilon}$ and the functions $v_{im}(x, y, t), m = 1, 2, 3, \dots$, are Y-periodic in y. If we define (compare [22, 35], e.g.)

$$\Psi_\varepsilon(x, t) := \Psi(x, \frac{x}{\varepsilon}, t),$$

then

$$\frac{\partial \Psi_\varepsilon}{\partial x_i} = \frac{\partial \Psi}{\partial x_i}(x, \frac{x}{\varepsilon}) + \frac{1}{\varepsilon}\frac{\partial \Psi}{\partial y_i}(x, \frac{x}{\varepsilon}). \tag{3.19}$$

We assume that $d_k^\varepsilon, k \in \{1, 2, 3, 4\}$ is $\varepsilon-$periodic and

$$d_k^\varepsilon(x) = d_k(\frac{x}{\varepsilon}),$$

where d_k is $1-$periodic. We investigate the asymptotic behavior of the solution $v_1^\varepsilon(x, t)$ as $\varepsilon \to 0$ of the following problem posed in the domain Ω_1^ε

$$
\begin{aligned}
\beta_1 \partial_s v_1^\varepsilon + \beta_1 \gamma_1 \text{div}(-d_1^\varepsilon \nabla v_1^\varepsilon) &= -\Phi_1^2 k_1^\varepsilon v_1^\varepsilon + \Phi_2^2 k_2^\varepsilon v_2^\varepsilon \ \text{ in } \ \Omega_1^\varepsilon, \\
n^\varepsilon \cdot (-d_1^\varepsilon \nabla v_1^\varepsilon)) &= -\varepsilon \frac{\Phi_3^2}{\gamma_1} \eta(v_1^\varepsilon, v_5^\varepsilon) \ \text{ on } \ \Gamma_1^\varepsilon, \\
n^\varepsilon \cdot (-d_1^\varepsilon \nabla v_1^\varepsilon)) &= 0 \ \text{ on } \ \Gamma_2^\varepsilon.
\end{aligned}
\tag{3.20}
$$

Using now the asymptotic expansion of the solution $v_1^\varepsilon(x, t)$ and the expansion of the normal vector (2.2) in (3.20) and collecting all the terms of order ε^{-2}, ε^{-1} and ε^0, we obtain:

$$
\begin{cases}
A_0 v_{10} = 0 \ \text{ in } \ Y_{1,x}, \\
v_{10} \ \ Y - \text{periodic in } \ y,
\end{cases}
\tag{3.21}
$$

where the operator A_0 is given by

$$A_0 := -\sum_{i,j=1}^{3} \frac{\partial}{\partial y_i}(d_1^{ij}\frac{\partial}{\partial y_j}),$$

where d_1^{ij} refers to the entry of the matrix d_1 in the ith row and jth column. As next step, we get

$$\begin{cases} A_0 v_{11} = -A_1 v_{10} \quad \text{in} \quad Y_{1,x}, \\ v_{11} \quad Y - \text{periodic in} \quad y, \\ (d_1\nabla_y v_{11}, \tilde{n}) = -(d_1\nabla_x v_{10}, \tilde{n}) \text{ on } \Gamma_{1,x} \cup \Gamma_{2,x}, \end{cases} \tag{3.22}$$

where

$$A_1 := -\sum_{i,j=1}^{3} \frac{\partial}{\partial x_i}(d_1^{ij}\frac{\partial}{\partial y_j}) - \sum_{i,j=1}^{3} \frac{\partial}{\partial y_i}(d_1^{ij}\frac{\partial}{\partial x_j}).$$

Furthermore, it holds that

$$\begin{aligned} \beta_1\gamma_1 A_0 v_{12} &= -\beta_1\gamma_1 A_1 v_{11} - \beta_1\gamma_1 A_2 v_{10} - \beta_1\partial_s v_{10} \\ &\quad - \Phi_1^2 k_1(y)v_{10} + \Phi_2^2 k_2(y)v_{20} \text{ in } Y_{1,x}, \\ &\quad v_{12} \quad Y - \text{periodic in} \quad y \end{aligned} \tag{3.23}$$

$$\begin{aligned} (d_1\nabla_y v_{12}, \tilde{n}) &= -(d_1\nabla_x v_{11}, \tilde{n}) - (d_1\nabla_x v_{10}, n') - (d_1\nabla_y v_{11}, n') \\ &\quad - \frac{\Phi_3^2}{\gamma_1}\eta(v_{10}, v_{50}) \text{ on } \Gamma_{1,x}, \end{aligned} \tag{3.24}$$

$$\begin{aligned} (d_1\nabla_y v_{12}, \tilde{n}) &= -(d_1\nabla_x v_{11}, \tilde{n}) - (d_1\nabla_x v_{10}, n') \\ &\quad - (d_1\nabla_y v_{11}, n') \text{ on } \Gamma_{2,x}, \end{aligned} \tag{3.25}$$

where

$$A_2 := -\sum_{i,j=1}^{3} \frac{\partial}{\partial x_i}(d_1^{ij}\frac{\partial}{\partial x_j}).$$

From (3.21), we obtain that v_{10} is independent of y. Since the elliptic equation for v_{11} [with right-hand side defined in terms of v_{10}] is linear, its solution can be represented in the following form

$$v_{11}(x, y, t) := -\sum_{k=1}^{3} \omega_1^k(x, y, t)\frac{\partial v_{10}(x,t)}{\partial x_k} + v_1(x, t),$$

where the functions $\omega_1^k(x, y, t)$ solve the cell problem(s) and are periodic w.r.t. y. The exact expression of v_1 does not matter much at this stage. Using the

expression of v_{11}, we obtain following cell problems in the standard manner:

$$A_0 \omega_1^k(x, y) = -\sum_{i=1}^{3} \frac{\partial}{\partial y_i} d_1^{ik}(y) \; k \in \{1, 2, 3\} \; \text{ in } \; Y_{1,x}, \qquad (3.26)$$

$$\sum_{i,j,k=1}^{3} \frac{\partial v_{10}}{\partial x_k} [d_1^{ij} \frac{\partial \omega_1^k}{\partial y_j} \tilde{n}_i - d_1^{jk} \tilde{n}_j] = 0 \; \text{ on } \; \Gamma_{1,x},$$

$$\sum_{i,j,k=1}^{3} \frac{\partial v_{10}}{\partial x_k} [d_1^{ij} \frac{\partial \omega_1^k}{\partial y_j} \tilde{n}_i - d_1^{jk} \tilde{n}_j] = 0 \; \text{ on } \; \Gamma_{2,x}.$$

In (3.26)n the cell function χ^k inherits the x-dependence from the perforation, and hence, instead of a standard periodic cell Y we now deal with with a x-dependent family of cells $Y_{1,x}$.

Since the right-hand side of (3.26) integrated over $Y_{1,x}$ is zero, this problem has a unique solution. Note also that (3.23) is leading to

$$\beta_1 \gamma_1 A_0 v_{12} = \beta_1 \gamma_1 [- \sum_{i,j,k=1}^{3} \frac{\partial v_{10}}{\partial x_k} \frac{\partial}{\partial y_i} (d_1^{ij} \frac{\partial \omega_1^k}{\partial x_j}) - \sum_{i,j,k=1}^{3} \frac{\partial^2 v_{10}}{\partial x_j \partial x_k} \frac{\partial}{\partial y_i} (d_1^{ij} \omega_1^k)$$

$$+ \sum_{i,j=1}^{3} \frac{\partial d_1^{ij}}{\partial y_i} \frac{\partial v_1}{\partial x_j} - \sum_{i,j,k=1}^{3} d_1^{ij} \frac{\partial^2 \omega_1^k}{\partial x_i \partial y_j} \frac{\partial v_{10}}{\partial x_k} - \sum_{i,j,k=1}^{3} d_1^{ij} \frac{\partial \omega_1^k}{\partial y_i} \frac{\partial^2 v_{10}}{\partial x_k \partial x_i}$$

$$+ \sum_{i,k=1}^{3} d_1^{ik} \frac{\partial^2 v_{10}}{\partial x_k \partial x_i}] - \beta_1 \partial_s v_{10} - \Phi_1^2 k_1(y) v_{10} + \Phi_2^2 k_2(y) v_{20}.$$

Moreover, we have

$$\beta_1 \gamma_1 (d_1 \nabla_y v_{12}, \tilde{n}) = \beta_1 \gamma_1 [\sum_{i,j,k=1}^{3} d_1^{ij} \frac{\partial v_{10}}{\partial x_k} \frac{\partial \omega_1^k}{\partial x_i} \tilde{n}_j - \frac{\Phi_3^2}{\gamma_1} \eta(v_{10}, v_{50}) - \sum_{i,j=1}^{3} d_1^{ij} \frac{\partial v_{10}}{\partial x_i} n'_j$$

$$+ \sum_{i,j,k=1}^{3} d_1^{ij} \frac{\partial^2 v_{10}}{\partial x_j \partial x_k} \omega_1^k \tilde{n}_j - \sum_{i,j=1}^{3} d_1^{ij} \frac{\partial v_1}{\partial x_i} \tilde{n}_j + \sum_{i,j,k=1}^{3} d_1^{ij} \frac{\partial \omega_1^k}{\partial x_i} \frac{\partial v_{10}}{\partial x_k} n'_j]. \quad (3.27)$$

Writing down the compatibility condition (see e.g. Lemma 2.1 in [120]), we get

$$\int_{Y_{1,x}} [\beta_1 \gamma_1 \{ \sum_{i,j,k=1}^{3} \frac{\partial v_{10}}{\partial x_k} \frac{\partial}{\partial y_i} (d_1^{ij} \frac{\partial \omega_1^k}{\partial x_j}) + \sum_{i,j,k=1}^{3} \frac{\partial^2 v_{10}}{\partial x_j \partial x_k} \frac{\partial}{\partial y_i} (d_1^{ij} \omega_1^k) - \sum_{i,j=1}^{3} \frac{\partial d_1^{ij}}{\partial y_i} \frac{\partial v_1}{\partial x_j}$$

$$+ \quad \sum_{i,j,k=1}^{3} d_1^{ij} \frac{\partial^2 \omega_1^k}{\partial x_i \partial y_j} \frac{\partial v_{10}}{\partial x_k} + \sum_{i,j,k=1}^{3} d_1^{ij} \frac{\partial \omega_1^k}{\partial y_i} \frac{\partial^2 v_{10}}{\partial x_k \partial x_i} - \sum_{i,j,k=1}^{3} d_1^{ij} \frac{\partial^2 v_{10}}{\partial x_j \partial x_i} \}$$

$$+ \quad \beta_1 \partial_s v_{10} + \Phi_1^2 k_1(y) v_{10} - \Phi_2^2 k_2(y) v_{20}] dy$$

$$= \quad \beta_1 \gamma_1 \int\limits_{\Gamma_{1,x} \cup \Gamma_{2,x}} \sum_{i,j,k=1}^{3} d_1^{ij} \frac{\partial v_{10}}{\partial x_k} \frac{\partial \omega_1^k}{\partial x_i} \tilde{n}_j d\gamma_y - \int\limits_{\Gamma_{1,x}} \frac{\Phi_3^2}{\gamma_1} \eta(v_{10}, v_{50}) d\gamma_y$$

$$+ \quad \beta_1 \gamma_1 \int\limits_{\Gamma_{1,x} \cup \Gamma_{2,x}} \left[\sum_{i,j,k=1}^{3} d_1^{ij} \frac{\partial^2 v_{10}}{\partial x_j \partial x_k} \omega_1^k \tilde{n}_j - \sum_{i,j=1}^{3} d_1^{ij} \frac{\partial v_{10}}{\partial x_i} n_j' \right] d\gamma_y$$

$$- \quad \beta_1 \gamma_1 \int\limits_{\Gamma_{1,x} \cup \Gamma_{2,x}} \left[\sum_{i,j=1}^{3} d_1^{ij} \frac{\partial v_1}{\partial x_i} \tilde{n}_j + \sum_{i,j,k=1}^{3} d_1^{ij} \frac{\partial \omega_1^k}{\partial x_i} \frac{\partial v_{10}}{\partial x_k} n_j' \right] d\gamma_y. \qquad (3.28)$$

We apply Stokes' theorem to the terms involving $\tilde{n}_j$ and, after straightforward calculations, we obtain

$$\beta_1 \partial_s v_{10} + \Phi_1^2 v_{10} \frac{1}{|Y_{1,x}|} \int\limits_{Y_{1,x}} k_1(y) dy - \Phi_2^2 v_{20} \frac{1}{|Y_{1,x}|} \int\limits_{Y_{1,x}} k_2(y) dy$$

$$- \beta_1 \gamma_1 \sum_{i,j,k=1}^{3} \frac{\partial^2 v_{10}}{\partial x_i \partial x_k} \langle d_1^{ij} \frac{\partial \omega_1^k}{\partial y_j} - d_1^{ik} \rangle - \beta_1 \gamma_1 \sum_{i,j,k=1}^{3} \langle d_1^{ij} \frac{\partial^2 \omega_1^k}{\partial x_i \partial y_j} \rangle \frac{\partial v_{10}}{\partial x_k}$$

$$= -\beta_1 \gamma_1 \sum_{i,j,k=1}^{3} \frac{\partial v_{10}}{\partial x_k} \frac{1}{|Y_{1,x}|} \int\limits_{\Gamma_{1,x} \cup \Gamma_{2,x}} (d_1^{kj} n_j' - d_1^{ij} \frac{\partial \chi^k}{\partial y_i} n_j') d\gamma_y$$

$$- \frac{\beta_1 \gamma_1}{\gamma_1} \Phi_3^2 v_{10} \frac{1}{|Y_{1,x}|} \int\limits_{\Gamma_{1,x}} v_{50}(x, y, t) k_3(y) d\gamma_y. \qquad (3.29)$$

In (3.29), we have $\langle f \rangle_V := \frac{1}{|V|} \int\limits_V f dx$ for any V a subset of either $Y_{1,x}$ or $Y_{2,x}$ and $|V|$ is the volume of V. The latter partial differential equation can be rewritten as

$$\beta_1 \partial_s v_{10} - \beta_1 \gamma_1 \sum_{i,j,k=1}^{3} \frac{\partial}{\partial x_i} (\langle d_1^{ij} \frac{\partial \omega_1^k}{\partial y_j} - d_1^{ik} \rangle \frac{\partial v_{10}}{\partial x_k}) + \Phi_1^2 v_{10} K_1 - \Phi_2^2 v_{20} K_2$$

$$= -\beta_1 \gamma_1 \sum_{k=1}^{3} \frac{\partial v_{10}}{\partial x_k} U_1^k - \beta_1 \Phi_3^2 v_{10} K_3 \quad \text{in } \Omega \times (0, T), \qquad (3.30)$$

where

$$K_\ell(x) \quad := \quad \frac{1}{|Y_{1,x}|} \int\limits_{Y_{1,x}} k_\ell(y) dy, \ \ell \in \{1, 2\}, \tag{3.31}$$

$$K_3(x) \quad := \quad \frac{1}{|Y_{1,x}|} \int\limits_{\Gamma_{1,x}} v_{50}(x, y, t) k_3(y) d\gamma_y, \tag{3.32}$$

and

$$U_1^k(x) := \frac{1}{|Y_{1,x}|} \sum_{i,j=1}^{3} \int\limits_{\Gamma_{1,x} \cup \Gamma_{2,x}} (d_1^{kj} n_j' - d_1^{ij} \frac{\partial \omega_1^k}{\partial y_i} n_j') d\gamma_y. \tag{3.33}$$

The terms U_1^{k2} are new. They occur due to the assumed deviation from a uniformly periodic distribution of perforations.

Now we apply the same procedure to the next mass-balance equation. To do this, we consider the auxiliary *cell problems*

$$A_0 \omega_2^k(x, y, t) = -\sum_{i=1}^{3} \frac{\partial}{\partial y_i} d_2^{ik}(y), \ k \in \{1, 2, 3\} \text{ in } Y_{1,x}, \tag{3.34}$$

$$\sum_{i,j,k=1}^{3} \frac{\partial v_{20}}{\partial x_k} [d_2^{ij} \frac{\partial \omega_2^k}{\partial y_j} \tilde{n}_i - d_2^{jk} \tilde{n}_j] = 0, \text{ on } \Gamma_{1,x},$$

$$\sum_{i,j,k=1}^{3} \frac{\partial v_{20}}{\partial x_k} [d_2^{ij} \frac{\partial \omega_2^k}{\partial y_j} \tilde{n}_i - d_2^{jk} \tilde{n}_j] = 0, \text{ on } \Gamma_{2,x},$$

whose solution is $\chi^k(x, y, t)$. We obtain the upscaled partial differential equation:

$$\beta_2 \partial_s v_{20} - \Phi_1^2 v_{10} k_1 + \Phi_2^2 v_{20} k_2 - \beta_2 \gamma_2 \sum_{i,j,k=1}^{3} \frac{\partial}{\partial x_i} (\langle d_2^{ij} \frac{\partial \omega_2^k}{\partial y_j} - d_2^{ik} \rangle \frac{\partial v_{20}}{\partial x_k})$$

$$= -\beta_2 \gamma_2 \sum_{k=1}^{3} \frac{\partial v_{20}}{\partial x_k} U_2^k - \beta_3 Bi^M v_{30} C + \beta_2 Bi^M v_{20} B, \tag{3.35}$$

holding in $\Omega \times (0, T)$ $v_{20} = 0$, on Γ, where

$$C(x) \quad := \quad \frac{1}{|Y_{1,x}|} \int\limits_{\Gamma_{2,x}} b(y) H(y) d\gamma_y, \tag{3.36}$$

---

[2]In [54], we do not specify the interfaces in the integral of extra terms in the homogenized system.

$$H(y) \quad := \quad \frac{a(y)}{b(y)}, \text{ with } y \in \Gamma_{2,x}, \tag{3.37}$$

$$B(x) \quad := \quad \frac{1}{|Y_{1,x}|} \int\limits_{\Gamma_{2,x}} b(y) d\gamma_y, \tag{3.38}$$

$$U_2^k(x) \quad := \quad \frac{1}{|Y_{1,x}|} \sum_{i,j=1}^{3} \int\limits_{\Gamma_{1,x} \cup \Gamma_{2,x}} (d_2^{kj} n_j' - d_2^{ij} \frac{\partial \omega_2^k}{\partial y_i} n_j') d\gamma_y. \tag{3.39}$$

We treat now the mass-balance equation for $H_2S(g)$. The corresponding *cell problems* are given by

$$A_0 \omega_3^k(x,y,t) = -\sum_{i=1}^{3} \frac{\partial}{\partial y_i} d_3^{ik}(y), \ k=1,2,3 \ \text{in} \ Y_{2,x},$$

$$\sum_{j,k=1}^{3} \frac{\partial v_{30}}{\partial x_k} [\sum_{i=1}^{3} d_3^{ij} \frac{\partial \omega_3^k}{\partial y_j} \tilde{n}_i - d_3^{jk} \tilde{n}_j] = 0 \ \text{on} \ \Gamma_{2,x},$$

while the macroscopic partial differential equation is

$$\partial_s v_{30} - \sum_{i,j,k=1}^{3} \frac{\partial}{\partial x_i} (\langle d_3^{ij} \frac{\partial \omega_3^k}{\partial y_j} - d_3^{ik} \rangle \frac{\partial v_{30}}{\partial x_k})$$

$$= -\sum_{k=1}^{3} \frac{\partial v_{30}}{\partial x_k} U_3^k + \beta_3 Bi^M v_{30} C - \beta_2 Bi^M v_{20} B \tag{3.40}$$

in $\Omega \times (0, T)$ with $v_{30} = v_{30}^D$ on Γ^D and $v_{30} = 0$ on Γ^N. Here we have

$$C(x) \quad := \quad \frac{1}{|Y_{2,x}|} \int\limits_{\Gamma_{2,x}} b(y) H(y) d\gamma_y, \quad B(x) := \frac{1}{|Y_{2,x}|} \int\limits_{\Gamma_{2,x}} b(y) d\gamma_y \tag{3.41}$$

$$U_3^k(x) \quad := \quad \frac{1}{|Y_{2,x}|} \sum_{i,j=1}^{3} \int\limits_{\Gamma_{2,x}} (d_3^{kj} n_j' - d_3^{ij} \frac{\partial \omega_3^k}{\partial y_i} n_j') d\gamma_y.. \tag{3.42}$$

Same procedure leads to

$$\beta_4 \partial_s v_{40} - \Phi_1^2 v_{10} k_1 - \beta_4 \gamma_4 \sum_{i,j,k=1}^{3} \frac{\partial}{\partial x_i} (\langle d_4^{ij} \frac{\partial \omega_4^k}{\partial y_j} - d_4^{ik} \rangle \frac{\partial v_{40}}{\partial x_k})$$

$$= -\beta_4 \gamma_4 \sum_{k=1}^{3} \frac{\partial v_{40}}{\partial x_k} U_4^k, \tag{3.43}$$

in $\Omega \times (0, T)$ with $v_{40} = 0$ on Γ and

$$U_4^k(x) \quad := \quad \frac{1}{|Y_{1,x}|} \sum_{i,j=1}^{3} \int\limits_{\Gamma_{1,x} \cup \Gamma_{2,x}} (d_4^{kj} n_j' - d_4^{ij} \frac{\partial \omega_4^k}{\partial y_i} n_j') d\gamma_y. \tag{3.44}$$

We also obtain following *cell problems*

$$A_0 \omega_4^k(x, y) = -\sum_{i=1}^{3} \frac{\partial}{\partial y_i} d_4^{ik}(y), \ k \in \{1, 2, 3\} \ \text{in} \ Y_{1,x}, \tag{3.45}$$

$$\sum_{i,j,k=1}^{3} \frac{\partial v_{40}}{\partial x_k} [d_4^{ij} \frac{\partial \omega_4^k}{\partial y_j} \tilde{n}_i - d_4^{jk} \tilde{n}_j] = 0, \ \text{on} \ \Gamma_{1,x},$$

$$\sum_{i,j,k=1}^{3} \frac{\partial v_{40}}{\partial x_k} [d_4^{ij} \frac{\partial \omega_4^k}{\partial y_j} \tilde{n}_i - d_4^{jk} \tilde{n}_j] = 0, \ \text{on} \ \Gamma_{2,x}.$$

Interestingly, the case of the ordinary differential equation for gypsum

$$\partial_s v_5^\varepsilon = \Phi_3^2 \eta(v_1^\varepsilon, v_5^\varepsilon) \ \text{on} \ \Gamma_{1,x}, \ s \in (0, T), \tag{3.46}$$

$$v_5^\varepsilon(x, 0) = v_{50}^\varepsilon(x), \tag{3.47}$$

seems to be more problematic. Let us firstly use the same homogenization ansatz as before and employ

$$\eta(v_1^\varepsilon, v_5^\varepsilon) = \eta_0^A(v_{10}(x, t), v_{50}(x, y, t)) + \mathcal{O}(\varepsilon).$$

We obtain

$$\partial_s v_{50}(x, y, t) = \Phi_3^2 \eta_0^A(v_{10}(x, t), v_{50}(x, y, t)) \ \text{with} \ y \in \Gamma_{1,x}, \tag{3.48}$$

$$v_{50}(x, y, 0) = v_{50}(x, y), \tag{3.49}$$

where $v_{50}(x, y, t)$ is periodic w.r.t y. Note that we can not obtain an expression for $v_{50}(x, y, t)$ that is independent of y. On the other hand, if we make another ansatz for v_5^ε, say

$$v_5^\varepsilon(x, t) = v_{50}(x, t) + \varepsilon v_{51}(x, y, t) + \varepsilon^2 v_{52}(x, y, t) + \dots, \tag{3.50}$$

then

$$\tilde{\eta}(v_1^\varepsilon, v_5^\varepsilon) = \eta_0^B(v_{10}(x, t), v_{50}(x, t)) + \mathcal{O}(\varepsilon)$$

and we obtain an averaged ordinary differential equation independent of y as given via

$$\partial_s v_{50}(x, t) = \Phi_3^2 \eta_0^B(v_{10}(x, t), v_{50}(x, t)), \tag{3.51}$$

$$v_{50}(x, 0) = v_{50}(x). \tag{3.52}$$

The advantage of the second choice is that it leads to the averaged reaction constant $\bar{k}_3 = \frac{1}{|\Gamma_{2,x}|} \int_{\Gamma_{2,x}} k_3(y) dy$, which is, in practice, much nicer than (3.48).

This raises the question: Which of the descriptions is correct: (3.48),(3.49) or (3.51), (3.52)? The Chapter 4 will shed light on this issue.

3.3.2   Case 2: Structured diffusion

In order to obtain distributed-microstructure models in the homogenized limit, it is necessary to consider diffusion coefficients scaled with certain power of the scale parameter ε. In this subsection, we take into account the fact that the diffusion of H_2S is much faster within the air-part of the pores than within the pore water. Particularly, we assume that d_3^ε is of order of $\mathcal{O}(1)$, while $d_k^\varepsilon = \mathcal{O}(\varepsilon^2)$ for all $k \in \{1, 2, 4\}$. Based on the existing literature, we expect that the latter assumption will finally lead to a distributed-microstructure model) for which the micro- and macro-structure need to be resolved simultaneously; see e.g. [49, 68, 87].

Assume the initial data to be given by $v_i^\varepsilon(x, 0) = v_i^0(x, \frac{x}{\varepsilon})$, $i \in \{1, 2, 3, 4, 5\}$ with functions $v_i^0 : \Omega \times Y \to \mathbb{R}$ being Y-periodic with respect to the second variable $y \in Y$. Assume also that $d_k^\varepsilon = \varepsilon^2 d_k$, for $k \in \{1, 2, 4\}$ and $d_3^\varepsilon = d_3$. We employ the same homogenization ansatz as before

$$v_i^\varepsilon(x, t) = w_{i0}(x, y, t) + \varepsilon w_{i1}(x, y, t) + \varepsilon^2 w_{i2}(x, y, t) + \dots \tag{3.53}$$

for all $i \in \{1, 2, 3, 4, 5\}$. Using the same strategy as in Section 3.3.1, we obtain

$$\beta_1 \partial_s w_{10}(x, y, t) - \beta_1 \gamma_1 \nabla_y \cdot (d_1 \nabla_y w_{10}(x, y, t))$$
$$= -k_1(y) w_{10}(x, y, t) + k_2(y) w_{20}(x, y, t) \tag{3.54}$$

in $\Omega \times Y_{1,x} \times (0, T)$. The boundary conditions become

$$\tilde{n}(x, y) \cdot (-d_1 \nabla_y w_{10}(x, y, t)) = 0 \quad \text{on} \quad \Omega \times \Gamma_{2,x} \times (0, T), \tag{3.55}$$

$$\tilde{n}(x, y) \cdot (-d_1 \nabla_y w_{10}(x, y, t)) = -\frac{\Phi_3^2}{\gamma_3} k_3(y) w_{10}(x, y, t) w_{50}(x, y, t) \tag{3.56}$$

on $\Omega \times \Gamma_{1,x} \times (0, T)$. Similarly,

$$\beta_2 \partial_s w_{20}(x, y, t) - \beta_2 \gamma_2 \nabla_y \cdot (d_2 \nabla_y w_{20}(x, y, t))$$
$$= k_1(y) w_{10}(x, y, t) - k_2(y) w_{20}(x, y, t) \text{ in } \Omega \times Y_{1,x} \times (0, T), \tag{3.57}$$

while the corresponding boundary conditions take the form

$$\tilde{n}(x, y) \cdot (-d_2 \nabla_y w_{20}(x, y, t)) = 0 \text{ on } \Omega \times \Gamma_{1,x} \times (0, T), \tag{3.58}$$

$$\tilde{n}(x, y) \cdot (-d_2 \nabla_y w_{20}(x, y, t)) = Bi^M b(y)[\frac{\beta_3}{\beta_2} H(y) w_{30}(x, t) - w_{20}(x, y, t)] \tag{3.59}$$

on $\Omega \times \Gamma_{2,x} \times (0, T)$. Since we consider $d_3^\varepsilon = d_3$, we obtain the same macroscopic partial differential equation as in Case 1:

$$\partial_s w_{30}(x, t) - \sum_{i,j,k=1}^{3} \frac{\partial}{\partial x_i}(\langle d_3^{ij} \frac{\partial \omega_3^k}{\partial y_j} - d_3^{ik} \rangle \frac{\partial w_{30}(x, t)}{\partial x_k}) = -\sum_{k=1}^{3} \frac{\partial w_{30}(x, t)}{\partial x_k} U_3^k$$

$$+ \frac{\beta_3 Bi^M w_{30}(x, t)}{|Y_{2,x}|} \int_{\Gamma_{2,x}} b(y) H(y) d\gamma_y - \frac{\beta_2 Bi^M}{|Y_{2,x}|} \int_{\Gamma_{2,x}} b(y) w_{20}(x, y, t) d\gamma_y$$

$$\tag{3.60}$$

in $x \in \Omega, s \in (0, T)$ and

$$w_{30}(x, t) = w_{30}^D(x, t) \ \text{on} \ \Gamma^D,$$

where

$$U_3^k(x) \quad := \quad \frac{1}{|Y_{2,x}|} \sum_{i,j=1}^{3} \int_{\Gamma_{2,x}} (d_1^{kj} n_j' - d_1^{ij} \frac{\partial \chi^k}{\partial y_i} n_j') d\gamma_y. \quad (3.61)$$

Next, we have

$$\beta_4 \partial_s w_{40}(x, y, t) - \beta_4 \gamma_4 \nabla_y . (d_4 \nabla_y w_{40}(x, y, t)) = k_1(y) w_{10}(x, y, t), \quad (3.62)$$

on $\Omega \times Y_1 \times (0, T)$, while the boundary conditions are now given by

$$\tilde{n}(x, y) \cdot (-d_4 \nabla_y w_{40}(x, y, t)) = 0 \ \text{on} \ \Omega \times \Gamma_{2,x} \times (0, T), \quad (3.63)$$
$$\tilde{n}(x, y) \cdot (-d_4 \nabla_y w_{40}(x, y, t)) = 0 \ \text{on} \ \Omega \times \Gamma_{1,x} \times (0, T). \quad (3.64)$$

The ordinary differential equation modelling gypsum growth takes finally the form

$$\beta_5 \partial_s w_{50}(x, y, t) = -\Phi_3^2 \eta(w_{10}(x, y, t) w_{50}(x, y, t)) \quad (3.65)$$

on $\Omega \times \Gamma_{1,x} \times (0, T)$.

3.4 Notes and comments

We performed the formal homogenization for locally-periodic domains and obtained two different upscaled models depending on the choice of the scaling parameter ε. To treat the ordinary differential equation posed at the boundary, we used two asymptotic expansions. We obtained some extra terms which pop up due to the locally-periodic assumption on the microstructure in the domain. The extra terms vanish due to the fact that the operators of the original and homogenized problem are self-adjoint and using the convergence of the corresponding bilinear forms, we obtain that the G-limit operator is self-adjoint, [30]. Here all the model parameters were assumed to be periodic. In case of the locally-periodic parameters, we expect that the same procedure is applicable without any additional difficulty.

At this point, the main issue is to justify rigorously these asymptotic behaviors of the concentrations. We address closely related aspects (focusing on uniformly periodic array of perforations) in forthcoming chapters.

At a later stage, we will need to perform extensive simulations for the distributed-microstructure model (3.54)–(3.65) for the case of fixed geometry. This should help understanding the long-time behavior of the concentrations for the case of *matched micro-macro transmission conditions* starting from regularized ones (with a large Biot number), see Chapter 7.

The asymptotic expansion method is based on the assumption of a periodic (or locally-periodic) structure and therefore the resulting equations may not be valid for an arbitrary non-periodic medium. In [63], the author generalized the asymptotic expansion from the periodic setting to stationary ergodic stochastic geometries. We aspect that a similar (formal) approach can also be used for our scenario.

To incorporate the concept of locally-periodic microstructures in our setting, we are very much inspired by Chechkin *et al.*, see [30, 31, 32] e.g. For the formal derivation, the connectedness of all constitutive parts of the microstructure does not matter much. Any periodic and locally-periodic microstructure with connected (or disconnected) parts can be considered.

It would be interesting to consider evolving microstructures. In this spirit, we could account for one of more of the following aspects:

1. The solid phase grows or shrinks due to precipitation or dissolution. In general, this results in changes of the shape of liquid phase.

2. The liquid phase grows or shrinks due to condensation or evaporation.

3. The liquid phase grows due to production of water by the chemical reaction (1.4).

4. The gypsum layer grows due to its volume expansion.

5. Different choices of scaling in ε of interfacial exchange.

For the formal homogenization of these types of systems of partial differential equations, we refer the reader to [121, 122, 123, 124] and the references cited therein.

Chapter 4

Derivation of the Two-scale Model

This chapter is devoted to a twofold aim: (i) the analysis of the microscopic model (2.16)–(2.22l) posed on a uniformly periodic domain and (ii) the derivation of the multiscale model stated in Theorem 4.5.1 by passing rigorously to the limit $\varepsilon \to 0$ in the microscopic model (2.16) – (2.22l). To deal with (ii), we apply the method of two-scale convergence by G. Nguestseng [106] and G. Allaire [8]. Our working technique combines the two-scale convergence method with basic properties of the periodic unfolding operator [34].

The chapter is organized as follows: In Section 4.1, we give the notations, functional spaces and the assumptions needed to perform the analysis. In Section 4.2, we show that the microscopic problem is well-posed. ε-independent *a priori* estimates for the solution to the microscopic problem are derived in Section 4.3. In Section 4.4, we extend the solution to the microscopic problem to the whole domain and introduce the central notion of two-scale convergence. In Section 4.5, we apply the procedure of two-scale convergence to derive upscaled equations together with explicit formulae for the effective diffusion coefficients and reaction constants. We conclude the section with the strong formulation of the upscaled system.

4.1   Geometry.   Microscopic model.   Notation. Function spaces. Weak formulation

4.1.1   Geometry

We refer the reader to Chapter 2 where we discussed possible choices of microstructures (periodic and locally-periodic). Here we focus only on periodic microstructures, see Fig 4.1. Note already at this stage that all the constituents (solid, water and air) are connected.

This chapter is built on the results published in [55] and on Appendix 8.2.3. This is a joint collaboration with A. Muntean (Eindhoven).
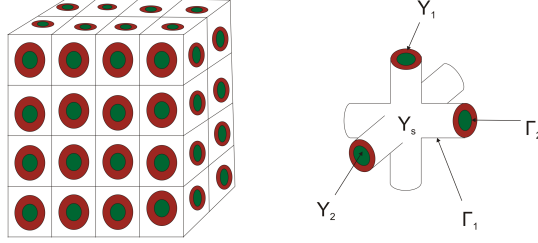
FIGURE 4.1: Left: Uniformly periodic array of microstructures. Right: The pore configuration.

4.1.2   Microscopic model equations

We consider the microscopic model given in Subsection 2.5.1.

4.1.3   Notation. Function spaces

Here φ^+ and φ^- refer to $\varphi^+ := \max\{0, \varphi\}, \varphi^- := -\min\{0, \varphi\}$, respectively. Note that $\varphi^+\varphi^- = 0$ and $\varphi^+ + \varphi^- = |\varphi|$. We denote by $C_\#^\infty(Y)$, $H_\#^1(Y)$, and $H_\#^1(Y)/\mathbb{R}$, the space of infinitely differentiable functions in $\mathbb{R}^n$ that are Y-periodic, the completion of $C_\#^\infty(Y)$ with respect to H^1-norm, and the respective quotient space. Furthermore, let

$$H_{\Gamma^D}^1(\Omega) := \{u \in H^1(\Omega) | u = 0 \text{ on } \Gamma^D\}.$$

The Sobolev space $H^\beta(\Omega)$ (β is a positive number, $\beta \in \mathbb{N}$) as a completion of $C_0^\infty(\Omega)$ is a Hilbert space equipped with the norm

$$\|\varphi\|_{H^\beta(\Omega)} := \|\varphi\|_{H^{[\beta]}(\Omega)} + \left(\int_\Omega \int_\Omega \frac{|\varphi(x) - \varphi(y)|^2}{|x - y|^{n + 2(\beta - [\beta])}} \mathrm{d}x dy \right)^{\frac{1}{2}}$$

and (cf. Theorem 5.7.7 in [77]) the embedding $H^\beta(\Omega) \hookrightarrow L^2(\Omega)$ is continuous. Since we deal here with an evolution problem, we use standard Bochner spaces like

$$L^2(0, T; H^1(\Omega)), L^2(0, T; L^2(\Omega)), L^2(0, T; H_{\Gamma^D}^1(\Omega)), \text{ and } L^2((0, T) \times \Omega; H_\#^1(Y)/\mathbb{R}).$$

For the analysis of the microscopic model, we employ frequently the following trace inequality for $\varepsilon-$dependent hypersurfaces Γ_1^ε: For $\varphi_\varepsilon \in H^1(\Omega^\varepsilon)$, there exists a constant C, which is independent of ε, such that

$$\varepsilon\|\varphi_\varepsilon\|_{L^2(\Gamma_\varepsilon)}^2 \leq C\left(\|\varphi_\varepsilon\|_{L^2(\Omega^\varepsilon)}^2 + \varepsilon^2 \|\nabla\varphi_\varepsilon\|_{L^2(\Omega^\varepsilon)}^2 \right). \tag{4.1}$$

The proof of (4.1) is given in Lemma 3 of [68] as well as in Lemma 2.7 of [91]. For a function $\varphi^\varepsilon \in H^\beta(\Omega^\varepsilon)$ with $\beta \in \left(\frac{1}{2}, 1\right)$, the inequality (4.1) refines into

$$\varepsilon \|\varphi_\varepsilon\|^2_{L^2(\Gamma_\varepsilon)} \leq C \left(\int\limits_{\Omega^\varepsilon} |\varphi_\varepsilon|^2 \mathrm{d}x + \varepsilon^{2\beta} \int\limits_{\Omega^\varepsilon} \int\limits_{\Omega^\varepsilon} \frac{|\varphi^\varepsilon(x) - \varphi^\varepsilon(y)|^2}{|x-y|^{n+2\beta}} \mathrm{d}x\mathrm{d}y \right). \qquad (4.2)$$

For the proof of (4.2), see [83].

The quantities like $Q, a, b, k_j, j \in \{1, 2, 3\}$ with superscript ∞ are the maximum of the $Q(u_5^\varepsilon), a^\varepsilon, b^\varepsilon, k_j^\varepsilon, j \in \{1, 2, 3\}$, while $a, b, k_j, j \in \{1, 2\}$ denote the minimum of the respective quantities. Constants are generically denoted by C and these may depend on the data of the problem but not on the solution. We always state explicitly whether C depends or not on the small parameter ε.

4.1.4 Restrictions on the data and parameters

We consider the following restrictions on the data and model parameters:

(A1) $d_i \in L^\infty(Y)^{3\times3}$, $(d_i(y)\xi, \xi) \geq d_{i0}|\xi|^2$ for $d_{i0} > 0$ and every $\xi \in \mathbb{R}^3$, $y \in Y$, $i \in \{1, 2, 3, 4\}$.

(A2) $\eta(\alpha, \beta) = k_3 R(\alpha)Q(\beta)$, where R is sub-linear and locally Lipschitz function with Lipschitz constant c_R, while Q is bounded and monotonically increasing. Furthermore, we assume

$$R(\alpha) := \begin{cases} \text{positive}, & \text{if } \alpha \geq 0, \\ 0, & \text{otherwise}, \end{cases} \qquad Q(\beta) := \begin{cases} \text{positive}, & \text{if } \beta < \beta_{\max}, \\ 0, & \text{otherwise}, \end{cases}$$

where $\beta_{\max} > 0$ represents the maximum amount of gypsum that can (locally) be produced.

(A3) $u_{i0} \in H^1(\Omega) \cap L^\infty_+(\Omega)$, $i \in \{1, 4\}$, $u_{j0} \in H^2(\Omega) \cap L^\infty_+(\Omega), j \in \{2, 3\}$, $u_{50} \in L^\infty_+(\Gamma_1)$.

(A4) The boundary mass transfer functions $a, b \in L^\infty(\Gamma_1), a, b > 0$ are assumed to satisfy $b(y)M_2 = a(y)M_3$ for a.e. $y \in \Gamma_1$. Furthermore,

$$\frac{k_1^\infty}{k_2} = \frac{M_2}{M_1} = \frac{k_1}{k_2^\infty} \text{ a.e. in } \Omega_1^\varepsilon$$

and $M_5 \geq k_3^\infty c_R Q^\infty M_1$ a.e. on Γ_1^ε. The constants M_1, M_2, M_3 and M_5 mentioned here are defined in (4.3).

(A5) $u_3^D \in H^2(0, T; H^1(\Omega_2^\varepsilon)) \cap L^\infty_+((0, T) \times \Omega_2^\varepsilon)$.

(A6) $k_3 \in L^\infty_+(\Gamma_1)$ and $k_j \in L^\infty_+(\bar{Y})$ for any $j \in \{1, 2\}$.

We also define the following constants

$$
\begin{aligned}
M_j &:= \|u_{j0}\|_{L^\infty(\Omega)} \ j \in \{1,4\}, \\
M_2 &:= \max\{\|u_{20}\|_{L^\infty(\Omega)}, \|u_{30}\|_{L^\infty(\Omega)}\}, \\
M_3 &:= \max\{M_2, \|u_{30}\|_{L^\infty(\Omega)}, \|u_3^D\|_{L^\infty(\Gamma^D)}\}, \\
M_5 &:= \max\{\|u_{50}\|_{L^\infty(\Gamma_1)}, \beta_{\max}\}.
\end{aligned}
\tag{4.3}
$$

$M_1, \ldots, M_5$ will play later on the role of essential supremum bounds on the active concentrations.

4.1.5   Weak formulation of the microscopic model

We start with defining the weak formulation of our system given in Section 2.5.1, see also Section 4.1.2.

Definition 4.1.1. Assume (A1) – (A6). We call the vector $u^\varepsilon = (u_1^\varepsilon, u_2^\varepsilon, u_3^\varepsilon, u_4^\varepsilon, u_5^\varepsilon)$, a weak solution to (2.16) – (2.22l) if $u_j^\varepsilon \in L^2(0,T;H^1(\Omega_1^\varepsilon))$, $\partial_t u_j^\varepsilon \in L^2((0,T) \times \Omega_1^\varepsilon)$, $j \in \{1,2,4\}$, $u_3^\varepsilon \in u_3^D + L^2(0,T;H^1_{\Gamma^D}(\Omega_2^\varepsilon))$, $\partial_t u_3^\varepsilon \in \partial_t u_3^D + L^2(0,T;L^2(\Omega_2^\varepsilon))$, $u_5^\varepsilon \in H^1(0,T;L^2(\Gamma_1^\varepsilon))$ and the following identities hold

$$
\int_0^T \int_{\Omega_1^\varepsilon} \left(\partial_t u_1^\varepsilon \varphi_1 + d_1^\varepsilon \nabla u_1^\varepsilon \nabla \varphi_1 + k_1^\varepsilon u_1^\varepsilon \varphi_1 - k_2^\varepsilon u_2^\varepsilon \varphi_1\right) \mathrm{d}x \mathrm{d}\tau = -\varepsilon \int_0^T \int_{\Gamma_1^\varepsilon} \eta^\varepsilon \varphi_1 \mathrm{d}\gamma_x \mathrm{d}\tau \tag{4.4}
$$

$$
\int_0^T \int_{\Omega_1^\varepsilon} \left(\partial_t u_2^\varepsilon \varphi_2 + d_2^\varepsilon \nabla u_2^\varepsilon \nabla \varphi_2 + k_1^\varepsilon u_1^\varepsilon \varphi_2 - k_2^\varepsilon u_2^\varepsilon \varphi_2\right) \mathrm{d}x \mathrm{d}\tau
$$

$$
= \varepsilon \int_0^T \int_{\Gamma_2^\varepsilon} (a^\varepsilon u_3^\varepsilon - b^\varepsilon u_2^\varepsilon) \varphi_2 \mathrm{d}\gamma_x \mathrm{d}\tau \tag{4.5}
$$

$$
\int_0^T \int_{\Omega_2^\varepsilon} \left(\partial_t u_3^\varepsilon \varphi_3 + d_3^\varepsilon \nabla u_3^\varepsilon \nabla \varphi_3\right) \mathrm{d}x \mathrm{d}\tau = -\varepsilon \int_0^T \int_{\Gamma_2^\varepsilon} (a^\varepsilon u_3^\varepsilon - b^\varepsilon u_2^\varepsilon) \varphi_3 \mathrm{d}\gamma_x \mathrm{d}\tau, \tag{4.6}
$$

$$
\int_0^T \int_{\Omega_1^\varepsilon} \left(\partial_t u_4^\varepsilon \varphi_4 + d_4^\varepsilon \nabla u_4^\varepsilon \nabla \varphi_4\right) \mathrm{d}x \mathrm{d}\tau = \int_0^T \int_{\Omega_1^\varepsilon} k_1^\varepsilon u_1^\varepsilon \varphi_4 \mathrm{d}x \mathrm{d}\tau, \tag{4.7}
$$

$$
\int_0^T \int_{\Gamma_1^\varepsilon} \partial_t u_5^\varepsilon \varphi_5 \mathrm{d}\gamma_x \mathrm{d}\tau = \int_0^T \int_{\Gamma_1^\varepsilon} \eta^\varepsilon \varphi_1 \mathrm{d}\gamma_x \mathrm{d}\tau, \tag{4.8}
$$

for all $\varphi_j \in L^2(0,T;H^1(\Omega_1^\varepsilon))$, $j \in \{1,2,4\}$, $\varphi_3 \in L^2(0,T;H^1_{\Gamma^D}(\Omega_2^\varepsilon))$ and $\varphi_5 \in L^2((0,T) \times \Gamma_1^\varepsilon)$.

4.2 Global solvability

In this section, we show that the microscopic model (2.16) – (2.22l) is well-posed.

4.2.1 Positivity and boundedness of microscopic solutions

We begin by showing the positivity of the solutions to (4.4) – (4.8).

Lemma 4.2.1. *(Positivity)* Assume (A1) – (A4), and let $t \in [0, T]$ be arbitrarily chosen. Then $u_i^\varepsilon(t) \geq 0$, $i \in \{1, 2, 4\}$ a.e. in Ω_1^ε, $u_3^\varepsilon(t) \geq 0$ a.e. Ω_2^ε and $u_5^\varepsilon(t) \geq 0$ a.e. on Γ_1^ε.

Proof. We test (4.4)-(4.7) with $\varphi = (-u_1^{\varepsilon-}, -u_2^{\varepsilon-}, -u_3^{\varepsilon-}, -u_4^{\varepsilon-}, -u_5^{\varepsilon-})$ element of the space $[L^2(0, T; H^1(\Omega_1^\varepsilon))]^2 \times L^2(0, T; H^1_{\Gamma^D}(\Omega_2^\varepsilon)) \times L^2(0, T; H^1(\Omega_1^\varepsilon)) \times L^2((0, T) \times \Gamma_1^\varepsilon)$. We obtain the following inequality

$$\frac{1}{2} \int_0^t \int_{\Omega_1^\varepsilon} \partial_t |u_1^{\varepsilon-}|^2 \mathrm{d}x\mathrm{d}t + d_{10} \int_0^t \int_{\Omega_1^\varepsilon} |\nabla u_1^{\varepsilon-}|^2 \mathrm{d}x\mathrm{d}\tau \leq -k_1 \int_0^t \int_{\Omega_1^\varepsilon} |u_1^{\varepsilon-}|^2 \mathrm{d}x\mathrm{d}\tau$$
$$+ k_2^\infty \int_0^t \int_{\Omega_1^\varepsilon} (u_1^{\varepsilon-}, u_2^{\varepsilon-}) \mathrm{d}x\mathrm{d}\tau - \varepsilon \int_0^t \int_{\Gamma_1^\varepsilon} (\eta^\varepsilon(u_1^\varepsilon, u_5^\varepsilon), -u_1^{\varepsilon-})_{\Gamma_1^\varepsilon} \mathrm{d}\gamma_x \mathrm{d}\tau, \tag{4.9}$$

where $k_1 := inf_{(0,T) \times \Omega_1^\varepsilon} |k_1^\varepsilon|$ and $k_2^\infty := sup_{(0,T) \times \Omega_1^\varepsilon} |k_2^\varepsilon|$. Note that the first term on the r.h.s. of (4.9) is negative, while the third term is zero because of (A2). We get

$$\int_0^t \int_{\Omega_1^\varepsilon} \partial_t |u_1^{\varepsilon-}|^2 \mathrm{d}x\mathrm{d}\tau + 2d_{10} \int_0^t \int_{\Omega_1^\varepsilon} |\nabla u_1^{\varepsilon-}|^2 \mathrm{d}x\mathrm{d}\tau \leq C \int_0^t \int_{\Omega_1^\varepsilon} \left(|u_1^{\varepsilon-}|^2 + |u_2^{\varepsilon-}|^2 \right) \mathrm{d}x\mathrm{d}\tau. \tag{4.10}$$

On the other hand, (4.5) leads to

$$\frac{1}{2} \int_0^t \int_{\Omega_1^\varepsilon} \partial_t |u_2^{\varepsilon-}|^2 \mathrm{d}x\mathrm{d}\tau + d_{20} \int_0^t \int_{\Omega_1^\varepsilon} |\nabla u_2^{\varepsilon-}|^2 \mathrm{d}x\mathrm{d}\tau \leq \frac{k_1^\infty}{2} \int_0^t \int_{\Omega_1^\varepsilon} \left(|u_1^{\varepsilon-}|^2 + |u_2^{\varepsilon-}|^2 \right) \mathrm{d}x\mathrm{d}\tau$$
$$+ \varepsilon a^\infty \int_0^t \int_{\Gamma_2^\varepsilon} u_2^{\varepsilon-} u_3^{\varepsilon-} \mathrm{d}\gamma_x \mathrm{d}\tau - \varepsilon b \int_0^t \int_{\Gamma_2^\varepsilon} |u_2^{\varepsilon-}|^2 \mathrm{d}\gamma_x \mathrm{d}\tau,$$

where $a^\infty := sup_{(0,T) \times \Gamma_2^\varepsilon} |a^\varepsilon|$ and $b := inf_{(0,T) \times \Gamma_2^\varepsilon} |b^\varepsilon|$. By the trace inequality (4.1), we get

$$\int_0^t \int_{\Omega_1^\varepsilon} \partial_t |u_2^{\varepsilon-}|^2 \mathrm{d}x\mathrm{d}t + (2d_{20} - C\varepsilon^2) \int_0^t \int_{\Omega_1^\varepsilon} |\nabla u_2^{\varepsilon-}|^2 \mathrm{d}x\mathrm{d}t$$

$$\leq C \int\limits_0^t \int\limits_{\Omega_1^\varepsilon} \left(|u_1^{\varepsilon-}|^2 + |u_2^{\varepsilon-}|^2\right) \mathrm{d}x\mathrm{d}t + C \int\limits_0^t \int\limits_{\Omega_2^\varepsilon} \left(|u_3^{\varepsilon-}|^2 + \varepsilon^2|\nabla u_3^{\varepsilon-}|^2\right)\mathrm{d}x\mathrm{d}t.$$

(4.11)

(4.6) leads to

$$\int\limits_0^t \int\limits_{\Omega_2^\varepsilon} \partial_t |u_3^{\varepsilon-}|^2 \mathrm{d}x\mathrm{d}t + (2d_{30} - C\varepsilon^2) \int\limits_0^t \int\limits_{\Omega_2^\varepsilon} |\nabla u_3^{\varepsilon-}|^2 \mathrm{d}x\mathrm{d}t \leq C \int\limits_0^t \int\limits_{\Omega_2^\varepsilon} |u_3^{\varepsilon-}|^2 \mathrm{d}x\mathrm{d}t$$

$$+ C \int\limits_0^t \int\limits_{\Omega_1^\varepsilon} \left(|u_2^{\varepsilon-}|^2 + \varepsilon^2|\nabla u_2^{\varepsilon-}|^2\right)\mathrm{d}x\mathrm{d}t,$$

(4.12)

while from (4.7), we see that

$$\int\limits_0^t \int\limits_{\Omega_1^\varepsilon} \partial_t |u_4^{\varepsilon-}|^2 \mathrm{d}x\mathrm{d}t + 2d_{40} \int\limits_0^t \int\limits_{\Omega_1^\varepsilon} |\nabla u_4^{\varepsilon-}|^2 \mathrm{d}x\mathrm{d}t \leq C \int\limits_0^t \int\limits_{\Omega_1^\varepsilon} \left(|u_1^{\varepsilon-}|^2 + |u_4^{\varepsilon-}|^2\right) \mathrm{d}x\mathrm{d}t.$$

(4.13)

We obtain from (4.8)

$$\int\limits_0^t \int\limits_{\Gamma_1^\varepsilon} \partial_t |u_5^{\varepsilon-}|^2 \mathrm{d}\gamma_x \mathrm{d}t = - \int\limits_0^t \int\limits_{\Gamma_1^\varepsilon} \eta^\varepsilon u_5^{\varepsilon-} \mathrm{d}\gamma_x \mathrm{d}t.$$

(4.14)

Adding up inequalities (4.10) – (4.14) and simplification gives

$$\int\limits_0^t \int\limits_{\Omega_1^\varepsilon} \partial_t (|u_1^{\varepsilon-}|^2 + |u_2^{\varepsilon-}|^2 + |u_4^{\varepsilon-}|^2) + \int\limits_0^t \int\limits_{\Omega_2^\varepsilon} \partial_t |u_3^{\varepsilon-}|^2 \mathrm{d}x\mathrm{d}t + 2d_{10} \int\limits_0^t \int\limits_{\Omega_1^\varepsilon} |\nabla u_1^{\varepsilon-}|^2$$

$$+ (2d_{20} - C\varepsilon^2) \int\limits_0^t \int\limits_{\Omega_1^\varepsilon} |\nabla u_2^{\varepsilon-}|^2 + (2d_{30} - C\varepsilon^2) \int\limits_0^t \int\limits_{\Omega_2^\varepsilon} |\nabla u_3^{\varepsilon-}|^2 + 2d_{40} \int\limits_0^t \int\limits_{\Omega_1^\varepsilon} |\nabla u_4^{\varepsilon-}|^2$$

$$+ \int\limits_0^t \int\limits_{\Gamma_1^\varepsilon} \partial_t |u_5^{\varepsilon-}|^2 \mathrm{d}\gamma_x \mathrm{d}t \leq C \int\limits_0^t \int\limits_{\Omega_1^\varepsilon} (|u_1^{\varepsilon-}|^2 + |u_2^{\varepsilon-}|^2 + |u_4^{\varepsilon-}|^2) + \int\limits_0^t \int\limits_{\Omega_2^\varepsilon} |u_3^{\varepsilon-}|^2 \mathrm{d}x\mathrm{d}t.$$

Choosing ε conveniently such that r.h.s. of above inequality is positive. Application of the Gronwall's inequality implies

$$\int\limits_{\Omega_1^\varepsilon} (|u_1^\varepsilon(t)^-|^2 + |u_2^\varepsilon(t)^-|^2 + |u_4^\varepsilon(t)^-|^2)\mathrm{d}x + \int\limits_0^t \int\limits_{\Omega_2^\varepsilon} |u_3^\varepsilon(t)^-|^2 \mathrm{d}x$$

$$\leq C \int\limits_{\Omega_1^\varepsilon} (|u_1^\varepsilon(0)^-|^2 + |u_2^\varepsilon(0)^-|^2 + |u_4^\varepsilon(0)^-|^2)\mathrm{d}x + \int\limits_0^t \int\limits_{\Omega_2^\varepsilon} |u_3^\varepsilon(0)^-|^2 \mathrm{d}x.$$

By the positivity of the initial data, we have the positivity of the weak solutions to the problem.

Next, we show that solution to (4.4) – (4.8) is bounded.

Lemma 4.2.2. *(Boundedness)* Assume (A1) – (A4). Then there exist constants such that $u_i^\varepsilon(t) \leq M_i$, $i \in \{1, 2\}$, $u_3^\varepsilon(t) \leq M_3$ a.e. in Ω_1^ε, $u_4^\varepsilon(t) \leq (t+1)M_4$ a.e. in Ω^ε and $u_5^\varepsilon(t) \leq M_5$ a.e. on Γ_ε^{ws} for arbitrarily $t \in [0, T]$.

*Proof.*We consider the test function

$$(\varphi_1, \varphi_2, \varphi_3, \varphi_4) = ((u_1^\varepsilon - M_1)^+, (u_2^\varepsilon - M_2)^+, (u_3^\varepsilon - M_3)^+, (u_4^\varepsilon - (t+1)M_4)^+),$$

where the constants M_i are defined in (4.3). By (4.4), we obtain:

$$\frac{1}{2}\int_0^t \int_{\Omega_1^\varepsilon} \partial_t |(u_1^\varepsilon - M_1)^+|^2 \mathrm{d}x\mathrm{d}t + d_{10}\int_0^t \int_{\Omega_1^\varepsilon} |\nabla(u_1^\varepsilon - M_1)^+|^2 \mathrm{d}x\mathrm{d}t + \varepsilon\int_0^t \int_{\Gamma_1^\varepsilon} \eta^\varepsilon (u_1^\varepsilon - M_1)^+ \mathrm{d}\gamma_x \mathrm{d}t$$

$$\leq -(k_1 M_1 - k_2^\infty M_2)\int_0^t \int_{\Omega_1^\varepsilon} (u_1^\varepsilon - M_1)^+ \mathrm{d}x\mathrm{d}t + C\int_0^t \int_{\Omega_1^\varepsilon} |(u_2^\varepsilon - M_2)^+|^2 \mathrm{d}x\mathrm{d}t.$$

Using (A2) and (A4), we get the estimate

$$\int_0^t \int_{\Omega_1^\varepsilon} \partial_t |(u_1^\varepsilon - M_1)^+|^2 \mathrm{d}x\mathrm{d}t \leq \quad C\int_0^t \int_{\Omega_1^\varepsilon} (|(u_1^\varepsilon - M_1)^+|^2 + |(u_2^\varepsilon - M_2)^+|^2)\mathrm{d}x\mathrm{d}t. \quad (4.15)$$

(4.5) in combination with (A4) gives that

$$\int_0^t \int_{\Omega_1^\varepsilon} \partial_t |(u_2^\varepsilon - M_2)^+|^2 \mathrm{d}x\mathrm{d}t + (2d_{20} - C\varepsilon^2)\int_0^t \int_{\Omega_1^\varepsilon} |\nabla(u_2^\varepsilon - M_2)^+|^2 \mathrm{d}x\mathrm{d}t$$

$$\leq C\int_0^t \int_{\Omega_1^\varepsilon} (|(u_1^\varepsilon - M_1)^+|^2 + |(u_2^\varepsilon - M_2)^+|^2)\mathrm{d}x\mathrm{d}t \quad\quad (4.16)$$

$$+ \int_0^t \int_{\Omega_2^\varepsilon} (|(u_3^\varepsilon - M_3)^+|^2 + \varepsilon^2 |\nabla(u_3^\varepsilon - M_3)^+|^2)\mathrm{d}x\mathrm{d}t.$$

By (4.6) and (A4), we obtain

$$\int_0^t \int_{\Omega_2^\varepsilon} \partial_t |(u_3^\varepsilon - M_3)^+|^2 \mathrm{d}x\mathrm{d}t + (2d_{30} - C\varepsilon^2)\int_0^t \int_{\Omega_2^\varepsilon} |\nabla(u_3^\varepsilon - M_3)^+|^2 \mathrm{d}x\mathrm{d}t$$

$$\leq C\int_0^t \int_{\Omega_2^\varepsilon} |(u_3^\varepsilon - M_3)^+|^2 \mathrm{d}x\mathrm{d}t + C\int_0^t \int_{\Omega_1^\varepsilon} (|u_2^\varepsilon - M_2)^+|^2 + |\nabla(u_2^\varepsilon - M_2)^+|^2)\mathrm{d}x\mathrm{d}t.$$

$$(4.17)$$

By (4.7), we get

$$
\int_0^t \int_{\Omega_1^\varepsilon} \partial_t |(u_4^\varepsilon - (t+1)M_4)^+|^2 \mathrm{d}x\mathrm{d}t + 2d_{40} \int_0^t \int_{\Omega_1^\varepsilon} |\nabla(u_4^\varepsilon - (t+1)M_4)^+|^2 \mathrm{d}x\mathrm{d}t
$$

$$
\leq C \int_0^t \int_{\Omega_1^\varepsilon} (|(u_1^\varepsilon - M_1)^+|^2 + |(u_4^\varepsilon - (t+1)M_4)^+|^2) \mathrm{d}x\mathrm{d}t. \tag{4.18}
$$

Adding up (4.15) – (4.18), we get

$$
\int_0^t \int_{\Omega_1^\varepsilon} \partial_t \left(|(u_1^\varepsilon - M_1)^+|^2 + |u_2^\varepsilon - M_2)^+|^2 + |(u_4^\varepsilon - (t+1)M_4)^+|^2 \right)
$$

$$
+ \int_0^t \int_{\Omega_2^\varepsilon} \partial_t |(u_3^\varepsilon - M_3)^+|^2 \mathrm{d}x\mathrm{d}t + (2d_{20} - C\varepsilon^2) \int_0^t \int_{\Omega_1^\varepsilon} |\nabla(u_2^\varepsilon - M_2)^+|^2 \mathrm{d}x\mathrm{d}t
$$

$$
+ (2d_{30} - C\varepsilon^2) \int_0^t \int_{\Omega_2^\varepsilon} |\nabla(u_3^\varepsilon - M_3)^+|^2 \mathrm{d}x\mathrm{d}t \leq C \int_0^t \int_{\Omega_2^\varepsilon} |(u_3^\varepsilon - M_3)^+|^2 \mathrm{d}x\mathrm{d}t
$$

$$
+ C \int_0^t \int_{\Omega_1^\varepsilon} (|(u_1^\varepsilon - M_1)^+|^2 + |(u_2^\varepsilon - M_2)^+|^2 + |(u_4^\varepsilon - (t+1)M_4)^+|^2) \mathrm{d}x\mathrm{d}t.
$$

Choosing ε small enough, then Gronwall's inequality yields the following estimate $u_j^\varepsilon(t) \leq M_j$, $j \in \{1, 2\}$ *a. e. in* Ω_1^ε, $u_3^\varepsilon(t) \leq M_3$, *a. e. in* Ω_2^ε $u_4^\varepsilon \leq (t+1)M_4$ a.e. in Ω_1^ε for all $t \in (0, T)$. Let us now point out the fact that the bound M_1 for u_1^ε also holds on Γ_1^ε; see Lemma 4.2.3 for this basic fact.

Claim 4.2.3. *If* $z \in H^1(\Omega) \cap L^\infty(\Omega)$, *then* $z \in L^\infty(\partial\Omega)$.

Proof of the Claim[1]. Let $z \in H^1(\Omega) \cap L^\infty(\Omega)$. Since the set of the restrictions to Ω of functions $C_0^\infty(\mathbb{R}^n)$ is dense in $H^1(\Omega)$, we consider a sequence of smooth functions $\{f_n\} \subset C_0^\infty(\overline{\Omega})$ such that $f_n \to z$ in $H^1(\Omega)$ and $\|f_n\|_{L^\infty(\Omega)} \leq \|z\|_{L^\infty(\Omega)}$. The trace theorem gives $f_n \to z$ in $L^2(\partial\Omega)$. So, there exists a subsequence $\{f_{n_i}\} \subset \{f_n\}$ converging pointwise, i.e., $f_{n_i}(x) \to z(x)$ for a.e $x \in \partial\Omega$. Therefore, $\|f_{ni}(x)\| \leq \|z\|_{L^\infty(\Omega)}$ and thus, $\|z\|_{L^\infty(\partial\Omega)} \leq \|z\|_{L^\infty(\Omega)}$.

By Lemma 4.3 and Claim 4.2.3, we see that u_1^ε is bounded on the interface Γ_ε^{sw}. Now testing (4.8) with $(u_5^\varepsilon - (t+1)M_5)^+$ and using the properties of R, Q, we derive

$$
\int_0^T \int_{\Gamma_1^\varepsilon} \left(\frac{1}{2} \partial_t |(u_5^\varepsilon - (t+1)M_5)^+|^2 + M_5(u_5^\varepsilon - (t+1)M_5)^+ \right) d\sigma_x \mathrm{d}\tau
$$

$$
\leq C \int_0^T \int_{\Gamma_1^\varepsilon} M_1(u_5^\varepsilon - (t+1)M_5)^+ d\sigma_x \mathrm{d}\tau,
$$

---

[1]Thanks are due to T. Aiki for showing us this proof.

$$\int\limits_0^T \int\limits_{\Gamma_1^\varepsilon} \partial_t |(u_5^\varepsilon - (t+1)M_5)^+|^2 d\sigma_x \mathrm{d}\tau \le -(M_5 - CM_1) \int\limits_0^T \int\limits_{\Gamma_1^\varepsilon} (u_5^\varepsilon - (t+1)M_5)^+ d\sigma_x \mathrm{d}\tau,$$

where $C := k_3^\infty c_R Q^\infty$. Using (A4) and Gronwall's inequality, we get $u_5^\varepsilon \le M_5$ a.e. in $(0,T) \times \Gamma_1^\varepsilon$.

4.2.2 Uniqueness and existence of solution to $(4.4) - (4.8)$

This subsection treats the uniqueness and global existence of the weak solutions to the system given in Section 2.5.1.

Proposition 4.2.4. *(Uniqueness)* Assume (A1)-(A6). Then there exists at most one weak solution in the sense of Definition 4.1.5.

Proof. We assume that $u^{j,\varepsilon} = (u_1^{j,\varepsilon}, u_2^{j,\varepsilon}, u_3^{j,\varepsilon}, u_4^{j,\varepsilon}, u_5^{j,\varepsilon}), j \in \{1,2\}$ are two distinct weak solutions in the sense of Definition 5.1.2 with same initial data. We set $u_i^\varepsilon := u_i^{1,\varepsilon} - u_i^{2,\varepsilon}$ for all $i \in \{1,2,3,4\}$. Firstly, we deal with (4.8). We obtain

$$\int\limits_0^t \int\limits_{\Gamma_1^\varepsilon} (\partial_t u_5^{1,\varepsilon} - \partial_t u_5^{2,\varepsilon}) \varphi_5 \mathrm{d}\gamma_x \mathrm{d}\tau = \int\limits_0^t \int\limits_{\Gamma_1^\varepsilon} \big(\eta^{1,\varepsilon}(u_1^{1,\varepsilon}, u_5^{1,\varepsilon}) - \eta^{2,\varepsilon}(u_1^{2,\varepsilon}, u_5^{2,\varepsilon})\big) \varphi_5 \mathrm{d}\gamma_x \mathrm{d}\tau.$$

$$(4.19)$$

Testing (4.19) with $u_5^{1,\varepsilon} - u_5^{2,\varepsilon}$ and making use of structure of η

$$\int\limits_0^t \int\limits_{\Gamma_1^\varepsilon} \partial_t |u_5^{1,\varepsilon} - u_5^{2,\varepsilon}|^2 \mathrm{d}\gamma_x \mathrm{d}\tau \le C \int\limits_0^t \int\limits_{\Gamma_1^\varepsilon} \big(|u_5^{1,\varepsilon} - u_5^{2,\varepsilon}|^2 + |u_1^{1,\varepsilon} - u_1^{2,\varepsilon}|^2\big) \mathrm{d}\gamma_x \mathrm{d}\tau.$$

Gronwall's inequality implies

$$\int\limits_{\Gamma_1^\varepsilon} |u_5^\varepsilon(t)|^2 \mathrm{d}\gamma_x \le C \int\limits_0^t \int\limits_{\Gamma_1^\varepsilon} |u_1^\varepsilon|^2 \mathrm{d}\gamma_x \mathrm{d}\tau \quad \text{for a.e. } t \in (0,T). \qquad (4.20)$$

We calculate

$$\frac{1}{2} \int\limits_0^t \int\limits_{\Omega_1^\varepsilon} \partial_t |u_1^\varepsilon|^2 \mathrm{d}x \mathrm{d}\tau + d_{10} \int\limits_0^t \int\limits_{\Omega_1^\varepsilon} |\nabla u_1^\varepsilon|^2 \mathrm{d}x \mathrm{d}\tau$$

$$\le -k_1 \int\limits_0^t \int\limits_{\Omega_1^\varepsilon} |u_1^\varepsilon|^2 \mathrm{d}x \mathrm{d}\tau + k_2^\infty \int\limits_0^t \int\limits_{\Omega_1^\varepsilon} u_1^\varepsilon u_2^\varepsilon \mathrm{d}x \mathrm{d}\tau - \varepsilon \int\limits_0^t \int\limits_{\Gamma_1^\varepsilon} (\eta^{1,\varepsilon} - \eta^{2,\varepsilon}) u_1^\varepsilon \mathrm{d}\gamma_x \mathrm{d}\tau.$$

We write

$$\int\limits_0^t \int\limits_{\Omega_1^\varepsilon} \partial_t |u_1^\varepsilon|^2 \mathrm{d}x \mathrm{d}\tau + 2d_{10} \int\limits_0^t \int\limits_{\Omega_1^\varepsilon} |\nabla u_1^\varepsilon|^2 \mathrm{d}x \mathrm{d}\tau + 2k_1 \int\limits_0^t \int\limits_{\Omega_1^\varepsilon} |u_1^\varepsilon|^2 \mathrm{d}x \mathrm{d}\tau$$

$$(4.21)$$

$$\le C \int\limits_0^t \int\limits_{\Omega_1^\varepsilon} (|u_1^\varepsilon|^2 + |u_2^\varepsilon|^2) \mathrm{d}x \mathrm{d}\tau + \varepsilon C \int\limits_0^t \int\limits_{\Gamma_1^\varepsilon} |u_5^\varepsilon|^2 \mathrm{d}\gamma_x \mathrm{d}\tau + \varepsilon C \int\limits_0^t \int\limits_{\Gamma_1^\varepsilon} |u_1^\varepsilon|^2 \mathrm{d}\gamma_x \mathrm{d}\tau.$$

Now, inserting (4.20) in (4.21) yields

$$\int_0^t \int_{\Omega_1^\varepsilon} \partial_t |u_1^\varepsilon|^2 \mathrm{d}x \mathrm{d}t + 2d_{10} \int_0^t \int_{\Omega_1^\varepsilon} |\nabla u_1^\varepsilon|^2 \mathrm{d}x \mathrm{d}\tau + 2k_1 \int_0^t \int_{\Omega_1^\varepsilon} |u_1^\varepsilon|^2 \mathrm{d}x \mathrm{d}\tau$$

$$\leq C \int_0^t \int_{\Omega_1^\varepsilon} (|u_1^\varepsilon|^2 + |u_2^\varepsilon|^2) \mathrm{d}x \mathrm{d}\tau + C\varepsilon \int_0^t \int_{\Gamma_1^\varepsilon} |u_1^\varepsilon|^2 \mathrm{d}\gamma_x \mathrm{d}\tau + \varepsilon C \int_0^t \int_0^\tau \int_{\Gamma_1^\varepsilon} |u_1^\varepsilon|^2 \mathrm{d}\gamma_x \mathrm{d}s \mathrm{d}\tau. \tag{4.22}$$

We estimate the last two terms in (4.22) to obtain the following inequality

$$\int_0^t \int_{\Omega_1^\varepsilon} \partial_t |u_1^\varepsilon|^2 \mathrm{d}x \mathrm{d}t + (2d_{10} - C\varepsilon^2) \int_0^t \int_{\Omega_1^\varepsilon} |\nabla u_1^\varepsilon|^2 \mathrm{d}x \mathrm{d}\tau + 2k_1 \int_0^t \int_{\Omega_1^\varepsilon} |u_1^\varepsilon|^2 \mathrm{d}x \mathrm{d}\tau \tag{4.23}$$

$$\leq C \int_0^t \int_{\Omega_1^\varepsilon} (|u_1^\varepsilon|^2 + |u_2^\varepsilon|^2) + C \int_0^t \int_0^\tau \int_{\Omega_1^\varepsilon} (|u_1^\varepsilon|^2 + \varepsilon^2 |\nabla u_1^\varepsilon|^2) \mathrm{d}x \mathrm{d}s \mathrm{d}\tau.$$

Following the same line of arguments as before, we obtain from (4.5) that

$$\int_0^t \int_{\Omega_1^\varepsilon} \partial_t |u_2^\varepsilon|^2 \mathrm{d}x \mathrm{d}t + (2d_{20} - C\varepsilon^2) \int_0^t \int_{\Omega_1^\varepsilon} |\nabla u_2^\varepsilon|^2 \mathrm{d}x \mathrm{d}\tau$$

$$\leq C \int_0^t \int_{\Omega_1^\varepsilon} (|u_1^\varepsilon|^2 + u_2^\varepsilon|^2) \mathrm{d}x \mathrm{d}\tau + C \int_0^t \int_{\Omega_2^\varepsilon} (|u_3^\varepsilon|^2 + \varepsilon^2 |\nabla u_3^\varepsilon|^2) \mathrm{d}x \mathrm{d}\tau,$$

while from (4.6), we deduce

$$\int_0^t \int_{\Omega_2^\varepsilon} \partial_t |u_3^\varepsilon|^2 \mathrm{d}x \mathrm{d}t + (2d_{30} - C\varepsilon^2) \int_0^t \int_{\Omega_2^\varepsilon} |\nabla u_3^\varepsilon|^2 \mathrm{d}x \mathrm{d}\tau \leq C \int_0^t \int_{\Omega_2^\varepsilon} |u_3^\varepsilon|^2 \mathrm{d}x \mathrm{d}\tau$$

$$+ C \int_0^t \int_{\Omega_1^\varepsilon} (|u_2^\varepsilon|^2 + \varepsilon^2 |\nabla u_2^\varepsilon|^2) \mathrm{d}x \mathrm{d}\tau. \tag{4.24}$$

Proceeding similarly, (4.7) yields

$$\int_0^t \int_{\Omega_1^\varepsilon} \partial_t |u_4^\varepsilon|^2 \mathrm{d}x \mathrm{d}\tau + 2d_{40} \int_0^t \int_{\Omega_1^\varepsilon} |\nabla u_4^\varepsilon|^2 \mathrm{d}x \mathrm{d}\tau \leq C \int_0^t \int_{\Omega_1^\varepsilon} (|u_1^\varepsilon|^2 + |u_4^\varepsilon|^2) \mathrm{d}x \mathrm{d}\tau. \tag{4.25}$$

Putting together (4.23) – (4.25) and re-arranging the terms, we get

$$\int_0^t \int_{\Omega_1^\varepsilon} \partial_t (|u_1^\varepsilon|^2 + |u_2^\varepsilon|^2 + |u_4^\varepsilon|^2) \mathrm{d}x \mathrm{d}\tau + (2d_{10} - C\varepsilon^2) \int_0^t \int_{\Omega_1^\varepsilon} |\nabla u_1^\varepsilon|^2 \mathrm{d}x \mathrm{d}\tau$$

$$+ (2d_{20} - C\varepsilon^2) \int\limits_0^t \int\limits_{\Omega_1^\varepsilon} |\nabla u_2^\varepsilon|^2 \mathrm{d}x\mathrm{d}\tau + \int\limits_0^t \int\limits_{\Omega_2^\varepsilon} \left(\partial_t |u_3^\varepsilon|^2 + (2d_{30} - C\varepsilon^2)|\nabla u_3^\varepsilon|^2 \right) \mathrm{d}x\mathrm{d}\tau$$

$$+ 2d_{40} \int\limits_0^t \int\limits_{\Omega_1^\varepsilon} |\nabla u_4^\varepsilon|^2 \mathrm{d}x\mathrm{d}\tau + 2k_1 \int\limits_0^t \int\limits_{\Omega_1^\varepsilon} |u_1^\varepsilon|^2 \mathrm{d}x\mathrm{d}\tau \le C \int\limits_0^t \int\limits_{\Omega_2^\varepsilon} |u_3^\varepsilon|^2 \mathrm{d}x\mathrm{d}\tau$$

$$+ C \int\limits_0^t \int\limits_{\Omega_1^\varepsilon} (|u_1^\varepsilon|^2 + u_2^\varepsilon|^2 + |u_4^\varepsilon|^2)\mathrm{d}x\mathrm{d}\tau + C \int\limits_0^t \int\limits_0^\tau \int\limits_{\Omega_1^\varepsilon} (|u_1^\varepsilon|^2 + \varepsilon^2 |\nabla u_1^\varepsilon|^2)\mathrm{d}x\mathrm{d}\tau \mathrm{d}s.$$

Let us choose ε such that the above inequality does not violate. Applying Gronwall's inequality with $k_1 > 0$, taking supremum along $t \in [0,T]$, we obtain the following estimate

$$\int\limits_{\Omega_1^\varepsilon} \left(|u_1^\varepsilon|^2 + |u_2^\varepsilon|^2 + |u_4^\varepsilon|^2 \right)\mathrm{d}x + C \int\limits_0^T \int\limits_{\Omega_1^\varepsilon} |\nabla u_1^\varepsilon|^2 \mathrm{d}x\mathrm{d}\tau + \int\limits_{\Omega_2^\varepsilon} |u_3^\varepsilon|^2 \mathrm{d}x \le 0.$$

Hence, we conclude that $u_i^{1,\varepsilon} = u_i^{2,\varepsilon}, i \in \{1, 2, 4\}$ a.e. $t \in (0,T)$ in Ω_1^ε and $u_3^{1,\varepsilon} = u_3^{2,\varepsilon}$ a.e. $t \in (0,T)$ in Ω_2^ε. Consequently, (4.20) gives $u_5^{1,\varepsilon} = u_5^{1,\varepsilon}$ a.e. $t \in (0,T)$ on Γ_1^ε.

Theorem 4.2.5. *(Global existence)* Assume $(A1) - (A6)$. Then there exists at least a global-in-time weak solution in the sense of Definition 4.1.5.

Proof. For the proof of this Theorem, see Appendix 8.2.3.

4.3 ε-independent estimates

Here, we derive *a priori* estimates for the sequence of solution to the problem (4.4) – (4.8).

Lemma 4.3.1. *(A priori* estimates) Assume $(A1) - (A6)$. Then the solution to microscopic problem (4.4) -(4.8) satisfies the following *a priori* estimates

$$\| u_j^\varepsilon \|_{L^2(0,T;L^2(\Omega^\varepsilon))} + \| \nabla u_j^\varepsilon \|_{L^2(0,T;L^2(\Omega^\varepsilon))} \le C, \text{ for } j \in \{1, 2, 4\}$$
$$\| u_3^\varepsilon \|_{L^2(0,T;L^2(\Omega_1^\varepsilon))} + \| \nabla u_3^\varepsilon \|_{L^2(0,T;L^2(\Omega_1^\varepsilon))} \le C,$$
$$\sqrt{\varepsilon} \, \| u_5^\varepsilon \|_{L^\infty((0,T)\times\Gamma_1^\varepsilon)} + \sqrt{\varepsilon} \, \| \partial_t u_5^\varepsilon \|_{L^2((0,T)\times\Gamma_1^\varepsilon)} \le C.$$

Proof. We test (4.4) with $\varphi_1 = u_1^\varepsilon$ to get

$$\int\limits_0^t \int\limits_{\Omega_1^\varepsilon} \partial_t |u_1^\varepsilon|^2 \mathrm{d}x\mathrm{d}\tau + 2d_{10} \int\limits_0^t \int\limits_{\Omega_1^\varepsilon} |\nabla u_1^\varepsilon|^2 \mathrm{d}x\mathrm{d}\tau \le k_2^\infty \int\limits_0^t \int\limits_{\Omega_1^\varepsilon} u_1^\varepsilon u_2^\varepsilon \mathrm{d}x\mathrm{d}\tau - \varepsilon \int\limits_0^t \int\limits_{\Gamma_1^\varepsilon} \eta^\varepsilon u_1^\varepsilon \mathrm{d}\gamma_x \mathrm{d}\tau,$$

$$\le C \int\limits_0^t \int\limits_{\Omega_1^\varepsilon} (|u_1^\varepsilon|^2 + |u_2^\varepsilon|^2)\mathrm{d}x\mathrm{d}\tau + \varepsilon C \int\limits_0^t \int\limits_{\Gamma_1^\varepsilon} |u_1^\varepsilon|^2 \mathrm{d}\gamma_x \mathrm{d}\tau.$$

$$(4.26)$$

Here we have used the structure of η and the properties of R and Q.

After applying the trace inequality (4.1) to the last term on r.h.s. of (4.26), we get

$$\int\limits_0^t \int\limits_{\Omega_1^\varepsilon} \partial_t |u_1^\varepsilon|^2 \mathrm{d}x \mathrm{d}\tau + (2d_{10} - C\varepsilon^2) \int\limits_0^t \int\limits_{\Omega_1^\varepsilon} |\nabla u_1^\varepsilon|^2 \mathrm{d}x \mathrm{d}\tau \le C \int\limits_0^t \int\limits_{\Omega_1^\varepsilon} (|u_1^\varepsilon|^2 + |u_2^\varepsilon|^2) \mathrm{d}x \mathrm{d}\tau.$$

(4.27)

Taking $\varphi_2 = u_2^\varepsilon$ in (4.5), we get

$$\int\limits_0^t \int\limits_{\Omega_1^\varepsilon} \partial_t |u_2^\varepsilon|^2 \mathrm{d}x \mathrm{d}\tau + 2d_{20} \int\limits_0^t \int\limits_{\Omega_1^\varepsilon} |\nabla u_2^\varepsilon|^2 \mathrm{d}x \mathrm{d}\tau \le 2k_1^\infty \int\limits_0^t \int\limits_{\Omega_1^\varepsilon} (|u_1^\varepsilon|^2 + |u_2^\varepsilon|^2) \mathrm{d}x \mathrm{d}\tau$$

$$+ \varepsilon C \int\limits_0^t \int\limits_{\Gamma_2^\varepsilon} u_3^\varepsilon u_2^\varepsilon \mathrm{d}\gamma_x \mathrm{d}\tau + \varepsilon C \int\limits_0^t \int\limits_{\Gamma_2^\varepsilon} |u_2^\varepsilon|^2 \mathrm{d}\gamma_x \mathrm{d}\tau.$$

Application of (4.1) leads to

$$\int\limits_0^t \int\limits_{\Omega_1^\varepsilon} \partial_t |u_2^\varepsilon|^2 \mathrm{d}x \mathrm{d}\tau + (2d_{20} - C\varepsilon^2) \int\limits_0^t \int\limits_{\Omega_1^\varepsilon} |\nabla u_2^\varepsilon|^2 \mathrm{d}x \mathrm{d}\tau$$

$$\le C \int\limits_0^t \int\limits_{\Omega_1^\varepsilon} (|u_1^\varepsilon|^2 + |u_2^\varepsilon|^2) \mathrm{d}x \mathrm{d}\tau + C \int\limits_0^t \int\limits_{\Omega_2^\varepsilon} (|u_3^\varepsilon|^2 + \varepsilon^2 |\nabla u_2^\varepsilon|^2) \mathrm{d}x \mathrm{d}t.$$

(4.28)

We choose $\varphi_3 = u_3^\varepsilon$ as a test function in (4.6) to calculate

$$\int\limits_0^t \int\limits_{\Omega_2^\varepsilon} \partial_t |u_3^\varepsilon|^2 \mathrm{d}x \mathrm{d}\tau + (2d_{30} - C\varepsilon^2) \int\limits_0^t \int\limits_{\Omega_2^\varepsilon} |\nabla u_3^\varepsilon|^2 \mathrm{d}x \mathrm{d}\tau$$

$$\le C \int\limits_0^t \int\limits_{\Omega_2^\varepsilon} |u_3^\varepsilon|^2 \mathrm{d}x \mathrm{d}\tau + C \int\limits_0^t \int\limits_{\Omega_1^\varepsilon} (|u_2^\varepsilon|^2 + \varepsilon^2 |\nabla u_2^\varepsilon|^2) \mathrm{d}x \mathrm{d}\tau.$$

(4.29)

Setting $\varphi_4 = u_4^\varepsilon$ in (4.7), we are led to

$$\int\limits_0^t \int\limits_{\Omega_1^\varepsilon} \partial_t |u_4^\varepsilon|^2 \mathrm{d}x \mathrm{d}\tau \quad + 2d_{40} \int\limits_0^t \int\limits_{\Omega_1^\varepsilon} |\nabla u_4^\varepsilon|^2 \mathrm{d}x \mathrm{d}\tau \le C \int\limits_0^t \int\limits_{\Omega_1^\varepsilon} (|u_1^\varepsilon|^2 + |u_4^\varepsilon|^2) \mathrm{d}x \mathrm{d}\tau. \quad (4.30)$$

Putting together (4.27) – (4.30), we obtain

$$\int\limits_0^t \int\limits_{\Omega_1^\varepsilon} \partial_t \left(|u_1^\varepsilon|^2 + |u_2^\varepsilon|^2 + |u_4^\varepsilon|^2\right) \mathrm{d}x \mathrm{d}\tau + \int\limits_0^t \int\limits_{\Omega_2^\varepsilon} \partial_t |u_3^\varepsilon|^2 \mathrm{d}x \mathrm{d}\tau + (2d_{20} - C\varepsilon^2) \int\limits_0^t \int\limits_{\Omega_1^\varepsilon} |\nabla u_2^\varepsilon|^2 \mathrm{d}x \mathrm{d}\tau$$

$$+ (2d_{10} - C\varepsilon^2) \int\limits_0^t \int\limits_{\Omega_1^\varepsilon} |\nabla u_1^\varepsilon|^2 \mathrm{d}x \mathrm{d}\tau + (2d_{30} - C\varepsilon^2) \int\limits_0^t \int\limits_{\Omega_2^\varepsilon} |\nabla u_3^\varepsilon|^2 \mathrm{d}x \mathrm{d}\tau + 2d_{40} \int\limits_0^t \int\limits_{\Omega_1^\varepsilon} |\nabla u_4^\varepsilon|^2 \mathrm{d}x \mathrm{d}\tau$$

(4.31)

$$\leq C \int\limits_0^t \int\limits_{\Omega_1^\varepsilon} (|u_1^\varepsilon|^2 + |u_2^\varepsilon|^2 + |u_4^\varepsilon|^2)\mathrm{d}x\mathrm{d}\tau + C \int\limits_0^t \int\limits_{\Omega_2^\varepsilon} |u_3^\varepsilon|^2 \mathrm{d}x\mathrm{d}\tau.$$

Choosing ε small enough and applying Gronwall's inequality, we have for $j \in \{1, 2, 4\}$

$$\| u_j^\varepsilon \|_{L^\infty(0,T;L^2(\Omega^\varepsilon))} \leq C, \quad \|u_3^\varepsilon\|_{L^\infty(0,T;L^2(\Omega_1^\varepsilon))} \leq C, \tag{4.32}$$

$$\| \nabla u_j^\varepsilon \|_{L^2(0,T;L^2(\Omega^\varepsilon))} \leq C, \quad \|\nabla u_3^\varepsilon\|_{L^2(0,T;L^2(\Omega_1^\varepsilon))} \leq C \tag{4.33}$$

We set as a test function $\varphi_5 = u_5^\varepsilon$ in (4.8)

$$\frac{\varepsilon}{2} \int\limits_0^t \int\limits_{\Gamma_1^\varepsilon} \partial_t |u_5^\varepsilon|^2 \mathrm{d}\gamma_x \mathrm{d}\tau \leq \varepsilon C \int\limits_0^t \int\limits_{\Gamma_1^\varepsilon} u_1^\varepsilon u_5^\varepsilon \mathrm{d}\gamma_x \mathrm{d}\tau,$$

$$\varepsilon \int\limits_0^t \int\limits_{\Gamma_1^\varepsilon} \partial_t |u_5^\varepsilon|^2 \mathrm{d}\gamma_x \mathrm{d}\tau \leq \varepsilon C \int\limits_0^t \int\limits_{\Gamma_1^\varepsilon} (|u_1^\varepsilon|^2 + |u_5^\varepsilon|^2)\mathrm{d}\gamma_x \mathrm{d}\tau.$$

Applying Gronwall's inequality together with (4.1), we obtain

$$\varepsilon \int\limits_{\Gamma_1^\varepsilon} |u_5^\varepsilon(t)|^2 \mathrm{d}\gamma_x \leq C \int\limits_0^t \int\limits_{\Omega_1^\varepsilon} (|u_1^\varepsilon|^2 + \varepsilon^2 |\nabla u_1^\varepsilon|^2)\mathrm{d}x\mathrm{d}\tau + C \int\limits_{\Gamma_1^\varepsilon} |u_5^\varepsilon(0)|^2 \mathrm{d}\gamma_x.$$

Hence by (4.32) and (4.33), $\varepsilon\|u_5^\varepsilon\|_{L^\infty((0,T)\times\Gamma_1^\varepsilon)} \leq C$. We take $\varphi_5 = \partial_t u_5^\varepsilon$ in (4.8) as a test function

$$\varepsilon \int\limits_0^t \int\limits_{\Gamma_1^\varepsilon} |\partial_t u_5^\varepsilon|^2 \mathrm{d}\gamma_x \mathrm{d}\tau \leq \varepsilon C \int\limits_0^t \int\limits_{\Gamma_1^\varepsilon} u_1^\varepsilon \partial_t u_5^\varepsilon \mathrm{d}\gamma_x \mathrm{d}\tau,$$

$$\varepsilon(1 - C\delta) \int\limits_0^t \int\limits_{\Gamma_1^\varepsilon} |\partial_t u_5^\varepsilon|^2 \mathrm{d}\gamma_x \mathrm{d}\tau \leq C \int\limits_0^t \int\limits_{\Omega_\varepsilon} (|u_1^\varepsilon|^2 + \varepsilon^2 |\nabla u_1^\varepsilon|^2)\mathrm{d}x\mathrm{d}\tau.$$

For convenient δ and by (4.32) and (4.33), we have

$$\varepsilon \| \partial_t u_5^\varepsilon \|_{L^2((0,T)\times\Gamma_1^\varepsilon)} \leq C. \tag{4.34}$$

Now we proceed with additional *a priori* estimates for the sequence of solutions defined in the domain and on the boundary.

Lemma 4.3.2. Assume (A1) – (A6). The following ε-independent bounds hold:

$$\| \nabla \partial_t u_2^\varepsilon \|_{L^2(0,T;L^2(\Omega^\varepsilon))} + \| \nabla \partial_t u_3^\varepsilon \|_{L^2(0,T;L^2(\Omega_1^\varepsilon))} \leq C, \tag{4.35}$$

$$\| \partial_t u_j^\varepsilon \|_{L^2(0,T;L^2(\Omega^\varepsilon))} + \| \partial_t u_3^\varepsilon \|_{L^2(0,T;L^2(\Omega_1^\varepsilon))} \leq C, \tag{4.36}$$

for $j \in \{1, 2, 4\}$ and C is a generic constant independent of ε.

Proof. Now, we focus on obtaining $\varepsilon-$independent estimates on the time derivative of the concentrations. Firstly, we choose $\varphi_1 = \partial_t u_1^\varepsilon$. We get

$$\int_0^t \int_{\Omega^\varepsilon} \partial_t u_1^\varepsilon \partial_t u_1^\varepsilon \mathrm{d}x \mathrm{d}\tau + \int_0^t \int_{\Omega^\varepsilon} d_1^\varepsilon \nabla u_1^\varepsilon \nabla \partial_t u_1^\varepsilon \mathrm{d}x \mathrm{d}\tau$$

$$= -\int_0^t \int_{\Omega^\varepsilon} k_1^\varepsilon u_1^\varepsilon \partial_t u_1^\varepsilon \mathrm{d}x \mathrm{d}\tau + \int_0^t \int_{\Omega^\varepsilon} k_2^\varepsilon u_2^\varepsilon \partial_t u_1^\varepsilon \mathrm{d}x \mathrm{d}\tau - \varepsilon \int_0^t \int_{\Gamma_1^\varepsilon} \eta^\varepsilon \partial_t u_1^\varepsilon \mathrm{d}\gamma_x \mathrm{d}\tau.$$

$$(1 - C\delta) \int_0^t \int_{\Omega^\varepsilon} |\partial_t u_1^\varepsilon|^2 \mathrm{d}x \mathrm{d}\tau + d_{10} \int_{\Omega^\varepsilon} |\nabla u_1^\varepsilon|^2 \mathrm{d}x \leq d_{10} \int_{\Omega^\varepsilon} |\nabla u_1^\varepsilon(0)|^2 \mathrm{d}x$$

$$+ C \int_0^t \int_{\Omega^\varepsilon} (|u_1^\varepsilon|^2 + |u_2^\varepsilon|^2) \mathrm{d}x \mathrm{d}\tau - \varepsilon \int_0^t \int_{\Gamma_1^\varepsilon} \eta^\varepsilon \partial_t u_1^\varepsilon \mathrm{d}\gamma_x \mathrm{d}\tau.$$

$$(4.37)$$

The last term in (4.37) can be estimated as follows:

$$|\varepsilon \int_0^t \int_{\Gamma_1^\varepsilon} \eta^\varepsilon \partial_t u_1^\varepsilon \mathrm{d}\gamma_x \mathrm{d}\tau| = |\varepsilon \int_0^t \int_{\Gamma_1^\varepsilon} k_3^\varepsilon R(u_1^\varepsilon) Q(u_5^\varepsilon) \partial_t u_1^\varepsilon \mathrm{d}\gamma_x \mathrm{d}\tau|$$

$$= |\varepsilon \int_0^t \int_{\Gamma_1^\varepsilon} k_3^\varepsilon \partial_t (\int_0^{u_1^\varepsilon} R(\alpha) d\alpha Q(u_5^\varepsilon)) \mathrm{d}\gamma_x \mathrm{d}\tau - \varepsilon \int_0^t \int_{\Gamma_1^\varepsilon} k_3^\varepsilon (\int_0^{u_1^\varepsilon} R(\alpha) d\alpha) \partial_{u_5^\varepsilon} Q(u_5^\varepsilon)) \partial_t u_5^\varepsilon \mathrm{d}\gamma_x \mathrm{d}\tau|,$$

$$\leq \varepsilon C \int_{\Gamma_1^\varepsilon} |u_1^\varepsilon(t)|^2 \mathrm{d}\gamma_x + \varepsilon C \int_{\Gamma_1^\varepsilon} |u_1^\varepsilon(0)|^2 \mathrm{d}\gamma_x + \varepsilon C \int_0^t \int_{\Gamma_1^\varepsilon} |u_1^\varepsilon|^2 |\partial_t u_5^\varepsilon| \mathrm{d}\gamma_x \mathrm{d}\tau$$

By Claim 4.2.3, u_1^ε is bounded on Γ_1^ε

$$\varepsilon |\int_0^t \int_{\Gamma_1^\varepsilon} \eta^\varepsilon \partial_t u_1^\varepsilon \mathrm{d}\gamma_x \mathrm{d}\tau| \leq C + C sup_{[0,T]} \int_{\Omega^\varepsilon} (|u_1^\varepsilon(t)|^2 + \varepsilon^2 |\nabla u_1^\varepsilon(t)|^2) \mathrm{d}x + C \int_{\Omega^\varepsilon} (|u_1^\varepsilon(0)|^2$$

$$+ \varepsilon^2 |\nabla u_1^\varepsilon(0)|^2) \mathrm{d}x + C sup_{[0,T]} \int_{\Omega^\varepsilon} (|u_1^\varepsilon|^2 + \varepsilon^2 |\nabla u_1^\varepsilon|^2) \mathrm{d}x + \varepsilon C \int_0^t \int_{\Gamma_1^\varepsilon} |\partial_t u_5^\varepsilon|^2 \mathrm{d}\gamma_x \mathrm{d}\tau,$$

$$(4.38)$$

Combine (4.38) in (4.37) and then choose $\delta > 0$ conveniently. Using Lemma 4.3, and taking supremum over the time variable, we get

$$\int_0^T \int_{\Omega^\varepsilon} |\partial_t u_1^\varepsilon|^2 \mathrm{d}x \mathrm{d}\tau + d_{10} sup_{[0,T]} \int_{\Omega^\varepsilon} |\nabla u_1^\varepsilon|^2 \mathrm{d}x \leq C.$$

Testing (4.5) with $\varphi_2 = \partial_t u_2^\varepsilon$ gives

$$\int_0^t \int_{\Omega_1^\varepsilon} |\partial_t u_2^\varepsilon|^2 \mathrm{d}x \mathrm{d}\tau + \frac{d_{20}}{2} \int_{\Omega_1^\varepsilon} |\nabla u_2^\varepsilon|^2 \mathrm{d}x \leq \frac{d_{20}}{2} \int_{\Omega_1^\varepsilon} |\nabla u_2^\varepsilon(0)|^2 \mathrm{d}x$$

$$+ \frac{C}{\delta} \int\limits_0^t \int\limits_{\Omega_1^\varepsilon} |u_1^\varepsilon|^2 \mathrm{d}x\mathrm{d}\tau + C \int\limits_{\Omega_1^\varepsilon} (|u_2^\varepsilon|^2 + |\nabla u_1^\varepsilon|^2)\mathrm{d}x + C\delta \int\limits_0^t \int\limits_{\Omega_1^\varepsilon} |\partial_t u_2^\varepsilon|^2 \mathrm{d}x\mathrm{d}\tau$$

$$+ \frac{C}{\delta} \int\limits_0^t \int\limits_{\Omega_2^\varepsilon} (|u_3^\varepsilon|^2 + |\nabla u_3^\varepsilon|^2)\mathrm{d}x\mathrm{d}\tau + C\delta \int\limits_0^t \int\limits_{\Omega_1^\varepsilon} (|\partial_t u_2^\varepsilon|^2 + \varepsilon^2 |\nabla \partial_t u_2^\varepsilon|^2)\mathrm{d}x\mathrm{d}\tau.$$

Choosing $\delta > 0$ small enough, we are led to

$$\int\limits_0^t \int\limits_{\Omega_1^\varepsilon} |\partial_t u_2^\varepsilon|^2 \mathrm{d}x\mathrm{d}\tau \le C(1 + \varepsilon^2 \int\limits_0^t \int\limits_{\Omega_1^\varepsilon} |\nabla \partial_t u_2^\varepsilon|^2 \mathrm{d}x\mathrm{d}\tau). \tag{4.39}$$

We consider now the Dirichlet data u_3^D to be extended in whole $\overline{\Omega}$. Testing now (4.6) with $\varphi_3 = \partial_t(u_3^\varepsilon - u_3^D)$ leads to

$$\int\limits_0^t \int\limits_{\Omega_1^\varepsilon} |\partial_t u_3^\varepsilon|^2 \mathrm{d}x\mathrm{d}\tau + \frac{d_{30}}{2} \int\limits_{\Omega_1^\varepsilon} |\nabla u_3^\varepsilon|^2 \mathrm{d}x\mathrm{d}\tau \le \frac{d_{30}}{2} \int\limits_{\Omega_1^\varepsilon} |\nabla u_3^\varepsilon(0)|^2 \mathrm{d}x\mathrm{d}\tau$$

$$+ \frac{1}{2} \int\limits_0^t \int\limits_{\Omega_1^\varepsilon} (|\partial_t u_3^\varepsilon|^2 + |\partial_t u_3^D|^2)\mathrm{d}x\mathrm{d}\tau + \frac{d_{30}}{2} \int\limits_0^t \int\limits_{\Omega_1^\varepsilon} (|\nabla u_3^\varepsilon|^2 + |\nabla \partial_t u_3^D|^2)\mathrm{d}x\mathrm{d}\tau$$

$$+ \varepsilon C \int\limits_0^t \int\limits_{\Gamma_2^\varepsilon} \left(|u_3^\varepsilon|^2 + |u_2^\varepsilon|^2\right)\mathrm{d}\gamma_x\mathrm{d}\tau + \varepsilon C \int\limits_0^t \int\limits_{\Gamma_2^\varepsilon} \left(|\partial_t u_3^\varepsilon|^2 + |\partial_t u_3^D|^2\right)\mathrm{d}\gamma_x\mathrm{d}\tau.$$

Using (4.1), (A6), (4.32) and (4.33), we end up with

$$\int\limits_0^t \int\limits_{\Omega_1^\varepsilon} |\partial_t u_3^\varepsilon|^2 \mathrm{d}x\mathrm{d}\tau \le C(1 + \varepsilon^2 \int\limits_0^t \int\limits_{\Omega_1^\varepsilon} |\nabla \partial_t u_3^\varepsilon|^2 \mathrm{d}x\mathrm{d}\tau). \tag{4.40}$$

From (4.7), we get

$$\int\limits_0^t \int\limits_{\Omega^\varepsilon} |\partial_t u_4^\varepsilon|^2 \mathrm{d}x\mathrm{d}\tau \quad \le \quad C. \tag{4.41}$$

To estimate (4.39) and (4.40), we proceed first with differentiating the partial differential equation in (2.17) with respect to time and then testing the result with $\partial_t u_2^\varepsilon$. Consequently, we derive

$$\frac{1}{2} \int\limits_{\Omega_1^\varepsilon} |\partial_t u_2^\varepsilon|^2 \mathrm{d}x + d_{20} \int\limits_0^t \int\limits_{\Omega_1^\varepsilon} |\nabla \partial_t u_2{}^\varepsilon|^2 \mathrm{d}x \le \frac{1}{2} \int\limits_{\Omega_1^\varepsilon} |\partial_t u_2^\varepsilon(0)|^2 \mathrm{d}x$$

$$+ C \int\limits_0^t \int\limits_{\Omega_1^\varepsilon} (|\partial_t u_1^\varepsilon|^2 + |\partial_t u_2^\varepsilon|^2)\mathrm{d}x\mathrm{d}\tau + \varepsilon C \int\limits_0^t \int\limits_{\Gamma_2^\varepsilon} (|\partial_t u_2^\varepsilon|^2 + |\partial_t u_3^\varepsilon|^2)\mathrm{d}\gamma_x\mathrm{d}\tau.$$

Using (4.1), it yields

$$\frac{1}{2}\int\limits_{\Omega_1^\varepsilon}|\partial_t u_2^\varepsilon|^2\mathrm{d}x + (d_{20}-C\varepsilon^2)\int\limits_0^t\int\limits_{\Omega_1^\varepsilon}|\nabla\partial_t u_2{}^\varepsilon|^2\mathrm{d}x\mathrm{d}\tau \le \frac{1}{2}\int\limits_{\Omega_1^\varepsilon}|\partial_t u_2^\varepsilon(0)|^2\mathrm{d}x$$

$$+ C\int\limits_0^t\int\limits_{\Omega_1^\varepsilon}|\partial_t u_1^\varepsilon|^2\mathrm{d}\tau\mathrm{d}x + C\int\limits_0^t\int\limits_{\Omega_2^\varepsilon}(|\partial_t u_3^\varepsilon|^2 + \varepsilon^2|\nabla\partial_t u_3^\varepsilon|^2)\mathrm{d}\tau\mathrm{d}x + C\int\limits_0^t\int\limits_{\Omega_1^\varepsilon}|\partial_t u_2^\varepsilon|^2\mathrm{d}\tau\mathrm{d}x.$$

$$(4.42)$$

Differentiating now the partial differential equation (2.18) with respect to time and then testing the result with $\partial_t(u_3^\varepsilon - u_3^D)$, we get

$$\frac{1}{2}\int\limits_{\Omega_1^\varepsilon}|\partial_t u_3^\varepsilon|^2\mathrm{d}x + d_{30}\int\limits_0^t\int\limits_{\Omega_1^\varepsilon}|\nabla\partial_t u_3{}^\varepsilon|^2\mathrm{d}x\mathrm{d}\tau \le \frac{1}{2}\int\limits_{\Omega_1^\varepsilon}|\partial_t u_3^\varepsilon(0)|^2\mathrm{d}x + \int\limits_0^t\int\limits_{\Omega_1^\varepsilon}\partial_{tt}u_3^\varepsilon\partial_t u_3{}^D\mathrm{d}x\mathrm{d}\tau$$

$$+ \int\limits_0^t\int\limits_{\Omega_1^\varepsilon}d_3^\varepsilon\nabla\partial_t u_3{}^\varepsilon\nabla\partial_t u_3{}^D\mathrm{d}x\mathrm{d}\tau + \varepsilon C\int\limits_0^t\int\limits_{\Gamma_2^\varepsilon}(|\partial_t u_2{}^\varepsilon|^2 + |\partial_t u_3{}^\varepsilon|^2 + |\partial_t u_3{}^D|^2)\mathrm{d}\gamma_x\mathrm{d}\tau.$$

$$(4.43)$$

The term with second-time derivative can be estimated by

$$\int\limits_0^t\int\limits_{\Omega_1^\varepsilon}\partial_{tt}u_3^\varepsilon\partial_t u_3{}^D\mathrm{d}x\mathrm{d}\tau = \int\limits_0^t\int\limits_{\Omega_1^\varepsilon}\partial_t u_3^\varepsilon\partial_t u_3{}^D\mathrm{d}x\mathrm{d}\tau$$

$$- \int\limits_0^t\int\limits_{\Omega_1^\varepsilon}\partial_t u_3^\varepsilon(0)\partial_t u_3{}^D(0)\mathrm{d}x\mathrm{d}\tau - \int\limits_0^t\int\limits_{\Omega_1^\varepsilon}\partial_{tt}u_3{}^D\partial_t u_3^\varepsilon\mathrm{d}x\mathrm{d}\tau.$$

Using (4.1) to deal with the boundary terms and (A5), we obtain

$$\frac{1}{2}\int\limits_{\Omega_2^\varepsilon}|\partial_t u_3^\varepsilon|^2\mathrm{d}x + (d_3-C\varepsilon^2)\int\limits_0^t\int\limits_{\Omega_2^\varepsilon}|\nabla\partial_t u_3{}^\varepsilon|^2\mathrm{d}x\mathrm{d}\tau \le C_0 + C\int\limits_0^t\int\limits_{\Omega_2^\varepsilon}|\partial_t u_3{}^\varepsilon|^2\mathrm{d}x\mathrm{d}\tau$$

$$+ C\int\limits_0^t\int\limits_{\Omega_1^\varepsilon}(|\partial_t u_2{}^\varepsilon|^2 + \varepsilon^2|\nabla\partial_t u_2{}^\varepsilon|^2)\mathrm{d}x\mathrm{d}\tau,$$

$$(4.44)$$

where C_0 contains bounded terms. The boundary data is smooth enough and regularity assumptions in u_{20} and u_{30} imply that $\|\partial_t u_2^\varepsilon(0)\|_{L^2(\Omega_1^\varepsilon)}$ and $\|\partial_t u_3^\varepsilon(0)\|_{L^2(\Omega_2^\varepsilon)}$ can be estimated by H^2-norm of the corresponding initial data. Adding (4.42) and (4.44), and re-arranging the terms gives

$$(d_2-C\varepsilon^2)\int\limits_0^t\int\limits_{\Omega_1^\varepsilon}|\nabla\partial_t u_2{}^\varepsilon|^2\mathrm{d}x\mathrm{d}\tau + (d_3-C\varepsilon^2)\int\limits_0^t\int\limits_{\Omega_2^\varepsilon}|\nabla\partial_t u_3{}^\varepsilon|^2\mathrm{d}x\mathrm{d}\tau \le C.$$

Choosing ε small and taking the supremum over the time interval in question, we get

$$\int\limits_0^T\int\limits_{\Omega_1^\varepsilon}|\nabla\partial_t u_2{}^\varepsilon|^2\mathrm{d}x\mathrm{d}\tau + \int\limits_0^T\int\limits_{\Omega_2^\varepsilon}|\nabla\partial_t u_3{}^\varepsilon|^2\mathrm{d}x\mathrm{d}\tau \le C. \qquad (4.45)$$

Inserting (4.45) in (4.39) and (4.40) yields the required result.

4.4 Extension. Two-scale convergence. Compactness. Cell problems

We intend to pass to the homogenization limit. We do this by following a three-steps procedure: In Step 1, we rely on the standard extension[2] results from [2] to extend all active concentrations u_ℓ^ε ($\ell \in \{1, \ldots, 4\}$) to Ω. As step 2, we use the notion of two-scale convergence and the corresponding two-scale compactness result developed by Nguetseng and Allaire to pass to the limit in the (weak form of the) partial differential equations. In step 3, we unfold the ordinary differential equation for u_5^ε to replace the oscillating boundary with a fixed one, say Γ_1; see Section 4.5.2. The last two steps will be detailed in the next section; here we focus more on the concept of two-scale convergence and available compactness properties.

4.4.1 Extension step

Since the concentrations are defined in the Ω_1^ε and Ω_2^ε, to get macroscopic equations we need to extend them into Ω. Note that according to our assumptions Ω_1^ε and Ω_2^ε are connected, standard results apply.

Remark 4.4.1. Take $\varphi^\varepsilon \in L^2(0, T; H^1(\Omega^\varepsilon))$. Note that since our microscopic geometry is sufficiently regular (and phases are connected), we can speak in terms of extensions. Recall the linearity of the extension operator

$$\mathcal{P}^\varepsilon : L^2(0, T; H^1(\Omega^\varepsilon)) \to L^2(0, T; H^1(\Omega))$$

defined by $\mathcal{P}^\varepsilon \varphi^\varepsilon = \tilde{\varphi}^\varepsilon$. To keep notation simple, we denote the extension $\tilde{\varphi}^\varepsilon$ again by φ^ε.

Lemma 4.4.2. (Extension) Consider the geometry described in Section 4.1.1 There exists an extension $\tilde{u}^\varepsilon$ of u^ε such that

1. $\| \tilde{u_i}^\varepsilon \|_{L^2(Y)} \leq \hat{C} \| u_i^\varepsilon \|_{L^2(Y_1)}$ for $i \in \{1, 2, 4\}, u^\varepsilon \in L^2(Y_1)$

2. $\| \nabla \tilde{u_i}^\varepsilon \|_{L^2(Y)} \leq \hat{C} \| \nabla u_i^\varepsilon \|_{L^2(Y_1)}$ for $\nabla u^\varepsilon \in L^2(Y_1)$

3. $\| \tilde{u_i}^\varepsilon \|_{H^1(\Omega)} \leq \hat{C} \| u_i^\varepsilon \|_{H^1(\Omega_1^\varepsilon)}$ for $u^\varepsilon \in H^1(\Omega_1^\varepsilon)$

Similar estimates hold for the concentration living in the air phase.

Proof. For the proof of this Lemma, see Section 2 in [39] or compare Lemma 5, p.214 in [68].

We identify u^ε with the extension $\tilde{u}^\varepsilon$. For the extended functions, we obtain *a priori* estimate by taking supremum norm of u^ε.

Lemma 4.4.3. For any solution of problem (4.4)-(4.7), the following estimate holds:

$$\| u_i^\varepsilon \|_{L^\infty(\Omega)} \leq C \quad i \in \{1, 2, 3, 4\}, \tag{4.46}$$

where C is a constant independent on u_i^ε.

The estimate (4.46) follows from the nonnegativity of u_i^ε.

---

[2]Since we deal here with an oscillating system posed in a perforated domain, the natural next step is to extend all concentrations to the whole Ω.

4.4.2   Two-scale convergence. Compactness. Basic convergences

In this subsection, the convergence of the sequence of solutions to the microscopic problem (4.4) – (4.8) associated with a sequence of parameters ε approaching to zero is discussed. Since we deal with periodic microstructures, the most natural type of convergence is the one presented in the next Definition:

Definition 4.4.4. Let $\{u^\varepsilon\}$ be a sequence of functions in $L^2((0,T) \times \Omega)$ (Ω being an open set of $\mathbb{R}^n$) where ε being a sequence of strictly positive numbers tends to zero. $\{u^\varepsilon\}$ is said to two-scale converge to a unique function $u_0 \in L^2((0,T) \times \Omega \times Y)$ if and only if for any $\phi \in C_0^\infty((0,T) \times \Omega, C_\#^\infty(Y))^3$, we have

$$\lim_{\varepsilon \to 0} \int_0^T \int_\Omega u^\varepsilon \phi(t, x, \frac{x}{\varepsilon}) \mathrm{d}x \mathrm{d}t = \int_0^T \int_\Omega \int_Y u_0(t, x, y) \phi(t, x, y) dy \mathrm{d}x \mathrm{d}t. \qquad (4.47)$$

We denote (4.47) by $u^\varepsilon \xrightarrow{2} u_0$.

The following compactness results allow us to extract converging sequences from the bounded sequences.

Theorem 4.4.5.   (i) From each bounded sequence $\{u^\varepsilon\}$ in $L^2((0,T) \times \Omega)$, one can extract a subsequence which two-scale converges to $u_0 \in L^2((0,T) \times \Omega \times Y)$.

(ii) Let $\{u^\varepsilon\}$ be a bounded sequence in $H^1((0,T) \times \Omega)$, then there exists $\tilde{u} \in L^2((0,T) \times \Omega; H_\#^1(Y)/\mathbb{R})$ such that up to a subsequence $\{u^\varepsilon\}$ two-scale converges to $u_0 \in L^2((0,T) \times \Omega)$ and $\nabla u^\varepsilon \xrightarrow{2} \nabla_x u_0 + \nabla_y \tilde{u}$.

Definition 4.4.6. A sequence of functions $\{u^\varepsilon\}$ in $L^2((0,T) \times \Gamma_\varepsilon)$ is said to two-scale converge to a limit $u_0 \in L^2((0,T) \times \Omega \times \Gamma)$ if and only if for any $\psi \in C_0^\infty((0,T) \times \Omega, C_\#^\infty(\Gamma))$ we have

$$\lim_{\varepsilon \to 0} \varepsilon \int_0^T \int_{\Gamma^\varepsilon} u^\varepsilon \phi(t, x, \frac{x}{\varepsilon}) \mathrm{d}\gamma_x \mathrm{d}t = \int_0^T \int_\Omega \int_\Gamma u_0(t, x, y) \phi(t, x, y) \mathrm{d}\gamma_y \mathrm{d}x \mathrm{d}t.$$

Theorem 4.4.7.   (i) From each bounded sequence $\{u^\varepsilon\} \in L^2((0,T) \times \Gamma^\varepsilon)$, one can extract a subsequence u^ε which two-scale converges to a function $u_0 \in L^2((0,T) \times \Omega \times \Gamma)$.

(ii) If a sequence of functions $\{u^\varepsilon\}$ is bounded in $L^\infty((0,T) \times \Gamma^\varepsilon)$, then u^ε two-scale converges to a function $u_0 \in L^\infty((0,T) \times \Omega \times \Gamma)$.

Proof. For the proof of (i), see [104, 10], while for the proof of (ii), see [83].

Estimates in Lemma 4.3.1 and Lemma 4.3.2 lead to the following convergence results:

Lemma 4.4.8. *(Compactness)* Assume (A1) – (A6). Then for $i \in \{1, 2, 3, 4\}$, it holds:

(a) $u_i^\varepsilon \rightharpoonup u_i$ weakly in $L^2(0, T; H^1(\Omega)$,

---

[3]$C_\#^\infty(Y)$ – the space of infinitely differentiable functions in $\mathbb{R}^n$ that are Y-periodic.

(b) $u_i^\varepsilon \overset{*}{\rightharpoonup} u_i$ weakly in $L^\infty((0,T) \times \Omega)$,

(c) $\partial_t u_i^\varepsilon \rightharpoonup \partial_t u_i$ weakly in $L^2((0,T) \times \Omega)$,

(d) $u_i^\varepsilon \to u_i$ strongly in $L^2(0,T; H^\beta(\Omega))$ for $\frac{1}{2} < \beta < 1$,
    also $\sqrt{\varepsilon} \parallel u_i^\varepsilon - u_i \parallel_{L^2((0,T) \times \Gamma_\varepsilon)} \to 0$ as $\varepsilon \to 0$,

(e) $u_i^\varepsilon \overset{2}{\rightharpoonup} u_i, \nabla u_j^\varepsilon \overset{2}{\rightharpoonup} \nabla_x u_j + \nabla_y u_{j1}, \; u_{j1} \in L^2((0,T) \times \Omega; H^1_\#(Y_1)/\mathbb{R}), j \in \{1,2\},$
    $\nabla u_3^\varepsilon \overset{2}{\rightharpoonup} \nabla_x u_3 + \nabla_y u_{31}, \; u_{31} \in L^2((0,T) \times \Omega; H^1_\#(Y_2)/\mathbb{R}),$

(f) $u_5^\varepsilon \overset{2}{\rightharpoonup} u_5$, and $u_5 \in L^\infty((0,T) \times \Omega \times \Gamma_1)$,

(g) $\partial_t u_5^\varepsilon \overset{2}{\rightharpoonup} \partial_t u_5$, and $\partial_t u_5 \in L^2((0,T) \times \Omega \times \Gamma_1)$.

Proof. (a) and (b) are obtained as a direct consequence of the fact that u_i^ε is bounded in $L^2(0,T; H^1(\Omega)) \cap L^\infty((0,T) \times \Omega)$; up to a subsequence (still denoted by u_i^ε) u_i^ε converges weakly to u_i in $L^2(0,T; H^1(\Omega)) \cap L^\infty((0,T) \times \Omega)$. A similar argument gives (c). To get (d), we use the compact embedding $H^{\beta'}(\Omega) \hookrightarrow H^\beta(\Omega)$, for $\beta \in (\frac{1}{2}, 1)$ and $0 < \beta < \beta' \leq 1$ (since Ω has Lipschitz boundary), see Proposition 5.4.4 in [132]. We have $W := \{u_i \in L^2(0,T; H^1(\Omega))$ and $\partial_t u_i \in L^2((0,T) \times \Omega)$ for all $i \in \{1,2,3,4\}\}$. For a fixed ε, W is compactly embedded in $L^2(0,T; H^\beta(\Omega))$ by the Lions-Aubin Lemma; cf. e.g. [80]. Using the trace inequality (4.2)

$$\begin{aligned} \sqrt{\varepsilon} \parallel u_i^\varepsilon - u_i \parallel_{L^2((0,T) \times \Gamma_\varepsilon)} &\leq C \parallel u_i^\varepsilon - u_i \parallel_{L^2(0,T; H^\beta(\Omega^\varepsilon))} \\ &\leq C \parallel u_i^\varepsilon - u_i \parallel_{L^2(0,T; H^\beta(\Omega))} \end{aligned}$$

where $\parallel u_i^\varepsilon - u_i \parallel_{L^2(0,T; H^\beta(\Omega))} \to 0$ as $\varepsilon \to 0$. To investigate (e), (f) and (g), we use the notion of two-scale convergence as indicated in Definition 4.4.4 and 4.4.6. Since u_i^ε are bounded in $L^2(0,T; H^1(\Omega))$, up to a subsequence $u_i^\varepsilon \overset{2}{\rightharpoonup} u_i$ in $L^2((0,T) \times \Omega)$, $\nabla u_j^\varepsilon \overset{2}{\rightharpoonup} \nabla_x u_j + \nabla_y u_{j1}, \; u_{j1} \in L^2((0,T) \times \Omega; H^1_\#(Y_1)/\mathbb{R}), j \in \{1,2\}, \nabla u_3^\varepsilon \overset{2}{\rightharpoonup} \nabla_x u_3 + \nabla_y u_{31}, \; u_{31} \in L^2((0,T) \times \Omega; H^1_\#(Y_2)/\mathbb{R})$. By Theorem 4.4.7, u_5^ε in $L^\infty((0,T) \times \Gamma_1^\varepsilon)$ converges two-scale to u_5 $L^\infty((0,T) \times \Omega \times \Gamma_1)$ and $\partial_t u_5^\varepsilon$ converges two-scale to $\partial_t u_5$ in $L^2((0,T) \times \Omega \times \Gamma_1)$.

4.4.3   Cell problems

To be able to formulate the limit (upscaled) equations in a compact manner, we define two classes of *cell problems* (local auxiliary problems) very much in the spirit of [67]. One class of problems refers to the water-filled parts of the pores, while the second class refers to the air-filled part of the pores.

Definition 4.4.9. The *cell problems for the water-filled part* are given by

$$\begin{cases} -\nabla_y.(d_\ell(y)\nabla_y \omega_\ell^k) &= \sum_{i=1}^3 \partial_{y_k} d_{\ell k i}(y) \text{ in } Y_1, \\ -d_\ell(y)\frac{\partial \omega_\ell^k}{\partial n} &= \sum_{i=1}^3 d_{\ell k i}(y)n_i \text{ on } \Gamma_1 \cup \Gamma_2, \end{cases} \tag{4.48}$$

for all $k \in \{1,2,3\}, \ell \in \{1,2,4\}$, ω_ℓ^k are Y-periodic in y.
The *cell problems for the air-filled part* are given by

$$\begin{cases} -\nabla_y.(d_3(y)\nabla_y \omega_3^k) &= \sum_{i=1}^3 \partial_{y_k} d_{3ki}(y) \text{ in } Y_2, \\ -d_3(y)\frac{\partial \omega_3^k}{\partial n} &= \sum_{i=1}^3 d_{3ki}(y)n_i \text{ on } \Gamma_1 \end{cases} \tag{4.49}$$

for all $k \in \{1,2,3\}$, ω_3^k are Y-periodic in y.

Note that standard theory of linear elliptic problems with periodic boundary conditions [35] ensures the solvability of the families of cell problems (4.48) – (4.49).

4.5   Derivation of two-scale limit equations

First we pass to the limit in the weak formulation of the partial differential equations and in Subsection 4.5.2, we pass to the limit in ordinary differential equation (4.8). We conclude this section with stating the strong formulation of two-scale problem.

Theorem 4.5.1. Assume (A1) – (A6). The sequences of the solutions of the weak formulation (4.4) – (4.8) converges to the weak solution $u_i, i \in \{1, 2, 3, 4\}$ as $\varepsilon \to 0$ such that $u_j \in H^1(0, T; L^2(\Omega)) \cap L^2(0, T; H^1(\Omega)), j \in \{1, 2, 4\}, u_3 \in u_3^D + L^2(0, T; H^1_{\Gamma^D}(\Omega))$, $\partial_t u_3 \in \partial_t u_3^D + L^2(0, T; L^2(\Omega))$ and $u_5 \in H^1(0, T; L^2(\Omega \times \Gamma_1))$. The weak formulation of the two-scale limit equations is given by

$$\int_0^T \int_\Omega (\partial_t u_i(t, x) - F_i(u))\phi_i(t, x) \mathrm{d}x \mathrm{d}t \quad + \quad \int_0^T \int_\Omega D_i \nabla u_i(t, x) \nabla \phi_i \mathrm{d}x \mathrm{d}t = 0, \quad (4.50)$$

where

$$F_1(u) \quad := \quad -\tilde{k}_1 u_1(t, x) + \tilde{k}_2 u_2(t, x) - \frac{1}{|Y_1|} \int_{\Gamma_1} k_3(y) R(u_1(t, x)) Q(u_5(t, x, y)) \mathrm{d}\gamma_y,$$

$$F_2(u) \quad := \quad \tilde{k}_1 u_1(t, x) - \tilde{k}_2 u_2(t, x) + \frac{|Y_2|}{|Y_1|} \tilde{a} u_3(t, x) - \tilde{b} u_2(t, x),$$

$$F_3(u) \quad := \quad -\tilde{a} u_3(t, x) + \frac{|Y_1|}{|Y_2|} \tilde{b} u_2(t, x), \qquad F_4(u) := \tilde{k}_1 u_1(t, x),$$

$$(D_\ell)_{jk} \quad := \quad \frac{1}{|Y_1|} \sum_{i=1}^3 \int_{Y_1} ((d_\ell)_{jk} + (d_\ell)_{ik} \partial_{y_i} \omega_\ell^j) dy, \text{ for } \ell \in \{1, 2, 4\}, j, k \in \{1, 2, 3\}$$

$$(D_3)_{jk} \quad := \quad \frac{1}{|Y_2|} \sum_{\ell=1}^3 \int_{Y_2} ((d_3)_{jk} + (d_3)_{\ell k} \partial_{y_\ell} \omega_3^j) dy, \quad \tilde{b} := \frac{1}{|Y_1|} \int_{\Gamma_1} b(y) \mathrm{d}\gamma_y$$

$$\tilde{a} \quad := \quad \frac{1}{|Y_2|} \int_{\Gamma_1} a(y) \mathrm{d}\gamma_y, \qquad \tilde{k}_m := \frac{1}{|Y_1|} \int_{Y_1} k_m(y) dy, \;\; m \in \{1, 2\},$$

with the initial values $u_i(0, x) = u_{i0}(x)$ for $x \in \Omega$ and $\omega_\ell^j, \omega_3^j$ being solutions of the cell problems defined in Definition 4.4.9. Furthermore, we have

$$\int_0^T \int_{\Omega \times \Gamma_1} \left(\partial_t u_5(t, x, y) - k_3(y) R(u_1(t, x)) Q(u_5(t, x, y)) \right) \phi_5(t, x, y) \mathrm{d}t \mathrm{d}x \mathrm{d}\gamma_y = 0, \quad (4.51)$$

with $u_5(0, x, y) = u_{50}(x, y)$ for $x \in \Omega, y \in \Gamma_1$. Also $\varphi_j \in L^2(0, T; H^1(\Omega)), j \in \{1, 2, 4\}$, $\varphi_3 \in L^2(0, T; H^1_{\Gamma^D}(\Omega))$ and $\varphi_5 \in L^2((0, T) \times \Omega \times \Gamma_1)$.

4.5.1 Passing to $\varepsilon \to 0$ in $(4.4) - (4.7)$

Proof. We apply two-scale convergence techniques together with Lemma 4.4.8 to get macroscopic equations. We take test functions incorporating the following oscillating behavior $\varphi_i(t,x) = \phi_i(t,x) + \varepsilon\psi_i(t,x,\frac{x}{\varepsilon}), \phi_j \in C^\infty((0,T) \times \Omega), \psi_j \in C^\infty((0,T) \times \Omega, ; C_\#^\infty(Y)), i \in \{1,2,3,4\}, j \in \{1,2,4\}$ and $\phi_3 \in C_0^\infty((0,T) \times \Omega), \psi_2 \in C_0^\infty((0,T) \times \Omega, ; C_\#^\infty(Y))$. Applying two-scale convergence yields for $i \in \{1,2,4\}$

$$|Y_1| \int\limits_0^T \int\limits_\Omega \partial_t u_i \phi_i(t,x) \mathrm{d}x\mathrm{d}t + \int\limits_0^T \int\limits_\Omega \int\limits_{Y_1} d_i(y)(\nabla_x u_i(t,x) \tag{4.52}$$

$$+ \quad \nabla_y \tilde{u}_i(t,x,y))(\nabla_x \phi_i(t,x) + \nabla_y \psi_i(t,x,y)) dy \mathrm{d}x\mathrm{d}t = \int\limits_0^T \int\limits_\Omega F_i(u)\phi_i(t,x)\mathrm{d}x\mathrm{d}t,$$

and

$$|Y_2| \int\limits_0^T \int\limits_\Omega \partial_t u_3 \phi_3(t,x) \mathrm{d}x\mathrm{d}t + \int\limits_0^T \int\limits_\Omega \int\limits_{Y_2} d_3(y)(\nabla_x u_3(t,x) \tag{4.53}$$

$$+ \quad \nabla_y \tilde{u}_3(t,x,y))(\nabla_x \phi_3(t,x) + \nabla_y \psi_3(t,x,y)) dy \mathrm{d}x\mathrm{d}t = \int\limits_0^T \int\limits_\Omega F_3(u)\phi_3(t,x)\mathrm{d}x\mathrm{d}t,$$

where

$$\int\limits_0^T \int\limits_\Omega F_1(u)\phi_1(t,x)\mathrm{d}x\mathrm{d}t = \lim_{\varepsilon \to 0} \int\limits_0^T \int\limits_\Omega \big(- k_1^\varepsilon u_1^\varepsilon + k_2^\varepsilon u_2^\varepsilon\big)(\phi_1(t,x) + \varepsilon\psi_1(t,x,\frac{x}{\varepsilon}))\mathrm{d}x\mathrm{d}t$$

$$- \lim_{\varepsilon \to 0} \varepsilon \int\limits_0^T \int\limits_{\Gamma_1^\varepsilon} \eta^\varepsilon(u_1^\varepsilon, u_5^\varepsilon)(\phi_1(t,x) + \varepsilon\psi_1(t,x,\frac{x}{\varepsilon}))\mathrm{d}\gamma_x\mathrm{d}t.$$

Using Lemma 4.4.8 and (4.8), we have

$$\int\limits_0^T \int\limits_\Omega F_1(u)\phi_1(t,x)\mathrm{d}x\mathrm{d}t \quad = \int\limits_0^T \int\limits_\Omega \int\limits_{Y_1} \big(- k_1(y)u_1(t,x) + k_2(y)u_2(t,x)\big)\phi_1(t,x) dy\mathrm{d}x\mathrm{d}t$$

$$- \lim_{\varepsilon \to 0} \varepsilon \int\limits_0^T \int\limits_{\Gamma_1^\varepsilon} \partial_t u_5^\varepsilon(\phi_1(t,x) + \varepsilon\psi_1(t,x,\frac{x}{\varepsilon}))\mathrm{d}\gamma_x\mathrm{d}t,$$

$$\int\limits_0^T \int\limits_\Omega F_1(u)\phi_1(t,x)\mathrm{d}x\mathrm{d}t \quad = |Y_1| \int\limits_0^T \int\limits_\Omega \big(- \tilde{k}_1 u_1(t,x) + \tilde{k}_2 u_2(t,x)\big)\phi_1(t,x)\mathrm{d}x\mathrm{d}t$$

$$- \int\limits_0^T \int\limits_\Omega \int\limits_{\Gamma_1} \partial_t u_5 \phi_1(t,x)\mathrm{d}\gamma_y\mathrm{d}x\mathrm{d}t.$$

$$\int\limits_0^T \int\limits_\Omega F_2(u)\phi_2(t,x)\mathrm{d}x\mathrm{d}t = \lim_{\varepsilon\to 0}\int\limits_0^T \int\limits_\Omega \big(k_1^\varepsilon u_1^\varepsilon - k_2^\varepsilon u_2^\varepsilon\big)(\phi_2(t,x)+\varepsilon\psi_2(t,x,\tfrac{x}{\varepsilon}))\mathrm{d}x\mathrm{d}t$$

$$+ \lim_{\varepsilon\to 0}\varepsilon\int\limits_0^T \int\limits_{\Gamma_2^\varepsilon} \big(a^\varepsilon u_3^\varepsilon - b^\varepsilon u_2^\varepsilon\big)(\phi_2(t,x)+\varepsilon\psi_2(t,x,\tfrac{x}{\varepsilon}))\mathrm{d}\gamma_x\mathrm{d}t.$$

Passage to the limits $\varepsilon \to 0$ gives

$$\int\limits_0^T \int\limits_\Omega F_2(u)\phi_2(t,x)\mathrm{d}x\mathrm{d}t \quad = |Y_1|\int\limits_0^T \int\limits_\Omega \big(\tilde{k}_1 u_1(t,x) - \tilde{k}_2 u_2(t,x)\big)\phi_2(t,x)\mathrm{d}x\mathrm{d}t$$

$$+ \int\limits_0^T \int\limits_\Omega \int\limits_{\Gamma_2} \big(a(y)u_3(t,x) - b(y)u_2(t,x)\big)\phi_2(t,x)\mathrm{d}x\mathrm{d}y\mathrm{d}t,$$

$$= |Y_1|\int\limits_0^T \int\limits_\Omega \big(-\tilde{k}_1 u_1(t,x) + \tilde{k}_2 u_2(t,x)\big)\phi_2(t,x)\mathrm{d}x\mathrm{d}t$$

$$+ \int\limits_0^T \int\limits_\Omega \big(|Y_2|\tilde{a}u_3(t,x) - |Y_1|\tilde{b}u_2(t,x)\big)\phi_2(t,x)\mathrm{d}x\mathrm{d}t.$$

We also obtain

$$\int\limits_0^T \int\limits_\Omega F_3(u)\phi_3(t,x)\mathrm{d}x\mathrm{d}t = -\int\limits_0^T \int\limits_\Omega \big(|Y_2|\tilde{a}u_3(t,x) - |Y_1|\tilde{b}u_2(t,x)\big)\phi_3(t,x)\mathrm{d}x\mathrm{d}t,$$

$$\int\limits_0^T \int\limits_\Omega F_4(u)\phi_4(t,x)\mathrm{d}x\mathrm{d}t = |Y_1|\int\limits_0^T \int\limits_\Omega \tilde{k}_1 u_1(t,x)\phi_4(t,x)\mathrm{d}x\mathrm{d}t.$$

We set $\phi_i = 0, i \in \{1,2,3,4\}$ in (4.52) to calculate the expression of the unknown function $\tilde{u}_1$ and obtain

$$\int\limits_0^T \int\limits_\Omega \int\limits_{Y_1} d_i(y)(\nabla_x u_i(t,x) + \nabla_y \tilde{u}_i(t,x,y))\nabla_y \psi_i(t,x,y)\mathrm{d}y\mathrm{d}x\mathrm{d}t = 0, \text{ for all } \psi_i.$$

Since $\tilde{u}_i$ depends linearly on $\nabla_x u_i$, it can be defined as

$$\tilde{u}_i := \sum_{j=1}^3 \partial_{x_j} u_i \omega_i^j,$$

where the function ω^j are the unique solutions of the cell problems defined in Definition 4.4.9. Similarly, we have $\tilde{u}_3 := \sum_{j=1}^3 \partial_{x_j} u_3 \varsigma_j$ where ς_j are the unique solutions of the

cell problems defined in Definition 4.4.9. Setting $\psi_i = 0$ in (4.52), we get

$$\int\limits_0^T \int\limits_\Omega \int\limits_{Y_1} \sum_{j,k=1}^3 d_{ijk}(y)(\partial_{x_k} u_i(t,x) + \sum_{m=1}^3 \partial_{y_k}\omega_m \partial_{x_m} u_i(t,x))\partial_{x_j}\phi_i(t,x)dy\mathrm{d}x\mathrm{d}t$$

$$= |Y_1| \int\limits_0^T \int\limits_\Omega \sum_{j,k=1}^3 (D_i)_{jk}\partial_{x_k} u_i(t,x)\partial_{x_j}\phi_i(t,x)\mathrm{d}x\mathrm{d}t.$$

Hence, the coefficients (entering the effective diffusion tensor in water) are given by

$$(D_i)_{jk} := \frac{1}{|Y_1|} \sum_{\ell=1}^3 \int\limits_{Y_1} ((d_i)_{jk} + (d_i)_{\ell k}\partial_{y_\ell}\omega_i^j)dy, \text{ for } i \in \{1,2,4\}.$$

Similarly, we obtain the following effective diffusion coefficient of $H_2S(g)$

$$(D_3)_{jk} := \frac{1}{|Y_2|} \sum_{\ell=1}^3 \int\limits_{Y_2} ((d_3)_{jk} + (d_3)_{\ell k}\partial_{y_\ell}\omega_3^j)dy.$$

These tensors are symmetric and positive definite, see [35].

4.5.2 Passing to the limit $\varepsilon \to 0$ in (4.8)

It is not yet possible to pass to the limit $\varepsilon \to 0$ in the ordinary differential equation (4.8) with the compactness results stated in Lemma 4.4.8. To overcome this difficulty, we use the notion of periodic boundary unfolding. It is worth mentioning that there is an intimate link between the two-scale convergence and weak convergence of the unfolded sequences; see [34, 83]. The key idea is to obtain strong convergence for the unfolded sequence of u_5^ε instead of getting strong convergence for u_5^ε.

Definition 4.5.2. (Boundary unfolding operator) For $\varepsilon > 0$, the boundary unfolding of a measurable function ϕ posed on oscillating surface Γ_1^ε is defined by

$$\mathcal{T}_{\Gamma_1}^\varepsilon \phi(x,y) = \phi(\varepsilon y + \varepsilon k), \ \ y \in \Gamma_1, x \in \Omega,$$

where $k := [\frac{x}{\varepsilon}]$ denotes the unique integer combination $\Sigma_{j=1}^3 k_j e_j$ of the periods such that $x - [\frac{x}{\varepsilon}]$ belongs to Y. Note that the oscillations due to the perforations are shifted into a second variable y which belongs to the fixed surface Γ_1.

Lemma 4.5.3. If φ_ε converges two-scale to φ and $\mathcal{T}_{\Gamma_1}^\varepsilon \varphi_\varepsilon$ converges weakly to φ^* in $L^2((0,T) \times \Omega; L_\#^2(\Gamma_1))$, then $\varphi = \varphi^*$ a.e. in $(0,T) \times \Omega \times \Gamma_1$.

Proof. The proof details for this statement can be found in Lemma 4.6 of [83]. ∎

Lemma 4.5.4. If $\varphi \in L^2((0,T) \times \Gamma_1^\varepsilon)$, then the following identity holds

$$\frac{1}{|Y|}\|\mathcal{T}_{\Gamma_1}^\varepsilon \varphi\|_{L^2((0,T)\times\Omega\times\Gamma_1)} = \sqrt{\varepsilon}\|\varphi\|_{L^2((0,T)\times\Gamma_1^\varepsilon)}.$$

Proof. See [83, 38, 36] for the proof details. ∎

Lemma 4.5.5. If $\varphi \in L^2(\Omega)$, then $\mathcal{T}_{\Gamma_1}^\varepsilon \varphi \to \varphi$ as $\varepsilon \to 0$ strongly in $L^2(\Omega \times \Gamma_1)$.

Proof. See e.g. [36, 38] for the details of the proof.

Lemma 4.5.6. If $\varphi \in L^2(\Gamma_1)$, then $\mathcal{T}_{\Gamma_1}^\varepsilon \varphi \to \varphi$ as $\varepsilon \to 0$ strongly in $L^2(\Omega \times \Gamma_1)$.

Proof. The proof goes on the same line as the proof of Lemma 4.5.5; see also Proposition 2.11(f) in [46].

Using the boundary unfolding operator $\mathcal{T}_{\Gamma_1}^\epsilon$, we unfold the ordinary differential equation (4.8). Changing then the variable, $x = \varepsilon y + \varepsilon k$ (for $x \in \Gamma_1^\varepsilon$) to the fixed domain $(0, T) \times \Omega \times \Gamma_1$, we have

$$\partial_t \mathcal{T}_{\Gamma_1}^\epsilon u_5^\epsilon(t, x, y) = \eta^\varepsilon(\mathcal{T}_{\Gamma_1}^\epsilon u_1^\epsilon(t, x, y), \mathcal{T}_{\Gamma_1}^\epsilon u_5^\epsilon(t, x, y)). \tag{4.54}$$

In the remainder of this section, we prove that $\mathcal{T}_{\Gamma_1}^\varepsilon u_5^\varepsilon$ converges strongly to u_5 in $L^2((0, T) \times \Omega \times \Gamma_1)$. From the two-scale convergence of u_5^ϵ, we obtain weak convergence of $\mathcal{T}^\epsilon u_5^\epsilon$ to u_5 in $L^2((0, T) \times \Omega; L_\#^2(\Gamma_1))$. We start with showing that $\{\mathcal{T}_{\Gamma_1}^\varepsilon u_5^\varepsilon\}$ is a Cauchy sequence in $L^2((0, T) \times \Omega \times \Gamma_1)$. We choose $m, n \in \mathbb{N}$ with $n > m$ arbitrary. Writing down (4.54) for the two different choices of ε (i.e. $\varepsilon_i = \varepsilon_n$ and $\varepsilon_i = \varepsilon_m$), we obtain after subtracting the corresponding equations that

$$\partial_t \int\limits_{\Omega \times \Gamma_1} |\mathcal{T}_{\Gamma_1}^{\epsilon_n} u_5^{\epsilon_n} - \mathcal{T}_{\Gamma_1}^{\epsilon_m} u_5^{\epsilon_m}|^2 \mathrm{d}\gamma_y \mathrm{d}x$$

$$= \int\limits_{\Omega \times \Gamma_1} [k_3(y) R(\mathcal{T}_{\Gamma_1}^{\epsilon_n} u_1^{\epsilon_n}) Q(\mathcal{T}_{\Gamma_1}^{\epsilon_n} u_5^{\epsilon_n}) - k_3(y) R(\mathcal{T}_{\Gamma_1}^{\epsilon_m} u_1^{\epsilon_m}) Q(\mathcal{T}_{\Gamma_1}^{\epsilon_m} u_5^{\epsilon_m}))$$

$$\times \quad (\mathcal{T}_{\Gamma_1}^{\epsilon_n} u_5^{\epsilon_n} - \mathcal{T}_{\Gamma_1}^{\epsilon_m} u_5^{\epsilon_m}) \mathrm{d}\gamma_y \mathrm{d}x,$$

$$\leq \quad C \int\limits_{\Omega \times \Gamma_1} |\mathcal{T}_{\Gamma_1}^{\epsilon_n} u_5^{\epsilon_n} - \mathcal{T}_{\Gamma_1}^{\epsilon_m} u_5^{\epsilon_m}|^2 \mathrm{d}\gamma_y \mathrm{d}x + C \int\limits_{\Omega \times \Gamma_1} |\mathcal{T}_{\Gamma_1}^{\epsilon_n} u_1^{\epsilon_n} - \mathcal{T}_{\Gamma_1}^{\epsilon_m} u_1^{\epsilon_m}|^2 \mathrm{d}\gamma_y \mathrm{d}x (4.55)$$

To get (4.55), we have used the uniform boundedness of $\mathcal{T}_{\Gamma_1}^{\epsilon_n} u_1^{\epsilon_n}$ and properties of R and Q. Since u_1^ε converges strongly to u_1 in $L^2((0, T) \times \Gamma_1^\varepsilon)$ by Lemma 4.4.8 (d), we get by Lemma 4.5.4 that

$$\int\limits_{\Omega \times \Gamma_1} |\mathcal{T}_{\Gamma_1}^\epsilon u_1^\epsilon - \mathcal{T}_{\Gamma_1}^\epsilon u_1|^2 \mathrm{d}\gamma_y \mathrm{d}x = \varepsilon \int\limits_{\Gamma_1^\varepsilon} |u_1^\epsilon - u_1|^2 \mathrm{d}\gamma_x \leq C\varepsilon. \tag{4.56}$$

Since u_1 is constant w.r.t. y, we have that $\mathcal{T}_{\Gamma_1}^\epsilon u_1 \to u_1$ strongly in $L^2((0, T) \times \Omega \times \Gamma_1)$ as $\varepsilon \to 0$. Combining (4.56) and the strong convergence of $\mathcal{T}_{\Gamma_1}^\epsilon u_1$ to u_1 to get

$$\int\limits_{\Omega \times \Gamma_1} |\mathcal{T}_{\Gamma_1}^{\epsilon_n} u_1^{\epsilon_n} - \mathcal{T}_{\Gamma_1}^{\epsilon_m} u_1^{\epsilon_m}|^2 \mathrm{d}\gamma_y \mathrm{d}x \quad \leq \varepsilon_n \int\limits_{\Gamma_1^\varepsilon} |u_1^{\epsilon_n} - u_1|^2 \mathrm{d}\gamma_x + \varepsilon_m \int\limits_{\Gamma_1^\varepsilon} |u_1^{\epsilon_m} - u_1|^2 \mathrm{d}\gamma_x$$

$$+ \int\limits_{\Omega \times \Gamma_1} \left(|\mathcal{T}_{\Gamma_1}^{\epsilon_n} u_1 - u_1|^2 + |\mathcal{T}_{\Gamma_1}^{\epsilon_m} u_1 - u_1|^2 \right) \mathrm{d}\gamma_y \mathrm{d}x,$$

$$\leq C(\varepsilon_n + \varepsilon_m),$$

while (4.55) becomes

$$\partial_t \int\limits_{\Omega \times \Gamma_1} |\mathcal{T}_{\Gamma_1}^{\epsilon_n} u_5^{\epsilon_n} - \mathcal{T}_{\Gamma_1}^{\epsilon_m} u_5^{\epsilon_m}|^2 \mathrm{d}\gamma_y \mathrm{d}x \leq C \int\limits_{\Omega \times \Gamma_1} |\mathcal{T}_{\Gamma_1}^{\epsilon_n} u_5^{\epsilon_n} - \mathcal{T}_{\Gamma_1}^{\epsilon_m} u_5^{\epsilon_m}|^2 \mathrm{d}\gamma_y \mathrm{d}x + C(\varepsilon_n + \varepsilon_m).$$

Applying Gronwall's inequality, we obtain:

$$\int\limits_{\Omega \times \Gamma_1} |\mathcal{T}_{\Gamma_1}^{\epsilon_n} u_5^{\epsilon_n}(t) - \mathcal{T}_{\Gamma_1}^{\epsilon_m} u_5^{\epsilon_m}(t)|^2 \mathrm{d}\gamma_y \mathrm{d}x$$

$$\leq \int\limits_{\Omega \times \Gamma_1} |\mathcal{T}_{\Gamma_1}^{\epsilon_n} u_5^{\epsilon_n}(0) - \mathcal{T}_{\Gamma_1}^{\epsilon_m} u_5^{\epsilon_m}(0)|^2 \mathrm{d}\gamma_y \mathrm{d}x + C(\varepsilon_n + \varepsilon_m)$$

$$\leq \int\limits_{\Omega \times \Gamma_1} |\mathcal{T}_{\Gamma_1}^{\epsilon_n} u_{50} - u_{50}|^2 \mathrm{d}\gamma_y \mathrm{d}x + \int\limits_{\Omega \times \Gamma_1} |\mathcal{T}_{\Gamma_1}^{\epsilon_m} u_{50} - u_{50}|^2 \mathrm{d}\gamma_y \mathrm{d}x + C(\varepsilon_n + \varepsilon_m).$$

Using Lemma 6.25, we get

$$\| \mathcal{T}_{\Gamma_1}^{\epsilon_n} u_5^{\epsilon_n} - \mathcal{T}_{\Gamma_1}^{\epsilon_m} u_5^{\epsilon_m} \|_{L^2((0,T) \times \Omega \times \Gamma_1)} \longrightarrow 0 \text{ as } \epsilon_n, \epsilon_m \to 0. \tag{4.57}$$

By (4.57), $\{\mathcal{T}_{\Gamma_1}^{\epsilon} u_5^{\epsilon}\}$ is a Cauchy sequence and hence converges strongly. Thus, $Q(\mathcal{T}_{\Gamma_1}^{\epsilon} u_5^{\epsilon}) \to Q(u_5)$ strongly in $(0,T) \times \Omega \times \Gamma_1$ as $\varepsilon \to 0$. Now, we take the two-scale limit in the ordinary differential equation (4.54) to get

$$\lim_{\varepsilon \to 0} \varepsilon \int\limits_0^T \int\limits_{\Omega \times \Gamma_1} \partial_t \mathcal{T}_{\Gamma_1}^{\epsilon} u_5^{\varepsilon} \phi_5(t,x,y) \mathrm{d}x \mathrm{d}\gamma_y \mathrm{d}\tau$$

$$= \lim_{\varepsilon \to 0} \varepsilon \int\limits_0^T \int\limits_{\Omega \times \Gamma_1} \eta^{\varepsilon}(\mathcal{T}_{\Gamma_1}^{\epsilon} u_1^{\varepsilon}, \mathcal{T}_{\Gamma_1}^{\epsilon} u_5^{\varepsilon}) \phi_5(t,x,y) \mathrm{d}x \mathrm{d}\gamma_y \mathrm{d}\tau. \tag{4.58}$$

Consequently, we have

$$\int\limits_0^T \int\limits_{\Omega \times \Gamma_1} \partial_t u_5 \phi_5(t,x,y) \mathrm{d}x \mathrm{d}\gamma_y \mathrm{d}t$$

$$= \lim_{\varepsilon \to 0} \varepsilon \int\limits_0^T \int\limits_{\Omega \times \Gamma_1} \mathcal{T}_{\Gamma_1}^{\epsilon} k_3^{\varepsilon} R(\mathcal{T}_{\Gamma_1}^{\epsilon} u_1^{\varepsilon}) Q(\mathcal{T}_{\Gamma_1}^{\epsilon} u_5^{\varepsilon}) \phi_5(t,x,\frac{x}{\varepsilon}) \mathrm{d}x \mathrm{d}\gamma_y \mathrm{d}t,$$

$$= \lim_{\varepsilon \to 0} \varepsilon \int\limits_0^T \int\limits_{\Omega \times \Gamma_1} k_3(y) R(\mathcal{T}_{\Gamma_1}^{\epsilon} u_1^{\varepsilon}) Q(u_5) \phi_5(t,x,\frac{x}{\varepsilon}) \mathrm{d}x \mathrm{d}\gamma_y \mathrm{d}t$$

$$+ \lim_{\varepsilon \to 0} \varepsilon \int\limits_0^T \int\limits_{\Omega \times \Gamma_1} k_3(y) R(\mathcal{T}_{\Gamma_1}^{\epsilon} u_1^{\varepsilon}) (Q(T_{\Gamma_1}^{\epsilon} u_5^{\varepsilon}) - Q(u_5)) \phi_5(t,x,\frac{x}{\varepsilon}) \mathrm{d}x \mathrm{d}\gamma_y \mathrm{d}t. \tag{4.59}$$

By (A2) and the strong convergence of u_1^{ε}, the first term on the right hand side of (4.59) converges two-scale to

$$\int\limits_0^T \int\limits_{\Omega} \int\limits_{\Gamma_1} k_3(t,y) R(u_1) Q(u_5) \phi_5(t,x,y) \mathrm{d}\gamma_y \mathrm{d}x \mathrm{d}t,$$

while the second integral of (4.59)

$$\varepsilon \int\limits_0^T \int\limits_{\Omega \times \Gamma_1} k_3(y) R(\mathcal{T}_{\Gamma_1}^\epsilon u_1^\varepsilon)(Q(\mathcal{T}_{\Gamma_1}^\epsilon u_5^\varepsilon) - Q(u_5))\phi_5(t, x, \frac{x}{\varepsilon})\mathrm{d}x\mathrm{d}\gamma_y\mathrm{d}t$$

$$\leq \; \varepsilon \left(\int\limits_0^T \int\limits_{\Omega \times \Gamma_1} |k_3(y) R(\mathcal{T}_{\Gamma_1}^\epsilon u_1^\varepsilon)\phi_5(t, x, \frac{x}{\varepsilon})|^2 \mathrm{d}x\mathrm{d}\gamma_y\mathrm{d}t \right)^{\frac{1}{2}}$$

$$\times \; \left(\int\limits_0^T \int\limits_{\Omega \times \Gamma_1} |Q(\mathcal{T}_{\Gamma_1}^\epsilon u_5^\varepsilon) - Q(u_5)|^2 \mathrm{d}x\mathrm{d}\gamma_y\mathrm{d}t \right)^{\frac{1}{2}} \quad \longrightarrow 0 \;\; \text{as} \;\; \varepsilon \to 0.$$

At this point, we have used again (A2) in combination with the strong convergence of $\mathcal{T}_{\Gamma_1}^\epsilon u_5^\varepsilon$. So, as result of passing to the limit $\varepsilon \to 0$ in (4.58), we get (4.51).

Since our positivity and L^∞-bounds are independent of the choice of ε, these properties hold true also for the weak solutions to the limit problem (4.50)-(4.51). Having these bounds available, the proof of the uniqueness follows very much in the same spirit as for the microscopic problem.

4.5.3   Strong formulation of the two-scale limit equations

Lemma 4.5.7. Assume the hypothesis of Lemma 4.4.8 to hold. Then the strong formulation of the two-scale limit equations (for all $t \in (0, T)$) reads

$$\partial_t u_1(t, x) + \nabla \cdot (-D_1 \nabla u_1(t, x)) = -\tilde{k}_1 u_1(t, x) + \tilde{k}_2 u_2(t, x)$$

$$- \frac{1}{|Y_1|} \int\limits_{\Gamma_1} k_3(y) R(u_1(t, x)) Q(u_5(t, x, y))\mathrm{d}\gamma_y, \; x \in \Omega$$

$$n \cdot (-D_1 \nabla u_1(t, x)) = 0, \; x \in \Gamma^D \cup \Gamma^N,$$

$$u_1(0, x) = u_{10}(x), \; x \in \bar{\Omega}, \tag{4.60}$$

$$\partial_t u_2(t, x) + \nabla \cdot (-D_2 \nabla u_2(t, x)) = \tilde{k}_1 u_1(t, x) - \tilde{k}_2 u_2(t, x)$$

$$+ \frac{|Y_2|}{|Y_1|} \tilde{a} u_3(t, x) - \tilde{b} u_2(t, x), \; x \in \Omega,$$

$$n \cdot (-D_2 \nabla u_2(t, x)) = 0, \; x \in \Gamma^D \cup \Gamma^N,$$

$$u_2(0, x) = u_{20}(x), \; x \in \bar{\Omega}, \tag{4.61}$$

$$\partial_t u_3(t, x) + \nabla \cdot (-D_3 \nabla u_3(t, x)) = -\tilde{a} u_3(t, x) + \frac{|Y_1|}{|Y_2|} \tilde{b} u_2(t, x), \; x \in \Omega,$$

$$u_3(0, x) = u_{30}(x), \; x \in \bar{\Omega},$$

$$u_3(t, x) = u_3^D(x), \; x \in \Gamma^D, \tag{4.62}$$

$$n \cdot (-D_3 \nabla u_3(t, x)) = 0, \; x \in \Gamma^N,$$

$$\partial_t u_4(t, x) + \nabla \cdot (-D_4 \nabla u_4(t, x)) = \tilde{k}_1 u_1(t, x), \; x \in \Omega,$$

$$u_4(0, x) = u_{40}(x), \; x \in \bar{\Omega}, \tag{4.63}$$

$$n \cdot (-D_4 \nabla u_4(t, x)) = 0, \; x \in \Gamma^D \cup \Gamma^N,$$

$$\partial_t u_5(t,x,y) = k_3(y) R(u_1(t,x)) Q(u_5(t,x,y)), \ x \in \Omega, y \in \Gamma_1,$$
$$u_5(0,x,y) = u_{50}(x,y) \ x \in \bar{\Omega}, y \in \Gamma_1, \tag{4.64}$$

where $D_i, i \in \{1,2,3,4\}$, $\tilde{a}, \tilde{b}$ and $\tilde{k}_j, j \in \{1,2\}$ are defined in Theorem 4.5.1.

4.6 Notes and comments

We applied the concept of two-scale convergence together with the periodic boundary unfolding to obtain the desired upscaled model equations[4]. In this way, we were able to provide a rigorous justification of the formal two-scale asymptotic expansion performed in Section 3.3 for the particular case of periodically-distributed microstructures.

We answer the question raised in Chapter 3 regarding the use of two different asymptotic expansions (3.18) and (3.50) for treating an ordinary differential equation posed on an oscillating boundary and justify rigorously the use of (3.18) in handling the ordinary differential equation.

There are some limitations of the two-scale convergence technique. The most important refer to:

1. In general, most of the microstructures are not periodic;

2. Boundary layers often arise inside microstructures;

3. Time-evolving microstructures.

The notion of stochastic homogenization was developed to deal with non-periodic structures. Zhikov and Pyatnitskii in [148] introduced a two-scale convergence method for stationary, ergodic cases on a compact probability space to homogenize a system posed for non-periodic structures of a certain class. This method was recently extended in [64] e.g. (also see [65]) to capture the effect of random geometries.

In many real world applications, boundary layers often arise at various length scales; see e.g., [71, 82]. They are induced by the presence of Dirichlet data or of especially ε−scaled geometries, see e.g. [6, 9, 21]. This averaging is cumbersome especially if one wants to capture information from the boundary layer.

Averaging scenarios with free and/or moving interfaces have been studied formally, for instance, in [79, 127]. Most such problems are hard to analyze mathematically and even basic solvability results may not hold. Here, we preferred to dwell on a class of x-dependent microstructures often named locally-periodic structures.

Local periodicity is included in the model equations in two ways: either the equations are defined in the locally-periodic domain or the transport coefficient and reaction rates are space-dependent in a non-monotonic way, see Remark 2.5.1.1 and [22].

We close this chapter by pointing out two multiscale convergence notions that possibly can treat some of the locally-periodic geometries. R. Alexandre introduced in [7] the notion of $\theta - 2$ convergence:

Definition 4.6.1. Let u^ε be a bounded sequence of functions in $L^2(\Omega)$. u^ε is said to converge $\theta - 2$ to $u_\theta \in L^2(\Omega; L^2_{\#\theta})$ [5] as $\varepsilon \to 0$ if and only if for any $\varphi \in \mathcal{D}(\Omega; C^\infty_{\#\theta})$[6],we

---

[4]The rigorous justification of the distributed-microstructure model derived in Subsection 3.3.2 of Chapter 3 for uniformly periodic and locally periodic domains is still to be done.

[5]$L^2(\Omega; L^2_{\#\theta})-$ the set of functions $\varphi(\cdot, z)$ which are L^2 in $x \in \Omega$ for all $z \in Y(x)$ ($Y(x)$ is defined in (4.66)) and for each $x \in \Omega$, the function $\varphi(x, \cdot)$ is L^2 and $Y(x)-$periodic.

[6]$\mathcal{D}(\Omega; C^\infty_{\#\theta})-$ the set of test functions $\varphi(\cdot, z)$ which are C^∞ in $x \in \Omega$ for all $z \in Y(x)$ and for each $x \in \Omega$, the function $\varphi(x, \cdot)$ is C^∞ and $Y(x)-$periodic.

have

$$\lim_{\varepsilon \to 0} \int\limits_{\Omega} u^{\varepsilon} \varphi_{\theta}^{\varepsilon}(x) \mathrm{d}x = \int\limits_{\Omega} \frac{1}{|Y(x)|} \int\limits_{Y(x)} u_{\theta}(x,z) \varphi(x,z) \mathrm{d}z \mathrm{d}x, \qquad (4.65)$$

where $\varphi_{\theta}^{\varepsilon}$ is defined by

$$\varphi_{\theta}^{\varepsilon}(x) := \varphi(x, \alpha_{\theta}^{\varepsilon}(x)), \text{ while },$$

$$\alpha_{\theta}^{\varepsilon}(x) := \nabla \theta(\theta^{-1}(x)) \cdot \left[\frac{\theta^{-1}(x) - \varepsilon k}{\varepsilon} \right] \text{ if } x \in \theta(P_{k}^{\varepsilon}), \ k \in \mathbb{Z}^{n},$$

$$\text{and} \qquad Y(x) \equiv \{ z, z = \nabla \theta(\theta^{-1}(x)) \alpha, \alpha \in Y \} \text{ for } x \in \Omega. \qquad (4.66)$$

$\theta : \mathbb{R}^{n} \to \mathbb{R}^{n}$ is a C^{2} diffeomorphism such that θ^{-1} has $1/2$ as Lipschitz constant. Recently, M. Ptashnyk introduced in [125] yet another extension of the two-scale convergence.

Definition 4.6.2. Let u^{ε} be a bounded sequence of functions in $L^{2}(\Omega)$. u^{ε} is said to converge locally-periodic two-scale to a unique function $u_{0} \in L^{2}(\Omega; L^{2}(Y_{x}))$ as $\varepsilon \to 0$ if and only if for any $\varphi \in C_{0}^{1}(\Omega; C_{\#}^{\infty}(Y_{x}))$

$$\lim_{\varepsilon \to 0} \int\limits_{\Omega} u^{\varepsilon}(x) \Sigma_{n=1}^{N(\varepsilon)} \varphi^{n}(x, \frac{x}{\varepsilon}) \chi_{\Omega_{n}^{\varepsilon}(x)} \mathrm{d}x = \frac{1}{|Y_{x}|} \int\limits_{\Omega} \int\limits_{Y_{x}} u_{0}(t,x,y) \varphi(t,x,y) \mathrm{d}y \mathrm{d}x, \qquad (4.67)$$

where φ^{n} is the locally-periodic approximation of φ and $\chi_{\Omega_{n}^{\varepsilon}(x)}$ are characteristic functions of Ω_{n}^{ε}.

Both notions of convergence are applicable to our partial differential equations but are not applicable to the nonlinear ordinary differential equation. In order to pass to the limit in the ordinary differential equation, a boundary unfolding operator designed for locally-periodic media would be needed. Note that the two concepts of locally-periodic two-scale convergence are somewhat similar. However they apply to different classes of microstructures [the notion by Alexandre is restricted to ball-like geometries, whereas the one by Ptashnyk seems more general]. We refer the reader to Theorem 2.2 in [7] and Theorem 6 in [125] for the corresponding compactness results.

Chapter 5

Corrector Estimates

Corrector estimates are useful tools to assess the quality of an averaging method. Basically, they emphasize the convergence rates measuring the error contribution produced while approximating macroscopic solutions by microscopic ones. The goal of this chapter is to obtain corrector estimates for our problem. We stress here on the fact that the corrector estimates obtained in this chapter require minimal regularity of the data and of the solutions to the cell problems, but work only for periodic microstructures.

The chapter is organized in the following fashion: In Section 5.1, we present a modified version of the microscopic model given in Chapter 2. We list the assumptions on the parameters and data involved in the model and give the definition of weak solutions. Section 5.2 is devoted to the analysis of the microscopic model. We introduce in Section 5.3 the notion of the periodic unfolding technique (introduced by Cioranescu *et al.* in [34]) as well as its basic properties. This section also includes the derivation of homogenized limit equations, this time using the unfolding idea. Section 5.4 contains the proofs of both corrector estimates and related technical lemmas. The main result of this chapter is Theorem 5.4.11 which basically states convergence results.

5.1 Geometry. Microscopic model. Assumptions

5.1.1 Geometry

We refer to the uniformly periodic geometry discussed in Chapter 2, Subsection 2.2.3.1; see also Fig. 5.1.

The results stated in this chapter have been reported in [57] as a joint collaboration with A. Muntean(Eindhoven) and M. Ptashnyk (Dundee).
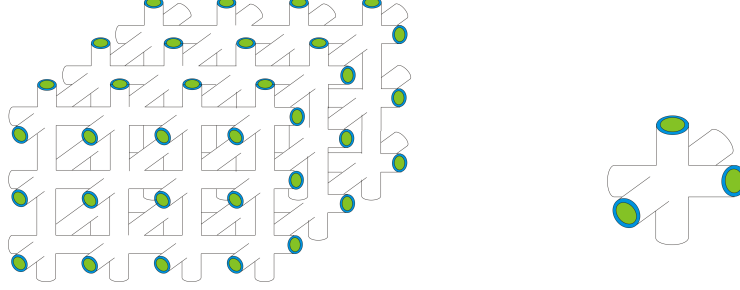
FIGURE 5.1: Left: Uniformly periodic system of connected "tubes". Right: Reference pore configuration.

5.1.2   Microscopic model

We modify the model equations described in Subsection 2.5.1 by replacing the linear reaction rates in the balance equations of for H_2SO_4 and $H_2S(aq)$ by non-linear reaction rates. To simplify the calculations, we neglect the partial differential equation for *moisture*. We consider here the following model equations:

$$\partial_t u_1^\varepsilon + \operatorname{div}(-d_1^\varepsilon \nabla u_1^\varepsilon) = -f(u_1^\varepsilon, u_2^\varepsilon) \qquad x \in \Omega_1^\varepsilon, \ t \in (0,T) \qquad (5.1)$$

$$\partial_t u_2^\varepsilon + \operatorname{div}(-d_2^\varepsilon \nabla u_2^\varepsilon) = f(u_1^\varepsilon, u_2^\varepsilon) \qquad x \in \Omega_1^\varepsilon, \ t \in (0,T) \qquad (5.2)$$

$$\partial_t u_3^\varepsilon + \operatorname{div}(-d_3^\varepsilon \nabla u_3^\varepsilon) = 0 \qquad x \in \Omega_2^\varepsilon, \ t \in (0,T) \qquad (5.3)$$

$$\partial_t u_5^\varepsilon = \eta^\varepsilon(u_1^\varepsilon, u_5^\varepsilon), \qquad x \in \Gamma_1^\varepsilon, \ t \in (0,T). \qquad (5.4)$$

The system is completed with the initial conditions

$$\begin{aligned} u_i^\varepsilon(x,0) &= u_{i0}(x) & x \in \Omega_1^\varepsilon, t = 0, i \in \{1,2\} & \qquad (5.5) \\ u_3^\varepsilon(x,0) &= u_{30}(x) & x \in \Omega_2^\varepsilon, t = 0 & \qquad (5.6) \\ u_5^\varepsilon(x,0) &= u_{50}(x) & x \in \Gamma_1^\varepsilon, t = 0. & \qquad (5.7) \end{aligned}$$

The associated boundary conditions are

$$\begin{aligned} -d_1^\varepsilon \nabla u_1^\varepsilon \cdot n^\varepsilon &= \varepsilon \eta(u_1^\varepsilon, u_5^\varepsilon) & x \in \Gamma_1^\varepsilon, t \in (0,T) & \qquad (5.8) \\ -d_1^\varepsilon \nabla u_1^\varepsilon \cdot n^\varepsilon &= 0 & x \in \Gamma_2^\varepsilon, t \in (0,T) & \qquad (5.9) \\ -d_2^\varepsilon \nabla u_2^\varepsilon \cdot n^\varepsilon &= 0 & x \in \Gamma_1^\varepsilon, t \in (0,T) & \qquad (5.10) \\ -d_2^\varepsilon \nabla u_2^\varepsilon \cdot n^\varepsilon &= -\varepsilon(a^\varepsilon(x)u_3^\varepsilon - b^\varepsilon(x)u_2^\varepsilon) & x \in \Gamma_2^\varepsilon, t \in (0,T) & \qquad (5.11) \\ -d_3^\varepsilon \nabla u_3^\varepsilon \cdot n^\varepsilon &= \varepsilon(a^\varepsilon(x)u_3^\varepsilon - b^\varepsilon(x)u_2^\varepsilon) & x \in \Gamma_2^\varepsilon, t \in (0,T) & \qquad (5.12) \\ u_1^\varepsilon, u_2^\varepsilon &= 0 & x \in \partial\Omega \cap \partial\Omega_1^\varepsilon, t \in (0,T) & \ (5.13) \\ u_3^\varepsilon &= 0 & x \in \partial\Omega \cap \partial\Omega_2^\varepsilon, t \in (0,T). & \ (5.14) \end{aligned}$$

Assumption 5.1.1. We assume the following restriction on the data and model parameters:

(A1) $d_k, \partial_t d_k \in L^\infty(0,T; L^\infty_\#(Y))^{3\times 3}$, $k \in \{1,2,3\}$, $(d_k(t,x)\xi, \xi) \geq d_k^0|\xi|^2$ for $d_k^0 > 0$, for every $\xi \in \mathbb{R}^3$ and a.e. $(t,x) \in (0,T) \times Y$.

(A2) $k_3 \in L^\infty_\#(\Gamma_1)$ is nonnegative and $\eta(\alpha, \beta) = k_3(y)R(\alpha)Q(\beta)$, where $R : \mathbb{R} \to \mathbb{R}_+$, $Q : \mathbb{R} \to \mathbb{R}_+$ are sublinear and locally Lipschitz continuous. Furthermore, $R(\alpha) = 0$ for $\alpha < 0$ and $Q(\beta) = 0$ for $\beta \geq \beta_{max}$, with some $\beta_{max} > 0$.

(A3) $f \in C^1(\mathbb{R}^2)$ is sublinear and globally Lipschitz continuous in both variables, i.e. $|f(\alpha,\beta)| \leq C_f(1 + |\alpha| + |\beta|)$, $|f(\alpha_1, \beta_1) - f(\alpha_2, \beta_2)| \leq C_L(|\alpha_1 - \alpha_2| + |\beta_1 - \beta_2|)$ for some $C_L, C_f > 0$, and $f(\alpha,\beta) = 0$ for $\alpha < 0$ or $\beta < 0$.

(A4) $a, b \in L^\infty_\#(\Gamma_2)$, $a(y)$ and $b(y)$ are positive for a.e. $y \in \Gamma_2$ and there exist M_2, M_3 such that $b(y)M_2 = a(y)M_3$ for a.e. $y \in \Gamma_2$.

(A5) Initial data $(u_1(0), u_2(0), u_3(0), u_5(0)) \in [H^2(\Omega) \cap H_0^1(\Omega) \cap L^\infty(\Omega)]^3 \times L^\infty_{\mathrm{per}}(\Gamma_1)$ are nonnegative and $u_2(0) \leq M_2$, $u_3(0) \leq M_3$ a.e. in Ω.

The oscillating coefficients are periodic and are defined in Subsection 2.5.1.1. Furthermore, we define the space

$$H_{\partial\Omega}^1(\Omega_i^\varepsilon) := \{u \in H^1(\Omega_i^\varepsilon) : u = 0 \text{ on } \partial\Omega \cap \partial\Omega_i^\varepsilon\}, \; i = 1, 2.$$

Definition 5.1.2. We call $(u_1^\varepsilon, u_2^\varepsilon, u_3^\varepsilon, u_5^\varepsilon)$ a weak solution of (6.1) – (6.8) if $u_1^\varepsilon, u_2^\varepsilon \in L^2(0,T; H_{\partial\Omega}^1(\Omega_2^\varepsilon)) \cap H^1(0,T; L^2(\Omega_2^\varepsilon))$, $u_3^\varepsilon \in L^2(0,T; H_{\partial\Omega}^1(\Omega_2^\varepsilon)) \cap H^1(0,T; L^2(\Omega_2^\varepsilon))$, $u_5^\varepsilon \in H^1(0,T; L^2(\Gamma_1^\varepsilon))$ and the following equations are satisfied:

$$\int_0^T \iint_{\Omega_1^\varepsilon} \left(\partial_t u_1^\varepsilon \phi_1 + d_1^\varepsilon \nabla u_1^\varepsilon \nabla \phi_1 + f(u_1^\varepsilon, u_2^\varepsilon)\phi_1\right) \mathrm{d}x\mathrm{d}t = -\varepsilon \int_0^T \iint_{\Gamma_1^\varepsilon} \eta(u_1^\varepsilon, u_5^\varepsilon)\phi_1 \mathrm{d}\gamma_x \mathrm{d}t, \quad (5.15)$$

$$\int_0^T \iint_{\Omega_1^\varepsilon} \left(\partial_t u_2^\varepsilon \phi_2 + d_2^\varepsilon \nabla u_2^\varepsilon \nabla \phi_2 - f(u_1^\varepsilon, u_2^\varepsilon)\phi_2\right) \mathrm{d}x\mathrm{d}t = \varepsilon \int_0^T \iint_{\Gamma_2^\varepsilon} \left(a^\varepsilon u_3^\varepsilon - b^\varepsilon u_2^\varepsilon\right)\phi_2 \mathrm{d}\gamma_x \mathrm{d}t, \quad (5.16)$$

$$\int_0^T \iint_{\Omega_2^\varepsilon} \left(\partial_t u_3^\varepsilon \phi_3 + d_3^\varepsilon \nabla u_3^\varepsilon \nabla \phi_3\right) \mathrm{d}x\mathrm{d}t = -\varepsilon \int_0^T \iint_{\Gamma_2^\varepsilon} \left(a^\varepsilon u_3^\varepsilon - b^\varepsilon u_2^\varepsilon\right)\phi_3 \mathrm{d}\gamma_x \mathrm{d}t, \quad (5.17)$$

$$\varepsilon \int_0^T \iint_{\Gamma_1^\varepsilon} \partial_t u_5^\varepsilon \phi_5 \mathrm{d}\gamma_x \mathrm{d}t = \varepsilon \int_0^T \iint_{\Gamma_1^\varepsilon} \eta(u_1^\varepsilon, u_5^\varepsilon)\phi_5 \mathrm{d}\gamma_x \mathrm{d}t \quad (5.18)$$

for all $\phi_j \in L^2(0,T; H_{\partial\Omega}^1(\Omega_1^\varepsilon))$, $j \in \{1,2\}$, $\phi_3 \in L^2(0,T; H_{\partial\Omega}^1(\Omega_2^\varepsilon))$, $\phi_5 \in L^2((0,T) \times \Gamma_1^\varepsilon)$ and $u_1^\varepsilon(t) \to u_{10}$, $u_2^\varepsilon(t) \to u_{20}$ in $L^2(\Omega_1^\varepsilon)$, $u_3^\varepsilon(t) \to u_{30}$ in $L^2(\Omega_2^\varepsilon)$, $u_5^\varepsilon(t) \to u_{50}$ in $L^2(\Gamma_1^\varepsilon)$ as $t \to 0$.

5.2   Analysis of the microscopic model

This section is devoted to the well-posedness of the microscopic model (5.1) – (5.14).

Lemma 5.2.1. *(a priori estimates)* Under the Assumption 5.1.1, solutions to the problem (5.15) – (5.18) satisfy the following *a priori* estimates:

$$
\begin{aligned}
\|u_1^\varepsilon\|_{L^\infty(0,T;L^2(\Omega_1^\varepsilon))} + \|\nabla u_1^\varepsilon\|_{L^2((0,T)\times\Omega_1^\varepsilon)} &\leq & C \\
\|u_2^\varepsilon\|_{L^\infty(0,T;L^2(\Omega_1^\varepsilon))} + \|\nabla u_2^\varepsilon\|_{L^2((0,T)\times\Omega_1^\varepsilon)} &\leq & C, \\
\|u_3^\varepsilon\|_{L^\infty(0,T;L^2(\Omega_2^\varepsilon))} + \|\nabla u_3^\varepsilon\|_{L^2((0,T)\times\Omega_2^\varepsilon)} &\leq & C, \\
\varepsilon^{1/2}\|u_5^\varepsilon\|_{L^\infty(0,T;L^2(\Gamma_1^\varepsilon))} + \varepsilon^{1/2}\|\partial_t u_5^\varepsilon\|_{L^2((0,T)\times\Gamma_1^\varepsilon)} &\leq & C,
\end{aligned}
\tag{5.19}
$$

where the constant C is independent of ε.

Proof. First, we consider as test functions $\phi_1 = u_1^\varepsilon$ in (5.15), $\phi_2 = u_2^\varepsilon$ in (5.16), $\phi_3 = u_3^\varepsilon$ in (5.17) and use Assumption 5.1.1, Young's inequality, and the trace inequality to get

$$
\varepsilon \int\limits_0^t \int\limits_{\Gamma_2^\varepsilon} u_3^\varepsilon u_2^\varepsilon \mathrm{d}\gamma_x d\tau \quad \leq C \int\limits_0^t \int\limits_{\Omega_2^\varepsilon} (|u_3^\varepsilon|^2 + \varepsilon^2|\nabla u_3^\varepsilon|^2)\mathrm{d}\gamma_x d\tau
$$

$$
+ C \int\limits_0^t \int\limits_{\Omega_1^\varepsilon} (|u_2^\varepsilon|^2 + \varepsilon^2|\nabla u_2^\varepsilon|^2)\mathrm{d}\gamma_x d\tau.
$$

Then, adding the obtained inequalities, choosing ε conveniently and applying Gronwall's inequality imply the first three estimates in Lemma.
Taking $\phi_5 = u_5^\varepsilon$ as a test function in (5.18) and using (A2) from Assumption 5.1.1 and the estimates for u_1^ε, yield the estimate for u_5^ε. The choice of test function $\phi_5 = \partial_t u_5^\varepsilon$ in (5.18), the sublinearity of R, the boundedness of Q and the estimates for u_1^ε imply the boundedness of $\varepsilon^{1/2}\|\partial_t u_5^\varepsilon\|_{L^2((0,T)\times\Gamma_1^\varepsilon)}$.

Lemma 5.2.2. (Positivity and boundedness) Let Assumption 5.1.1 be fulfilled. Then the following estimates hold:

(i) $u_1^\varepsilon(t), u_2^\varepsilon(t) \geq 0$ a.e. in Ω_1^ε, $u_3^\varepsilon(t) \geq 0$ a.e. in Ω_2^ε and $u_1^\varepsilon(t), u_5^\varepsilon(t) \geq 0$ a.e. on Γ_1^ε, for a.e. $t \in (0,T)$.

(ii) $u_1^\varepsilon(t) \leq M_1 e^{A_1 t}$, $u_2^\varepsilon(t) \leq M_2 e^{A_2 t}$ a.e. in Ω_1^ε, $u_3^\varepsilon(t) \leq M_3 e^{A_3 t}$ a.e. in Ω_2^ε, and $u_1^\varepsilon(t) \leq M_1 e^{A_1 t}$, $u_5^\varepsilon(t) \leq M_5 e^{A_5 t}$ a.e. on Γ_1^ε, for a.e. $t \in (0,T)$, with some positive numbers A_j, M_j, where $j = 1, 2, 3, 5$.

Proof. (i) To show the positivity of a weak solution we consider $-u_1^{\varepsilon-}$ as test function in (5.15), $-u_2^{\varepsilon-}$ in (5.16), $-u_3^{\varepsilon-}$ in (5.17) , and $-u_5^{\varepsilon-}$ in (5.18). The integrals involving $f(u_1^\varepsilon, u_2^\varepsilon)u_1^{\varepsilon-}$, $f(u_1^\varepsilon, u_2^\varepsilon)u_2^{\varepsilon-}$ and $\eta(u_1^\varepsilon, u_5^\varepsilon)u_1^{\varepsilon-}$ are zero by Assumption 5.1.1. In the integrals over Γ_2^ε we use the positivity of a and b and

the estimate $-u_2^\varepsilon u_3^{\varepsilon-} = -(u_2^{\varepsilon+} - u_2^{\varepsilon-})u_3^{\varepsilon-} \leq u_2^{\varepsilon-}u_3^{\varepsilon-}$. Due to the positivity of η, the right hand side in the equation for u_5^ε, with the test function $\phi_5 = -u_5^{\varepsilon-}$, is nonpositive. Adding the obtained inequalities, applying both Young's and the trace inequalities, considering ε sufficiently small, we obtain, due to positivity of the initial data and using Gronwall's inequality, that

$$\|u_1^{\varepsilon-}(t)\|_{L^2(\Omega_1^\varepsilon)} + \|u_2^{\varepsilon-}(t)\|_{L^2(\Omega_1^\varepsilon)} + \|u_3^{\varepsilon-}(t)\|_{L^2(\Omega_2^\varepsilon)} + \|u_5^{\varepsilon-}(t)\|_{L^2(\Gamma_1^\varepsilon)} \leq 0,$$

for a.e. $t \in (0,T)$. Thus, negative parts of the involved concentrations are equal zero a.e. in $(0,T) \times \Omega_i^\varepsilon$, $i = 1,2$, or in $(0,T) \times \Gamma_1^\varepsilon$, respectively.

(ii) To show the boundedness of solutions, we consider $U_1^\varepsilon = (u_1^\varepsilon - e^{A_1 t}M_1)^+$ as a test function in (5.15), $U_2^\varepsilon = (u_2^\varepsilon - e^{A_2 t}M_2)^+$ in (5.16) $U_3^\varepsilon = (u_3^\varepsilon - e^{A_3 t}M_3)^+$ in (5.17), where $(\phi - M)^+ = \max\{0, \phi - M\}$ and M_i, $i = 1,2,3$, are positive numbers, such that $u_{10}(x) \leq M_1$, $u_{20}(x) \leq M_2$, $u_{30}(x) \leq M_3$ a.e in Ω, also $A_2 = A_3$ and M_2, M_3 are given by $(A4)$ in Assumption 5.1.1. Addition of the obtained equations combined with Assumption 5.1.1 yields

$$\int_0^\tau \left(\int_{\Omega_1^\varepsilon} \partial_t(|U_1^\varepsilon|^2 + |U_2^\varepsilon|^2) + |\nabla U_1^\varepsilon|^2 + |\nabla U_2^\varepsilon|^2 \mathrm{d}x + \int_{\Omega_2^\varepsilon} \partial_t |U_3^\varepsilon|^2 + |\nabla U_3^\varepsilon|^2 \mathrm{d}x \right) \mathrm{d}t$$

$$\leq C \int_0^\tau \left[\int_{\Omega_1^\varepsilon} \left((e^{A_1 t}M_1(C_f - A_1) + C_f e^{A_2 t}M_2)U_1^\varepsilon + |U_1^\varepsilon|^2 + |U_2^\varepsilon|^2 + \varepsilon^2 |\nabla U_2^\varepsilon|^2 \right. \right.$$

$$\left. + (C_f e^{A_1 t}M_1 + e^{A_2 t}M_2(C_f - M_2))U_2^\varepsilon \right) \mathrm{d}x + \int_{\Omega_2^\varepsilon} \left(|U_3^\varepsilon|^2 + \varepsilon^2 |\nabla U_3^\varepsilon|^2 \right) \mathrm{d}x \right] \mathrm{d}t.$$

Choosing A_1, M_1 such that $C_f e^{A_1 t}M_1 + C_f e^{A_2 t}M_2 - A_1 e^{A_1 t}M_1 \leq 0$ and $C_f e^{A_1 t}M_1 + C_f e^{A_2 t}M_2 - A_2 e^{A_2 t}M_2 \leq 0$ for a.e. $t \in (0,T)$, and ε sufficiently small, Gronwall's inequality implies the estimates for u_1^ε, u_2^ε, u_3^ε, stated in Lemma 5.2.2. Lemma 4.2.3 in Chapter 4 and H^1-estimates for u_1^ε in Lemma 5.2.1 imply $u_1^\varepsilon(t) \geq 0$ and $u_1^\varepsilon(t) \leq e^{A_1 t}M_1$ a.e on Γ_1^ε for a.e. $t \in (0,T)$. The assumption on η and equation (5.18) with the test function $(u_5^\varepsilon - e^{A_5 t}M_5)^+$, where $u_{50}(x) \leq M_5$ a.e. on Γ_1, yield

$$\varepsilon \int_0^\tau \int_{\Gamma_1^\varepsilon} \left(\frac{1}{2}\partial_t |(u_5^\varepsilon - e^{A_5 t}M_5)^+|^2 + A_5 e^{A_5 t}M_5(u_5^\varepsilon - e^{A_5 t}M_5)^+ \right) \mathrm{d}\gamma_x \mathrm{d}t =$$

$$\varepsilon \int_0^\tau \int_{\Gamma_1^\varepsilon} \eta(u_1^\varepsilon, u_5^\varepsilon)(u_5^\varepsilon - e^{A_5 t}M_5)^+ \mathrm{d}\gamma_x \mathrm{d}t \leq C_\eta(A_1, M_1)\varepsilon \int_0^\tau \int_{\Gamma_1^\varepsilon} (u_5^\varepsilon - e^{A_5 t}M_5)^+ \mathrm{d}\gamma_x \mathrm{d}t.$$

This, for convenient A_5 and M_5 such that $C_\eta \leq A_5 M_5 e^{A_5 t}$, implies the boundedness of u_5^ε on Γ_1^ε for a.e. $t \in (0,T)$.

Lemma 5.2.3. Under Assumption 5.1.1, we obtain the following estimates independent of ε:

$$\|\partial_t u_1^\varepsilon\|_{L^2((0,T)\times\Omega_1^\varepsilon)} + \|\partial_t u_2^\varepsilon\|_{L^2(0,T;H^1(\Omega_1^\varepsilon))} + \|\partial_t u_3^\varepsilon\|_{L^2(0,T;H^1(\Omega_2^\varepsilon))} \le C.$$

Proof We test (5.15) with $\phi_1 = \partial_t u_1^\varepsilon$, and using the structure of η, the regularity assumptions on R, Q and the boundedness of u_1^ε and u_5^ε on Γ_1^ε, we estimate the boundary integral by

$$\varepsilon \int\limits_0^\tau \int\limits_{\Gamma_1^\varepsilon} \eta(u_1^\varepsilon, u_5^\varepsilon)\partial_t u^\varepsilon \mathrm{d}\gamma_x \mathrm{d}t$$

$$= \varepsilon \int\limits_0^\tau \int\limits_{\Gamma_1^\varepsilon} k_3^\varepsilon \Big(\partial_t\big(\mathcal{R}(u_1^\varepsilon)Q(u_5^\varepsilon)\big) - \mathcal{R}(u_1^\varepsilon)Q'(u_5^\varepsilon)\partial_t u_5^\varepsilon\Big)\mathrm{d}\gamma_x \mathrm{d}t$$

$$\le C \int\limits_{\Omega_1^\varepsilon} \Big(|u_1^\varepsilon(\tau)|^2 + \varepsilon^2|\nabla u_1^\varepsilon(\tau)|^2 + |u_{10}|^2 + \varepsilon^2|\nabla u_{10}|^2\Big)\mathrm{d}x$$

$$+ C\varepsilon \int\limits_0^\tau \int\limits_{\Gamma_1^\varepsilon} \Big(1 + |\partial_t u_5^\varepsilon|^2\Big)\mathrm{d}\gamma_x \mathrm{d}t,$$

where $\mathcal{R}(\alpha) = \int\limits_0^\alpha R(\xi)d\xi$. Then, Assumption 5.1.1, the estimates in Lemma 5.2.1 and the fact that $d_1^0/2 - \varepsilon^2 \ge 0$ for appropriate ε, imply the estimate for $\partial_t u_1^\varepsilon$.

In order to estimate $\partial_t u_2^\varepsilon$ and $\partial_t u_3^\varepsilon$, we differentiate the corresponding equations with respect to the time variable and then test the resulting partial differential equations with $\partial_t u_2^\varepsilon$ and $\partial_t u_3^\varepsilon$, respectively. Due to assumptions on f and using the trace inequality, we obtain

$$\int\limits_{\Omega_1^\varepsilon} |\partial_t u_2^\varepsilon|^2 \mathrm{d}x + C \int\limits_0^\tau\int\limits_{\Omega_1^\varepsilon} |\nabla\partial_t u_2^\varepsilon|^2 \mathrm{d}x\mathrm{d}t \le C \int\limits_0^\tau\int\limits_{\Omega_2^\varepsilon} \big(|\partial_t u_3^\varepsilon|^2 + \varepsilon^2|\nabla\partial_t u_3^\varepsilon|^2\big)\mathrm{d}x\mathrm{d}t$$

$$+ C \int\limits_0^\tau\int\limits_{\Omega_1^\varepsilon} \big(|\partial_t u_1^\varepsilon|^2 + |\partial_t u_2^\varepsilon|^2 + |\nabla u_2^\varepsilon|^2\big)\mathrm{d}x\mathrm{d}t + \int\limits_{\Omega_1^\varepsilon} |\partial_t u_2^\varepsilon(0)|^2 \mathrm{d}x, \qquad (5.20)$$

and

$$\int\limits_{\Omega_2^\varepsilon} |\partial_t u_3^\varepsilon|^2 \mathrm{d}x + C \int\limits_0^\tau\int\limits_{\Omega_2^\varepsilon} |\nabla\partial_t u_3^\varepsilon|^2 \mathrm{d}x\mathrm{d}t \le C \int\limits_0^\tau\int\limits_{\Omega_2^\varepsilon} \big(|\partial_t u_3^\varepsilon|^2 + |\nabla u_3^\varepsilon|^2\big)\mathrm{d}x\mathrm{d}t$$

$$+ \int\limits_{\Omega_2^\varepsilon} |\partial_t u_3^\varepsilon(0)|^2 \mathrm{d}x + C \int\limits_0^\tau\int\limits_{\Omega_1^\varepsilon} \big(|\partial_t u_2^\varepsilon|^2 + \varepsilon^2|\nabla\partial_t u_2^\varepsilon|^2\big)\mathrm{d}x\mathrm{d}t. \qquad (5.21)$$

The regularity assumptions imply that $\|\partial_t u_2^\varepsilon(0)\|_{L^2(\Omega_1^\varepsilon)}$ and $\|\partial_t u_3^\varepsilon(0)\|_{L^2(\Omega_2^\varepsilon)}$ can be estimated by the H^2-norm of u_{20} and u_{30}. Adding (5.20) and (5.21), making use of estimates for $\partial_t u_1^\varepsilon$, ∇u_2^ε and ∇u_3^ε, and applying Gronwall's lemma, give the desired estimates.

Theorem 5.2.4. (Existence and uniqueness) Let Assumption 5.1.1 be fulfilled. Then there exists a unique global-in-time weak solution in the sense of Definition 5.1.2.

Proof. The Lipschitz continuity of f, local Lipschitz continuity of η and the boundedness of u_1^ε and u_5^ε on Γ_1^ε ensure the uniqueness result. The existence of weak solutions follows by a standard Galerkin approach given in [80] by using the *a priori* estimates in Lemmas 5.2.1, 5.2.2 and 5.2.3.

5.3 Upscaled model

We begin with introducing the unfolding operator and describe some of its properties. For more properties and proofs, we refer to [34, 36, 37, 110]. First we present the unfolding operators defined for perforated domains and then we define boundary unfolding operators for $\varepsilon-$dependent hypersurfaces. The notion of unfolding provides a way to connect the unfolded sequence defined on the fixed domain to the sequences defined in $\varepsilon-$dependent domain. We define

$$
\begin{aligned}
(\mathbb{R}^n)^i &= \mathbb{R}^n \cap \{\varepsilon(Y_i + \xi), \xi \in \mathbb{Z}^n\}, \\
\tilde{\Omega}_i^{\varepsilon,l} &= \{x \in (\mathbb{R}^n)^i : \text{dist}(x, \Omega_i^\varepsilon) < l\sqrt{n}\varepsilon\}, \\
\tilde{\Omega}^{\varepsilon,l} &= \{x \in \mathbb{R}^n : \text{dist}(x, \Omega) < l\sqrt{n}\varepsilon\}, \\
\tilde{\Omega}_{int}^\varepsilon &= \text{Int}(\cup_{k\in\mathbb{Z}^3}\{\varepsilon\overline{Y^k}, \varepsilon Y^k \subset \Omega\}),
\end{aligned}
$$

for $l = 1, 2$, and $\tilde{\Gamma}_{i,int}^\varepsilon = \cup_{k\in\mathbb{Z}^3}\{\varepsilon\overline{\Gamma_i^k}, \varepsilon Y^k \subset \Omega\}$, where $i = 1, 2$.

Definition 5.3.1. (Domain and boundary unfolding operator)

1. For any function ϕ which is Lebesgue-measurable on the perforated domain Ω_i^ε, the unfolding operators $\mathcal{T}_{Y_i}^\varepsilon : \Omega_i^\varepsilon \to \Omega \times Y_i$, $i = 1, 2$, are defined

$$
\mathcal{T}_{Y_i}^\varepsilon(\phi)(x,y) = \begin{cases} \phi(\varepsilon\left[\frac{x}{\varepsilon}\right]_Y + \varepsilon y) & \text{a.e. for } y \in Y_i, \ x \in \tilde{\Omega}_{int}^\varepsilon, \\ 0 & \text{a.e. for } y \in Y_i, \ x \in \Omega \setminus \tilde{\Omega}_{int}^\varepsilon, \end{cases}
$$

   where $k := \left[\frac{x}{\varepsilon}\right]$ is the unique integer combination, such that $x - \left[\frac{x}{\varepsilon}\right]$ belongs to Y_i. We note that for $w \in H^1(\Omega)$ it holds that $\mathcal{T}_{Y_i}^\varepsilon(w|_{\Omega_i^\varepsilon}) = \mathcal{T}_{Y_i}^\varepsilon(w)|_{\Omega \times Y_i}$.

2. For any function ϕ which is Lebesgue-measurable on the oscillating boundary Γ_i^ε, the boundary unfolding operators $\mathcal{T}_{\Gamma_i}^\varepsilon : \Gamma_i^\varepsilon \to \Omega \times \Gamma_i$, $i = 1, 2$ are defined by

$$
\mathcal{T}_{\Gamma_i}^\varepsilon(\phi)(x,y) = \begin{cases} \phi(\varepsilon\left[\frac{x}{\varepsilon}\right]_Y + \varepsilon y) & \text{a.e. for } y \in \Gamma_i, \ x \in \tilde{\Omega}_{int}^\varepsilon, \\ 0 & \text{a.e. for } y \in \Gamma_i, \ x \in \Omega \setminus \tilde{\Omega}_{int}^\varepsilon. \end{cases}
$$

In the following lemma, we state some important properties of the unfolding operator which will be used frequently in the next sections.

Lemma 5.3.2. (Some properties of the unfolding operator)

1. Let $v \in L^p_{\#}(Y_i)$ and $v^\varepsilon(x) = v(\frac{x}{\varepsilon})$, then $\mathcal{T}^\varepsilon_{Y_i}(v^\varepsilon)(x, y) = v(y)$.

2. For $v, w \in L^p(\Omega^\varepsilon_i)$ and $\phi, \psi \in L^p(\Gamma^\varepsilon_i)$, it holds that $\mathcal{T}^\varepsilon_{Y_i}(v\, w) = \mathcal{T}^\varepsilon_{Y_i}(v)\mathcal{T}^\varepsilon_{Y_i}(w)$ and $\mathcal{T}^\varepsilon_{\Gamma_i}(\phi\, \psi) = \mathcal{T}^\varepsilon_{\Gamma_i}(\phi)\mathcal{T}^\varepsilon_{\Gamma_i}(\psi)$.

3. For $w \in L^p(\Omega^\varepsilon_i)$ for $p \in [1, \infty)$, we have

$$\|\mathcal{T}^\varepsilon_{Y_i} w\|_{L^p(\Omega \times Y_i)} = |Y|^{1/p} \|w\|_{L^p(\tilde{\Omega}^\varepsilon_{i,int})} \le |Y|^{1/p} \|w\|_{L^p(\Omega^\varepsilon_i)}.$$

4. For $w \in L^p(\Gamma^\varepsilon_i)$, $p \in [1, \infty)$, we have

$$\|\mathcal{T}^\varepsilon_{\Gamma_i} w\|_{L^p(\Omega \times \Gamma_i)} = \varepsilon^{1/p} |Y|^{1/p} \|w\|_{L^p(\tilde{\Gamma}^\varepsilon_{i,int})} \le \varepsilon^{1/p} |Y|^{1/p} \|u\|_{L^p(\Gamma^\varepsilon_i)}.$$

5. If $w \in L^p(\Omega)$, $p \in [1, \infty)$, then $\mathcal{T}^\varepsilon_{Y_i} w \to w$ strongly in $L^p(\Omega \times Y_i)$ as $\varepsilon \to 0$.

6. For $w \in W^{1,p}(\Omega^\varepsilon_i)$, $1 < p < +\infty$,

$$\|\mathcal{T}^\varepsilon_{\Gamma_i} w\|_{L^p(\Omega \times \Gamma_i)} \le C\big(\|w\|_{L^p(\Omega^\varepsilon_i)} + \varepsilon\|\nabla w\|_{L^p(\Omega^\varepsilon_i)^n}\big).$$

7. For $w \in W^{1,p}(\Omega^\varepsilon_i)$, it holds that $\mathcal{T}^\varepsilon_{Y_i}(w) \in L^p(\Omega, W^{1,p}(Y_i))$ and $\nabla_y \mathcal{T}^\varepsilon_{Y_i}(w) = \varepsilon \mathcal{T}^\varepsilon_{Y_i}(\nabla w)$.

For proofs and details, see [33].

Now we state two important results which are needed in order to get strong convergence on the boundary.

Theorem 5.3.3. Let $p \in (1, \infty)$ and $i = 1, 2$.

1. For any $\{\phi_\varepsilon\} \subset W^{1,p}(\Omega^\varepsilon_i)$ that satisfies $\|\phi_\varepsilon\|_{W^{1,p}(\Omega^\varepsilon_i)} \le C$, there exists a subsequence of $\{\phi_\varepsilon\}$ (still denoted by ϕ_ε), and $\phi \in W^{1,p}(\Omega)$, $\hat{\phi} \in L^p(\Omega; W^{1,p}_{\#}(Y_i))$, such that

$$\mathcal{T}^\varepsilon_{Y_1} \phi_\varepsilon \to \phi \quad \text{strongly in} \quad L^p_{loc}(\Omega; W^{1,p}(Y_i)),$$
$$\mathcal{T}^\varepsilon_{Y_1} \phi_\varepsilon \rightharpoonup \phi \quad \text{weakly in} \quad L^p(\Omega; W^{1,p}(Y_i)),$$
$$\mathcal{T}^\varepsilon_{Y_1}(\nabla \phi_\varepsilon) \rightharpoonup \nabla \phi + \nabla_y \hat{\phi} \quad \text{weakly in} \quad L^p(\Omega \times Y_i).$$

2. For $\{\phi_\varepsilon\} \subset W^{1,p}_0(\Omega^\varepsilon_i)$, such that $\|\phi_\varepsilon\|_{W^{1,p}_0(\Omega^\varepsilon_i)} \le C$, there exists a subsequence of $\{\phi^\varepsilon\}$ (still denoted by ϕ_ε) and $\phi \in W^{1,p}_0(\Omega)$, $\hat{\phi} \in L^p(\Omega; W^{1,p}_{\#}(Y_i))$, such that

$$\mathcal{T}^\varepsilon_{Y_i} \phi_\varepsilon \to \phi \quad \text{strongly in} \quad L^p(\Omega; W^{1,p}(Y_i)),$$
$$\mathcal{T}^\varepsilon_{Y_i}(\nabla \phi_\varepsilon) \rightharpoonup \nabla \phi + \nabla_y \hat{\phi} \quad \text{weakly in} \quad L^p(\Omega \times Y_i).$$

3. For $\{\phi_\varepsilon\} \subset L^p(\Gamma_i^\varepsilon)$ such that $\varepsilon^{1/p}\|\phi_\varepsilon\|_{L^p(\Gamma_i^\varepsilon)} \leq C$ there exists a subsequence of $\{\phi_\varepsilon\}$ and $\phi \in L^p(\Omega \times \Gamma_i)$ such that

$$\mathcal{T}_{\Gamma_i}^\varepsilon(\phi_\varepsilon) \rightharpoonup \phi \quad \text{weakly in} \quad L^p(\Omega \times \Gamma_i).$$

For proofs and details, see [33].

Lemma 5.3.4. (Compactness) Under Assumption 5.1.1, there exist $u_1, u_2, u_3 \in L^2(0,T; H_0^1(\Omega)) \cap H^1(0,T; L^2(\Omega))$, $\tilde{u}_1, \tilde{u}_2 \in L^2((0,T) \times \Omega; H_\#^1(Y_1))$, $\tilde{u}_3 \in L^2((0,T) \times \Omega; H_\#^1(Y_2))$, and $u_5 \in H^1(0,T, L^2(\Omega \times \Gamma_1))$ such that (up to a subsequence) for $\varepsilon \to 0$

$$
\begin{aligned}
\mathcal{T}_{Y_1}^\varepsilon(u_1^\varepsilon) \to u_1, \mathcal{T}_{Y_1}^\varepsilon(u_2^\varepsilon) \to u_2 && \text{in } L^2((0,T) \times \Omega; H^1(Y_1)), \\
\partial_t \mathcal{T}_{Y_1}^\varepsilon(u_1^\varepsilon) \rightharpoonup \partial_t u_1, \partial_t \mathcal{T}_{Y_1}^\varepsilon(u_2^\varepsilon) \rightharpoonup \partial_t u_2 && \text{in } L^2((0,T) \times \Omega \times Y_1), \\
\mathcal{T}_{Y_2}^\varepsilon(u_3^\varepsilon) \to u_3, \partial_t \mathcal{T}_{Y_2}^\varepsilon(u_3^\varepsilon) \rightharpoonup \partial_t u_3 && \text{in } L^2((0,T) \times \Omega; H^1(Y_2)), \\
\mathcal{T}_{Y_1}^\varepsilon(\nabla u_1^\varepsilon) \rightharpoonup \nabla u_1 + \nabla_y \tilde{u}_1 && \text{in } L^2((0,T) \times \Omega \times Y_1), \\
\mathcal{T}_{Y_1}^\varepsilon(\nabla u_2^\varepsilon) \rightharpoonup \nabla u_2 + \nabla_y \tilde{u}_2 && \text{in } L^2((0,T) \times \Omega \times Y_1), \\
\mathcal{T}_{Y_2}^\varepsilon(\nabla u_3^\varepsilon) \rightharpoonup \nabla u_3 + \nabla_y \tilde{u}_3 && \text{in } L^2((0,T) \times \Omega \times Y_2),
\end{aligned}
\tag{5.22}
$$

and

$$
\begin{aligned}
\mathcal{T}_{\Gamma_1}^\varepsilon(u_5^\varepsilon) \to u_5, \partial_t \mathcal{T}_{\Gamma_1}^\varepsilon(u_5^\varepsilon) \rightharpoonup \partial_t u_5, \mathcal{T}_{\Gamma_1}^\varepsilon(u_1^\varepsilon) \to u_1 && \text{in } L^2((0,T) \times \Omega \times \Gamma_1), \\
\mathcal{T}_{\Gamma_2}^\varepsilon(u_2^\varepsilon) \to u_2, \mathcal{T}_{\Gamma_2}^\varepsilon(u_3^\varepsilon) \to u_3 && \text{in } L^2((0,T) \times \Omega \times \Gamma_2).
\end{aligned}
\tag{5.23}
$$

Proof. Applying the Convergence Theorems in [34, 37] and Theorem 5.3.3 to the estimates stated in Lemmas 5.2.1 and 5.2.3 we obtain convergence for u_1^ε, u_2^ε, u_3^ε in (5.22). The strong convergence of u_5^ε is achieved by showing that $\mathcal{T}_{\Gamma_1}^\varepsilon(u_5^\varepsilon)$ is a Cauchy sequence in $L^2((0,T) \times \Omega \times \Gamma_1)$. For the proof see Subsection 4.5.2 or [55] and a similar proof can be found in [83]. The *a priori* estimate for $\partial_t u_5^\varepsilon$ and the convergence properties of $\mathcal{T}_{\Gamma_1}^\varepsilon$ given in [38] imply the convergence of $\partial_t \mathcal{T}_{\Gamma_1}^\varepsilon(u_5^\varepsilon)$. To show the other results in (5.23), we make use of the trace theorem stated in [52], and of the strong convergence of $\mathcal{T}_{Y_1}^\varepsilon(u_1^\varepsilon)$

$$\|\mathcal{T}_{\Gamma_1}^\varepsilon(u_1^\varepsilon) - u_1\|_{L^2((0,T) \times \Omega \times \Gamma_1)} \leq C\|\mathcal{T}_{Y_1}^\varepsilon(u_1^\varepsilon) - u_1\|_{L^2((0,T) \times \Omega; H^1(Y_1))} \to 0$$

as $\varepsilon \to 0$.

Theorem 5.3.5. (Unfolded limit equations) Under the Assumption 5.1.1, the sequences of weak solutions of the problem (5.1)-(5.14) converges as $\varepsilon \to 0$ to a weak solution (u_1, u_2, u_3, u_5) of a macroscopic model, i.e. $u_1, u_2, u_3 \in L^2(0,T; H_0^1(\Omega)) \cap H^1(0,T; L^2(\Omega))$, $u_5 \in H^1(0,T; L^2(\Omega \times \Gamma_1))$ and u_1, u_2, u_3, u_5

satisfy the macroscopic equations

$$\int\limits_0^T \int\limits_{\Omega \times Y_1} \partial_t u_1 \phi_1 + d_1(t,y)\Big(\nabla u_1 + \sum_{j=1}^n \frac{\partial u_1}{\partial x_j}\nabla_y \omega_1^j\Big)(\nabla \phi_1 + \nabla_y \tilde{\phi}_1)$$

$$+f(u_1,u_2)\phi_1 \mathrm{dydxdt} = -\int\limits_0^T \int\limits_{\Omega \times \Gamma_1} \eta(u_1,u_5)\phi_1 \mathrm{d}\gamma_y \mathrm{dxdt},$$

$$\int\limits_0^T \int\limits_{\Omega \times Y_1} \partial_t u_2 \phi_2 + d_2(t,y)\Big(\nabla u_2 + \sum_{j=1}^n \frac{\partial u_2}{\partial x_j}\nabla_y \omega_2^j\Big)(\nabla \phi_2 + \nabla_y \tilde{\phi}_1)$$

$$-f(u_1,u_2)\phi_2 \mathrm{dydxdt} = \int\limits_0^T \int\limits_{\Omega \times \Gamma_2} (a(y)u_3 - b(y)u_2)\phi_2 d\gamma_y \mathrm{dxdt}, \qquad (5.24)$$

$$\int\limits_0^T \int\limits_{\Omega \times Y_2} \partial_t u_3 \phi_3 + d_3(t,y)\Big(\nabla u_3 + \sum_{j=1}^n \frac{\partial u_3}{\partial x_j}\nabla_y \omega_3^j\Big)(\nabla \phi_3 + \nabla_y \tilde{\phi}_3) \mathrm{dydxdt}$$

$$= -\int\limits_0^T \int\limits_{\Omega \times \Gamma_2} (a(y)u_3 - b(y)u_2)\phi_3 d\gamma_y \mathrm{dxdt},$$

$$\int\limits_0^T \int\limits_{\Omega \times \Gamma_1} \partial_t u_5 \phi_5 \mathrm{d}\gamma_y \mathrm{dxdt} = \int\limits_0^T \int\limits_{\Omega \times \Gamma_1} \eta(u_1,u_5)\phi_5 \mathrm{d}\gamma_y \mathrm{dxdt},$$

for $\phi_1, \phi_2, \phi_3 \in L^2(0,T;H_0^1(\Omega))$, $\tilde{\phi}_1, \tilde{\phi}_2 \in L^2((0,T)\times \Omega; H_\#^1(Y_1))$, $\tilde{\phi}_3 \in L^2((0,T)\times \Omega; H_\#^1(Y_2))$ and $\phi_5 \in L^2((0,T) \times \Omega \times \Gamma_1)$, where ω_1^j, ω_2^j and ω_3^j, for $j = 1, \ldots, n$, are solutions of the correspondent unit cell problems

$$-\nabla_y(d_\zeta(t,y)\nabla_y \omega_\zeta^j) \quad = \sum_{k=1}^n \partial_{y_k} d_\zeta^{kj}(t,y) \ in \ Y_1, \ \zeta = 1, 2, \qquad (5.25)$$

$$-d_\zeta(t,y)\nabla \omega_\zeta^j \cdot \nu \quad = \sum_{k=1}^n d_\zeta^{kj}(t,y)\nu_k \ on \ \Gamma_1 \cup \Gamma_2, \qquad (5.26)$$

$$\omega_\zeta^j \ is \ Y\text{-}periodic, \ \int\limits_{Y_1} \omega_\zeta^j(y)\mathrm{d}y = 0,$$

$$-\nabla_y(d_3(t,y)\nabla_y \omega_3^j) \quad\quad = \sum_{k=1}^n \partial_{y_k} d_3^{kj}(t,y) \ in \ Y_2, \qquad (5.27)$$

$$-d_3(t,y)\nabla \omega_3^j \cdot \nu \quad\quad = \sum_{k=1}^n d_3^{kj}(t,y)\nu_k \ on \ \Gamma_2, \qquad (5.28)$$

$$\omega_3^j \ is \ Y\text{-}periodic, \ \int\limits_{Y_2} \omega_3^j(y)\mathrm{d}y = 0.$$

Proof. Due to considered geometry of Ω_1^ε and Ω_2^ε, we have

$$\int\limits_0^T \int\limits_{\Omega_i^\varepsilon} u^\varepsilon \phi \mathrm{dxdt} = \int\limits_0^T \int\limits_{\Omega \times Y_i} \mathcal{T}_{Y_i}^\varepsilon(u^\varepsilon)\mathcal{T}_{Y_i}^\varepsilon(\phi)\mathrm{dydxdt}, \quad i = 1, 2.$$

Applying the unfolding operator to (5.15)-(5.18), using $\mathcal{T}_{Y_1}^{\varepsilon} d_i(t, \frac{x}{\varepsilon}) = d_i(t, y), i \in \{1, 2\}$ and $\mathcal{T}_{Y_2}^{\varepsilon} d_3(t, \frac{x}{\varepsilon}) = d_3(t, y)$, considering the limit as $\varepsilon \to 0$ and the convergence results stated in Theorem 5.3.4, we obtain the unfolded limit problem. The functions $\tilde{u}_1, \tilde{u}_2, \tilde{u}_3$ are defined in terms of u_1, u_2, u_3 and solutions $\omega_1^j, \omega_2^j, \omega_3^j$ of unit cell problems (5.25) and (5.27), see [55, 83].

In a similar way, using local Lipschitz continuity of the functions η and f, and boundedness of macroscopic solutions, which follows directly from the boundedness of microscopic solutions, we can show the uniqueness of a solution of the macroscopic model. Thus, the whole sequence of microscopic solutions converges to a solution of the limit problem.

5.4   Definitions. Basis estimates. Periodicity defect. Error estimates

First of all, we introduce the definition of local average and averaging operators. Then we show some technical estimates needed in the following sections.

5.4.1   Some averaging operators

Definition 5.4.1.   1. For any $\phi \in L^p(\Omega_i^{\varepsilon})$, $p \in [1, \infty]$ and $i = 1, 2$, we define the local average operator (mean in the cells) $\mathcal{M}_{Y_i}^{\varepsilon} : L^p(\Omega_i^{\varepsilon}) \to L^p(\Omega)$

$$\mathcal{M}_{Y_i}^{\varepsilon}(\phi)(x) = \frac{1}{|Y_i|} \int_{Y_i} \mathcal{T}_{Y_i}^{\varepsilon}(\phi)(x, y) \mathrm{d}y = \frac{1}{\varepsilon^n |Y_i|} \int_{\varepsilon[\frac{x}{\varepsilon}]+\varepsilon Y_i} \phi(y) \mathrm{d}y, \quad x \in \Omega.$$

2. The operator $\mathcal{Q}_{Y_i}^{\varepsilon} : L^p(\tilde{\Omega}_i^{\varepsilon,2}) \to W^{1,\infty}(\Omega)$, for $p \in [1, \infty]$ and $i = 1, 2$, is defined as Q_1-interpolation of $\mathcal{M}_{Y_i}^{\varepsilon}(\phi)$, i.e. $\mathcal{Q}_{Y_i}^{\varepsilon}(\phi)(\varepsilon\xi) = \mathcal{M}_{Y_i}^{\varepsilon}(\phi)(\varepsilon\xi)$ for $\xi \in \mathbb{Z}^n$ and

$$\mathcal{Q}_{Y_i}^{\varepsilon}(\phi)(x) = \sum_{k\in\{0,1\}^n} \mathcal{Q}_{Y_i}^{\varepsilon}(\phi)(\varepsilon\xi+\varepsilon k)\bar{x}_1^{k_1} \ldots \bar{x}_n^{k_n} \quad \text{for } x \in \varepsilon(Y+\xi), \quad \xi \in \mathbb{Z}^n,$$

where for $k = (k_1, \ldots, k_n) \in \{0, 1\}^n$ points $\bar{x}_l^{k_l}$ are given by

$$\bar{x}_l^{k_l} = \begin{cases} \frac{x_l - \varepsilon\xi_l}{\varepsilon}, & \text{if } k_l = 1, \\ 1 - \frac{x_l - \varepsilon\xi_l}{\varepsilon}, & \text{if } k_l = 0. \end{cases}$$

3. The operator $\mathcal{Q}_{Y_i}^{\varepsilon} : W^{1,p}(\Omega_i^{\varepsilon}) \to W^{1,\infty}(\Omega)$, $p \in [1, \infty]$ and $i = 1, 2$, is defined by $\mathcal{Q}_{Y_i}^{\varepsilon}(\phi) = \mathcal{Q}_{Y_i}^{\varepsilon}(\mathcal{P}(\phi))|_{\Omega_i^{\varepsilon}}$, where $\mathcal{Q}_{Y_i}^{\varepsilon}$ is given above. and

$$\mathcal{P} : W^{1,p}(\Omega_i^{\varepsilon}) \to W^{1,p}((\mathbb{R}^n)^i)$$

is an extension operator such that

$$\|\mathcal{P}(\phi)\|_{W^{1,p}((\mathbb{R}^n)^i)} \leq C\|\phi\|_{W^{1,p}(\Omega_i^{\varepsilon})}.$$

Note that $\mathcal{T}_{Y_i}^\varepsilon \circ \mathcal{M}_{Y_i}^\varepsilon(\phi) = \mathcal{M}_{Y_i}^\varepsilon(\phi)$ for $\phi \in L^p(\Omega_i^\varepsilon)$ and $\mathcal{M}_{Y_i}^\varepsilon(\phi)(x)$
$= \mathcal{M}_{Y_i}(\mathcal{T}_{Y_i}^\varepsilon(\phi))(x)$, where $\mathcal{M}_{Y_i}$ is the mean value over Y_i, additionally

$$\sum_{k \in \{0,1\}^n} \bar{x}_1^{k_1} \dots \bar{x}_n^{k_n} = 1.$$

See more details in [34, 59].

Definition 5.4.2.   1. For $p \in [1 + \infty]$ and $i = 1, 2$, the averaging operator
$\mathcal{U}_{Y_i}^\varepsilon : L^p(\Omega \times Y_i) \to L^p(\Omega_i^\varepsilon)$ is defined as

$$\mathcal{U}_{Y_i}^\varepsilon(\Phi)(x) = \begin{cases} \frac{1}{|Y|} \int\limits_Y \Phi(\varepsilon \left[\frac{x}{\varepsilon}\right]_Y + \varepsilon z, \left\{\frac{x}{\varepsilon}\right\}_Y) dz & \text{for a.e. } x \in \tilde{\Omega}_{i,int}^\varepsilon, \\ 0 & \text{for a.e. } x \in \Omega_i^\varepsilon \setminus \tilde{\Omega}_{i,int}^\varepsilon. \end{cases}$$

2. $\mathcal{U}_{\Gamma_i}^\varepsilon : L^p(\Omega \times \Gamma_i) \to L^p(\Gamma_i^\varepsilon)$ is defined as

$$\mathcal{U}_{\Gamma_i}^\varepsilon(\Phi)(x) = \begin{cases} \frac{1}{|Y|} \int\limits_Y \Phi(\varepsilon \left[\frac{x}{\varepsilon}\right]_Y + \varepsilon z, \left\{\frac{x}{\varepsilon}\right\}_Y) dz & \text{for a.e. } x \in \tilde{\Gamma}_{i,int}^\varepsilon, \\ 0 & \text{for a.e. } x \in \Gamma_i^\varepsilon \setminus \tilde{\Gamma}_{i,int}^\varepsilon. \end{cases}$$

The above definition can be seen in [37, 33].
For $\omega^i \in H_\#^1(Y_i)$, due to $\nabla_y \omega^i(y) = \nabla_y \mathcal{T}_{Y_i}^\varepsilon \left(\omega^i\left(\frac{x}{\varepsilon}\right)\right) = \varepsilon \mathcal{T}_{Y_i}^\varepsilon \left(\nabla_x \omega^i\left(\frac{x}{\varepsilon}\right)\right)$ and

$$\mathcal{U}_{Y_i}^\varepsilon(\nabla_y \omega^i(y)) = \varepsilon \mathcal{U}_{Y_i}^\varepsilon \left(\mathcal{T}_{Y_i}^\varepsilon \left(\nabla_x \omega^i\left(\frac{x}{\varepsilon}\right)\right)\right) = \varepsilon \nabla_x \omega^i\left(\frac{x}{\varepsilon}\right) = \nabla_y \omega^i\left(\frac{x}{\varepsilon}\right),$$

we have that $\mathcal{U}_{Y_i}^\varepsilon(\nabla_y \omega^i(y)) = \nabla_y \omega^i\left(\frac{x}{\varepsilon}\right)$.

Proposition 5.4.3.   1. The operator $\mathcal{U}_{Y_i}^\varepsilon$ is formal adjoint and left inverse of
$\mathcal{T}_{Y_i}^\varepsilon$, i.e for $\phi \in L^p(\Omega_i^\varepsilon)$, where $p \in [1, \infty)$,

$$\mathcal{U}_{Y_i}^\varepsilon(\mathcal{T}_{Y_i}^\varepsilon(\phi))(x) = \begin{cases} \phi(x) & \text{a.e. for } \in \tilde{\Omega}_{i,int}^\varepsilon, \\ 0 & \text{a.e. for } \in \Omega_i^\varepsilon \setminus \tilde{\Omega}_{i,int}^\varepsilon. \end{cases}$$

2. For $\phi \in L^p(\Omega \times Y_i)$, it holds that $\|\mathcal{U}_{Y_i}^\varepsilon(\phi)\|_{L^p(\Omega_i^\varepsilon)} \le |Y|^{-1/p} \|\phi\|_{L^p(\Omega \times Y_i)}$.

5.4.2   Basic unfolding estimates

In this subsection, we prove some technical estimates which will be used in the derivation of corrector estimates.

Proposition 5.4.4. For $\phi_1 \in L^2(0, T; H^1(\Omega))$ and $\phi_2 \in L^2(0, T; H^1(\Omega_i^\varepsilon))$, we have

$$\begin{aligned} \|\phi_1 - \mathcal{M}_{Y_i}^\varepsilon(\phi_1)\|_{L^2((0,T) \times \Omega)} &\le \varepsilon C \|\nabla \phi_1\|_{L^2((0,T) \times \Omega)}, \\ \|\phi_2 - \mathcal{M}_{Y_i}^\varepsilon(\phi_2)\|_{L^2((0,T) \times \Omega_i^\varepsilon)} &\le \varepsilon C \|\nabla \phi_2\|_{L^2((0,T) \times \Omega_i^\varepsilon)}. \end{aligned} \tag{5.29}$$

Proof. This proof goes on the lines as proved in [59]. For $\phi_1 \in L^2(0, T; H^1(\Omega))$ we can write

$$x \to \phi_1|_{\varepsilon(\xi+Y)}(x) - \mathcal{M}_{Y_i}^\varepsilon(\phi_1)(\varepsilon\xi) \in L^2(0, T; H^1(\varepsilon\xi + \varepsilon Y)) \text{ with } \varepsilon(\xi+Y) \subset \Omega.$$

Using $Y_i \subset Y$ and applying Poincaré's inequality, we obtain

$$\int_0^T \int_{\varepsilon(\xi+Y)} |\phi_1 - \mathcal{M}_{Y_i}^\varepsilon(\phi_1)(\varepsilon\xi)|^2 \mathrm{d}x\mathrm{d}t = \int_0^T \int_{\xi+Y} \left|\phi_1(\varepsilon y) - \frac{1}{|Y_i|}\int_{\xi+Y_i} \phi_1(\varepsilon z)dz\right|^2 \varepsilon^n \mathrm{d}y\mathrm{d}t$$

$$\leq C\varepsilon^n \int_0^T \int_{\xi+Y} |\nabla_y \phi_1(\varepsilon y)|^2 \mathrm{d}y\mathrm{d}t = C\varepsilon^2 \int_0^T \int_{\varepsilon(\xi+Y)} |\nabla_x \phi_1(x)|^2 \mathrm{d}x\mathrm{d}t.$$

Then, we add up all inequalities for $\xi \in \mathbb{Z}^n$, such that $\varepsilon(\xi + Y) \subset \Omega$, and obtain the first estimate in (5.29). The second estimate follows from the decomposition of Ω_i^ε into $\cup_{\xi \in \mathbb{Z}^n} \varepsilon(\xi + Y_i)$ and Poincaré's inequality similar to the previous estimate.

Lemma 5.4.5. For $\phi \in L^2(0, T; H^2(\tilde{\Omega}^{\varepsilon,2}))$, $\phi_2 \in L^2(0, T; H^1(\tilde{\Omega}_i^{\varepsilon,2}))$ and $\omega \in H_\#^1(Y_i)$, with $i = 1, 2$, we have the following estimates

$$\left\|\nabla\phi - \mathcal{M}_{Y_i}^\varepsilon(\nabla\phi)\right\|_{L^2((0,T)\times\Omega)} \leq \varepsilon C\|\phi\|_{L^2(0,T;H^2(\Omega))},$$

$$\left\|(\mathcal{M}_{Y_i}^\varepsilon(\partial_{x_i}\phi) - \mathcal{Q}_{Y_i}^\varepsilon(\partial_{x_i}\phi))\nabla_y\omega\right\|_{L^2((0,T)\times\Omega_i^\varepsilon)} \leq \varepsilon C\|\phi\|_{L^2(0,T;H^2(\tilde{\Omega}^{\varepsilon,2}))}\|\nabla\omega\|_{L^2(Y_i)},$$

$$\left\|\mathcal{Q}_{Y_i}^\varepsilon(\phi_2) - \mathcal{M}_{Y_i}^\varepsilon(\phi_2)\right\|_{L^2((0,T)\times\Omega)} \leq \varepsilon C\|\nabla\phi_2\|_{L^2((0,T)\times\tilde{\Omega}_i^{\varepsilon,2})},$$

$$\left\|\mathcal{Q}_{Y_i}^\varepsilon(\phi) - \phi\right\|_{L^2((0,T)\times\Omega)} \leq \varepsilon C\|\nabla\phi\|_{L^2((0,T)\times\tilde{\Omega}^{\varepsilon,2})},$$

$$\left\|\mathcal{Q}_{Y_i}^\varepsilon(\phi_2) - \phi_2\right\|_{L^2((0,T)\times\Omega_i^\varepsilon)} \leq \varepsilon C\|\nabla\phi_2\|_{L^2((0,T)\times\tilde{\Omega}_i^{\varepsilon,2})}, \qquad (5.30)$$

$$\left\|\phi - \mathcal{T}_{\Gamma_i}^\varepsilon(\phi)\right\|_{L^2((0,T)\times\Omega\times\Gamma_i)} \leq \varepsilon C\|\nabla\phi\|_{L^2((0,T)\times\Omega)} + \varepsilon C\|\nabla\phi\|_{L^2((0,T)\times\Omega_i^\varepsilon)},$$

$$\left\|\nabla\mathcal{Q}_{Y_i}^\varepsilon(\phi_2)\right\|_{L^2((0,T)\times\Omega)} \leq C\|\nabla\phi_2\|_{L^2((0,T)\times\tilde{\Omega}_i^{\varepsilon,2})},$$

$$\left\|\mathcal{M}_{Y_i}(\omega) - \omega\right\|_{L^2(Y_i)} \leq C\|\nabla_y\omega\|_{L^2(Y_i)},$$

$$\left\|\mathcal{T}_{Y_i}^\varepsilon(\mathcal{Q}_{Y_i}^\varepsilon(\phi_2)) - \mathcal{Q}_{Y_i}^\varepsilon(\phi_2)\right\|_{L^2((0,T)\times\Omega\times Y_i)} \leq \varepsilon C\|\nabla\phi_2\|_{L^2((0,T)\times\tilde{\Omega}_i^{\varepsilon,2})}.$$

Proof. The first inequality follows directly from the first estimate in (5.29) applied to $\nabla\phi$. To show the second estimate, we use the definition of the operator $\mathcal{Q}_{Y_i}^\varepsilon$ and the equality $\sum_{k\in\{0,1\}^n} \bar{x}_1^{k_1}\ldots\bar{x}_n^{k_n} = 1$, and obtain

$$\mathcal{Q}_{Y_i}^\varepsilon(\phi)(x) - \mathcal{M}_{Y_i}^\varepsilon(\phi)(x) = \sum_{k\in\{0,1\}^n} \left(\mathcal{Q}_{Y_i}^\varepsilon(\phi)(\varepsilon\xi + \varepsilon k) - \mathcal{M}_{Y_i}^\varepsilon(\phi)(\varepsilon\xi)\right)\bar{x}_1^{k_1}\ldots\bar{x}_n^{k_n}.$$

Then, it follows that

$$\int\limits_{\varepsilon(\xi+Y_i)} \left|\mathcal{Q}^\varepsilon_{Y_i}(\phi)(x) - \mathcal{M}^\varepsilon_{Y_i}(\phi)(x)\right|^2 \left|\nabla_y\omega\left(\frac{x}{\varepsilon}\right)\right|^2 \mathrm{d}x$$

$$\leq 2^n \sum_{k\in\{0,1\}^n} \left|\mathcal{Q}^\varepsilon_{Y_i}(\phi)(\varepsilon\xi+\varepsilon k) - \mathcal{Q}^\varepsilon_{Y_i}(\phi)(\varepsilon\xi)\right|^2 \varepsilon^n \int\limits_{Y_i} |\nabla_y\omega(y)|^2\,\mathrm{d}y.$$

For any $\phi\in W^{1,p}(\mathrm{Int}(\overline{Y_i\cup(Y_i+e_j)}))$, the following estimate holds

$$|\mathcal{M}_{Y_i+e_j}(\phi) - \mathcal{M}_{Y_i}(\phi)| = |\mathcal{M}_{Y_i}(\phi(\cdot+e_j) - \phi(\cdot))|$$

$$\leq \|\phi(\cdot+e_j) - \phi(\cdot)\|_{L^p(Y_i)} \leq C\|\nabla\phi\|_{L^p(Y_i\cup(Y_i+e_j))}.$$

Thus, by the definition of $\mathcal{Q}^\varepsilon_{Y_i}(\phi)$ and by a scaling argument this implies

$$|\mathcal{Q}^\varepsilon_{Y_i}(\phi)(\varepsilon\xi+\varepsilon k) - \mathcal{Q}^\varepsilon_{Y_i}(\phi)(\varepsilon\xi)| \leq \varepsilon C\|\nabla\phi\|_{L^2(\varepsilon(\xi+Y_i)\cup\varepsilon(\xi+k+Y_i))}. \qquad (5.31)$$

We sum over $\xi\in\mathbb{Z}^n$ with $\varepsilon(\xi+Y_i)\subset\tilde{\Omega}^\varepsilon_i$ and obtain the desired estimate. Using (5.31), we obtain also that

$$\int\limits_\Omega |\mathcal{Q}^\varepsilon_{Y_i}(\phi_2) - \mathcal{M}^\varepsilon_{Y_i}(\phi_2)|^2\mathrm{d}x$$

$$\leq \varepsilon^2 C \sum_{\varepsilon(\xi+Y_i)\subset\tilde{\Omega}^{\varepsilon,1}_i} \varepsilon^n \sum_{k\in\{0,1\}^n} \|\nabla\phi_2\|^2_{L^2(\varepsilon(\xi+Y_i)\cup\varepsilon(\xi+k+Y_i))}$$

$$\leq \varepsilon^2 C \int\limits_{\tilde{\Omega}^{\varepsilon,2}_i} |\nabla\phi_2|^2\mathrm{d}x.$$

In the same way, using the estimates stated in Proposition 5.4.4, the fourth and fifth estimates in (5.30) follow from:

$$\|\mathcal{Q}^\varepsilon_{Y_i}(\phi_2) - \phi_2\|_{L^2((0,T)\times\Omega^\varepsilon_i)}$$
$$\leq \|\mathcal{Q}^\varepsilon_{Y_i}(\phi_2) - \mathcal{M}^\varepsilon_{Y_i}(\phi_2)\|_{L^2((0,T)\times\Omega)} + \|\mathcal{M}^\varepsilon_{Y_i}(\phi_2) - \phi_2\|_{L^2((0,T)\times\Omega^\varepsilon_i)}$$
$$\leq \varepsilon C\|\nabla\phi_2\|_{L^2((0,T)\times\tilde{\Omega}^{\varepsilon,2}_i)}.$$

For $\phi\in H^1(\Omega)$, applying the trace theorem to a function in $L^2(\Gamma_i)$ yields

$$\int\limits_{\Omega\times\Gamma_i} |\phi - \mathcal{T}^\varepsilon_{\Gamma_i}(\phi)|^2\mathrm{d}\gamma_y\mathrm{d}x \leq \int\limits_{\Omega\times\Gamma_i} \left(|\phi - \mathcal{M}^\varepsilon_{Y_i}(\phi)|^2 + |\mathcal{M}^\varepsilon_{Y_i}(\phi) - \mathcal{T}^\varepsilon_{\Gamma_i}(\phi)|^2\right)\mathrm{d}\gamma_y\mathrm{d}x$$

$$\leq C\varepsilon^2|\Gamma_i|\int\limits_\Omega |\nabla\phi|^2\mathrm{d}x + C\int\limits_{\Omega\times Y_i} \left(|\mathcal{M}^\varepsilon_{Y_i}(\phi) - \mathcal{T}^\varepsilon_{Y_i}(\phi)|^2 + |\nabla_y(\mathcal{M}^\varepsilon_{Y_i}(\phi) - \mathcal{T}^\varepsilon_{Y_i}(\phi))|^2\right)\mathrm{d}y\mathrm{d}x$$

$$\leq C\varepsilon^2|\Gamma_i|\int\limits_\Omega |\nabla\phi|^2\mathrm{d}x + C\int\limits_{\Omega^\varepsilon_i} |\mathcal{M}^\varepsilon_{Y_i}(\phi) - \phi|^2\mathrm{d}x + \int\limits_{\Omega\times Y_i} |\nabla_y\mathcal{T}^\varepsilon_{Y_i}(\phi))|^2\mathrm{d}y\mathrm{d}x$$

$$\leq \varepsilon^2 C\left(\int\limits_\Omega |\nabla\phi|^2\mathrm{d}x + \int\limits_{\Omega^\varepsilon_i} |\nabla\phi|^2\mathrm{d}x\right).$$

To obtain an estimate for the gradient of $\mathcal{Q}^\varepsilon_{Y_i}(\phi_2)$ where $\phi_2 \in L^2(0, T; H^1(\tilde{\Omega}^\varepsilon))$, we define $\tilde{k}^j = (k_1, \ldots, k_{j-1}, k_{j+1}, \ldots, k_n)$, $\tilde{k}^j_1 = (k_1, \ldots, k_{j-1}, 1, k_{j+1}, \ldots, k_n)$, $\tilde{k}^j_0 = (k_1, \ldots, k_{j-1}, 0, k_{j+1}, \ldots, k_n)$ and calculate

$$\frac{\partial \mathcal{Q}^\varepsilon_{Y_i}(\phi_2)}{\partial x_j} = \sum_{\tilde{k}^j} \frac{\mathcal{Q}^\varepsilon_{Y_i}(\phi_2)(\varepsilon\xi + \varepsilon\tilde{k}^j_1) - \mathcal{Q}^\varepsilon_{Y_i}(\phi_2)(\varepsilon\xi + \varepsilon\tilde{k}^j_0)}{\varepsilon} \bar{x}_1^{k_1} \ldots \bar{x}_{j-1}^{k_{j-1}} \bar{x}_{j+1}^{k_{j+1}} \bar{x}_n^{k_n}.$$

Now, by applying (5.31) we obtain the estimates for $\nabla \mathcal{Q}^\varepsilon_{Y_i}(\phi_2)$ in $L^2((0, T) \times \Omega)$. The estimate for $\mathcal{M}^\varepsilon_{Y_i}(\omega) - \omega$ follows directly by applying the Poincaré's inequality. To derive the last estimate, we consider

$$\left\| \mathcal{T}^\varepsilon_{Y_i}(\mathcal{Q}^\varepsilon_{Y_i}(\phi_2)) - \mathcal{Q}^\varepsilon_{Y_i}(\phi_2)) \right\|_{L^2(\Omega \times Y_i)}$$
$$\leq \left\| \mathcal{T}^\varepsilon_{Y_i}(\mathcal{Q}^\varepsilon_{Y_i}(\phi_2)) - \mathcal{M}^\varepsilon_{Y_i}(\mathcal{Q}^\varepsilon_{Y_i}(\phi_2)) \right\|_{L^2(\Omega \times Y_i)} + \left\| \mathcal{M}^\varepsilon_{Y_i}(\mathcal{Q}^\varepsilon_{Y_i}(\phi_2)) - \mathcal{Q}^\varepsilon_{Y_i}(\phi_2) \right\|_{L^2(\Omega \times Y_i)}$$
$$\leq C \left\| \mathcal{Q}^\varepsilon_{Y_i}(\phi_2) - \mathcal{M}^\varepsilon_{Y_i}(\mathcal{Q}^\varepsilon_{Y_i}(\phi_2)) \right\|_{L^2(\Omega^\varepsilon_i)} + C \left\| \mathcal{M}^\varepsilon_{Y_i}(\mathcal{Q}^\varepsilon_{Y_i}(\phi_2)) - \mathcal{Q}^\varepsilon_{Y_i}(\phi_2) \right\|_{L^2(\Omega)}$$
$$\leq \varepsilon C \left\| \nabla \mathcal{Q}^\varepsilon_{Y_i}(\phi_2) \right\|_{L^2(\Omega)} \leq \varepsilon C \left\| \nabla \phi_2 \right\|_{L^2(\tilde{\Omega}^{\varepsilon,2}_i)}.$$

Theorem 5.4.6. For any $\phi \in W^{1,p}(Y_i)$, with $i = 1, 2$ and $p \in (1, \infty]$, there exists a function $\hat{\phi} \in W^{1,p}_\#(Y_i)$ such that

$$\|\phi - \hat{\phi}\|_{W^{1,p}(Y_i)} \leq C \sum_{j=1}^n \|\phi|_{e_j + Y_i^j} - \phi_{Y_i^j}\|_{W^{1-\frac{1}{p}, p}(Y_i^j)},$$

where $Y_i^j = \{y \in \bar{Y}_i \,|\, y_j = 0\}$, for $j = 1, \ldots, n$, and C depends only on n.

Lemma 5.4.7. For any $\phi \in W^{1,p}(Y_i)$, where $p \in (1, \infty]$, $i = 1, 2$, and for $k \in \{1, \ldots, n\}$, there exists $\hat{\phi}_k \in W_k = \{\phi \in W^{1,p}(Y_i), \phi(\cdot) = \phi(\cdot + e_j), j \in \{1, \ldots, k\}\}$, where as $W_0 = W^{1,p}(Y_i)$, such that

$$\|\phi - \hat{\phi}_k\|_{W^{1,p}(Y_i)} \leq C \sum_{j=1}^k \|\phi|_{e_j + Y_i^j} - \phi|_{Y_i^j}\|_{W^{1-1/p}(Y_i^j)}.$$

The constant C is independent of n.

Theorem 5.4.8. For any $\phi \in H^1(Y_i, X)$ and X a separable Hilbert space, there exists a unique $\hat{\phi} \in H^1_\#(Y_i, X)$, $i = 1, 2$ such that $\phi - \hat{\phi} \in (H^1_\#(Y_i, X))^\perp$ and

$$\|\hat{\phi}\|_{H^1(Y_i, X)} \leq \|\phi\|_{H^1(Y_i, X)},$$
$$\|\phi - \hat{\phi}\|_{H^1(Y_i, X)} \leq C \sum_{j=1}^n \|\phi|_{e_j + Y_i^j} - \phi|_{Y_i^j}\|_{H^{1/2}(Y_i^j, X)}.$$

Lemma 5.4.7, Theorems 5.4.6 and 5.4.8 follow directly from the corresponding Lemma 2.2, Theorem 2.1, and Theorem 2.3 in [59], replacing Y by Y_1 and Y_2.

5.4.3   Periodicity defect

In the derivation of error estimates, we have to test the equations with the gradient of the concentration to get the estimates for the gradient. Therefore we need to have a generalization of Theorem 3.4 (for the domain without holes) proved in [59] to the functions defined in a perforated domain.[1]

Proposition 5.4.9. For $\phi \in H^1(\Omega_i^\varepsilon)$ there exists a unique $\hat{\psi}^\varepsilon \in L^2(\Omega; H_{\#}^1(Y_i))$, such that

$$
\begin{aligned}
\|\hat{\psi}_\varepsilon\|_{L^2(\Omega; H^1(Y_i))} &\leq C\big(\|\phi\|_{L^2(\Omega_i^\varepsilon)} + \varepsilon\|\nabla\phi\|_{L^2(\Omega_i^\varepsilon)^n}\big), \\
\|\mathcal{T}_{Y_i}^\varepsilon(\phi) - \hat{\psi}_\varepsilon\|_{H^{-1}(\Omega; H^1(Y_i))} &\leq C\varepsilon\big(\|\phi\|_{L^2(\Omega_i^\varepsilon)} + \varepsilon\|\nabla\phi\|_{L^2(\Omega_i^\varepsilon)^n}\big).
\end{aligned}
$$

Proof. We consider

$$
K_j = \mathrm{Int}(Y_i \cup (Y_i + e_j)) \text{ and } \varepsilon(K_i + [x/\varepsilon]_{Y_i}) \subset \tilde{\Omega}_i^{\varepsilon,2} \text{ for } x \in \Omega_i^\varepsilon,
$$

where $\tilde{\Omega}_i^{\varepsilon,k}$ are introduced in Subsection 5.3. Then for all $\phi \in L^2(\tilde{\Omega}_i^{\varepsilon,2})$, we define

$$
\mathcal{T}_{Y_i}^{\varepsilon,j}(\phi)(x,y) = \phi\left(x, \varepsilon\left[\frac{x}{\varepsilon}\right]_Y + \varepsilon y\right) \quad \text{for } x \in \Omega \text{ and a.e. } y \in K_j.
$$

For a.e. $\phi \in H_0^1(\Omega)$ and $y \in Y_i$, extended by zero to $\mathbb{R}^n \setminus \Omega$, we obtain

$$
\int\limits_{\Omega} \mathcal{T}_{Y_i}^{\varepsilon,j}(\phi)(x, y + e_j)\psi(x)\mathrm{d}x = \int\limits_{\Omega + \varepsilon e_j} \mathcal{T}_{Y_i}^{\varepsilon,j}(\phi)(x,y)\psi(x - \varepsilon e_j)\mathrm{d}x.
$$

Notice, that

$$
\begin{aligned}
\mathcal{T}_{Y_i}^{\varepsilon,j}(\phi)(x, y + e_j) \quad &= \phi\big(x, \varepsilon[\tfrac{x}{\varepsilon}]_Y + \varepsilon y + \varepsilon e_j\big) \\
&= \phi\big(x, \varepsilon\big[\tfrac{x + \varepsilon e_j}{\varepsilon}\big]_Y + \varepsilon y\big) \\
&= \mathcal{T}_{Y_i}^{\varepsilon,j}(\phi)(x + \varepsilon e_j, y)
\end{aligned}
$$

for $x \in \Omega$ and $y \in K_j$ and $\mathcal{T}_{Y_i}^{\varepsilon,j}(\phi)|_{\Omega \times Y_i} = \mathcal{T}_{Y_i}^\varepsilon(\phi)$. Thus

$$
\left| \int\limits_{\Omega} \big(\mathcal{T}_{Y_i}^{\varepsilon,j}(\phi)(\cdot, y + e_j) - \mathcal{T}_{Y_i}^{\varepsilon,j}(\phi)(\cdot, y)\big)\psi\,\mathrm{d}x - \int\limits_{\Omega} \mathcal{T}_{Y_i}^{\varepsilon,j}(\phi)(\cdot, y)\big(\psi(\cdot - \varepsilon e_j) - \psi\big)\mathrm{d}x \right|
$$

$$
\leq C\|\mathcal{T}_{Y_i}^{\varepsilon,j}(\phi)(\cdot, y))\|_{L^2(\tilde{\Omega}^{\varepsilon,1})}\|\psi\|_{L^2(\Omega \setminus (\Omega + \varepsilon e_j))},
$$

where $\tilde{\Omega}^{\varepsilon,k} := \{x \in \mathbb{R}^n, \mathrm{dist}(\Omega, x) < k\varepsilon\sqrt{n}\}$. The Lipschitz continuity of $\partial\Omega$ and $\psi \in H_0^1(\Omega)$ imply, for $j = 1, \dots, n$,

$$
\|\psi\|_{L^2(\Omega \setminus (\Omega + \varepsilon e_j))} \leq C\varepsilon\|\nabla\psi\|_{L^2(\Omega)^n}, \quad \|\psi(\cdot - \varepsilon e_j) - \psi\|_{L^2(\Omega)} \leq C\varepsilon\|\partial_{x_j}\psi\|_{L^2(\Omega)}.
$$

---

[1] The terminology "periodicity defect" is due to G. Griso, see [59].

Due to Lipschitz continuity of $\partial\Omega_i^\varepsilon$, a function $\phi \in H^1(\Omega_i^\varepsilon)$ can be extended into $H^1(\tilde{\Omega}_i^{\varepsilon,2})$, such that

$$\|\mathcal{P}(\phi)\|_{L^2(\tilde{\Omega}_i^{\varepsilon,2})} \leq C\big(\|\phi\|_{L^2(\Omega_i^\varepsilon)} + \varepsilon\|\nabla\phi\|_{L^2(\Omega_i^\varepsilon)^n}\big)$$

and

$$\|\nabla\mathcal{P}(\phi)\|_{L^2(\tilde{\Omega}_i^{\varepsilon,2})^n} \leq C\|\nabla\phi\|_{L^2(\Omega_i^\varepsilon)^n}.$$

Hence for $\phi \in H^1(\Omega_i^\varepsilon)$ and $\psi \in H_0^1(\Omega)$, it follows for a.e. $y \in Y_i$

$$\langle \mathcal{T}_{Y_i}^{\varepsilon,j}(\phi)(\cdot,\cdot + e_j) - \mathcal{T}_{Y_i}^{\varepsilon,j}(\phi)(\cdot,\cdot), \psi \rangle_{H^{-1}(\Omega), H_0^1(\Omega)}$$

$$= \int_\Omega (\mathcal{T}_{Y_i}^{\varepsilon,j}(\phi)(\cdot, y + e_j) - \mathcal{T}_{Y_i}^{\varepsilon,j}(\phi)(\cdot, y))\psi \, dx$$

$$\leq C\varepsilon\|\nabla\psi\|_{L^2(\Omega)^n}\|\mathcal{T}_{Y_i}^{\varepsilon,j}(\phi)(\cdot, y)\|_{L^2(\tilde{\Omega}^{\varepsilon,1})}.$$

The last estimate, the definition of $\mathcal{T}_{Y_i}^{\varepsilon,j}$ and the extension properties yield

$$\|\mathcal{T}_{Y_i}^{\varepsilon,j}(\phi)(\cdot,\cdot + e_j) - \mathcal{T}_{Y_i}^{\varepsilon,j}(\phi)(\cdot,\cdot)\|_{H^{-1}(\Omega; L^2(Y_i))} \leq C\varepsilon\|\mathcal{T}_{Y_i}^{\varepsilon,j}(\phi)\|_{L^2(\tilde{\Omega}^{\varepsilon,1} \times Y_i)}$$

$$\leq C\varepsilon\|\phi\|_{L^2(\tilde{\Omega}_i^{\varepsilon,2})} \leq C\varepsilon\big(\|\phi\|_{L^2(\Omega_i^\varepsilon)} + \varepsilon\|\nabla\phi\|_{L^2(\Omega_i^\varepsilon)}\big) \leq \varepsilon C\|\nabla\phi\|_{L^2(\Omega_i^\varepsilon)}.$$

Using $\nabla_y \mathcal{T}_{Y_i}^{\varepsilon,j}(\phi) = \varepsilon\mathcal{T}_{Y_i}^{\varepsilon,j}(\nabla\phi)$, we obtain the following estimate in $H^1(Y_i)$

$$\|\mathcal{T}_{Y_i}^{\varepsilon,j}(\phi)(\cdot,\cdot + e_j) - \mathcal{T}_{Y_i}^{\varepsilon,j}(\phi)(\cdot,\cdot)\|_{H^{-1}(\Omega; H^1(Y_i))}$$

$$\leq C\varepsilon\big(\|\phi\|_{L^2(\Omega_i^\varepsilon)} + \varepsilon\|\nabla\phi\|_{L^2(\Omega_i^\varepsilon)}\big) \leq \varepsilon C\|\nabla\phi\|_{L^2(\Omega_i^\varepsilon)}.$$

This implies also the following estimate for the traces of $y \to \mathcal{T}_{Y_i}^\varepsilon(\phi)$ on Y_i^j and $e_j + Y_i^j$

$$\|\mathcal{T}_{Y_i}^{\varepsilon,j}(\phi)(\cdot,\cdot + e_j) - \mathcal{T}_{Y_i}^{\varepsilon,j}(\phi)(\cdot,\cdot)\|_{H^{-1}(\Omega; H^{1/2}(Y_i^j))} \leq C\varepsilon\big(\|\phi\|_{L^2(\Omega_i^\varepsilon)} + \varepsilon\|\nabla\phi\|_{L^2(\Omega_i^\varepsilon)}\big).$$

Using Theorem 5.4.8, we decompose $\mathcal{T}_{Y_i}^\varepsilon(\phi) = \hat{\psi}^\varepsilon + \bar{\phi}^\varepsilon$, where $\hat{\psi}^\varepsilon \in L^2(\Omega; H_\#^1(Y_i))$ and $\bar{\phi}^\varepsilon \in (L^2(\Omega; H_\#^1(Y_i)))^\perp$ such that

$$\|\bar{\phi}^\varepsilon\|_{L^2(\Omega; H^1(Y_i))} + \|\hat{\psi}^\varepsilon\|_{L^2(\Omega; H^1(Y_i))} \leq C\left(\|\phi\|_{L^2(\Omega_i^\varepsilon)} + \varepsilon\|\nabla\phi\|_{L^2(\Omega_i^\varepsilon)}\right),$$

$$\|\bar{\phi}^\varepsilon\|_{H^{-1}(\Omega; H^1(Y_i))} \leq C\sum_{j=1}^n \|\mathcal{T}_{Y_i}^\varepsilon(\cdot,\cdot + e_j) - \mathcal{T}_{Y_i}^\varepsilon(\cdot,\cdot)\|_{H^{-1}(\Omega; H^{1/2}(Y_i^j))}$$

$$\leq C\varepsilon\left(\|\phi\|_{L^2(\Omega_i^\varepsilon)} + \varepsilon\|\nabla\phi\|_{L^2(\Omega_i^\varepsilon)}\right).$$

Theorem 5.4.10. For any $\phi \in H^1(\Omega_i^\varepsilon)$, $i = 1, 2$, there exists $\hat{\psi}^\varepsilon \in L^2(\Omega; H_\#^1(Y_i))$ satisfying

$$\|\hat{\psi}^\varepsilon\|_{L^2(\Omega; H^1(Y_i))} \leq C\|\nabla\phi\|_{L^2(\Omega_i^\varepsilon)^n},$$

$$\|\mathcal{T}_{Y_i}^\varepsilon(\nabla\phi) - \nabla\phi^\varepsilon - \nabla_y\hat{\psi}^\varepsilon\|_{H^{-1}(\Omega; L^2(Y_i))} \leq C\varepsilon\|\nabla\phi\|_{L^2(\Omega_i^\varepsilon)^n}.$$

Here $\phi^\varepsilon = \mathcal{Q}_{Y_i}^\varepsilon(\phi)$.

Proof. The proof is similar to that of Theorem 3.4 in [59]. For $\phi \in H^1(\Omega_i^\varepsilon)$, we consider $\phi = \phi^\varepsilon + \varepsilon\underline{\phi}$, where $\phi^\varepsilon = \mathcal{Q}_{Y_i}^\varepsilon(\phi)$ and $\underline{\phi} = \frac{1}{\varepsilon}\left(\phi - \mathcal{Q}_{Y_i}^\varepsilon(\phi)\right)$. Then, it follows that

$$\|\nabla\phi^\varepsilon\|_{L^2(\Omega_i^\varepsilon)} + \|\underline{\phi}\|_{L^2(\Omega_i^\varepsilon)} + \varepsilon\|\nabla\underline{\phi}\|_{L^2(\Omega_i^\varepsilon)} \leq C\|\nabla\phi\|_{L^2(\Omega_i^\varepsilon)}. \tag{5.32}$$

For $\underline{\phi} \in H^1(\Omega_i^\varepsilon)$, it follows from Proposition 5.4.9 and (5.32) that there exists $\hat{\psi}^\varepsilon \in L^2(\Omega; H_\#^1(Y_i))$ such that

$$\|\mathcal{T}_{Y_i}^\varepsilon(\underline{\phi}) - \hat{\psi}^\varepsilon\|_{H^{-1}(\Omega; H^1(Y_i))} \leq C\varepsilon\|\nabla\phi\|_{L^2(\Omega_i^\varepsilon)}, \tag{5.33}$$

$$\|\hat{\psi}^\varepsilon\|_{L^2(\Omega; H^1(Y_i))} \leq C\|\nabla\phi\|_{L^2(\Omega_i^\varepsilon)}. \tag{5.34}$$

Using the definition and properties of $\mathcal{M}_{Y_i}^\varepsilon$ and $\mathcal{Q}_{Y_i}^\varepsilon$, it implies

$$\|\partial_{x_j}\phi^\varepsilon - \mathcal{M}_{Y_i}^\varepsilon(\partial_{x_j}\phi^\varepsilon)\|_{H^{-1}(\Omega)} \leq C\varepsilon\|\nabla\phi^\varepsilon\|_{L^2(\Omega)^n} \leq C\varepsilon\|\nabla\phi\|_{L^2(\Omega_i^\varepsilon)^n}. \tag{5.35}$$

For $\psi \in H_0^1(\Omega)$ we have that

$$\langle\mathcal{T}_{Y_i}^\varepsilon(\partial_{x_j}\phi^\varepsilon) - \mathcal{M}_{Y_i}^\varepsilon(\partial_{x_j}\phi^\varepsilon)), \psi\rangle_{H^{-1}(\Omega), H_0^1(\Omega)}$$

$$= \int_\Omega \left(\mathcal{T}_{Y_i}^\varepsilon(\partial_{x_j}\phi^\varepsilon)) - \mathcal{M}_{Y_i}^\varepsilon(\partial_{x_j}\phi^\varepsilon)\right)\psi\mathrm{d}x$$

$$= \int_\Omega \left(\mathcal{T}_{Y_i}^\varepsilon(\partial_{x_j}\phi^\varepsilon)(\cdot, y) - \mathcal{M}_{Y_i}^\varepsilon(\partial_{x_j}\phi^\varepsilon))\right)\mathcal{M}_{Y_i}^\varepsilon(\psi)\mathrm{d}x.$$

Then, due to the definition of $\mathcal{T}_{Y_i}^\varepsilon(\partial_{x_j}Q_{Y_i}^\varepsilon(\phi))$, it follows in the same way as in [59],

$$\int_\Omega \left(\mathcal{T}_{Y_i}^\varepsilon(\partial_{x_j}\phi^\varepsilon)(\cdot, y) - \mathcal{M}_{Y_i}^\varepsilon(\partial_{x_j}\phi^\varepsilon)\right)\mathcal{M}_{Y_i}^\varepsilon(\psi)\mathrm{d}x$$

$$= \varepsilon^n \sum_\xi \frac{\mathcal{M}_{Y_i}^\varepsilon(\phi)(\varepsilon\xi + \varepsilon e_j) - \mathcal{M}_{Y_i}^\varepsilon(\phi)(\varepsilon\xi)}{\varepsilon} \times$$

$$\sum_{\tilde{k}^j} \left(\mathcal{M}_{Y_i}^\varepsilon(\psi)(\varepsilon\xi - \varepsilon\tilde{k}_0^j) - \frac{1}{2^{n-1}}\sum_{\tilde{k}^j}\mathcal{M}_{Y_i}^\varepsilon(\psi)(\varepsilon\xi - \varepsilon\tilde{k}_0^j)\right)\bar{y}^j,$$

where $\tilde{k}^j = (k_1, \ldots, k_{j-1}, k_{j+1}, \ldots, k_n)$, $\tilde{k}_1^j = (k_1, \ldots, k_{j-1}, 1, k_{j+1}, \ldots, k_n)$, $\tilde{k}_0^j = (k_1, \ldots, k_{j-1}, 0, k_{j+1}, \ldots, k_n)$, $\bar{y}^j = \bar{y}_1^{k_1} \cdots \bar{y}_{j-1}^{k_{j-1}} \bar{y}_{j+1}^{k_{j+1}} \cdots \bar{y}_n^{k_n}$. This together with the estimates for $\mathcal{M}_{Y_i}^\varepsilon$ (see Section 5.4) implies, for every $y \in Y_i$, the inequality

$$\langle\mathcal{T}_{Y_i}^\varepsilon(\partial_{x_j}\phi^\varepsilon)(\cdot, y) - \mathcal{M}_{Y_i}^\varepsilon(\partial_{x_j}\phi^\varepsilon), \psi\rangle_{H^{-1}(\Omega), H_0^1(\Omega)} \leq C\varepsilon|\bar{y}^j|\|\nabla\phi\|_{L^2(\Omega_i^\varepsilon)^n}\|\nabla\psi\|_{L^2(\Omega)^n}.$$

Moreover, the following holds:

$$\|\mathcal{T}_{Y_i}^\varepsilon(\partial_{x_j}\phi^\varepsilon) - \mathcal{M}_{Y_i}^\varepsilon(\partial_{x_j}\phi^\varepsilon)\|_{H^{-1}(\Omega; L^2(Y_i))} \leq C\varepsilon\|\nabla\phi\|_{L^2(\Omega_i^\varepsilon)}.$$

Using the last estimate together with (5.33) – (5.35) and $\nabla\phi = \nabla\phi^\varepsilon + \varepsilon\nabla\underline{\phi}^\varepsilon$, yield

$$\|\mathcal{T}_{Y_i}^\varepsilon(\nabla\phi) - \nabla\phi^\varepsilon - \nabla_y\hat{\psi}^\varepsilon\|_{H^{-1}(\Omega;L^2(Y_i))}$$
$$\leq \|\mathcal{T}_{Y_i}^\varepsilon(\nabla\phi^\varepsilon) - \nabla\phi^\varepsilon\|_{H^{-1}(\Omega;L^2(Y_i))} + \|\nabla_y(\mathcal{T}_{Y_i}^\varepsilon(\underline{\phi}^\varepsilon)) - \nabla_y\hat{\psi}^\varepsilon\|_{H^{-1}(\Omega;L^2(Y_i))}$$
$$\leq C\varepsilon\|\nabla\phi\|_{L^2(\Omega_i^\varepsilon)}.$$

5.4.4 Corrector estimates

Under additional regularity assumptions on the solution of the macroscopic problem, we obtain a set of error estimates. We emphasize here again that only H^1-regularity for the solutions to the microscopic model and to the cell problems is required.

The main result of this chapter is:

Theorem 5.4.11. Suppose $(u_1^\varepsilon, u_2^\varepsilon, u_3^\varepsilon, u_5^\varepsilon)$ are solutions of the microscopic problem $(6.1) - (6.8)$ and $u_1, u_2, u_3 \in L^2(0,T;H^2(\Omega)) \cap H^1((0,T)\times\Omega))$, $u_5 \in H^1(0,T; L^2(\Omega\times\Gamma_1))$ are nonnegative and bounded solutions of the macroscopic equations (**??**). Then we have the following corrector estimates:

$$\|u_1^\varepsilon - u_1\|_{L^2((0,T)\times\Omega_1^\varepsilon)} + \|\nabla u_1^\varepsilon - \nabla u_1 - \sum_{j=1}^n \mathcal{Q}_{Y_1}^\varepsilon(\partial_{x_j}u_1)\nabla_y\omega_1^j\|_{L^2((0,T)\times\Omega_1^\varepsilon)}^2 \leq C\varepsilon^{\frac{1}{2}},$$

$$\|u_2^\varepsilon - u_2\|_{L^2((0,T)\times\Omega_1^\varepsilon)} + \|\nabla u_2^\varepsilon - \nabla u_2 - \sum_{j=1}^n \mathcal{Q}_{Y_1}^\varepsilon(\partial_{x_j}u_2)\nabla_y\omega_2^j\|_{L^2((0,T)\times\Omega_1^\varepsilon)}^2 \leq C\varepsilon^{\frac{1}{2}},$$

$$\|u_3^\varepsilon - u_3\|_{L^2((0,T)\times\Omega_2^\varepsilon)} + \|\nabla u_3^\varepsilon - \nabla u_3 - \sum_{j=1}^n \mathcal{Q}_{Y_2}^\varepsilon(\partial_{x_j}u_3)\nabla_y\omega_3^j\|_{L^2((0,T)\times\Omega_2^\varepsilon)}^2 \leq C\varepsilon^{\frac{1}{2}},$$

$$\varepsilon^{\frac{1}{2}}\|u_5^\varepsilon - \mathcal{U}_{\Gamma_1}^\varepsilon(u_5)\|_{L^2((0,T)\times\Gamma_1^\varepsilon)} \leq C\varepsilon^{\frac{1}{2}}. \tag{5.36}$$

5.4.5 Proof of Theorem 5.4.11

We define the distance function $\rho(x) = \mathrm{dist}(x,\partial\Omega)$, and the domains $\hat{\Omega}_{\rho,in}^\varepsilon := \{x \in \Omega, \rho(x) < \varepsilon\}$ as well as $\hat{\Omega}_{i,\rho,in}^\varepsilon := \{x \in \Omega_i^\varepsilon, \rho(x) < \varepsilon\}$, and $\rho^\varepsilon(\cdot) := \inf\{\frac{\rho(\cdot)}{\varepsilon}, 1\}$. The definition of ρ^ε yields

$$\|\nabla\rho^\varepsilon\|_{L^\infty(\Omega)^n} = \|\nabla\rho^\varepsilon\|_{L^\infty(\hat{\Omega}_{\rho,in}^\varepsilon)^n} = \varepsilon^{-1}. \tag{5.37}$$

Then, for $\Phi \in H^2(\Omega)$ and $\omega \in H^1(Y_i)$, where $i = 1, 2$, we obtain the following estimates in the same way as in [59],

$$\|\nabla\Phi\|_{L^2(\hat{\Omega}^\varepsilon_{\rho,in})^n} + \|Q^\varepsilon_{Y_i}(\nabla\Phi)\|_{L^2(\hat{\Omega}^\varepsilon_{\rho,in})^n} + \|\mathcal{M}^\varepsilon_{Y_i}(\nabla\Phi)\|_{L^2(\hat{\Omega}^\varepsilon_{\rho,in})^n} \leq C\varepsilon^{\frac{1}{2}}\|\Phi\|_{H^2(\Omega)},$$

$$\left\|\omega\left(\frac{\cdot}{\varepsilon}\right)\right\|_{L^2(\hat{\Omega}^\varepsilon_{i,\rho,in})} + \left\|\nabla\omega\left(\frac{\cdot}{\varepsilon}\right)\right\|_{L^2(\hat{\Omega}^\varepsilon_{i,\rho,in})^n} \leq C\varepsilon^{\frac{1}{2}}\|\nabla_y\omega\|_{L^2(Y_i)^n},$$

$$\|(1 - \rho_\varepsilon)\nabla_x\Phi\|_{L^2(\Omega)^n} \leq \|\nabla_x\Phi\|_{L^2(\hat{\Omega}^\varepsilon_{\rho,in})^n} \leq C\varepsilon^{\frac{1}{2}}\|\Phi\|_{H^2(\Omega)}, \qquad (5.38)$$

$$\|\nabla_x(\rho_\varepsilon\partial_{x_j}\Phi)\|_{L^2(\Omega)^n} \leq C(\varepsilon^{-\frac{1}{2}} + 1)\|\Phi\|_{H^2(\Omega)},$$

$$\left\|\varepsilon\partial_{x_i}\rho_\varepsilon\mathcal{Q}^\varepsilon_{Y_i}(\partial_{x_j}\Phi)\omega\left(\frac{\cdot}{\varepsilon}\right)\right\|_{L^2(\Omega^\varepsilon_i)} \leq C\varepsilon^{\frac{1}{2}}\|\Phi\|_{H^2(\Omega)}\|\omega\|_{L^2(Y_i)},$$

$$\left\|\varepsilon\rho_\varepsilon\partial_{x_i}\mathcal{Q}^\varepsilon_{Y_i}(\partial_{x_j}\Phi)\omega\left(\frac{\cdot}{\varepsilon}\right)\right\|_{L^2(\Omega^\varepsilon_i)} \leq C\varepsilon\|\Phi\|_{H^2(\Omega)}\|\omega\|_{L^2(Y_i)}.$$

Note that for a bounded Lipschitz domain Ω, there exists an extension of Φ from Ω into $\Omega^{\varepsilon,2}$ such that

$$\|\mathcal{P}(\Phi)\|_{L^2(\tilde{\Omega}^{\varepsilon,2})} \leq C\left(\|\Phi\|_{L^2(\Omega)} + \varepsilon\|\nabla\Phi\|_{L^2(\Omega)^n}\right)$$

and

$$\|\nabla\mathcal{P}(\Phi)\|_{L^2(\tilde{\Omega}^{\varepsilon,2})^n} \leq C\|\nabla\Phi\|_{L^2(\Omega)^n}.$$

Now, for $\phi_1 \in L^2(0, T; H^1_{\partial\Omega}(\Omega^\varepsilon_1))$ given by

$$\phi_1(x) = u^\varepsilon_1(x) - u(x) - \varepsilon\rho^\varepsilon(x)\sum_{j=1}^n \mathcal{Q}^\varepsilon_{Y_1}(\partial_{x_j}u)(x)\omega^j_1\left(\frac{x}{\varepsilon}\right),$$

we consider an extension $\tilde{\phi}^\varepsilon_1$ of ϕ_1 from $(0, T) \times \Omega^\varepsilon_1$ into $(0, T) \times \Omega$, such that

$$\|\tilde{\phi}^\varepsilon_1\|_{L^2((0,T)\times\Omega)} \leq C\|\phi_1\|_{L^2((0,T)\times\Omega^\varepsilon_1)}$$

and

$$\|\nabla\tilde{\phi}^\varepsilon_1\|_{L^2((0,T)\times\Omega)} \leq C\|\nabla\phi_1\|_{L^2((0,T)\times\Omega^\varepsilon_1)}.$$

Due to the presence of zero boundary conditions and since all phases are connected, standard extension results apply, see [40]. We consider $\tilde{\phi}^\varepsilon_1 \in L^2(0, T; H^1_0(\Omega))$ and $\hat{\psi}^\varepsilon_1 \in L^2((0, T) \times \Omega, H^1_\#(Y_1))$ given by Theorem 5.4.10 applied to ϕ_1, as test functions in the macroscopic equation (**??**) for u_1:

$$\int_0^\tau \int_{\Omega\times Y_1} \partial_t u_1\tilde{\phi}^\varepsilon_1 + d_1(y)\Big(\nabla u_1 + \sum_{j=1}^n \frac{\partial u_1}{\partial x_j}\nabla_y\omega^j_1\Big)\big(\nabla\tilde{\phi}^\varepsilon_1 + \nabla_y\hat{\psi}^\varepsilon_1\big)\mathrm{d}y\mathrm{d}x\mathrm{d}t$$

$$+ \int_0^\tau \int_{\Omega\times Y_1} f(u_1, u_2)\tilde{\phi}^\varepsilon_1\mathrm{d}y\mathrm{d}x\mathrm{d}t + \int_0^\tau \int_{\Omega\times\Gamma_1} \eta(u_1, u_5)\tilde{\phi}^\varepsilon_1\mathrm{d}\gamma_y\mathrm{d}x\mathrm{d}t = 0.$$

In the first term and in the last two integrals, we replace $\tilde{\phi}_1^\varepsilon$ by $\mathcal{M}_{Y_1}^\varepsilon(\phi_1)$, $\tilde{\phi}_1^\varepsilon$ by $\mathcal{T}_{\Gamma_1}^\varepsilon(\phi_1)$, and u_1 by $\mathcal{T}_{Y_1}^\varepsilon(u_1)$. As next step, we introduce ρ^ε in front of ∇u_1 and $\partial_{x_j} u_1$, and replace $\nabla \tilde{\phi}_1^\varepsilon$ by $\nabla \mathcal{Q}_{Y_1}^\varepsilon(\phi_1)$. Notice that $\mathcal{Q}_{Y_i}^\varepsilon(\partial_{x_j} u_1)$ and ∇u_1 are in $L^2(0,T;H^1(\Omega))$, but not in $L^2(0,T;H_0^1(\Omega))$. Now, using Theorem 5.4.10, we replace $\nabla \phi_1^\varepsilon + \nabla_y \hat{\psi}_1^\varepsilon$ by $\mathcal{T}_{Y_1}^\varepsilon(\nabla \phi_1)$, where $\phi_1^\varepsilon = \mathcal{Q}_{Y_1}^\varepsilon(\phi_1)$, and obtain

$$
\int_0^\tau \int_{\Omega \times Y_1} \partial_t \mathcal{T}_{Y_1}^\varepsilon(u_1) \mathcal{M}_{Y_1}^\varepsilon(\phi_1) + d_1(y)\rho^\varepsilon \Big(\nabla u_1 + \sum_{j=1}^n \frac{\partial u_1}{\partial x_j} \nabla_y \omega_1^j \Big) \mathcal{T}_{Y_1}^\varepsilon(\nabla \phi_1) \mathrm{d}y \mathrm{d}x \mathrm{d}t
$$

$$
+ \int_0^\tau \int_{\Omega \times Y_1} \mathcal{T}_{Y_1}^\varepsilon(f(u_1,u_2)) \mathcal{M}_{Y_1}^\varepsilon(\phi_1) \mathrm{d}y \mathrm{d}x \mathrm{d}t + \int_0^\tau \int_{\Omega \times \Gamma_1} \eta(u_1,u_5) \mathcal{T}_{\Gamma_1}^\varepsilon(\phi_1) \mathrm{d}\gamma_y \mathrm{d}x \mathrm{d}t = R_1^1,
$$

where

$$
R_1^1 = \int_0^\tau \int_{\Omega \times Y_1} \Big[\partial_t (u_1 - \mathcal{T}_{Y_1}^\varepsilon(u_1)) \mathcal{M}_{Y_1}^\varepsilon(\phi_1) + \partial_t u_1 (\tilde{\phi}_1^\varepsilon - \mathcal{M}_{Y_1}^\varepsilon(\phi_1))
$$

$$
+ \rho^\varepsilon d_1 \Big(\nabla u_1 + \sum_{j=1}^n \frac{\partial u_1}{\partial x_j} \nabla_y \omega_1^j \Big) \Big(\nabla(\mathcal{Q}_{Y_i}^\varepsilon(\phi_1) - \tilde{\phi}_1^\varepsilon) + (\mathcal{T}_{Y_1}^\varepsilon(\nabla \phi_1) - \nabla \phi_1^\varepsilon - \nabla_y \hat{\psi}_1^\varepsilon) \Big)
$$

$$
+ (\rho^\varepsilon - 1) d_1 \Big(\nabla u_1 + \sum_{j=1}^n \frac{\partial u_1}{\partial x_j} \nabla_y \omega_1^j \Big) (\nabla \tilde{\phi}_1^\varepsilon + \nabla_y \hat{\psi}_1^\varepsilon) + f(u_1,u_5)(\mathcal{M}_{Y_1}^\varepsilon(\phi_1) - \tilde{\phi}_1^\varepsilon)
$$

$$
+ (\mathcal{T}_{Y_1}^\varepsilon(f) - f) \mathcal{M}_{Y_1}^\varepsilon(\phi_1) \Big] \mathrm{d}y \mathrm{d}x \mathrm{d}t + \int_0^\tau \int_{\Omega \times \Gamma_1} \eta(u_1,u_5)(\mathcal{T}_{\Gamma_1}^\varepsilon(\phi_1) - \tilde{\phi}_1^\varepsilon) \mathrm{d}\gamma_y \mathrm{d}x \mathrm{d}t.
$$

Then we remove ρ^ε, replace ∇u_1 by $\mathcal{M}_{Y_1}^\varepsilon(\nabla u_1)$, $\partial_{x_j} u_1$ by $\mathcal{M}_{Y_1}^\varepsilon(\partial_{x_j} u_1)$ and, using $\mathcal{M}_{Y_1}^\varepsilon(\phi) = \mathcal{T}_{Y_1}^\varepsilon \circ \mathcal{M}_{Y_1}^\varepsilon(\phi)$, we apply the inverse unfolding

$$
\int_0^\tau \int_{\Omega_1^\varepsilon} \Big(\partial_t u_1 \mathcal{M}_{Y_1}^\varepsilon(\phi_1) + d_1^\varepsilon \Big(\mathcal{M}_{Y_1}^\varepsilon(\nabla u_1) + \sum_{j=1}^n \mathcal{M}_{Y_1}^\varepsilon(\partial_{x_j} u_1) \nabla_y \omega_1^j \Big(\frac{x}{\varepsilon}\Big) \Big) \nabla \phi_1 \Big) \mathrm{d}x \mathrm{d}t
$$

$$
+ \int_0^\tau \int_{\Omega_1^\varepsilon} f(u_1,u_2) \mathcal{M}_{Y_1}^\varepsilon(\phi_1) \mathrm{d}x \mathrm{d}t + \int_0^\tau \int_{\Omega \times \Gamma_1} \eta(u_1,u_5) \mathcal{T}_{\Gamma_1}^\varepsilon(\phi_1) \mathrm{d}\gamma_y \mathrm{d}x \mathrm{d}t = R_1^1 + R_1^2,
$$

where

$$
R_1^2 = \int_0^\tau \int_{\Omega \times Y_1} \Big[(1 - \rho^\varepsilon) d_1(y) \Big(\nabla u_1 + \sum_{j=1}^n \partial_{x_j} u_1 \nabla_y \omega_1^j(y) \Big) \mathcal{T}_{Y_1}^\varepsilon(\nabla \phi_1) +
$$

$$
d_1(y) \Big(\mathcal{M}_{Y_1}^\varepsilon(\nabla u_1) - \nabla u_1 + \sum_{j=1}^n \big(\mathcal{M}_{Y_1}^\varepsilon(\partial_{x_j} u_1) - \partial_{x_j} u_1 \big) \nabla_y \omega_1^j(y) \Big) \mathcal{T}_{Y_1}^\varepsilon(\nabla \phi_1) \Big] \mathrm{d}y \mathrm{d}x \mathrm{d}t.
$$

If we introduce ρ^ε in front of $\mathcal{M}^\varepsilon_{Y_i}(\partial_{x_j} u_1)$ and replace $\mathcal{M}^\varepsilon_{Y_1}(\phi_1)$ by ϕ_1, $\mathcal{M}^\varepsilon_{Y_1}(\nabla u_1)$ by ∇u_1, $\mathcal{M}^\varepsilon_{Y_1}(\partial_{x_j} u_1)$ by $\mathcal{Q}^\varepsilon_{Y_1}(\partial_{x_j} u_1)$, we obtain

$$\int\limits_0^\tau \int\limits_{\Omega_1^\varepsilon} \Big[\partial_t u_1 \phi_1 + d_1^\varepsilon \Big(\nabla u_1 + \sum_{j=1}^n \rho^\varepsilon \mathcal{Q}^\varepsilon_{Y_1}(\partial_{x_j} u_1) \nabla_y \omega_1^j\big(\tfrac{x}{\varepsilon}\big) \Big) \nabla \phi_1 + f(u_1, u_2)\phi_1 \Big] \mathrm{d}x\mathrm{d}t$$

$$= -\int\limits_0^\tau \int\limits_{\Omega\times\Gamma_1} \eta(u_1, u_5) \mathcal{T}^\varepsilon_{Y_1}(\phi_1) \mathrm{d}\gamma_y \mathrm{d}x\mathrm{d}t + R_1^1 + R_1^2 + R_1^3, \qquad (5.39)$$

where

$$R_1^3 = \int\limits_0^\tau \int\limits_{\Omega_1^\varepsilon} \Big[(\partial_t u_1 + f)(\phi_1 - \mathcal{M}^\varepsilon_{Y_1}(\phi_1)) + (\rho^\varepsilon - 1)d_1^\varepsilon \sum_{j=1}^n \mathcal{M}^\varepsilon_{Y_i}(\partial_{x_j} u_1) \nabla_y \omega_1^j\big(\tfrac{x}{\varepsilon}\big) \nabla \phi_1$$

$$+ d_1^\varepsilon \Big(\nabla u_1 - \mathcal{M}^\varepsilon_{Y_1}(\nabla u_1) + \sum_{j=1}^n \rho^\varepsilon \big(\mathcal{Q}^\varepsilon_{Y_1}(\partial_{x_j} u_1) - \mathcal{M}^\varepsilon_{Y_1}(\partial_{x_j} u_1) \big) \nabla_y \omega_1^j\big(\tfrac{x}{\varepsilon}\big) \Big) \nabla \phi_1 \Big] \mathrm{d}x\mathrm{d}t.$$

Now, we subtract (5.39) from (5.15) for u_1^ε and obtain for the test function $\phi_1 = u_1^\varepsilon - u_1 - \varepsilon\rho^\varepsilon \sum_{j=1}^n \mathcal{Q}^\varepsilon_{Y_1}(\partial_{x_j} u_1)\omega_1^j$ the equality

$$\int\limits_0^\tau \int\limits_{\Omega_1^\varepsilon} \Big[\partial_t(u_1^\varepsilon - u_1)(u_1^\varepsilon - u_1 - \varepsilon\rho^\varepsilon \sum_{j=1}^n \mathcal{Q}^\varepsilon_{Y_i}(\partial_{x_j} u_1)\omega_1^j) +$$

$$d_1^\varepsilon \big(\nabla(u_1^\varepsilon - u_1) - \rho^\varepsilon \sum_{j=1}^n \mathcal{Q}^\varepsilon_{Y_i}(\partial_{x_j} u_1) \nabla_y \omega_1^j \big) \big(\nabla(u_1^\varepsilon - u_1) - \varepsilon \sum_{j=1}^n \nabla_x \big(\rho^\varepsilon \mathcal{Q}^\varepsilon_{Y_i}(\partial_{x_j} u_1)\omega_1^j \big) \big)$$

$$+ \big(f(u_1^\varepsilon, u_2^\varepsilon) - f(u_1, u_2) \big) \big(u_1^\varepsilon - u_1 - \varepsilon\rho^\varepsilon \sum_{j=1}^n \mathcal{Q}^\varepsilon_{Y_i}(\partial_{x_j} u_1)\omega_1^j \big) \Big] \mathrm{d}x\mathrm{d}t +$$

$$\int\limits_0^\tau \int\limits_{\Omega\times\Gamma_1} \big(\eta(\mathcal{T}^\varepsilon_{\Gamma_1} u_1^\varepsilon, \mathcal{T}^\varepsilon_{\Gamma_1} u_5^\varepsilon) - \eta(u_1, u_5) \big) \mathcal{T}^\varepsilon_{\Gamma_1} \big(u_1^\varepsilon - u_1 - \varepsilon\rho^\varepsilon \sum_{j=1}^n \mathcal{Q}^\varepsilon_{Y_i}(\partial_{x_j} u_1)\omega_1^j \big) \mathrm{d}\gamma_y \mathrm{d}x\mathrm{d}t$$

$$= R_1, \qquad \text{where } R_1 = R_1^1 + R_1^2 + R_1^3.$$

We consider $\psi^\varepsilon := \mathcal{T}^\varepsilon_{\Gamma_1} u_5^\varepsilon - u_5$ as a test function in the equations for u_5 in (**??**) and $\mathcal{T}^\varepsilon_{\Gamma_1}(u_5^\varepsilon)$ obtained from (5.18) by applying the unfolding operator. Using the local Lipschitz continuity of η and the boundedness of u_1^ε, u_1, u_5^ε, and u_5, we obtain

$$\int\limits_0^\tau \int\limits_{\Omega\times\Gamma_1} \partial_t |\mathcal{T}^\varepsilon_{\Gamma_1} u_5^\varepsilon - u_5|^2 \mathrm{d}\gamma_y \mathrm{d}x\mathrm{d}t \le C \int\limits_0^\tau \int\limits_{\Omega\times\Gamma_1} \big(|\mathcal{T}^\varepsilon_{\Gamma_1} u_5^\varepsilon - u_5|^2 + |\mathcal{T}^\varepsilon_{\Gamma_1} u_1^\varepsilon - u_1|^2 \big) \mathrm{d}\gamma_y \mathrm{d}x\mathrm{d}t.$$

Applying Gronwall's inequality and considering $\mathcal{T}_{\Gamma_1}^\varepsilon(u_{50}^\varepsilon)(x,y) = u_{50}(y)$ yields

$$\|(\mathcal{T}_{\Gamma_1}^\varepsilon(u_5^\varepsilon) - u_5)(t)\|_{L^2(\Omega \times \Gamma_1)}^2$$
$$\leq C\|\mathcal{T}_{\Gamma_1}^\varepsilon(u_1^\varepsilon) - u_1\|_{L^2((0,\tau)\times\Omega\times\Gamma_1)}^2 + \|\mathcal{T}_{\Gamma_1}^\varepsilon(u_{50}^\varepsilon) - u_{50}\|_{L^2(\Omega\times\Gamma_1)}^2$$
$$\leq C\Big(\|\mathcal{T}_{\Gamma_1}^\varepsilon(u_1^\varepsilon - u_1)\|_{L^2((0,\tau)\times\Omega\times\Gamma_1)}^2 + \|\mathcal{T}_{\Gamma_1}^\varepsilon(u_1) - u_1\|_{L^2((0,\tau)\times\Omega\times\Gamma_1)}^2\Big).$$

Then, for the boundary integral, it follows from the estimate stated in Lemma 5.4.5 that

$$\int_0^\tau \int_{\Omega\times\Gamma_1} \big(\eta(\mathcal{T}_{\Gamma_1}^\varepsilon(u_5^\varepsilon), \mathcal{T}_{\Gamma_1}^\varepsilon(u_1^\varepsilon)) - \eta(r,u)\big)\mathcal{T}_{\Gamma_1}^\varepsilon(\phi_1)\mathrm{d}\gamma_y\mathrm{d}x\mathrm{d}t \leq$$

$$C\big(\|\mathcal{T}_{\Gamma_1}^\varepsilon(u_5^\varepsilon)-u_5\|_{L^2((0,\tau)\times\Omega\times\Gamma_1)}+\|\mathcal{T}_{\Gamma_1}^\varepsilon(u_1^\varepsilon)-u_1\|_{L^2((0,\tau)\times\Omega\times\Gamma_1)}\big)\varepsilon^{\frac{1}{2}}\|\phi_1\|_{L^2((0,\tau)\times\Gamma_1^\varepsilon)}$$
$$\leq C\big(\|u_1^\varepsilon - u_1\|_{L^2((0,\tau)\times\Omega_1^\varepsilon)} + \varepsilon\|\nabla(u_1^\varepsilon - u_1)\|_{L^2((0,\tau)\times\Omega_1^\varepsilon)} + \varepsilon\|\nabla u_1\|_{L^2((0,\tau)\times\Omega)}\big) \times$$
$$\big(\|\phi_1\|_{L^2((0,\tau)\times\Omega_1^\varepsilon)} + \varepsilon\|\nabla\phi_1\|_{L^2((0,\tau)\times\Omega_1^\varepsilon)}\big). \tag{5.40}$$

The ellipticity assumption, Lipschitz continuity of f, the estimate (5.40), and Young's inequality imply

$$\int_0^\tau \int_{\Omega_1^\varepsilon} \Big(\partial_t\big|\hat{u}_1^\varepsilon - \varepsilon\rho^\varepsilon\sum_{j=1}^n \mathcal{Q}_{Y_1}^\varepsilon(\partial_{x_j}u_1)\omega_1^j\big|^2 + \big|\nabla\hat{u}_1^\varepsilon - \rho^\varepsilon\sum_{j=1}^n \mathcal{Q}_{Y_1}^\varepsilon(\partial_{x_j}u_1)\nabla_y\omega_1^j\big|^2\Big)\mathrm{d}x\mathrm{d}t$$

$$\leq C\int_0^\tau \int_{\Omega_1^\varepsilon} \Big(\big|\hat{u}_1^\varepsilon - \varepsilon\rho^\varepsilon\sum_{j=1}^n \mathcal{Q}_{Y_1}^\varepsilon(\partial_{x_j}u_1)\omega_1^j\big|^2 + \big|\hat{u}_2^\varepsilon - \varepsilon\rho^\varepsilon\sum_{j=1}^n Q_{Y_1}^\varepsilon(\partial_{x_j}u_2)\omega_2^j\big|^2\Big)\mathrm{d}x\mathrm{d}t$$
$$+ C\varepsilon^2\|\nabla u_1\|_{L^2((0,T)\times\Omega)}^2 + R_1 + C_1^\varepsilon,$$

where $\hat{u}_1^\varepsilon := u_1^\varepsilon - u_1$, $\hat{u}_2^\varepsilon := u_2^\varepsilon - u_2$, and

$$C_1^\varepsilon := C\varepsilon^2\int_0^\tau\int_{\Omega_1^\varepsilon}\sum_{j=1}^n\Big(|\mathcal{Q}_{Y_1}^\varepsilon(\partial_t\partial_{x_j}u_1)\omega_1^j|^2 + (1+\varepsilon^2)|\nabla\mathcal{Q}_{Y_1}^\varepsilon(\partial_{x_j}u_1)\omega_1^j|^2$$

$$+|\mathcal{Q}_{Y_1}^\varepsilon(\partial_{x_j}u_1)\omega_1^j|^2 + |\mathcal{Q}_{Y_1}^\varepsilon(\partial_{x_j}u_2)\omega_2^j|^2 + |\mathcal{Q}_{Y_1}^\varepsilon(\partial_{x_j}u_1)\nabla_y\omega_1^j|^2\Big)\mathrm{d}x\mathrm{d}t$$

$$+ C\int_0^\tau\int_{\hat{\Omega}_{1,\rho,in}^\varepsilon}\sum_{j=1}^n|\mathcal{Q}_{Y_1}^\varepsilon(\partial_{x_j}u_1)\omega_1^j|^2\mathrm{d}x\mathrm{d}t$$

$$\leq C\big(\varepsilon^2\|u_1\|_{L^2(0,T;H^2(\Omega))}^2 + \varepsilon^2\|u_1\|_{H^1((0,T)\times\Omega)}^2 + \varepsilon\|u_1\|_{L^2(0,T;H^2(\Omega))}^2\big)\|\omega_1\|_{H^1(Y_1)^n}^2$$
$$+ C\varepsilon^2\|u_2\|_{L^2(0,T;H^1(\Omega))}^2\|\omega_1\|_{L^2(Y_1)^n}^2.$$

Here we used that

$$\varepsilon^2 \int_{\hat{\Omega}_1^\varepsilon} |\nabla\big(\rho^\varepsilon \mathcal{Q}_{Y_1}^\varepsilon(\partial_{x_j} u_1)\big)\omega_1^j|^2 \mathrm{d}x \le \varepsilon^2 \int_{\hat{\Omega}_1^\varepsilon} |\nabla\mathcal{Q}_{Y_1}^\varepsilon(\partial_{x_j} u_1)\omega_1^j|^2 \mathrm{d}x$$
$$+ \int_{\hat{\Omega}_{1,\rho,in}^\varepsilon} |\mathcal{Q}_{Y_1}^\varepsilon(\partial_{x_j} u_1)\omega_1^j|^2 \mathrm{d}x.$$

The estimates of the error terms in the Subsection 5.4.6 imply

$$|R_1| = |R_1^1 + R_1^2 + R_1^3| \le \varepsilon^{1/2} C\big(1 + \|u_1\|_{H^1((0,T)\times\Omega)} + \|u_1\|_{L^2(0,T;H^2(\Omega))}$$
$$+ \|u_2\|_{L^2(0,T;H^1(\Omega))} + \|u_5\|_{L^2((0,T)\times\Omega\times\Gamma_1)}\big)\|\phi_1\|_{L^2(0,T;H^1(\Omega_1^\varepsilon))}.$$

Then, applying Young's inequality, we obtain

$$\int_0^\tau \int_{\Omega_1^\varepsilon} \big(\partial_t |\hat{u}_1^\varepsilon - \varepsilon\rho^\varepsilon \sum_{j=1}^n \mathcal{Q}_{Y_i}^\varepsilon(\partial_{x_j} u_1)\omega_1^j|^2 + |\nabla\hat{u}_1^\varepsilon - \rho^\varepsilon \sum_{j=1}^n \mathcal{Q}_{Y_1}^\varepsilon(\partial_{x_j} u_1)\nabla_y\omega_1^j|^2\big) \mathrm{d}x\mathrm{d}t$$
$$\le C \int_0^\tau \int_{\Omega_1^\varepsilon} \big(|\hat{u}_1^\varepsilon - \varepsilon\rho^\varepsilon \sum_{j=1}^n \mathcal{Q}_{Y_1}^\varepsilon(\partial_{x_j} u_1)\omega_1^j|^2 + |\hat{u}_2^\varepsilon - \varepsilon\rho^\varepsilon \sum_{j=1}^n \mathcal{Q}_{Y_1}^\varepsilon(\partial_{x_j} u_2)\omega_2^j|^2\big) \mathrm{d}x\mathrm{d}t$$
$$+ C(\varepsilon + \varepsilon^2)(1 + \|u_1\|_{H^1((0,T)\times\Omega)}^2 + \|u_1\|_{L^2(0,T;H^2(\Omega))}^2)\big(1 + \|\omega_1\|_{H^1(Y_1)^n}^2\big)$$
$$+ C\varepsilon^2 \|u_2\|_{L^2(0,T;H^1(\Omega))}^2\big(1 + \|\omega_2\|_{H^1(Y_1)^n}^2\big) + \varepsilon^2 \|u_5\|_{L^\infty((0,T)\times\Omega\times\Gamma_1)}^2.$$

Analogously, the estimates for $u_2^\varepsilon - u_2 - \varepsilon \sum_{j=1}^n \mathcal{Q}_{Y_1}^\varepsilon(\partial_{x_j} v_2)\omega_2^j$ and

$u_3^\varepsilon - u_3 - \varepsilon \sum_{j=1}^n \mathcal{Q}_{Y_2}^\varepsilon(\partial_{x_j} u_3)\omega_3^j$ are obtained. The only difference is the bound-
ary term. Applying the trace theorem and the estimates in Lemma 5.4.5, the
boundary term can be estimated by

$$\int_{\Omega\times\Gamma_2} \Big((a(y)u_3 - b(y)u_2)\tilde{\phi}_2^\varepsilon - (a(y)\mathcal{T}_{\Gamma_2}^\varepsilon(u_3) - b(y)\mathcal{T}_{\Gamma_2}^\varepsilon(u_2))\mathcal{T}_{\Gamma_2}^\varepsilon(\phi_2)\Big)\mathrm{d}\gamma_y\mathrm{d}x$$
$$\le C \int_{\Omega\times\Gamma_2} \big(|u_3 - \mathcal{T}_{\Gamma_2}^\varepsilon(u_3)| + |u_2 - \mathcal{T}_{\Gamma_2}^\varepsilon(u_2)|\big)\mathcal{T}_{\Gamma_2}^\varepsilon(\phi_2) + (u_3 + u_2)|\tilde{\phi}_2^\varepsilon - \mathcal{M}_{Y_1}^\varepsilon(\phi_2)|$$
$$+ (u_3 + u_2)|\mathcal{M}_{Y_1}^\varepsilon(\phi_2) - \mathcal{T}_{\Gamma_2}^\varepsilon(\phi_2)|\big)\mathrm{d}\gamma_y\mathrm{d}x \le \varepsilon C\big(\|u_2\|_{H^1(\Omega)} + \|u_3\|_{H^1(\Omega)}\big)\|\phi_2\|_{H^1(\Omega_2^\varepsilon)},$$

where $\phi_2 = u_2^\varepsilon - u_2 - \varepsilon\rho^\varepsilon \sum_{j=1}^n \mathcal{Q}_{Y_1}^\varepsilon(\partial_{x_j} u_2)\omega_2^j$. Thus, for $\hat{u}_2^\varepsilon = u_2^\varepsilon - u_2$ and $\hat{u}_3^\varepsilon = u_3^\varepsilon - u_3$ we have

$$\int_0^\tau \int_{\Omega_1^\varepsilon} \Big(\partial_t\big|\hat{u}_2^\varepsilon - \varepsilon\rho^\varepsilon \sum_{j=1}^n \mathcal{Q}_{Y_1}^\varepsilon\big(\frac{\partial u_2}{\partial x_j}\big)\omega_2^j\big|^2 + \big|\nabla\hat{u}_2^\varepsilon - \rho^\varepsilon \sum_{j=1}^n \mathcal{Q}_{Y_1}^\varepsilon\big(\frac{\partial u_2}{\partial x_j}\big)\nabla_y\omega_2^j\big|^2\Big)\mathrm{d}x\mathrm{d}t$$

$$\leq C\int_0^\tau \int_{\Omega_1^\varepsilon} \Big(\big|\hat{u}_1^\varepsilon - \varepsilon\rho^\varepsilon \sum_{j=1}^n \mathcal{Q}_{Y_1}^\varepsilon\big(\frac{\partial u_1}{\partial x_j}\big)\omega_1^j\big|^2 + \big|\hat{u}_2^\varepsilon - \varepsilon\rho^\varepsilon \sum_{j=1}^n \mathcal{Q}_{Y_1}^\varepsilon\big(\frac{\partial u_2}{\partial x_j}\big)\omega_2^j\big|^2\Big)\mathrm{d}x\mathrm{d}t+$$

$$C\int_0^\tau \int_{\Omega_2^\varepsilon} \Big(\big|\hat{u}_3^\varepsilon - \varepsilon\rho^\varepsilon \sum_{j=1}^n \mathcal{Q}_{Y_2}^\varepsilon\big(\frac{\partial u_3}{\partial x_j}\big)\omega_3^j\big|^2 + \varepsilon^2\big|\nabla\hat{u}_3^\varepsilon - \rho^\varepsilon \sum_{j=1}^n \mathcal{Q}_{Y_2}^\varepsilon\big(\frac{\partial u_3}{\partial x_j}\big)\nabla_y\omega_3^j\big)\big|^2\Big)\mathrm{d}x\mathrm{d}t$$

$$+C(\varepsilon+\varepsilon^2)\big(1 + \|u_2\|_{L^2(0,T;H^2(\Omega))}^2 + \|u_2\|_{H^1((0,T)\times\Omega)}^2\big)\big(1 + \|\omega_2\|_{H^1(Y_1)^n}^2\big)$$
$$+C\big(\varepsilon^2\|u_1\|_{L^2(0,T;H^1(\Omega))}^2 + \varepsilon^2\|u_3\|_{L^2(0,T;H^1(\Omega))}^2 + C_2^\varepsilon\big),$$

and

$$\int_0^\tau \int_{\Omega_2^\varepsilon} \Big(\partial_t\big|\hat{u}_3^\varepsilon - \varepsilon\rho^\varepsilon \sum_{j=1}^n \mathcal{Q}_{Y_2}^\varepsilon\big(\frac{\partial u_3}{\partial x_j}\big)\omega_3^j\big|^2 + \big|\nabla\hat{u}_3^\varepsilon - \rho^\varepsilon \sum_{i=j}^n \mathcal{Q}_{Y_2}^\varepsilon\big(\frac{\partial u_3}{\partial x_j}\big)\nabla_y\omega_3^j\big|^2\Big)\mathrm{d}x\mathrm{d}t$$

$$\leq C\int_0^\tau \int_{\Omega_1^\varepsilon} \Big(\big|\hat{u}_2^\varepsilon - \varepsilon\rho^\varepsilon \sum_{j=1}^n \mathcal{Q}_{Y_1}^\varepsilon\big(\frac{\partial u_2}{\partial x_j}\big)\omega_2^j\big|^2 + \varepsilon^2\big|\nabla\hat{u}_2^\varepsilon - \rho^\varepsilon \sum_{j=1}^n \mathcal{Q}_{Y_1}^\varepsilon\big(\frac{\partial u_2}{\partial x_j}\big)\nabla_y\omega_2^j\big|^2\Big)\mathrm{d}x\mathrm{d}t$$

$$+C\int_0^\tau \int_{\Omega_2^\varepsilon} \Big(\big|\hat{u}_3^\varepsilon - \varepsilon\rho^\varepsilon \sum_{i=1}^n \mathcal{Q}_{Y_2}^\varepsilon\big(\frac{\partial u_3}{\partial x_j}\big)\omega_3^j\big|^2 + \varepsilon^2\big|\nabla\hat{u}_3^\varepsilon - \rho^\varepsilon \sum_{j=1}^n \mathcal{Q}_{Y_2}^\varepsilon\big(\frac{\partial u_3}{\partial x_j}\big)\nabla_y\omega_3^j\big|^2\Big)\mathrm{d}x\mathrm{d}t$$

$$+C(\varepsilon+\varepsilon^2)\big(1 + \|u_3\|_{L^2(0,T;H^2(\Omega))}^2 + \|u_3\|_{H^1((0,T)\times\Omega)}^2\big)\big(1 + \|\omega_2\|_{H^1(Y_1)^n}^2\big)$$
$$+C\big(\varepsilon^2\|u_2\|_{L^2(0,T;H^1(\Omega)}^2 + C_3^\varepsilon\big),$$

where

$$C_2 := \varepsilon^2\int_0^\tau \int_{\Omega_1^\varepsilon} \sum_{j=1}^n \Big(\big|\mathcal{Q}_{Y_1}^\varepsilon\big(\frac{\partial^2 u_2}{\partial t\partial x_j}\big)\omega_2^j\big|^2 + (1+\varepsilon^2)\big|\nabla\mathcal{Q}_{Y_1}^\varepsilon\big(\frac{\partial u_2}{\partial x_j}\big)\omega_2^j\big|^2 + \big|\mathcal{Q}_{Y_1}^\varepsilon\big(\frac{\partial u_1}{\partial x_j}\big)\omega_1^j\big|^2$$

$$+\big|\mathcal{Q}_{Y_1}^\varepsilon\big(\frac{\partial u_2}{\partial x_j}\big)\omega_2^j\big|^2 + \big|\mathcal{Q}_{Y_1}^\varepsilon\big(\frac{\partial u_2}{\partial x_j}\big)\nabla_y\omega_2^j\big|^2\Big)\mathrm{d}x\mathrm{d}t + \int_0^\tau \int_{\hat{\Omega}_{1,\rho,in}^\varepsilon} \big|\mathcal{Q}_{Y_1}^\varepsilon\big(\frac{\partial u_2}{\partial x_j}\big)\omega_2^j\big|^2\mathrm{d}x\mathrm{d}t$$

$$+\varepsilon^2\int_0^\tau \int_{\Omega_2^\varepsilon} \sum_{i=1}^n \Big(\big|\mathcal{Q}_{Y_2}^\varepsilon\big(\frac{\partial u_3}{\partial x_j}\big)\omega_3^j\big|^2 + \big|\mathcal{Q}_{Y_2}^\varepsilon\big(\frac{\partial u_3}{\partial x_j}\big)\nabla_y\omega_3^j\big|^2\Big)\mathrm{d}x\mathrm{d}t$$

$$\leq C\big(\varepsilon^2\|u_2\|^2_{L^2(0,T;H^2(\Omega))} + \varepsilon^2\|u_2\|^2_{H^1((0,T)\times\Omega)} + \varepsilon\|u_2\|^2_{L^2(0,T;H^2(\Omega))}\big)\|\omega_2\|^2_{H^1(Y_1)^n}$$
$$+\varepsilon^2 C\big(\|u_1\|^2_{L^2(0,T;H^1(\Omega))}\|\omega_1\|^2_{L^2(Y_1)^n} + \|u_3\|^2_{L^2(0,T;H^1(\Omega))}\|\omega_3\|^2_{H^1(Y_2)^n}\big).$$

For C_3, we have the same expression as for C_2, with u_2 replaced by u_3, ω_2^j by ω_3^j, Ω_1^ε by Ω_2^ε, and without the term $|Q_{Y_1}^j(\partial_{x_j}u_1)\omega_1^j|^2$. Thus, we can estimate

$$
\begin{aligned}
C_3 \quad &\leq \varepsilon^2 C\|u_2\|^2_{L^2(0,T;H^1(\Omega))}\|\omega_2\|^2_{H^1(Y_1)^n} + C\big(\varepsilon\|u_3\|^2_{L^2(0,T;H^2(\Omega))}\\
&\quad +\varepsilon^2\|u_3\|^2_{L^2(0,T;H^2(\Omega))} + \varepsilon^2\|u_3\|^2_{H^1((0,T)\times\Omega)}\big)\|\omega_3\|^2_{H^1(Y_2)^n}.
\end{aligned}
$$

For sufficiently small ε, adding all estimates, removing ρ^ε by using the estimates (5.38), applying Gronwall's inequality and noting that by definition $u_1^\varepsilon(0) = u_{10}$, $u_2^\varepsilon(0) = u_{20}$, $u_3^\varepsilon(0) = u_{30}$, we obtain the estimates for u_1^ε, u_2^ε, u_3^ε, stated in the theorem.

To obtain the estimate for $u_5^\varepsilon - \mathcal{U}_{\Gamma_1}^\varepsilon(u_5)$, we consider the equations for $\mathcal{T}_{\Gamma_1}^\varepsilon u_5^\varepsilon$ obtained from (5.18) by applying the unfolding operator and the equation for u_5 in (??) with the test function $\mathcal{T}_{\Gamma_1}^\varepsilon u_5^\varepsilon - u_5$. Using the properties of $\mathcal{U}_{\Gamma_1}^\varepsilon$, the local Lipschitz continuity of η, and Gronwall's inequality, yields

$$\varepsilon\int_{\Gamma_1^\varepsilon}|u_5^\varepsilon - \mathcal{U}_{\Gamma_1}^\varepsilon(u_5)|^2\mathrm{d}\gamma_x \leq C\int_{\Omega\times\Gamma_1}|\mathcal{T}_{\Gamma_1}^\varepsilon(u_5^\varepsilon) - u_5|^2\mathrm{d}\gamma_y\mathrm{d}x$$

$$\leq C\int_0^\tau\int_{\Omega\times\Gamma_1}|\mathcal{T}_{\Gamma_1}^\varepsilon(u_1^\varepsilon) - u_1|^2\mathrm{d}\gamma_y\mathrm{d}x\mathrm{d}t + \int_{\Omega\times\Gamma_1}|\mathcal{T}_{\Gamma_1}^\varepsilon(u_{50}) - u_{50}|^2\mathrm{d}\gamma_y\mathrm{d}x$$

$$\leq \int_0^\tau\int_{\Omega\times\Gamma_1}\Big(|\mathcal{T}_{\Gamma_1}^\varepsilon(u_1) - \mathcal{M}_{Y_1}^\varepsilon(u_1)|^2 + |\mathcal{M}_{Y_1}^\varepsilon(u_1) - u_1|^2\Big)\mathrm{d}\gamma_y\mathrm{d}x\mathrm{d}t$$

$$+C\int_0^\tau\int_{\Omega_1^\varepsilon}\Big[\big|\hat{u}_1^\varepsilon - \varepsilon\sum_{j=1}^n \mathcal{Q}_{Y_1}^\varepsilon(\partial_{x_j}u_1)\omega_1^j\big|^2 + \varepsilon^2\big|\nabla\hat{u}_1^\varepsilon - \sum_{j=1}^n \mathcal{Q}_{Y_1}^\varepsilon(\partial_{x_j}u_1)\nabla_y\omega_1^j\big|^2$$

$$+\varepsilon^2\sum_{j=1}^n\Big(\big|\mathcal{Q}_{Y_1}^\varepsilon(\partial_{x_j}u_1)\omega_1^j\big|^2 + \varepsilon^2\big|\nabla\mathcal{Q}_{Y_1}^\varepsilon(\partial_{x_j}u_1)\omega_1^j\big|^2 + \big|\mathcal{Q}_{Y_1}^\varepsilon(\partial_{x_j}u_1)\nabla_y\omega_1^j\big|^2\Big)\Big]\mathrm{d}x\mathrm{d}t$$

$$\leq C(\varepsilon + \varepsilon^2)\Big(\|u_1\|^2_{L^2(0,T;H^2(\Omega))} + \|u_1\|^2_{H^1((0,T)\times\Omega)} + \|u_2\|^2_{L^2(0,T;H^2(\Omega))}$$

$$+\|u_2\|^2_{H^1((0,T)\times\Omega)} + \|u_3\|^2_{L^2(0,T;H^2(\Omega))} + \|u_3\|^2_{H^1((0,T)\times\Omega)} + \|u_5\|^2_{L^\infty((0,T)\times\Omega\times\Gamma_1)}\Big).$$

5.4.6 Estimates of the error terms

Now, we proceed to estimate the error terms R_1^1, R_1^2, and R_1^3. Using the definition of ρ^ε, the extension properties of $\tilde{\phi}_1^\varepsilon$, Theorem 5.4.10, and the estimates (5.38)

we obtain

$$\int\limits_0^\tau \int\limits_{\Omega\times Y_1} \left| d_1(y)(\rho^\varepsilon - 1)\Big(\nabla u_1 + \sum_{j=1}^n \frac{\partial u_1}{\partial x_j}\nabla_y\omega_1^j\Big)(\nabla\tilde{\phi}_1^\varepsilon + \nabla\hat{\psi}_1^\varepsilon)\right| \mathrm{d}y\mathrm{d}x\mathrm{d}t$$

$$\leq C\|\nabla u_1\|_{L^2((0,T)\times\hat{\Omega}_{1,\rho,in})}\Big(1+\sum_{j=1}^n \|\nabla_y\omega_1^j\|_{L^2(Y_1)}\Big)\big(\|\nabla\tilde{\phi}_1^\varepsilon\|_{L^2((0,\tau)\times\Omega)}+\|\nabla\hat{\psi}_1^\varepsilon\|_{L^2(\Omega_\tau\times Y_1)}\big)$$

$$\leq C\varepsilon^{1/2}\|u_1\|_{L^2(0,T;H^2(\Omega))}\Big(1+\sum_{j=1}^n \|\nabla_y\omega_1^j\|_{L^2(Y_1)}\Big)\|\nabla\phi_1\|_{L^2((0,\tau)\times\Omega_1^\varepsilon)}. \tag{5.41}$$

Theorem 5.4.10 and the estimates (5.37) and (5.38) imply

$$\int\limits_0^\tau \int\limits_{\Omega\times Y_1} \rho^\varepsilon d_1(y)\Big(\nabla u_1 + \sum_{j=1}^n \partial_{x_j}u_1\nabla_y\omega_1^j\Big)\Big(\mathcal{T}_{Y_1}^\varepsilon(\nabla\phi_1) - \nabla\phi_1^\varepsilon - \nabla_y\hat{\psi}_1^\varepsilon\Big)\mathrm{d}y\mathrm{d}x\mathrm{d}t$$

$$\leq C(\varepsilon^{1/2}+\varepsilon)\|u_1\|_{L^2(0,T;H^2(\Omega))}\Big(1+\sum_{j=1}^n \|\nabla_y\omega_1^j\|_{L^2(Y_1)}\Big)\|\nabla\phi_1\|_{L^2((0,T)\times\Omega_2^\varepsilon)}. \tag{5.42}$$

We notice $\mathcal{M}_{Y_1}^\varepsilon(\tilde{\phi}_1^\varepsilon) = \mathcal{M}_{Y_1}^\varepsilon(\phi_1)$ and using estimates (5.37) and (5.38), Lemma 5.4.5. the fact that $\tilde{\phi}_1^\varepsilon$ is an extension of ϕ_1 from Ω_1^ε into Ω and $\phi_1 = \tilde{\phi}_1$ a.e in $(0,T)\times\Omega_1^\varepsilon$, implies

$$\int\limits_0^\tau \int\limits_{\Omega\times Y_1} \rho^\varepsilon d_1\Big(\nabla u_1 + \sum_{j=1}^n \frac{\partial u_1}{\partial x_j}\nabla_y\omega_1^j\Big)\nabla\big(\mathcal{Q}_{Y_i}^\varepsilon(\phi_1) - \tilde{\phi}_1^\varepsilon\big)\mathrm{d}y\mathrm{d}x\mathrm{d}t$$

$$\leq \left\|\nabla\Big(\rho^\varepsilon d_1\Big(\nabla u_1 + \sum_{j=1}^n \frac{\partial u_1}{\partial x_j}\nabla_y\omega_1^j\Big)\Big)\right\|_{L^2((0,\tau)\times\Omega\times Y_1)} \|\mathcal{Q}_{Y_i}^\varepsilon(\tilde{\phi}_1^\varepsilon) - \tilde{\phi}_1^\varepsilon\|_{L^2((0,\tau)\times\Omega)}$$

$$\leq C\varepsilon\big(\varepsilon^{-1}\|\nabla u_1\|_{L^2((0,T)\times\hat{\Omega}_{1,\rho,in})}+\|\nabla^2 u_1\|_{L^2}\big)\Big(1+\sum_{j=1}^n \|\nabla\omega_1^j\|_{L^2(Y_1)}\Big)\|\nabla\tilde{\phi}_1^\varepsilon\|_{L^2((0,\tau)\times\Omega)}$$

$$\leq C(\varepsilon^{1/2} + \varepsilon)\|u\|_{L^2(0,T;H^2(\Omega))}\Big(1 + \sum_{j=1}^n \|\nabla_y\omega_1^j\|_{L^2(Y_1)}\Big)\|\nabla\phi_1\|_{L^2((0,\tau)\times\Omega_2^\varepsilon)}. \tag{5.43}$$

Applying the estimates in Lemma 5.4.5, yields

$$\int\limits_0^\tau \int\limits_{\Omega\times Y_1} \Big(\partial_t\big(u_1 - \mathcal{T}_{Y_1}^\varepsilon(u_1)\big)\mathcal{M}_{Y_1}^\varepsilon(\phi_1) + \partial_t u_1\big(\tilde{\phi}_1^\varepsilon - \mathcal{M}_{Y_1}^\varepsilon(\phi_1)\big)\Big)\mathrm{d}y\mathrm{d}x\mathrm{d}t$$

$$\leq C\varepsilon\big(\|\partial_t\nabla u_1\|_{L^2(\Omega_T)}\|\phi_1\|_{L^2(0,\tau)\times\Omega_1^\varepsilon)} + \|\partial_t u_1\|_{L^2(\Omega_T)}\|\nabla\phi_1\|_{L^2((0,\tau)\times\Omega_1^\varepsilon)}\big) \tag{5.44}$$

Due to Lipschitz continuity of f, we can estimate

$$\int_0^\tau \int_{\Omega \times Y_1} \Big(\big(\mathcal{T}_{Y_1}^\varepsilon(f) - f(u_1, u_2) \big) \mathcal{M}_{Y_1}^\varepsilon(\phi_1) + f(u_1, u_2) \big(\mathcal{M}_{Y_1}^\varepsilon(\phi_1) - \tilde\phi_1^\varepsilon \big) \Big) \mathrm{d}y \mathrm{d}x \mathrm{d}t$$

$$\leq \varepsilon C \big(\|\nabla u_1\|_{L^2((0,T) \times \Omega)} + \|\nabla u_2\|_{L^2(\Omega_T)} \big) \|\phi_1\|_{L^2((0,\tau) \times \Omega_1^\varepsilon)}$$

$$+ \varepsilon C \big(1 + \|u_1\|_{L^2((0,T) \times \Omega)} + \|u_2\|_{L^2(\Omega_T)} \big) \|\nabla \phi_1\|_{L^2((0,\tau) \times \Omega_1^\varepsilon)}. \tag{5.45}$$

For the boundary integral, we have

$$\int_0^\tau \int_{\Omega \times \Gamma_1} \eta(u_1, u_5) (\mathcal{T}_{\Gamma_1}^\varepsilon(\phi_1) - \tilde\phi_1^\varepsilon)) \mathrm{d}\gamma_y \mathrm{d}x \mathrm{d}t \leq \|\eta(u_1, u_5)\|_{L^2((0,\tau) \times \Omega \times \Gamma_1)} \times$$

$$\big(\|\mathcal{T}_{\Gamma_1}^\varepsilon(\phi_1) - \mathcal{M}_{Y_1}^\varepsilon(\phi_1)\|_{L^2((0,\tau) \times \Omega \times \Gamma_1)} + \|\mathcal{M}_{Y_1}^\varepsilon(\phi_1) - \tilde\phi_1^\varepsilon\|_{L^2((0,\tau) \times \Omega \times \Gamma_1)} \big)$$

$$\leq C \big(1 + \|u_1\|_{L^2(\Omega_T)} + \|u_5\|_{L^\infty((0,T) \times \Omega \times \Gamma_1)} \big) \|\mathcal{T}_{Y_1}^\varepsilon(\phi_1) - \mathcal{M}_{Y_1}^\varepsilon(\phi_1)\|_{L^2((0,\tau) \times \Omega; H^1(Y_1))}$$

$$+ C \big(1 + \|u_1\|_{L^2((0,T) \times \Omega)} + \|u_5\|_{L^\infty((0,T) \times \Omega \times \Gamma_1)} \big) \|\mathcal{M}_{Y_1}^\varepsilon(\phi_1) - \tilde\phi_1^\varepsilon\|_{L^2((0,\tau) \times \Omega)}$$

$$\leq \varepsilon C \big(1 + \|u_1\|_{L^2((0,T) \times \Omega)} + \|u_5\|_{L^\infty((0,T) \times \Omega \times \Gamma_1)} \big) \|\nabla \phi_1\|_{L^2((0,\tau) \times \Omega_1^\varepsilon)}. \tag{5.46}$$

Thus, collecting all estimates (5.43) – (5.46) we obtain for R_1^1:

$$|R_1^1| \leq C(\varepsilon^{\frac{1}{2}} + \varepsilon) \|u_1\|_{L^2(0,T; H^2(\Omega))} \Big(1 + \sum_{j=1}^n \|\nabla_y \omega_1^j\|_{L^2(Y_1)} \Big) \|\nabla \phi_1\|_{L^2((0,\tau) \times \Omega_i^\varepsilon)}$$

$$+ C\varepsilon \big(\|u_1\|_{H^1((0,T) \times \Omega)} + \|u_2\|_{L^2(0,T; H^1(\Omega))} \big) \|\phi_1\|_{L^2(0,\tau; H^1(\Omega_i^\varepsilon))}.$$

Using the estimates (5.38) implies

$$\int_0^\tau \int_{\Omega_1^\varepsilon} (1 - \rho^\varepsilon) d_1^\varepsilon \sum_{j=1}^n \mathcal{M}_{Y_i}^\varepsilon(\partial_{x_j} u_1) \nabla_y \omega_1^j \Big(\frac{x}{\varepsilon} \Big) \nabla \phi_1 \mathrm{d}x \mathrm{d}t$$

$$\leq \sum_{j=1}^n \|\mathcal{M}_{Y_i}^\varepsilon(\partial_{x_j} u_1)\|_{L^2((0,\tau) \times \hat\Omega_{1,\rho,in}^\varepsilon)} \left\| \nabla_y \omega_1^j \Big(\frac{x}{\varepsilon} \Big) \right\|_{L^2(\hat\Omega_{1,\rho,in}^\varepsilon)} \|\nabla \phi_1\|_{L^2((0,\tau) \times \Omega_1^\varepsilon)}$$

$$\leq \varepsilon C \sum_{j=1}^n \|u_1\|_{L^2(0,T; H^2(\Omega_1^\varepsilon))} \|\nabla_y \omega_1^j\|_{L^2(Y_1)} \|\nabla \phi_1\|_{L^2((0,\tau) \times \Omega_1^\varepsilon)}. \tag{5.47}$$

Thus, (5.47) together with (5.30) and (5.38) yields

$$|R_1^2| \leq \|\nabla u_1\|_{L^2((0,\tau) \times \hat\Omega_{1,\rho,in}^\varepsilon)} (1 + \|\nabla_y \omega_1\|_{L^2(Y_1)^{n \times n}}) \|\mathcal{T}_{Y_1}^\varepsilon(\nabla \phi_1)\|_{L^2((0,\tau) \times \Omega \times Y_1)}$$

$$+ C\varepsilon \|u_1\|_{L^2(0,\tau; H^2(\Omega))} (1 + \|\nabla_y \omega_1^j\|_{L^2(Y_1)^{n \times n}}) \|\mathcal{T}_{Y_1}^\varepsilon(\nabla \phi_1)\|_{L^2((0,\tau) \times \Omega \times Y_1)}$$

$$\leq (\varepsilon^{1/2} + \varepsilon) C \|u_1\|_{L^2(0,T; H^2(\Omega))} (1 + \|\nabla_y \omega_1^j\|_{L^2(Y_1)^{n \times n}}) \|\nabla \phi_1\|_{L^2((0,\tau) \times \Omega_1^\varepsilon)}.$$

Due to estimates in (5.38) and in Lemma 5.4.5 we obtain also

$$|R_1^3| \leq \varepsilon C \Big(\|\partial_t u_1\|_{L^2((0,T) \times \Omega_1^\varepsilon)} + \|f\|_{L^2((0,T) \times \Omega_1^\varepsilon)} + \|u_1\|_{L^2(0,T; H^2(\Omega_1^\varepsilon))} \|\nabla_y \omega_1\|_{L^2(Y_1)^{n \times n}}$$

$$+ \|\nabla^2 u_1\|_{L^2((0,T) \times \Omega_1^\varepsilon)} + \|\nabla^2 u_1\|_{L^2((0,T) \times \Omega_1^\varepsilon)} \|\nabla_y \omega_1\|_{L^2(Y_1)^{n \times n}} \Big) \|\nabla \phi_1\|_{L^2((0,\tau) \times \Omega_1^\varepsilon)}.$$

In the similar way, we show the estimates for the error terms in the equations for u_2 and u_3:

$$|R_2| \le C\varepsilon^{\frac{1}{2}} \left(1 + \|u_2\|_{L^2(0,T;H^2(\Omega))} + \|u_2\|_{H^1((0,T)\times\Omega)} + \|u_2\|_{L^2(0,T;H^1(\Omega))} \right.$$

$$\left. + \|u_3\|_{L^2(0,T;H^1(\Omega))} \right) \|\phi_2\|_{L^2(0,\tau;H^1(\Omega_2^\varepsilon))}, \tag{5.48}$$

$$|R_3| \le C\varepsilon^{\frac{1}{2}} \left(1 + \|u_3\|_{L^2(0,T;H^2(\Omega))} + \|u_3\|_{H^1(\Omega_T)} \right.$$

$$\left. + \|u_2\|_{L^2(0,T;H^1(\Omega))} \right) \|\phi_3\|_{L^2(0,\tau;H^1(\Omega_2^\varepsilon))}. \tag{5.49}$$

5.5 Notes and comments

In this chapter, we obtained the desired convergence rates as indicated in (5.36). Hence, we now have a *confidence measure* for our averaging results. The main ideas of the methodology we used here were presented in [59, 60] for linear elliptic equations with oscillating coefficients, posed in a fixed domain. We applied the same methodology to derive corrector estimates in perforated media.

It is worth noting that often in the context of real-world applications it is not sufficient to consider only leading-order terms in the derivation of corrector estimates. They simply do not capture enough information from the physics of the problem. This is the case when ε is necessarily not very small. To face such situation, it is necessary to obtain higher-order correctors to capture the information at not-very-small scales (requiring also much more regularity). To see an example of first-order correctors, we refer the reader, for instance, to [90], where Taylor dispersion formulae are derived.

We believe that further research can go on here at least in three different directions:

1. Driving corrector estimates for locally-periodic domains (see e.g., the preliminary result in [102]);

2. Driving goal-oriented *a posteriori* error estimates for perforated domains (see e.g., [137, 138] for the general philosophy of goal-oriented *a posteriori* estimates);

3. For the extended system containing the mobility of the water, error estimates can be proved using first-order asymptotic expansions in energy-like estimates, see [147].

Chapter 6

Solvability of a Parabolic System with Distributed-microstructure

This chapter deals with the solvability of a semilinear parabolic system that incorporates transport (diffusion) and reaction effects emerging from two separated spatial scales: x - macro and y - micro. Our motivation originates from the fact that often problems in material science involve multiple spatial scales and, in addition, several processes occur at highly different time scales. To capture information at separated spatial scales, distributed-microstructure models are the right tool to use.

The chapter is organized in the following fashion: Section 6.1 includes the geometry, functional setting and assumptions on the data as well as on the model parameters. We present the main results of the chapter at the end of the section. In Section 6.2, we introduce axillary problems and treat them in Section 6.3. Existence and uniqueness of solutions to (6.1) – (6.15) is ensured in Section 6.4 together with the needed positivity and L^∞ bounds. The main ingredients to prove existence of solutions include fixed-point arguments and convergent two-scale Galerkin approximations.

6.1 Geometry. Model equations. Functional setting and assumptions

In this section, we present our two-scale geometry, the setting of model equations, the assumptions on the model parameters and data needed to define our concept of solution to perform the mathematical analysis.

6.1.1 Geometry

We consider here a two-scale geometry where to each macroscopic point $x \in \Omega$, we associate the constant microstructure Y, see Fig. 6.1. The microstructure Y
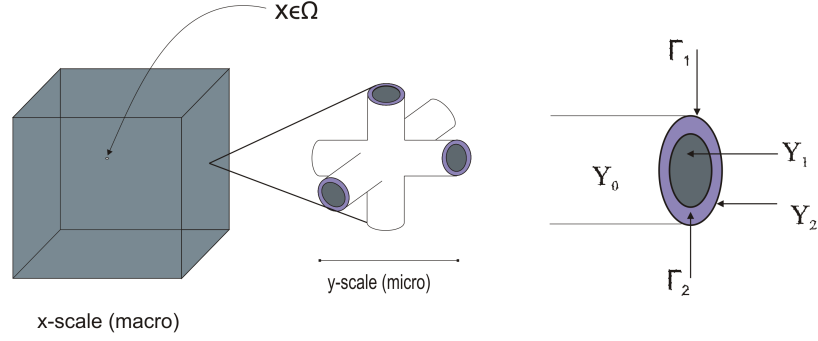
FIGURE 6.1: Left: Zoomed out cubic piece from the concrete wall. This is the scale we refer to as *macroscopic*. Middle: Reference pore (*microscopic*) configuration. Right: Zoomed out one end of the pore.

contains three disjoint parts, Y_0, Y_1 and Y_2 representing the solid part, water-filled part and air-filled part of the pore, respectively. Γ_1 denotes the interface between solid and water-filled parts whereas Γ_2, the interface between water and air-filled parts. We refer to Subsection 2.2.3.3 for details.

6.1.2   Distributed-microstructure system

The distributed-microstructure system, we deal here, is obtained from the system given in Subsection 2.5.2 by replacing the linear reaction rates by nonlinear ones. Our system consists of the following set of partial differential equations coupled with an ordinary differential equation:

$$\partial_t w_1 - \nabla_y \cdot (d_1 \nabla_y w_1) = -f_1(w_1) + f_2(w_2) \qquad \text{in } (0,T) \times \Omega \times Y_1, \tag{6.1}$$
$$\partial_t w_2 - \nabla_y \cdot (d_2 \nabla_y w_2) = f_1(w_1) - f_2(w_2) \qquad \text{in } (0,T) \times \Omega \times Y_1, \tag{6.2}$$
$$\partial_t w_3 - \nabla \cdot (d_3 \nabla w_3) = -\alpha \int_{\Gamma_2} \left(H w_3 - w_2 \right) \mathrm{d}\gamma_y \qquad \text{in } (0,T) \times \Omega, \tag{6.3}$$
$$\partial_t w_5 = \eta(w_1, w_5) \qquad \text{on } (0,T) \times \Omega \times \Gamma_1 \tag{6.4}$$

The system (6.1)-(6.4) is equipped with two-scale initial conditions

$$w_j(0,x,y) = w_j^0(x,y), \quad j \in \{1,2\} \qquad \text{in } \Omega \times Y_1, \tag{6.5}$$
$$w_3(0,x) = w_3^0(x) \quad \text{in } \Omega, \tag{6.6}$$
$$w_5(0,x,y) = w_5^0(x,y) \quad \text{on } \Omega \times \Gamma_1, \tag{6.7}$$

while the boundary conditions are

$$-n(y) \cdot d_1 \nabla_y w_1 \; = \eta(w_1, w_5) \qquad \text{on } (0, T) \times \Omega \times \Gamma_1, \qquad (6.8)$$
$$-n(y) \cdot d_1 \nabla_y w_1 \; = 0 \qquad \text{on } (0, T) \times \Omega \times \Gamma_2, \qquad (6.9)$$
$$-n(y) \cdot d_1 \nabla_y w_1 \; = 0 \qquad \text{on } (0, T) \times \Omega \times (\partial Y_1 \cap \partial Y), (6.10)$$
$$-n(y) \cdot d_2 \nabla_y w_2 \; = 0 \qquad \text{on } (0, T) \times \Omega \times \Gamma_1, \qquad (6.11)$$
$$-n(y) \cdot d_2 \nabla_y w_2 \; = 0 \qquad \text{on } (0, T) \times \Omega \times (\partial Y_1 \cap \partial Y), (6.12)$$
$$-n(y) \cdot d_2 \nabla_y w_2 \; = -\alpha(Hw_3 - w_2) \quad \text{on } (0, T) \times \Omega \times \Gamma_2, \qquad (6.13)$$
$$-n(x) \cdot d_3 \nabla w_3 \; = 0 \qquad \text{on } (0, T) \times \Gamma_N, \qquad (6.14)$$
$$w_3 \; = w_3^D \qquad \text{on } (0, T) \times \Gamma_D. \qquad (6.15)$$

Here w_1 denotes the concentration of H_2SO_4 in $\Omega \times Y_1$, w_2 the concentration of H_2S aqueous species in $\Omega \times Y_1$, w_3 the concentration of H_2S gaseous species in Ω and w_5 of *gypsum* concentration on $\Omega \times \Gamma_1$. ∇ without subscript denotes the differentiation w.r.t. macroscopic variable x, while ∇_y is the respective differential operators w.r.t. the micro-variable y. α is the mass-transfer coefficient for the reaction taking place on the interface Γ_2 and H is the Henry's constant. The microscale information is connected to the macroscale via the right-hand side of (6.3) and the *micro-macro transmission condition* (6.13).

6.1.3 Functional setting. Assumptions

In this subsection, we enumerate the assumptions on the model parameters and data needed to perform the analysis of the system of (6.1)–(6.15). We also discuss our concept of solutions. We give the main results of the chapter at the end of this section. To keep notation simple, we set

$$X := \{z \in H^1(\Omega) | z = 0 \text{ on } \Gamma_D\}.$$

Assumption 6.1.1. *(A1)* $d_k \in L^\infty(\Omega \times Y_1), k \in \{1, 2\}$ and $d_3 \in L^\infty(\Omega)$ such that $(d_k(x, y)\xi, \xi) \geq d_k^0 |\xi|^2$ for $d_k^0 > 0$ for every $\xi \in \mathbb{R}^3$, a.e. $(x, y) \in \Omega \times Y_1$ and $(d_3(x)\xi, \xi) \geq d_3^0 |\xi|^2$ for $d_3^0 > 0$ for every $\xi \in \mathbb{R}^3$ and a.e. $x \in \Omega$.

(A2) The functions $f_i, i \in \{1, 2\}$, are increasing and locally Lipschitz continuous with $f_i(\alpha) = 0$ for $\alpha \leq 0$ and $f_i(\alpha) > 0$ for $\alpha > 0$, $i \in \{1, 2\}$. Furthermore, $\mathcal{R}(f_1) = \mathcal{R}(f_2)$, where $\mathcal{R}(f)$ denotes the range of the function f. Moreover, for $M_1, M_2 > 0$ there exist positive constants $M_1', M_2' > 0$ such that

$$f_1(M_1') = f_2(M_2'), M_1' \geq M_1 \text{ and } M_2' \geq M_2.$$

(A3) $\eta(\alpha, \beta) := R(\alpha)Q(\beta)$, where R and Q are locally Lipschitz continuous functions such that $R' \geq 0$ and $Q' \leq 0$ a.e. on $\mathbb{R}$ and

$$R(\alpha) := \begin{cases} \text{positive,} & \text{if } \alpha > 0, \\ 0, & \text{otherwise,} \end{cases} \qquad Q(\beta) := \begin{cases} \text{positive,} & \text{if } \beta < \beta_{max}, \\ 0, & \text{otherwise,} \end{cases}$$

where β_{max} is a positive constant. Also, we denote by $\mathcal{R}$ the primitive of R with $\mathcal{R}(0) = 0$, i.e. $\mathcal{R}(r) = \int_0^r R(\xi)d\xi$ for $r \in \mathbb{R}$.

(A4) $w_{10} \in L^2(\Omega; H^1(Y_1)) \cap L_+^\infty(\Omega \times Y_1), w_{20} \in L^2(\Omega; H^1(Y_1)) \cap L_+^\infty(\Omega \times Y_1)$, $w_{30} \in H^1(\Omega) \cap L_+^\infty(\Omega), w_{30} - w_3^D(0, \cdot) \in X, w_3^D \in L^2(0, T; H^2(\Omega)) \cap H^1(0, T; L^2(\Omega)) \cap L_+^\infty((0, T) \times \Omega)$ with $\nabla w_3^D \cdot n = 0$ on $(0, T) \times \Gamma_N, w_{50} \in L_+^\infty(\Omega \times \Gamma_1)$.

In (A4) we define $L_+^\infty(\Omega') := L^\infty(\Omega') \cap \{u | u \geq 0 \text{ on } \Omega'\}$ for a domain Ω'.

6.1.4 Definition of solutions

Next, we give the definition of a suitable concept of solution to our problem:

Definition 6.1.2. We call the multiplet (w_1, w_2, w_3, w_5) a solution to the problem (6.1) – (6.8) if (S1) – (S5) hold:

(S1) $w_1, w_2 \in H^1(0, T; L^2(\Omega \times Y_1)) \cap L^\infty(0, T; L^2(\Omega; H^1(Y_1))) \cap L^\infty((0, T) \times \Omega \times Y_1), w_3 \in H^1(0, T; L^2(\Omega)) \cap L^\infty((0, T) \times \Omega), w_3 - w_3^D \in L^\infty(0, T; X), w_5 \in H^1(0, T; L^2(\Omega \times \Gamma_1)) \cap L^\infty((0, T) \times \Omega \times \Gamma_1)$.

(S2) It holds that

$$\int_{\Omega \times Y_1} \partial_t w_1 (w_1 - v_1) \mathrm{d}x\mathrm{d}y + \int_{\Omega \times Y_1} d_1 \nabla_y w_1 \cdot \nabla_y (w_1 - v_1) \mathrm{d}x\mathrm{d}y$$

$$+ \int_{\Omega \times \Gamma_1} Q(w_5)(\mathcal{R}(w_1) - \mathcal{R}(v_1)) \mathrm{d}x\mathrm{d}\gamma_y \leq \int_{\Omega \times Y_1} (-f_1(w_1) + f_2(w_2))(w_1 - v_1) \mathrm{d}x\mathrm{d}y$$

$$\text{for } v_1 \in L^2(\Omega; H^1(Y_1)) \text{ with } \mathcal{R}(v_1) \in L^1(\Omega \times \Gamma_1) \text{ a.e. on } [0, T].$$

(S3) It holds that

$$\int_{\Omega \times Y_1} \partial_t w_2 v_2 \mathrm{d}x\mathrm{d}y + \int_{\Omega \times Y_1} d_2 \nabla_y w_2 \cdot \nabla_y v_2 \mathrm{d}x\mathrm{d}y - \alpha \int_{\Omega \times \Gamma_2} (H w_3 - w_2) v_2 \mathrm{d}x\mathrm{d}\gamma_y$$

$$= \int_{\Omega \times Y_1} (f_1(w_1) - f_2(w_2)) v_2 \mathrm{d}x\mathrm{d}y \quad \text{for } v_2 \in L^2(\Omega; H^1(Y_1)) \text{ a.e. on } [0, T].$$

(S4) It holds that

$$\int_{\Omega \times Y_1} \partial_t w_3 v_3 \mathrm{d}x + \int_{\Omega} d_3 \nabla_y w_3 \cdot \nabla v_3 \mathrm{d}x\mathrm{d}y = -\alpha \int_{\Omega \times \Gamma_2} (H w_3 - w_2) v_3 \mathrm{d}x\mathrm{d}\gamma_y$$

$$\text{for } v_3 \in X \text{ a.e. on } [0, T].$$

(S5) (6.4) holds a.e. on $(0, T) \times \Omega \times \Gamma_1$.

Note that we have introduced a variational inequality in the above definition. The idea of inclusion of the variational inequality is due to the absence of the Laplacian term with respect to $x-$variable. It is not easy to show that the boundary condition for w_1 holds, since the boundary condition is nonlinear. Variational inequality helps in proving the existence and uniqueness of solutions, see Section 6.3. To get the inequality, we use the convexity of $\mathcal{R}$ and positivity of Q such that

$$Q(\beta)R(\alpha)(\alpha - \delta) \geq Q(\beta)(\mathcal{R}(\alpha) - \mathcal{R}(\delta)) \quad \text{for any } \alpha, \delta \in \mathbb{R}.$$

6.1.5 Statement of the main result

Theorem 6.1.3. Assume $(A1) - (A4)$, then there exists a solution (w_1, w_2, w_3, w_5) of the problem $(6.1) - (6.8)$. Moreover, it holds that

(i) $w_1(t), w_2(t) \geq 0$ a.e. in $\Omega \times Y_1$, $w_3(t) \geq 0$ a.e. in Ω and $w_5(t) \geq 0$ a.e. on $\Omega \times \Gamma_1$ for a.a. $t \in [0, T]$.

(ii) $w_1(t) \leq M_1$, $w_2(t) \leq M_2$ a.e. in $\Omega \times Y_1$, $w_3(t) \leq M_3$ a.e. in Ω and $w_5(t) \leq M_5$ a.e. on $\Omega \times \Gamma_1$ for a.a. $t \in [0, T]$, where M_1, M_2, M_3 and M_5 are positive constants satisfying $M_1 \geq \|w_{10}\|_{L^\infty(\Omega \times Y_1)}$, $M_2 \geq \|w_{20}\|_{L^\infty(\Omega \times Y_1)}$, $M_3 \geq \max\{\|w_{30}\|_{L^\infty(\Omega)}, \|w_3^D\|_{L^\infty(\Omega \times Y_1)}\}$, $f_1(M_1) = f_2(M_2)$ and $M_2 = HM_3$ and $M_5 = \max\{\beta_{max}, \|w_{40}\|_{L^\infty(\Omega \times \Gamma_1)}\}$.

Proof. The proof is contained in Section 6.4.

Theorem 6.1.4. Assume $(A1)$ – $(A4)$, then there exists at most one solution in the sense of Definition 5.1.2.

Proof. For the proof, see Subsection 6.4.1.

6.2 Auxiliary problems

In order to prove the existence of solutions, we first introduce the following auxiliary problems:

Problem $\mathbf{P}_1(g, h)$

$$\partial_t w_1 - \nabla_y \cdot (d_1 \nabla_y w_1) = g \quad \text{in } (0, T) \times \Omega \times Y_1,$$
$$d_1 \nabla_y w_1 \cdot n(y) = -hR(w_1) \quad \text{on } (0, T) \times \Omega \times \Gamma_1,$$
$$d_1 \nabla_y w_1 \cdot n(y) = 0 \quad \text{on } (0, T) \times \Omega \times \Gamma_2 \text{ and } (0, T) \times \Omega \times (\partial Y_1 \cap \partial Y),$$
$$w_1(0) = w_{10} \quad \text{on } \Omega \times Y_1.$$

We solve this in Lemma 6.3.1 for given functions g and h.

Problem $\mathbf{P}_2(g)$

Next, for a given function g on $(0, T) \times \Omega \times Y_1$, we consider the following problem $\mathrm{P}_2(g)$:

$$\partial_t w_1 - \nabla_y \cdot (d_1 \nabla_y w_1) = g \quad \text{in } (0, T) \times \Omega \times Y_1,$$
$$d_1 \nabla_y w_1 \cdot n(y) = -\eta(w_1, w_5) \quad \text{on } (0, T) \times \Omega \times \Gamma_1,$$
$$d_1 \nabla_y w_1 \cdot n(y) = 0 \quad \text{on } (0, T) \times \Omega \times \Gamma_2 \text{ and } (0, T) \times \Omega \times (\partial Y_1 \cap \partial Y),$$
$$\partial_t w_5 = \eta(w_1, w_5) \quad \text{a.e. on } (0, T) \times \Omega \times \Gamma_1,$$
$$w_1(0) = w_{10} \text{ on } \Omega \times Y_1 \text{ and } w_4(0) = w_{40} \text{ on } \Omega \times \Gamma_1.$$

We solve this problem in Lemma 6.3.2 for given functions g.

Problem $\mathbf{P}_3(g)$

As a third step of the proof, we show the existence of a solution of the following problem $\mathrm{P}_3(g)$ for a given function g on $(0, T) \times \Omega \times Y_1$:

$$\partial_t w_2 - \nabla_y \cdot (d_2 \nabla_y w_2) = g \quad \text{in } (0, T) \times \Omega \times Y_1,$$
$$\partial_t w_3 - \nabla \cdot (d_3 \nabla w_3) = -\alpha \int_{\Gamma_2} \left(H w_3 - w_2 \right) \mathrm{d}\gamma_y \quad \text{in } (0, T) \times \Omega,$$
$$d_2 \nabla_y w_2 \cdot n = 0 \quad \text{on } (0, T) \times \Omega \times \Gamma_1 \text{ and } (0, T) \times \Omega \times (\partial Y_1 \cap \partial Y),$$
$$d_2 \nabla_y w_2 \cdot n = \alpha(H w_3 - w_2) \quad \text{on } (0, T) \times \Omega \times \Gamma_2,$$
$$d_3 \nabla w_3 \cdot n(x) = 0 \quad \text{on } (0, T) \times \Gamma_N,$$
$$w_3 = w_3^D \quad \text{on } (0, T) \times \Gamma_D,$$
$$w_2(0) = w_{20} \text{ on } \Omega \times Y_1 \text{ and } w_3(0) = w_{30} \text{ on } \Omega.$$

See Lemma 6.3.3 for solution.

6.3   Proof of the technical lemmas

This section contains the solvability of the lemmas given in Section 6.2.

Lemma 6.3.1. Assume (A1), (A3), (A4), $h \in H^1(0, T; L^2(\Omega \times \Gamma_1)) \cap L^\infty_+((0, T) \times \Omega \times \Gamma_1)$ and $g \in L^2((0, T) \times \Omega \times Y_1)$. If R is Lipschitz continuous and bounded on $\mathbb{R}$, then there exists a solution w_1 of $\mathrm{P}_1(g, h)$ in the following sense: $w_1 \in H^1(0, T; L^2(\Omega \times Y_1)) \cap L^\infty(0, T; L^2(\Omega; H^1(Y_1)))$ satisfying

$$\int_{\Omega \times Y_1} \partial_t w_1 (w_1 - v_1) \mathrm{d}x \mathrm{d}y + \int_{\Omega \times Y_1} d_1 \nabla_y w_1 \cdot \nabla_y (w_1 - v_1) \mathrm{d}x \mathrm{d}y$$

$$+ \int\limits_{\Omega \times \Gamma_1} h(\mathcal{R}(w_1) - \mathcal{R}(v_1)) \mathrm{d}x \mathrm{d}\gamma_y$$

$$\leq \int\limits_{\Omega \times Y_1} g(w_1 - v_1) \mathrm{d}x \mathrm{d}y \quad \textit{for } v_1 \in L^2(\Omega; H^1(Y_1)) \textit{ a.e. on } [0, T], (6.16)$$

$$w_1(0) = w_{10} \quad \textit{on } \Omega \times Y_1.$$

Proof. Let $\{\zeta_j\}$ be a Schauder basis of $L^2(\Omega; H^1(Y_1))$. More precisely, $\{\zeta_j\}$ is an orthonormal system of a Hilbert space $L^2(\Omega \times Y_1)$ and is a fundamental of $L^2(\Omega; H^1(Y_1))$, i.e., for any $z \in L^2(\Omega \times Y_1)$, we can take a sequence $\{z^n\}$ such that $z^n = \sum_{j=1}^{N_n} a_j^n \zeta_j$ and $z^n \to z$ in $L^2(\Omega; H^1(Y_1))$ as $n \to \infty$, where $a_j^n \in \mathbb{R}$. Then there exists a sequence $\{w_{10}^n\}$ such that $w_{10}^n := \sum_{j=1}^{N_n} \alpha_{j0}^n \zeta_j$ and $w_{10}^n \to w_{10}$ in $L^2(\Omega; H^1(Y_1))$ as $n \to \infty$.

Here, we are interested in the finite-dimensional approximations of the function w_1 that is of the form

$$w_1^n(t, x, y) := \sum_{j=1}^{N_n} \alpha_j^n(t)\zeta(x, y) \quad \text{for } (t, x, y) \in (0, T) \times \Omega \times Y_1, \qquad (6.17)$$

where the coefficients α_j^n, $j = 1, 2, \ldots, N_n$, are determined by the following relations: For each n

$$\int\limits_{\Omega \times Y_1} (\partial_t w_1^n(t)\phi_1 + d_1 \nabla_y w_1^n(t)\nabla_y \phi_1) \mathrm{d}x \mathrm{d}y + \int\limits_{\Omega \times \Gamma_1} hR(w_1^n(t))\phi_1 \mathrm{d}x \mathrm{d}\gamma_y$$

$$= \int\limits_{\Omega \times Y_1} g(t)\phi_1 \mathrm{d}x \mathrm{d}y \quad \text{for } \phi_1 \in \text{ span}\{\zeta_i : i = 1, 2, .., N_n\} \text{ and } t \in (0, T], (6.18)$$

$$\alpha_j^n(0) = \alpha_{j0}^n \quad \text{for } j = 1, 2, ...N_n. \qquad (6.19)$$

Consider $\phi_1 = \zeta_j$, $j = 1, 2, ...N_n$, as a test functions in (6.18). This yields a system of ordinary differential equations for $t \in (0, T]$

$$\partial_t \alpha_j^n(t) + \sum_{i=1}^{N_n} (A_i)_j \alpha_i^n(t) + F_j^n(t, \alpha^n(t)) = J_j(t) \quad \text{for } t \in (0, T] j = 1, 2, \ldots, N_n,$$

$$(6.20)$$

where

$$\alpha^n(t) := (\alpha_1^n(t), \ldots, \alpha_{N_n}^n(t)), \quad F_j^n(t, \alpha^n) := \int\limits_{\Omega \times \Gamma_1} h(t)R(\sum_{i=1}^{N_n} \alpha_i^n \zeta_i)\zeta_j \mathrm{d}x \mathrm{d}\gamma_y$$

$$(A_i)_j := \int\limits_{\Omega \times Y_1} d_1 \nabla_y \zeta_i \cdot \nabla_y \zeta_j \mathrm{d}x \mathrm{d}y, \quad J_j(t) := \int\limits_{\Omega \times Y_1} g(t)\zeta_j \mathrm{d}x \mathrm{d}y \text{ for } t \in (0, T].$$

Now we show that F_j^n is globally Lipschitz continuous due to the assumptions given in the statement of the lemma.

$$F_j^n(t, \alpha^n) - F_j^n(t, \tilde{\alpha}^n) \quad = \int\limits_{\Omega \times \Gamma_1} h(t) R(\sum_{i=1}^{N_n} (\alpha_i^n - \tilde{\alpha}_i^n)\zeta_i)\zeta_j \mathrm{d}x \mathrm{d}\gamma_y$$

$$\leq C \int\limits_{\Omega \times \Gamma_1} |R(\sum_{i=1}^{N_n} (\alpha_i^n - \tilde{\alpha}_i^n)\zeta_i)| \, |\zeta_j| \mathrm{d}x \mathrm{d}\gamma_y$$

$$\leq C \int\limits_{\Omega \times \Gamma_1} \sum_{i=1}^{N_n} |(\alpha_i^n - \tilde{\alpha}_i^n)\zeta_i| \, |\zeta_j| \mathrm{d}x \mathrm{d}\gamma_y$$

$$\leq C \sum_{i=1}^{N_n} |\alpha_i^n - \tilde{\alpha}_i^n| \int\limits_{\Omega \times \Gamma_1} |\zeta_i| \, |\zeta_j| \mathrm{d}x \mathrm{d}\gamma_y$$

$$\leq C max\{c_{ij}\} \sum_{i=1}^{N_n} |\alpha_i^n - \tilde{\alpha}_i^n|,$$

where the coefficient c_{ij} is given by

$$c_{ij} := \int\limits_{\Omega \times \Gamma_1} |\zeta_i| \, |\zeta_j| \mathrm{d}x \mathrm{d}\gamma_y.$$

According to the standard existence theory for ordinary differential equations, there exists a unique solution α_j^n, $j = 1, 2, .., N_n$, satisfying (8.9) for $0 \leq t \leq T$ and (6.19). Thus the solution w_1^n defined in (8.1) solves (6.18) – (6.19).

Next, we show uniform estimates for solutions w_1^n with respect to N. We take $\phi_1 = w_1^n$ in (6.18) to obtain

$$\int\limits_{\Omega \times Y_1} \partial_t w_1^n(t) w_1^n(t) \mathrm{d}x \mathrm{d}y + \int\limits_{\Omega \times Y_1} d_1 |\nabla_y w_1^n(t)|^2 \mathrm{d}x \mathrm{d}y + \int\limits_{\Omega \times \Gamma_1} h(t) R(w_1^n(t)) w_1^n(t) \mathrm{d}x \mathrm{d}\gamma_y$$

$$= \int\limits_{\Omega \times Y_1} g(t) w_1^n(t) \mathrm{d}x \mathrm{d}y \quad \text{for } t \in (0, T].$$

Since $R(r)r \geq 0$ for any $r \in \mathbb{R}$, we see that

$$\frac{1}{2} \frac{\mathrm{d}}{\mathrm{d}t} \int\limits_{\Omega \times Y_1} |w_1^n(t)|^2 \mathrm{d}x \mathrm{d}y + d_1^0 \int\limits_{\Omega \times Y_1} |\nabla_y w_1^n(t)|^2 \mathrm{d}x \mathrm{d}y$$

$$\leq \frac{1}{2} \int\limits_{\Omega \times Y_1} |g(t)|^2 \mathrm{d}x \mathrm{d}y + \frac{1}{2} \int\limits_{\Omega \times Y_1} |w_1^n(t)|^2 \mathrm{d}x \mathrm{d}y \quad \text{for } t \in (0, T].$$

Applying Gronwall's inequality, we have

$$\int\limits_{\Omega\times Y_1} |w_1^n(t)|^2 \mathrm{d}x\mathrm{d}y + d_1^0 \int\limits_0^t \int\limits_{\Omega\times Y_1} |\nabla_y w_1^n(t)|^2 \mathrm{d}x\mathrm{d}y \le C \quad \text{for } t \in (0,T],$$

where C is a positive constant independent of n.

To obtain bounds on the time-derivative, we take $\phi_1 = \partial_t w_1^n$ as test function in (6.18). We see that

$$\int\limits_{\Omega\times Y_1} |\partial_t w_1^n(t)|^2 \mathrm{d}x\mathrm{d}y + \frac{1}{2}\frac{d}{dt} \int\limits_{\Omega\times Y_1} d_1 |\nabla_y w_1^n(t)|^2 \mathrm{d}x\mathrm{d}y + \int\limits_{\Omega\times\Gamma_1} h(t)\partial_t \mathcal{R}(w_1^n(t))\mathrm{d}x\mathrm{d}\gamma_y$$

$$= \int\limits_{\Omega\times Y_1} g(t)\partial_t w_1^n(t)\mathrm{d}x\mathrm{d}y$$

$$\le \frac{1}{2}\int\limits_{\Omega\times Y_1} |g(t)|^2 \mathrm{d}x\mathrm{d}y + \frac{1}{2}\int\limits_{\Omega\times Y_1} |\partial_t w_1^n(t)|^2 \mathrm{d}x\mathrm{d}y \quad \text{for a.e. } t \in (0,T].$$

Accordingly, we have

$$\frac{1}{2}\int\limits_{\Omega\times Y_1} |\partial_t w_1^n|^2 \mathrm{d}x\mathrm{d}y + \frac{1}{2}\frac{d}{dt} \int\limits_{\Omega\times Y_1} d_1 |\nabla_y w_1^n|^2 \mathrm{d}x\mathrm{d}y + \frac{d}{dt} \int\limits_{\Omega\times\Gamma_1} h\mathcal{R}(w_1^n)\mathrm{d}x\mathrm{d}\gamma_y$$

$$\le \frac{1}{2}\int\limits_{\Omega\times Y_1} |g|^2 \mathrm{d}x\mathrm{d}y + \int\limits_{\Omega\times\Gamma_1} \partial_t h\mathcal{R}(w_1^n)\mathrm{d}x\mathrm{d}\gamma_y \quad \text{a.e. on } \in (0,T].$$

By integrating the latter equation, we have

$$\frac{1}{2}\int\limits_0^\tau \int\limits_{\Omega\times Y_1} |\partial_t w_1^n|^2 \mathrm{d}x\mathrm{d}y\mathrm{d}t + \frac{d_1^0}{2} \int\limits_{\Omega\times Y_1} |\nabla_y w_1^n(\tau)|^2 \mathrm{d}x\mathrm{d}y + \int\limits_{\Omega\times\Gamma_1} h(t)\mathcal{R}(w_1^n(\tau))\mathrm{d}x\mathrm{d}\gamma_y$$

$$\le \frac{1}{2}\int\limits_{\Omega\times Y_1} d_1 |\nabla_y w_1^n(0)|^2 \mathrm{d}x\mathrm{d}y + \int\limits_{\Omega\times\Gamma_1} h(0)\mathcal{R}(w_1^n(0))\mathrm{d}x\mathrm{d}\gamma_y$$

$$+\frac{1}{2}\int\limits_0^\tau \int\limits_{\Omega\times Y_1} |g|^2 \mathrm{d}x\mathrm{d}y\mathrm{d}t + \int\limits_0^\tau \int\limits_{\Omega\times\Gamma_1} \partial_t h\mathcal{R}(w_1^n)\mathrm{d}x\mathrm{d}\gamma_y\mathrm{d}t \quad \text{for } \tau \in (0,T].$$

Note that

$$\int\limits_0^T \int\limits_{\Omega\times\Gamma_1} |\mathcal{R}(w_1^n)|^2 \mathrm{d}x\mathrm{d}\gamma_y\mathrm{d}t \le C\int\limits_0^T \int\limits_{\Omega\times\Gamma_1} |w_1^n|^2 \mathrm{d}x\mathrm{d}\gamma_y\mathrm{d}t$$

$$\le C\int\limits_0^T \int\limits_{\Omega\times Y_1} (|\nabla_y w_1^n|^2 + |w_1^n|^2)\mathrm{d}x\mathrm{d}y\mathrm{d}t.$$

Here, we have used the trace inequality. Hence, we observe that $\{w_1^n\}$ is bounded in $H^1(0, T; L^2(\Omega \times Y_1))$ and $L^\infty(0, T; L^2(\Omega; H^1(Y_1)))$. From these estimates, we can choose a subsequence $\{n_i\}$ of $\{n\}$ such that $w_1^{n_i} \to w_1$ weakly in $H^1(0, T; L^2(\Omega \times Y_1))$ and weakly* in $L^\infty(0, T; L^2(\Omega \times Y_1))$ and $L^\infty(0, T; L^2(\Omega; H^1(Y_1)))$. Also, the above convergence results imply that $w_1^{n_i}(T) \to w_1(T)$ weakly in $L^2(\Omega \times Y_1)$.

Now, to show that (6.16) holds, let $v \in L^2(0, T; L^2(\Omega; H^1(Y_1)))$. We take a sequence $\{v^k\}$ such that $v^k(t) := \sum_{j=1}^{m_k} \lambda_j^k(t) \zeta_j$ and $v^k \to v$ in $L^2(0, T; L^2(\Omega; H^1(Y_1)))$ as $k \to \infty$, where $\lambda_i^k \in C([0, T])$ for $i = 1, 2, \ldots, m_k$ and $k = 1, 2, \ldots$. For each k and i with $N_{n_i} \geq m_k$, it follows from (6.18) that

$$
\int_0^T \int_{\Omega \times Y_1} \partial_t w_1^{n_i}(w_1^{n_i} - v_1^k) \mathrm{d}x \mathrm{d}y \mathrm{d}t + \int_{\Omega \times Y_1} d_1 \nabla_y w_1^{n_i} \cdot \nabla_y(w_1^{n_i} - v_1^k) \mathrm{d}x \mathrm{d}y \mathrm{d}t
$$

$$
+ \int_0^T \int_{\Omega \times \Gamma_1} hR(w_1^{n_i})(w_1^{n_i} - v_1^k) \mathrm{d}x \mathrm{d}\gamma_y \mathrm{d}t \leq \int_0^T \int_{\Omega \times Y_1} g(w_1^{n_i} - v_1^k) \mathrm{d}x \mathrm{d}y \mathrm{d}t.
$$

By the lower semi-continuity of the norm and the convex function $\mathcal{R}$, we have

$$
\liminf_{i \to \infty} \left(\int_0^T \int_{\Omega \times Y_1} \{\partial_t w_1^{n_i}(w_1^{n_i} - v_1^k) + d_1 \nabla_y w_1^{n_i} \cdot \nabla_y(w_1^{n_i} - v_1^k)\} \mathrm{d}x \mathrm{d}y \mathrm{d}t \right.
$$

$$
\left. + \int_0^T \int_{\Omega \times \Gamma_1} hR(w_1^{n_i})(w_1^{n_i} - v_1^k) \mathrm{d}x \mathrm{d}\gamma_y \mathrm{d}t \right)
$$

$$
\geq \int_0^T \int_{\Omega \times Y_1} \partial_t w_1(w_1 - v_1^k) \mathrm{d}x \mathrm{d}y \mathrm{d}t + \int_{\Omega \times Y_1} d_1 \nabla_y w_1 \cdot \nabla_y(w_1 - v_1^k) \mathrm{d}x \mathrm{d}y \mathrm{d}t
$$

$$
+ \int_0^T \int_{\Omega \times \Gamma_1} h(\mathcal{R}(w_1) - \mathcal{R}(v_1^k)) \mathrm{d}x \mathrm{d}\gamma_y \mathrm{d}t \quad \text{for each } k.
$$

Then we show that (6.16) holds for each v^k. Moreover, by letting $k \to \infty$ we obtain the conclusion of this lemma.

Next, we deal with the problem $P_2(g)$.

Lemma 6.3.2. Assume (A1) – (A3) and (A4), and $g \in L^2((0, T) \times \Omega \times Y_1)$. If R and Q are Lipschitz continuous and bounded on $\mathbb{R}$, then there exists a solution (w_1, w_5) of $P_2(g)$ in the following sense: $w_1 \in H^1(0, T; L^2(\Omega \times Y_1)) \cap$

$L^\infty(0, T; L^2(\Omega; H^1(Y_1)))$ and $w_5 \in H^1(0, T; L^2(\Omega \times \Gamma_1))$ satisfying

$$\int\limits_{\Omega \times Y_1} \partial_t w_1 (w_1 - v_1) \mathrm{d}x \mathrm{d}y + \int\limits_{\Omega \times Y_1} d_1 \nabla_y w_1 \cdot \nabla_y (w_1 - v_1) \mathrm{d}x \mathrm{d}y$$

$$+ \int\limits_{\Omega \times \Gamma_1} Q(w_5)(\mathcal{R}(w_1) - \mathcal{R}(v_1)) \mathrm{d}x \mathrm{d}\gamma_y$$

$$\leq \int\limits_{\Omega \times Y_1} g(w_1 - v_1) \mathrm{d}x \mathrm{d}y \quad \textit{for } v_1 \in L^2(\Omega; H^1(Y_1)) \textit{ a.e. on } [0, T], (6.21)$$

$$\partial_t w_5 = \eta(w_1, w_5) \quad \textit{on } (0, T) \times \Omega \times \Gamma, \tag{6.22}$$

$$w_1(0) = w_{10} \quad \textit{on } \Omega \times Y_1 \textit{ and } w_5(0) = w_{50} \quad \textit{on } \Omega \times \Gamma_1.$$

Proof. Let $\bar{w}_5 \in V := \{z \in H^1(0, T; L^2(\Omega \times \Gamma_1)) : z(0) = w_{50}\}$.
Since $Q(\bar{w}_5) \in H^1(0, T; L^2(\Omega \times \Gamma_1)) \cap L^\infty_+((0, T) \times \Omega \times \Gamma_1)$, Lemma 6.3.1 implies that the problem $P_1(g, Q(\bar{w}_5))$ has a solution w_1 in the sense stated in Lemma 6.3.1. Also, we put

$$w_5(t) := \int\limits_0^t \eta(w_1(\tau), \bar{w}_5(\tau)) d\tau + w_{50} \quad \text{on } \Omega \times \Gamma_1 \text{ for } t \in [0, T].$$

Accordingly, we can define an operator $\Lambda_T : V \to V$ by $\Lambda_T(\bar{w}_5) = w_5$. Now, we show that Λ_T is a contraction mapping for sufficiently small $T > 0$. Let $\bar{w}_5^i \in H^1(0, T; L^2(\Omega \times \Gamma_1))$ and w_1^i be a solution to $P_1(g, Q(\bar{w}_5^i))$ and $w_5^i = \Lambda_T(\bar{w}_5^i)$ for $i = 1, 2$, and $w_1 = w_1^1 - w_1^2$, $w_5 = w_5^1 - w_5^2$ and $\bar{w}_5 = \bar{w}_5^1 - \bar{w}_5^2$.

First, from (6.16) with $v_1 = w_1^2$ we see that

$$\int\limits_{\Omega \times Y_1} \partial_t w_1^1 (w_1^1 - w_1^2) \mathrm{d}x \mathrm{d}y + \int\limits_{\Omega \times Y_1} d_1 \nabla_y w_1^1 \cdot \nabla_y (w_1^1 - w_1^2) \mathrm{d}x \mathrm{d}y$$

$$+ \int\limits_{\Omega \times \Gamma_1} Q(\bar{w}_5^1)(\mathcal{R}(w_1^1) - \mathcal{R}(w_1^2)) \mathrm{d}x \mathrm{d}\gamma_y$$

$$\leq \int\limits_{\Omega \times Y_1} g(w_1^1 - w_1^2) \mathrm{d}x \mathrm{d}y \quad \text{a.e. on } [0, T].$$

Similarly, we have

$$\int\limits_{\Omega \times Y_1} \partial_t w_1^2 (w_1^2 - w_1^1) \mathrm{d}x \mathrm{d}y + \int\limits_{\Omega \times Y_1} d_1 \nabla_y w_1^2 \cdot \nabla_y (w_1^2 - w_1^1) \mathrm{d}x \mathrm{d}y$$

$$+ \int\limits_{\Omega \times \Gamma_1} Q(\bar{w}_5^2)(\mathcal{R}(w_1^2) - \mathcal{R}(w_1^1)) \mathrm{d}x \mathrm{d}\gamma_y$$

$$\leq \int\limits_{\Omega \times Y_1} g(w_1^2 - w_1^1) \mathrm{d}x \mathrm{d}y \quad \text{a.e. on } [0, T].$$

By subtracting these inequalities, for any $\varepsilon > 0$ we obtain

$$
\frac{1}{2}\frac{d}{dt}\int\limits_{\Omega\times Y_1} |w_1|^2 \mathrm{d}x\mathrm{d}y + \int\limits_{\Omega\times Y_1} d_1|\nabla_y w_1|^2 \mathrm{d}x\mathrm{d}y
$$

$$
\leq \quad -\int\limits_{\Omega\times\Gamma_1} (Q(\bar{w}_5^1) - Q(\bar{w}_5^2))(\mathcal{R}(w_1^2) - \mathcal{R}(w_1^1))\mathrm{d}x\mathrm{d}\gamma_y \qquad (6.23)
$$

$$
\leq \quad C_\varepsilon \int\limits_{\Omega\times\Gamma_1} |\bar{w}_5|^2 \mathrm{d}x\mathrm{d}\gamma_y + \varepsilon \int\limits_{\Omega\times\Gamma_1} |w_1|^2 \mathrm{d}x\mathrm{d}\gamma_y
$$

$$
\leq \quad C_\varepsilon \int\limits_{\Omega\times\Gamma_1} |\bar{w}_5|^2 \mathrm{d}x\mathrm{d}\gamma_y + C_{Y_1}\varepsilon \int\limits_{\Omega\times Y_1} (|\nabla_y w_1|^2 + |w_1|^2)\mathrm{d}x\mathrm{d}y \quad \text{a.e. on } [0,T],
$$

where C_{Y_1} is a positive constant depending only on Y_1. Here, by taking $\varepsilon > 0$ with $C_{Y_1}\varepsilon = \frac{1}{2}d_1^0$ and using Gronwall's inequality we see that

$$
\frac{1}{2}\int\limits_{\Omega\times Y_1} |w_1(t)|^2 \mathrm{d}x\mathrm{d}y + \frac{d_1^0}{2}\int\limits_0^t \int\limits_{\Omega\times Y_1} |\nabla_y w_1|^2 \mathrm{d}x\mathrm{d}y d\tau
$$

$$
\leq \quad e^{Ct}\int\limits_0^t \int\limits_{\Omega\times\Gamma_1} |\bar{w}_5|^2 \mathrm{d}x\mathrm{d}\gamma_y d\tau \quad \text{for } t \in [0,T]. \qquad (6.24)
$$

Next, on account of the definition of w_5, we that

$$
\frac{1}{2}\frac{d}{dt}\int\limits_{\Omega\times\Gamma_1} |w_5(t)|^2 \mathrm{d}x\mathrm{d}\gamma_y
$$

$$
\leq \quad \frac{1}{2}\int\limits_{\Omega\times\Gamma_1} (|\eta(w_1^1(t), \bar{w}_5^1(t)) - \eta(w_1^2(t), \bar{w}_5^2(t))|^2 + |w_5(t)|^2)\mathrm{d}x\mathrm{d}\gamma_y
$$

$$
\leq \quad C\int\limits_{\Omega\times\Gamma_1} (|w_1(t)|^2 + |\bar{w}_5(t)|^2 + |w_5(t)|^2)\mathrm{d}x\mathrm{d}\gamma_y \quad \text{for a.e. } t \in [0,T].
$$

Gronwall's inequality, viewed in the context of (6.24), implies that

$$
\int\limits_{\Omega\times\Gamma_1} |w_5(t)|^2 \mathrm{d}x\mathrm{d}\gamma_y
$$

$$
\leq \quad Ce^{Ct}\left(\int\limits_0^t \int\limits_{\Omega\times\Gamma_1} |\bar{w}_5|^2 \mathrm{d}x\mathrm{d}\gamma_y d\tau + \int\limits_0^t \int\limits_{\Omega\times Y_1} (|\nabla_y w_1|^2 + |w_1|^2)\mathrm{d}x\mathrm{d}y d\tau\right)
$$

$$
\leq \quad Ce^{Ct}\int\limits_0^t \int\limits_{\Omega\times\Gamma_1} |\bar{w}_5|^2 \mathrm{d}x\mathrm{d}\gamma_y d\tau \quad \text{for } t \in [0,T].
$$

Hence, we obtain

$$
\begin{aligned}
\left\|\partial_t w_5\right\|_{L^2(0,T;L^2(\Omega \times \Gamma_1))} &\leq \left\|\eta(w_1^1, \bar{w}_5^1) - \eta(w_1^2, \bar{w}_5^2)\right\|_{L^2(0,T;L^2(\Omega \times \Gamma_1))} \\
&\leq C\left(\left\|w_1\right\|_{L^2(0,T;L^2(\Omega;H^1(Y_1)))} + \left\|\bar{w}_5\right\|_{L^2(0,T;L^2(\Omega \times \Gamma_1))}\right) \\
&\leq C\left\|\bar{w}_5\right\|_{L^2(0,T;L^2(\Omega \times \Gamma_1))} \\
&\leq CT^{1/2}\left\|\partial_t \bar{w}_5\right\|_{L^2(0,T;L^2(\Omega \times \Gamma_1))},
\end{aligned}
$$

and

$$
\begin{aligned}
&\left\|\Lambda_T(\bar{w}_5^1) - \Lambda_T(\bar{w}_5^2)\right\|_{H^1(0,T;L^2(\Omega \times \Gamma_1))} \\
&\leq \quad \left\|w_5\right\|_{L^2(0,T;L^2(\Omega \times \Gamma_1))} + \left\|\partial_t w_5\right\|_{L^2(0,T;L^2(\Omega \times \Gamma_1))} \\
&\leq \quad CT^{1/2}\left\|\bar{w}_5\right\|_{H^1(0,T;L^2(\Omega \times \Gamma_1))}.
\end{aligned}
$$

This concludes that there exists $0 < T_0 \leq T$ such that Λ_{T_0} is a contraction mapping. Here, we note that the choice of T_0 is independent of initial values. Therefore, by applying Banach's fixed point theorem we have proved this lemma.

As third step, we treat the auxiliary problem $P_3(g)$.

Lemma 6.3.3. Assume (A1), (A3), (A4), and $g \in L^2((0,T) \times \Omega \times Y_1)$. Then there exists a pair (w_2, w_3) such that $w_2 \in H^1(0,T;L^2(\Omega \times Y_1)) \cap L^\infty(0,T; L^2(\Omega;H^1(Y_1)))$, $w_3 \in H^1(0,T;L^2(\Omega)) \cap L^\infty(0,T;H^1(\Omega))$,

$$
\begin{aligned}
&\int_{\Omega \times Y_1} \partial_t w_2 v_2 \mathrm{d}x\mathrm{d}y + \int_{\Omega \times Y_1} d_2 \nabla_y w_2 \cdot \nabla_y v_2 \mathrm{d}x\mathrm{d}y - \alpha \int_{\Omega \times \Gamma_2} (H w_3 - w_2) v_2 \mathrm{d}x\mathrm{d}\gamma_y \\
&= \int_{\Omega \times Y_1} g v_2 \mathrm{d}x\mathrm{d}y \quad \text{for } v_2 \in L^2(\Omega;H^1(Y_1)) \text{ a.e. on } [0,T]. \quad (6.25)
\end{aligned}
$$

and (S4).

Proof. Let $\{\zeta_j\}$ be the same set of bases functions as in the proof of Lemma 6.3.1 and $\{\mu_j\}$ be an orthonormal system of the Hilbert space $L^2(\Omega)$ and a fundamental of X. Then we can take sequences $\{w_{20}^n\}$ and $\{W_{30}^n\}$ such that $w_{20}^n \to w_{20}$ in $L^2(\Omega;H^1(Y_1))$ and $W_{30}^n \to w_{30} - w_3^D(0)$ in X as $n \to \infty$.

We approximate w_2 and $W_3 := w_3 - w_3^D$ by functions w_2^n and W_3^n of the forms

$$
w_2^n(t) = \sum_{j=1}^{N_n} \beta_j^n(t)\zeta_j, \quad W_3^n(t) = \sum_{j=1}^{N_n} \gamma_j^n(t)\mu_j \quad \text{for } n, \quad (6.26)
$$

where the coefficients β_j^n and γ_j^n, $j = 1, 2, \ldots, N_n$ are determined in the following

relations: For each n , we have

$$\int\limits_{\Omega\times Y_1} \partial_t w_2^n \phi_2 \mathrm{d}x\mathrm{d}y + \int\limits_{\Omega\times Y_1} d_2 \nabla_y w_2^n \cdot \nabla_y \phi_2 \mathrm{d}x\mathrm{d}y - \alpha \int\limits_{\Omega\times\Gamma_2} (HW_3^n - w_2^n)\phi_2 \mathrm{d}x\mathrm{d}\gamma_y$$

$$= \int\limits_{\Omega\times Y_1} g\phi_2 \mathrm{d}x\mathrm{d}y + \alpha \int\limits_{\Omega\times\Gamma_2} Hw_3^D \phi_2 \mathrm{d}x\mathrm{d}\gamma_y \qquad (6.27)$$

$$\text{for } \phi_2 \in \text{ span}\{\zeta_i : i = 1,..,N_n\}, t \in (0,T],$$
$$\beta_j^n(0) = \beta_{j0}^n \quad \text{for } j = 1,2,..,N_n,$$

$$\int\limits_{\Omega} \partial_t W_3^n \phi_3 \mathrm{d}x + \int\limits_{\Omega} d_3 \nabla W_3^n \cdot \nabla \phi_3 \mathrm{d}x + \alpha \int\limits_{\Omega\times\Gamma_2} (HW_3^n - w_2^n)\phi_3 \mathrm{d}x\mathrm{d}\gamma_y$$

$$= -\int\limits_{\Omega} (\partial_t w_3^D - \nabla d_3(\nabla w_3^D))\phi_3 \mathrm{d}x\mathrm{d}y - \alpha \int\limits_{\Omega\times\Gamma_2} Hw_3^D \phi_3 \mathrm{d}x\mathrm{d}\gamma_y \qquad (6.28)$$

$$\text{for } \phi_3 \in \text{ span}\{\mu_i : i = 1,2,...,N_n\}, t \in (0,T],$$
$$\gamma_j^n(0) = \gamma_{j0}^n \quad \text{for } j = 1,2,..,N_n.$$

Consider $\phi_2 = \zeta_j$ and $\phi_3 = \mu_j$, $j = 1,2,..,N_n$, as a test functions in (6.27) and (6.28), respectively, these yield a system of ordinary differential equations

$$\partial_t \beta_j^n(t) + \sum_{i=1}^{N_n} (B_i)_j \beta_i^n(t) + \sum_{i=1}^{N_n} (\tilde{B}_i)_j \gamma_i^n(t) = J_{j2}(t),$$

$$\partial_t \gamma_j^n(t) + \sum_{i=1}^{N_n} (C_i)_j \gamma_i^n(t) + \sum_{i=1}^{N_n} (\tilde{C}_i)_j \beta_i^n(t) = J_{j3}(t),$$

for $t \in (0,T]$ and $j = 1,2,\ldots,N_n$ and

$$(B_i)_j := \int\limits_{\Omega\times Y_1} d_2 \nabla_y \zeta_i \cdot \nabla_y \zeta_j \mathrm{d}x\mathrm{d}y, \qquad (\tilde{B}_i)_j := \int\limits_{\Omega\times\Gamma_2} \mu_i \zeta_j \mathrm{d}x\mathrm{d}\gamma_y,$$

$$(C_i)_j := \int\limits_{\Omega} d_3 \nabla\mu_i \cdot \nabla\mu_j \mathrm{d}x + \alpha H \int\limits_{\Omega\times\Gamma_2} \mu_i\mu_j \mathrm{d}x\mathrm{d}\gamma_y,$$

$$(\tilde{C}_i)_j := -\alpha \int\limits_{\Omega\times\Gamma_2} \mu_j \zeta_i \mathrm{d}x\mathrm{d}\gamma_y, \qquad J_{2j}(t) := \int\limits_{\Omega\times Y_1} g(t)\zeta_j \mathrm{d}x\mathrm{d}y,$$

$$J_{3j}(t) := \int\limits_{\Omega\times Y_1} (\partial_t w_3^D - \nabla(\nabla w_3^D))\zeta_j \mathrm{d}x\mathrm{d}y + \alpha H \int\limits_{\Omega\times\Gamma_2} w_3^D \zeta_j \mathrm{d}x\mathrm{d}\gamma_y \text{ for } t \in (0,T].$$

Clearly, this linear system of ordinary differential equations has a solution β_j^n and γ_j^n. Thus the solutions w_2^n and W_3^n defined in (6.26) solve (6.27) and (6.28), respectively.

Next, we shall obtain some uniform estimates for w_2^n and W_3^N. We take $\phi_2 = w_2^n$ and $\phi_3 = W_3^n$ in (6.27) and (6.28), respectively, to have

$$\frac{1}{2}\frac{d}{dt}\int\limits_{\Omega\times Y_1}|w_2^n(t)|^2\mathrm{d}x\mathrm{d}y + \int\limits_{\Omega\times Y_1}d_2|\nabla_y w_2^n(t)|^2\mathrm{d}x\mathrm{d}y + \frac{\alpha}{4}\int\limits_{\Omega\times\Gamma_2}|w_2^n(t)|^2\mathrm{d}x\mathrm{d}\gamma_y$$

$$\leq \frac{\alpha}{2}H|\Gamma_2|\int\limits_{\Omega}|W_3^n(t)|^2\mathrm{d}x + \frac{1}{2}\int\limits_{\Omega\times Y_1}|g(t)|^2\mathrm{d}x\mathrm{d}y$$

$$+ \frac{1}{2}\int\limits_{\Omega\times Y_1}|w_2^n(t)|^2\mathrm{d}x\mathrm{d}y + \alpha H^2\int\limits_{\Omega\times\Gamma_2}|w_3^D(t)|^2\mathrm{d}x\mathrm{d}y \quad \text{for a.e. } t \in [0, T],$$

and

$$\frac{1}{2}\frac{d}{dt}\int\limits_{\Omega}|W_3^n(t)|^2\mathrm{d}x + \int\limits_{\Omega}d_3|\nabla W_3^n(t)|^2\mathrm{d}x + \alpha H|\Gamma_2|\int\limits_{\Omega}|W_3^n(t)|^2\mathrm{d}x\mathrm{d}\gamma_y$$

$$\leq \frac{1}{4}\int\limits_{\Omega\times\Gamma_2}|w_2^n(t)|^2\mathrm{d}x\mathrm{d}\gamma_y + (\alpha^2|\Gamma_2| + \frac{1}{2})\int\limits_{\Omega}|W_3^n(t)|^2\mathrm{d}x$$

$$+ \frac{1}{2}\int\limits_{\Omega}|g^D(t)|^2\mathrm{d}x \quad \text{for a.e. } t \in [0, T],$$

where $|\Gamma_2| := \int\limits_{\Gamma_2}\mathrm{d}\gamma_y$, and $g^D := \partial_t w_3^D - \nabla(\nabla w_3^D) + \alpha H|\Gamma_2|w_3^D$. By adding these inequalities, we get

$$\frac{1}{2}\frac{d}{dt}\int\limits_{\Omega\times Y_1}|w_2^n(t)|^2\mathrm{d}x\mathrm{d}y + d_2^0\int\limits_{\Omega\times Y_1}|\nabla_y w_2^n(t)|^2\mathrm{d}x\mathrm{d}y$$

$$+ \frac{1}{2}\frac{d}{dt}\int\limits_{\Omega}|W_3^n(t)|^2\mathrm{d}x + d_3^0\int\limits_{\Omega}|\nabla W_3^n(t)|^2\mathrm{d}x$$

$$\leq (\alpha^2|\Gamma_2| + \frac{1}{2} + \frac{\alpha}{2}H|\Gamma_2|)\int\limits_{\Omega}|W_3^n(t)|^2\mathrm{d}x + \frac{1}{2}\int\limits_{\Omega\times Y_1}|g(t)|^2\mathrm{d}x\mathrm{d}y$$

$$+ \frac{3}{4}\int\limits_{\Omega\times Y_1}|w_2^n(t)|^2\mathrm{d}x\mathrm{d}y + \frac{1}{2}\int\limits_{\Omega}|g^D(t)|^2\mathrm{d}x \quad \text{for a.e. } t \in [0, T].$$

Consequently, Gronwall's inequality implies that for some positive constant C

$$\int\limits_{\Omega\times Y_1}|w_2^n(t)|^2\mathrm{d}x\mathrm{d}y + \int\limits_{\Omega}|W_3^n(t)|^2\mathrm{d}x \leq C \quad \text{for } t \in [0, T] \text{ and } n, \quad (6.29)$$

$$\int\limits_0^T\int\limits_{\Omega\times Y_1}|\nabla_y w_2^n(t)|^2\mathrm{d}x\mathrm{d}y\mathrm{d}t + \int\limits_0^T\int\limits_{\Omega}|\nabla W_3^n(t)|^2\mathrm{d}x\mathrm{d}t \leq C \text{ for } n. \quad (6.30)$$

Now we obtain a uniform estimate for the time derivative by taking $\phi_2 = \partial_t w_2^n$ in (6.27), we observe that

$$
\int\limits_{\Omega \times Y_1} |\partial_t w_2^n(t)|^2 \mathrm{d}x\mathrm{d}y + \frac{1}{2}\frac{d}{dt}\int\limits_{\Omega \times Y_1} d_2|\nabla_y w_2^n(t)|^2 \mathrm{d}x\mathrm{d}y
$$

$$
-\alpha \int\limits_{\Omega \times \Gamma_2} (H(W_3^n(t) + w_3^D(t)) - w_2^n(t))\partial_t w_2^n(t)\mathrm{d}x\mathrm{d}\gamma_y
$$

$$
= \int\limits_{\Omega \times Y_1} g(t)\partial_t w_2^n(t)\mathrm{d}x\mathrm{d}y \quad \text{for a.e. } t \in [0, T]. \tag{6.31}
$$

Here, we denote the third term in the left hand side of (6.31) by $J(t)$ and see that

$$
J(t) \quad := \quad -\alpha\frac{d}{dt}\int\limits_{\Omega \times \Gamma_2} H(W_3^n(t) + w_3^D(t))w_2^n(t)\mathrm{d}x\mathrm{d}\gamma_y + \alpha\frac{1}{2}\frac{d}{dt}\int\limits_{\Omega \times \Gamma_2} |w_2^n(t)|^2 \mathrm{d}x\mathrm{d}\gamma_y
$$

$$
+\alpha H \int\limits_{\Omega \times \Gamma_2} \partial_t(W_3^n(t) + w_3^D(t))w_2^n(t)\mathrm{d}x\mathrm{d}\gamma_y \quad \text{for a.e. } t \in [0, T].
$$

Then we have

$$
\frac{1}{2}\int\limits_{\Omega \times Y_1} |\partial_t w_2^n(t)|^2 \mathrm{d}x\mathrm{d}y + \frac{1}{2}\frac{d}{dt}\int\limits_{\Omega \times Y_1} d_2|\nabla_y w_2^n(t)|^2 \mathrm{d}x\mathrm{d}y + \frac{\alpha}{2}\frac{d}{dt}\int\limits_{\Omega \times \Gamma_2} |w_2^n(t)|^2 \mathrm{d}x\mathrm{d}\gamma_y
$$

$$
\leq \frac{1}{2}\int\limits_{\Omega \times Y_1} |g(t)|^2 \mathrm{d}x\mathrm{d}y + \alpha\frac{d}{dt}\int\limits_{\Omega \times \Gamma_2} H(W_3^n(t) + w_3^D(t))w_2^n(t)\mathrm{d}x\mathrm{d}\gamma_y
$$

$$
+\alpha H|\Gamma_2|^{1/2}\int\limits_{\Omega} |\partial_t(W_3^n(t) + w_3^D(t))|\,\|w_2^n(t)\|_{L^2(\Gamma_2)}\mathrm{d}x \quad \text{for a.e. } t \in [0, T]. \tag{6.32}
$$

Considering the last term in (6.32) and by Young's inequality, we have

$$
\alpha H|\Gamma_2|^{1/2}\int\limits_{\Omega} |\partial_t(W_3^n(t) + w_3^D(t))|\,\|w_2^n(t)\|_{L^2(\Gamma_2)}\mathrm{d}x
$$

$$
\leq \quad \alpha H|\Gamma_2|^{1/2}\|w_2^n(t)\|_{L^2(\Gamma_2)}\int\limits_{\Omega} |\partial_t(W_3^n(t) + w_3^D(t))|\mathrm{d}x
$$

$$
\leq \quad \alpha H|\Gamma_2|^{1/2}\|w_2^n(t)\|_{L^2(\Gamma_2)}\int\limits_{\Omega} \left(|\partial_t(W_3^n(t)| + |w_3^D(t))|\right)\mathrm{d}x
$$

$$
\leq \quad \alpha H|\Gamma_2|^{1/2}|\Omega|^{1/2}\|w_2^n(t)\|_{L^2(\Gamma_2)}\left(\|\partial_t(W_3^n(t)\|_{L^2(\Gamma_2)} + \|w_3^D(t))\|_{L^2(\Gamma_2)}\right)
$$

$$
\leq \quad \frac{1}{4}\|\partial_t(W_3^n(t)\|_{L^2(\Gamma_2)}^2 + \frac{3}{2}\alpha^2 H^2|\Gamma_2||\Omega|\|w_2^n(t)\|_{L^2(\Gamma_2)}^2 + \frac{1}{2}\|w_3^D(t))\|_{L^2(\Gamma_2)}^2\right)
$$

Similarly, by taking $\phi_3 = \partial_t W_3^n$ in (6.28) we have

$$
\int_\Omega |\partial_t W_3^n(t)|^2 \mathrm{d}x + \frac{1}{2}\frac{d}{dt}\int_\Omega d_3|\nabla W_3^n(t)|^2 \mathrm{d}x
$$

$$
= -\alpha \int_{\Omega\times\Gamma_2} (H(W_3^n(t)+w_3^D(t))-w_2^n(t))\partial_t W_3^n(t)\mathrm{d}x\mathrm{d}\gamma_y - \int_\Omega g^D(t)\partial_t W_3^n(t)\mathrm{d}x
$$

$$
\leq -\alpha H|\Gamma_2|\frac{d}{dt}\int_\Omega |W_3^n(t)|^2\mathrm{d}x + 2\alpha^2 H^2|\Gamma_2|^2\int_\Omega |w_3^D(t)|^2\mathrm{d}x
$$

$$
+2\alpha^2|\Gamma_2|\int_{\Omega\times\Gamma_2} |w_2^n(t)|^2\mathrm{d}x\mathrm{d}\gamma_y + \frac{1}{2}\int_\Omega |\partial_t W_3^n(t)|^2\mathrm{d}x + \int_\Omega |g^D(t)|^2\mathrm{d}x
$$
$$
\text{for a.e. } t\in[0,T].
$$

From these inequalities, it follows that

$$
\frac{1}{2}\int_{\Omega\times Y_1} |\partial_t w_2^n(t)|^2\mathrm{d}x\mathrm{d}y + \frac{1}{2}\frac{d}{dt}\int_{\Omega\times Y_1} d_2|\nabla_y w_2^n(t)|^2\mathrm{d}x\mathrm{d}y + \frac{1}{2}\frac{d}{dt}\int_{\Omega\times\Gamma_2} |w_2^n(t)|^2\mathrm{d}x\mathrm{d}\gamma_y
$$

$$
+\frac{1}{8}\int_\Omega |\partial_t W_3^n(t)|^2\mathrm{d}x + \frac{1}{2}\frac{d}{dt}\int_\Omega d_3|\nabla W_3^n(t)|^2\mathrm{d}x + \alpha H|\Gamma_2|\frac{d}{dt}\int_\Omega |W_3^n(t)|^2\mathrm{d}x
$$

$$
\leq \frac{1}{2}\int_{\Omega\times Y_1} |g(t)|^2\mathrm{d}x\mathrm{d}y + \frac{d}{dt}\int_{\Omega\times\Gamma_2} H(W_3^n(t)+w_3^D(t))w_2^n(t)\mathrm{d}x\mathrm{d}\gamma_y
$$

$$
+(2|\Gamma_2|+2\alpha^2|\Gamma_2|)\int_{\Omega\times\Gamma_2} |w_2^n(t)|^2\mathrm{d}x\mathrm{d}\gamma_y + \int_\Omega |g^D(t)|^2\mathrm{d}x \quad \text{for a.e. } t\in[0,T].
$$

Here, we use Gronwall's inequality to have

$$
\frac{1}{2}\int_0^{t_1}\int_{\Omega\times Y_1} |\partial_t w_2^n|^2\mathrm{d}x\mathrm{d}y\mathrm{d}t + \frac{1}{2}\int_{\Omega\times Y_1} d_2|\nabla_y w_2^n(t_1)|^2\mathrm{d}x\mathrm{d}y + \frac{1}{2}\int_{\Omega\times\Gamma_2} |w_2^n(t_1)|^2\mathrm{d}x\mathrm{d}\gamma_y
$$

$$
+\frac{1}{8}\int_0^{t_1}\int_\Omega |\partial_t W_3^n|^2\mathrm{d}x\mathrm{d}t + \frac{1}{2}\int_\Omega d_3|\nabla W_3^n(t_1)|^2\mathrm{d}x + \alpha H|\Gamma_2|\int_{\Omega\times\Gamma_2} |W_3^n(t_1)|^2\mathrm{d}x
$$

$$
\leq e^{Ct_1}\int_0^{t_1}\left(\int_{\Omega\times Y_1} |g|^2\mathrm{d}x\mathrm{d}y + \int_\Omega |g^D|^2\mathrm{d}x\right)\mathrm{d}t
$$

$$
+ e^{Ct_1}\int_0^{t_1} e^{-Ct}\left(\alpha\frac{d}{dt}\int_{\Omega\times\Gamma_2} H(W_3^n+w_3^D)w_2^n\mathrm{d}x\mathrm{d}\gamma_y\right)\mathrm{d}t
$$

$$\leq \; e^{Ct_1}\int_0^{t_1}\Big(\int_{\Omega\times Y_1}|g|^2\mathrm{d}x\mathrm{d}y+\int_\Omega|g^D|^2\mathrm{d}x\Big)\mathrm{d}t+\alpha\int_{\Omega\times\Gamma_2}H\big(W_3^n(t_1)+w_3^D(t_1)\big)w_2^n(t_1)\mathrm{d}x\mathrm{d}\gamma_y$$

$$+\;\; \alpha e^{Ct_1}\Big|\int_{\Omega\times\Gamma_2}H(W_3^n(0)+w_3^D(0))w_2^n(0)\mathrm{d}x\mathrm{d}\gamma_y\Big|$$

$$+\;\; \alpha e^{Ct_1}\int_0^{t_1}\int_{\Omega\times\Gamma_2}H\big(W_3^n+w_3^D\big)w_2^n\mathrm{d}x\mathrm{d}\gamma_y\mathrm{d}t \quad \text{for } t_1\in[0,T].$$

This inequality together with (6.29) and (6.30) lead to

$$\int_{\Omega\times Y_1}|\nabla_y w_2^n(t)|^2\mathrm{d}x\mathrm{d}y + \int_\Omega|\nabla W_3^n(t)|^2\mathrm{d}x \leq C \quad \text{for } t\in[0,T] \text{ and } n, \quad (6.33)$$

$$\int_0^T\int_{\Omega\times Y_1}|\partial_t w_2^n|^2\mathrm{d}x\mathrm{d}y\mathrm{d}t + \int_0^T\int_\Omega|\partial_t W_3^n|^2\mathrm{d}x\mathrm{d}t \leq C \text{ for } n. \quad (6.34)$$

By (6.29) - (6.34), there exists a subsequence $\{n_i\}$ such that $w_2^{n_i}\to w_2$ weakly in $H^1(0,T;L^2(\Omega\times Y_1))$, weakly* in $L^\infty(0,T;L^2(\Omega;H^1(Y_1))$ and $W_3^{n_i}\to W_3$ weakly in $H^1(0,T;L^2(\Omega))$, weakly* in $L^\infty(0,T;H^1(\Omega))$ as $i\to\infty$. Clearly, $w_2^{n_i}\to w_2$ weakly in $L^2((0,T)\times\Omega\times\Gamma_2)$ as $i\to\infty$. Here, we put $w_3=W_3+w_3^D$.

Since the problem $P_3(g)$ is linear, similarly to the last part of the proof of Lemma 6.3.1, we can show (6.25) and (S4).

6.4   Proof of Theorem 6.1.3 (main results)

First, we consider our problem (6.1) – (6.8) in the case when f_1, f_2, R and Q are Lipschitz continuous and bounded on $\mathbb{R}$.

Proposition 6.4.1. If (A1)– (A4) hold and f_1, f_2, R and Q are Lipschitz continuous and bounded on $\mathbb{R}$, then there exists one and only one multiplet (w_1,w_2,w_3,w_5) satisfying
(S)

$$\begin{cases} w_1,w_2\in H^1(0,T;L^2(\Omega\times Y_1))\cap L^\infty(0,T;L^2(\Omega;H^1(Y_1))), \\ w_3\in H^1(0,T;L^2(\Omega)), w_3-w_3^D\in L^\infty((0,T;X)), w_5\in H^1(0,T;L^2(\Omega\times\Gamma_1)), \\ \text{(S2) holds for any } v_1\in L^2(\Omega;H^1(Y_1)), \text{ and (S3), (S4) and (S5) hold.} \end{cases}$$

Proof.   Let $(\bar{w}_1,\bar{w}_2)\in L^2((0,T)\times\Omega\times Y_1)^2$. Then, by Lemmas 6.3.2 and 6.3.3, there exist solutions (w_1,w_5) of $P_2(-f_1(\bar{w}_1)+f_2(\bar{w}_2))$ and (w_2,w_3) of $P_3(f_1(\bar{w}_1)-f_2(\bar{w}_2))$, respectively. Accordingly, we can define an operator $\bar{\Lambda}_T$ from $L^2((0,T)\times\Omega\times Y_1)^2$ into itself. Henceforth, we show that $\bar{\Lambda}_T$ is contraction for small T. To do so, let $(\bar{w}_1^i,\bar{w}_2^i)\in L^2((0,T)\times\Omega\times Y_1)^2$, (w_1^i,w_5^i) and (w_2^i,w_3^i)

be solutions of $P_2(-f_1(\bar{w}_1^i) + f_2(\bar{w}_2^i))$ and $P_3(f_1(\bar{w}_1^i) - f_2(\bar{w}_2^i))$, respectively, for $i = 1, 2$, and put $\bar{w}_1 = \bar{w}_1^1 - \bar{w}_1^2$, $\bar{w}_2 = \bar{w}_2^1 - \bar{w}_2^2$, $w_j = w_j^1 - w_j^2$, $j = 1, 2, 3, 5$.

Similarly to (6.23), we see that

$$
\frac{1}{2}\frac{d}{dt}\int\limits_{\Omega\times Y_1} |w_1|^2 \mathrm{d}x\mathrm{d}y + \int\limits_{\Omega\times Y_1} d_1|\nabla_y w_1|^2 \mathrm{d}x\mathrm{d}y
$$

$$
\leq \quad -\int\limits_{\Omega\times\Gamma_1} (Q(\bar{w}_5^1) - Q(\bar{w}_5^2))(\mathcal{R}(w_1^2) - \mathcal{R}(w_1^1))\mathrm{d}x\mathrm{d}\gamma_y
$$

$$
-\int\limits_{\Omega\times Y_1} (f_1(\bar{w}_1^1) - f_1(\bar{w}_1^2))w_1\mathrm{d}x\mathrm{d}y + \int\limits_{\Omega\times Y_1} (f_2(\bar{w}_1^1) - f_2(\bar{w}_1^2))w_1\mathrm{d}x\mathrm{d}y
$$

$$
\leq \quad \frac{d_1^0}{2}\int\limits_{\Omega\times Y_1} |\nabla_y w_1|^2 \mathrm{d}x\mathrm{d}y + C\int\limits_{\Omega\times Y_1} |w_1|^2 \mathrm{d}x\mathrm{d}y + C\int\limits_{\Omega\times\Gamma_1} |w_5|^2 \mathrm{d}x\mathrm{d}\gamma_y
$$

$$
+C\int\limits_{\Omega\times Y_1} (|\bar{w}_1|^2 + |\bar{w}_2|^2)\mathrm{d}x\mathrm{d}y \quad \text{a.e. on } [0, T]. \tag{6.35}
$$

Next, we test (6.25) by w_2. Consequently, by elementary calculations, we obtain

$$
\frac{1}{2}\frac{d}{dt}\int\limits_{\Omega\times Y_1} |w_2|^2 \mathrm{d}x\mathrm{d}y + d_2^0\int\limits_{\Omega\times Y_1} |\nabla_y w_2|^2 \mathrm{d}x\mathrm{d}y + \alpha\int\limits_{\Omega\times\Gamma_2} |w_2|^2 \mathrm{d}x\mathrm{d}\gamma_y
$$

$$
\leq \quad \int\limits_{\Omega\times Y_1} (f_1(\bar{w}_1^1) - f_1(\bar{w}_1^2))w_2\mathrm{d}x\mathrm{d}y - \int\limits_{\Omega\times Y_1} (f_1(\bar{w}_2^1) - f_1(\bar{w}_2^2))w_2\mathrm{d}x\mathrm{d}y
$$

$$
+\alpha\int\limits_{\Omega\times\Gamma_2} Hw_3 w_2\mathrm{d}x\mathrm{d}\gamma_y
$$

$$
\leq \quad C\int\limits_{\Omega\times Y_1} (|\bar{w}_1| + |\bar{w}_2|)|w_2|\mathrm{d}x\mathrm{d}y + \frac{\alpha}{2}\int\limits_{\Omega\times\Gamma_2} |w_2|^2 \mathrm{d}x\mathrm{d}\gamma_y + \frac{\alpha}{2}H^2|\Gamma_2|\int\limits_\Omega |w_3|^2 \mathrm{d}x
$$

and

$$
\frac{1}{2}\frac{d}{dt}\int\limits_{\Omega\times Y_1} |w_2|^2 \mathrm{d}x\mathrm{d}y + d_2^0\int\limits_{\Omega\times Y_1} |\nabla_y w_2|^2 \mathrm{d}x\mathrm{d}y + \frac{\alpha}{2}\int\limits_{\Omega\times\Gamma_2} |w_2|^2 \mathrm{d}x\mathrm{d}\gamma_y \tag{6.36}
$$

$$
\leq \quad C\int\limits_{\Omega\times Y_1} (|\bar{w}_1|^2 + |\bar{w}_2|^2 + |w_2|^2)\mathrm{d}x\mathrm{d}y + C\int\limits_\Omega |w_3|^2 \mathrm{d}x \quad \text{a.e. on } [0, T].
$$

It follows form (S4) that

$$
\frac{1}{2}\frac{d}{dt}\int_{\Omega}|w_3|^2 dx + d_3^0 \int_{\Omega}|\nabla w_3|^2 dx + \alpha H \int_{\Omega\times\Gamma_2}|w_3|^2 dx d\gamma_y \quad (6.37)
$$

$$
\leq \quad \frac{\alpha}{4}\int_{\Omega\times\Gamma_2}|w_2|^2 dx d\gamma_y + \alpha|\Gamma_2|\int_{\Omega}|w_3|^2 dx \quad \text{a.e. on } [0,T].
$$

Moreover, by using the trace inequality and (6.22), we see that for $\varepsilon > 0$ we can write

$$
\frac{1}{2}\frac{d}{dt}\int_{\Omega\times\Gamma_1}|w_5|^2 dx \leq \int_{\Omega\times\Gamma_1}\left|\eta(w_1^1,w_5^1)-\eta(w_1^2,w_5^2)\right||w_5|dx d\gamma_y
$$

$$
\leq \quad C\int_{\Omega\times\Gamma_1}\left(|w_1||w_5|+|w_5|^2\right)dx d\gamma_y \quad\quad\quad\quad (6.38)
$$

$$
\leq \quad C_{Y_1}\varepsilon\int_{\Omega\times Y_1}\left(|\nabla_y w_1|^2+|w_1|^2\right)dx dy + C\int_{\Omega\times\Gamma_1}|w_5|^2 dx d\gamma_y \quad \text{a.e. on } [0,T].
$$

Here, we take ε with $C_{Y_1}\varepsilon = \frac{d_1^0}{4}$ and add (6.35) – (6.38). Then it holds that

$$
\frac{1}{2}\frac{d}{dt}\int_{\Omega\times Y_1}|w_1|^2 dx dy + \frac{d_1^0}{4}\int_{\Omega\times Y_1}|\nabla_y w_1|^2 dx dy + \frac{1}{2}\frac{d}{dt}\int_{\Omega\times\Gamma_1}|w_5|^2 dx
$$

$$
+\frac{1}{2}\frac{d}{dt}\int_{\Omega\times Y_1}|w_2|^2 dx dy + d_2^0\int_{\Omega\times Y_1}|\nabla_y w_2|^2 dx dy + \frac{\alpha}{4}\int_{\Omega\times\Gamma_2}|w_2|^2 dx d\gamma_y
$$

$$
+\frac{1}{2}\frac{d}{dt}\int_{\Omega}|w_3|^2 dx + d_3^0\int_{\Omega}|\nabla w_3|^2 dx + \alpha H\int_{\Omega\times\Gamma_2}|w_3|^2 dx d\gamma_y
$$

$$
\leq \quad C\int_{\Omega\times Y_1}\left(|\bar{w}_1|^2+|\bar{w}_2|^2\right)dx dy + C\int_{\Omega\times Y_1}\left(|w_1|^2+|w_2|^2\right)dx dy
$$

$$
+C\int_{\Omega}|w_3|^2 dx + C\int_{\Omega\times\Gamma_1}|w_5|^2 dx dy \quad \text{a.e. on } [0,T].
$$

Hence, Gronwall's inequality implies that

$$
\int_{\Omega\times Y_1}\left(|w_1(t)|^2+|w_2(t)|^2\right)dx dy + \int_{\Omega}|w_3(t)|^2 dx + \int_{\Omega\times\Gamma_1}|w_5(t)|^2 dx d\gamma_y
$$

$$
\leq e^{Ct}\int_0^t\int_{\Omega\times Y_1}\left(|\bar{w}_1|^2+|\bar{w}_2|^2\right)dx dy d\tau \quad \text{for } t \in [0,T].
$$

This leads to

$$\left\|\bar{\Lambda}_T(\bar{w}_1^1, \bar{w}_2^1) - \bar{\Lambda}_T(\bar{w}_1^2, \bar{w}_2^2)\right\|_{L^2((0,T)\times\Omega\times Y_1)}$$
$$\leq \quad \|w_1\|_{L^2((0,T)\times\Omega\times Y_1)} + \|w_2\|_{L^2((0,T)\times\Omega\times Y_1)}$$
$$\leq \quad 2\Big(\int\limits_0^{T_0} e^{Ct} \int\limits_0^t \int\limits_{\Omega\times Y_1} (|\bar{w}_1(\tau)|^2_{L^2(\Omega\times Y_1)} + |\bar{w}_2(\tau)|^2_{L^2(\Omega\times Y_1)})\mathrm{d}x\mathrm{d}\tau\mathrm{d}t\Big)$$
$$\leq \quad Ce^{Ct}T^{1/2}\left\|(\bar{w}_1^1, \bar{w}_2^1) - (\bar{w}_1^2, \bar{w}_2^2)\right\|_{L^2((0,T)\times\Omega\times Y_1)}$$

Therefore, there exists a positive number T_0 such that $\bar{\Lambda}_{T_0}$ is a contraction mapping for $0 < T_0 \leq T$. Since the choice of T_0 is independent of initial values, by Banach's fixed point theorem we conclude that the problem (6.1)–(6.8) has a solution in the sense of (S).

Proof of Theorem 6.1.3. First, for $m > 0$ we define f_{im}, $i = 1, 2$, R_m and Q_m by

$$f_{im}(r) := \begin{cases} f_i(m) & \text{for } r > m, \\ f_i(r) & \text{otherwise}, \end{cases} \qquad R_m(r) := \begin{cases} R(m) & \text{for } r > m, \\ R(r) & \text{otherwise}. \end{cases}$$

$$Q_m(r) := \begin{cases} Q(m) & \text{for } r > m, \\ Q(r) & \text{for } |r| \leq m, \\ Q(-m) & \text{for } r < -m. \end{cases}$$

Then, by Proposition 6.4.1 for each $m > 0$, the problem (6.1)–(6.8) with $f_1 = f_{1m}$, $f_2 = f_{2m}$, $R = R_m$ and $Q = Q_m$ has a solution $(w_{1m}, w_{2m}, w_{3m}, w_{5m})$ in the sense of (S).

Now, for each m we shall prove
(i) $w_{1m}, w_{2m}(t) \geq 0$ a.e. on $(0, T) \times \Omega \times Y_1$, $w_{3m} \geq 0$ a.e. on $(0, T) \times \Omega$ and $w_{5m} \geq 0$ a.e. on $(0, T) \times \Omega \times \Gamma_1$.
In order to prove (i) we test $(S2)$ by $w_{1m} + w_{1m}^-$, where $\phi^- := -\min\{0, \phi\}$ with $\phi^+\phi^- = 0$. Then we see that

$$\frac{1}{2}\frac{d}{dt}\int\limits_{\Omega\times Y_1} |w_{1m}^-|^2\mathrm{d}x\mathrm{d}y + \int\limits_{\Omega\times Y_1} d_1|\nabla_y w_{1m}^-|^2\mathrm{d}x\mathrm{d}y$$
$$+ \int\limits_{\Omega\times\Gamma_1} Q_m(w_5)(\mathcal{R}_m(w_{1m}) - \mathcal{R}_m(w_{1m} + w_{1m}^-))\mathrm{d}x\mathrm{d}\gamma_y$$
$$\leq \int\limits_{\Omega\times Y_1} (f_{1m}(w_{1m}) - f_{2m}(w_{2m}))w_{1m}^-\mathrm{d}x\mathrm{d}y \quad \text{a.e. on } [0, T],$$

where $\mathcal{R}_m$ is the primitive of R_m with $\mathcal{R}_m(0) = 0$. Note that

$$\mathcal{R}_m(w_{1m}) - \mathcal{R}_m(w_{1m} + w_{1m}^-) = 0$$

and $(f_{1m}(w_{1m}) - f_{2m}(w_{2m}))w_{1m}^- \leq 0$, since $f_{2m} \geq 0$ on $\mathbb{R}$. Clearly,

$$\frac{1}{2}\frac{d}{dt}\int\limits_{\Omega \times Y_1}|w_{1m}^-|^2 \mathrm{d}x\mathrm{d}y + \int\limits_{\Omega \times Y_1}d_1|\nabla_y w_{1m}^-|^2\mathrm{d}x\mathrm{d}y \leq 0 \quad \text{a.e. on } [0,T]$$

so that $w_{1m} \geq 0$ a.e. on $(0,T) \times \Omega \times Y_1$.

Next, because $-[w_{3m}]^- \in X$, we can test $(S3)$ by $-w_{2m}^-$ and $(S4)$ by $-w_{3m}^-$ to obtain

$$\frac{1}{2}\frac{d}{dt}\int\limits_{\Omega \times Y_1}|w_{2m}^-|^2\mathrm{d}x\mathrm{d}y + d_2^0\int\limits_{\Omega \times Y_1}|\nabla_y w_{2m}^-|^2\mathrm{d}x\mathrm{d}y + \alpha\int\limits_{\Omega \times \Gamma_2}|w_{2m}^-|^2\mathrm{d}x\mathrm{d}\gamma_y$$

$$\leq \quad -\int\limits_{\Omega \times Y_1}(f_{1m}(w_{1m}) - f_{2m}(w_{2m}))w_{2m}^-\mathrm{d}x\mathrm{d}y - \alpha\int\limits_{\Omega \times \Gamma_2}Hw_{3m}w_{2m}^-\mathrm{d}x\mathrm{d}\gamma_y$$

$$\leq \quad \frac{\alpha}{2}\int\limits_{\Omega \times \Gamma_2}|w_{2m}^-|^2\mathrm{d}x\mathrm{d}\gamma_y + \frac{\alpha}{2}H^2|\Gamma_2|\int\limits_{\Omega}|w_{3m}^-|^2\mathrm{d}x \quad \text{a.e. on } [0,T], \qquad (6.39)$$

and

$$\frac{1}{2}\frac{d}{dt}\int\limits_{\Omega}|w_{3m}^-|^2\mathrm{d}x + d_3^0\int\limits_{\Omega}|\nabla w_{3m}^-|^2\mathrm{d}x \quad = \quad \alpha\int\limits_{\Omega \times \Gamma_2}(Hw_{3m} - w_{2m})w_{3m}^-\mathrm{d}x\mathrm{d}\gamma_y$$

$$\leq \alpha\int\limits_{\Omega \times \Gamma_2}|w_{2m}^-||w_{3m}^-|\mathrm{d}x\mathrm{d}\gamma_y \text{ a.e. on } [0,T]. \qquad (6.40)$$

Adding (6.39) and (6.40) and then applying Young's inequality, we get

$$\frac{1}{2}\frac{d}{dt}(\int\limits_{\Omega \times Y_1}|w_{2m}^-|^2\mathrm{d}x\mathrm{d}y + \int\limits_{\Omega}|w_{3m}^-|^2\mathrm{d}x) + d_2^0\int\limits_{\Omega \times Y_1}|\nabla_y w_{2m}^-|^2\mathrm{d}x\mathrm{d}y \qquad (6.41)$$

$$+d_3^0\int\limits_{\Omega}|\nabla w_{3m}^-|^2\mathrm{d}x \leq (\frac{\alpha}{2}H^2|\Gamma_2| + \alpha|\Gamma_2|)\int\limits_{\Omega}|w_{3m}^-|^2\mathrm{d}x \quad \text{a.e. on } [0,T].$$

The application of Gronwall's inequality and the positivity of initial data give $w_{2m} \geq 0$ a.e. on $(0,T) \times \Omega \times Y_1$ and $w_{3m} \geq 0$ a.e. on $(0,T) \times \Omega$.

Since $\eta \geq 0$, it is easy to see that

$$\frac{1}{2}\frac{d}{dt}\int\limits_{\Omega \times \Gamma_1}|w_{5m}^-|\mathrm{d}x\mathrm{d}\gamma_y \leq 0 \quad \text{a.e. on } [0,T].$$

Hence, we see that $w_{5m} \geq 0$ a.e. on $(0,T) \times \Omega \times \Gamma_1$. Thus (i) is true.

Next, we shall show upper bounds of solutions. By (A1) we can take M_1 and M_2 such that $M_1 \geq \|w_{10}\|_{L^\infty(\Omega \times Y_1)}$,

$$M_2 \geq \max\{\|w_{20}\|_{L^\infty(\Omega \times Y_1)}, H\|w_{30}\|_{L^\infty(\Omega)}, H\|w_3^D\|_{L^\infty(\Omega \times Y_1)}\}$$

and $f_1(M_1) = f_2(M_2)$. Also, we put $M_3 = \frac{M_2}{H}$, $M_5 = \max\{\beta_{max}, \|w_{50}\|_{L^\infty(\Omega \times \Gamma_1)}\}$ and $M_0 = \max\{M_1, M_2, M_3, M_5\}$. Then it holds:

(ii) For any $m \geq M_0$ we have $w_{1m}(t) \leq M_1$, $w_{2m}(t) \leq M_2$ a.e. in $\Omega \times Y_1$, $w_{3m}(t) \leq M_3$ a.e. in Ω and $w_{5m}(t) \leq M_5$ a.e. on $\Omega \times \Gamma_1$ for a.e. $t \in [0, T]$.

In fact, let $m \geq M_0$ and consider $w_{1m} - (w_{1m} - M_1)^+$, $(w_{2m} - M_2)^+$ and $(w_{3m} - M_3)^+$ as test functions in (S2) - (S4). Then we observe that

$$\frac{1}{2}\frac{d}{dt}\int\limits_{\Omega \times Y_1} |(w_{1m} - M_1)^+|^2 \mathrm{d}x\mathrm{d}y + d_1^0 \int\limits_{\Omega \times Y_1} |\nabla_y(w_{1m} - M_1)^+|^2 \mathrm{d}x\mathrm{d}y$$

$$+ \int\limits_{\Omega \times \Gamma_1} Q_m(w_{5m})(\mathcal{R}_m(w_{1m}) - \mathcal{R}_m(w_{1m} - (w_{1m} - M_1)^+)) \mathrm{d}x\mathrm{d}\gamma_y$$

$$\leq \int\limits_{\Omega \times Y_1} (-f_{1m}(w_{1m}) + f_{2m}(w_{2m}))(w_{1m} - M_1)^+ \mathrm{d}x\mathrm{d}y, \tag{6.42}$$

$$\frac{1}{2}\frac{d}{dt}\int\limits_{\Omega \times Y_1} |(w_{2m} - M_2)^+|^2 \mathrm{d}x\mathrm{d}y + d_2^0 \int\limits_{\Omega \times Y_1} |\nabla_y(w_{2m} - M_2)^+|^2 \mathrm{d}x\mathrm{d}y$$

$$\leq \int\limits_{\Omega \times Y_1} (f_{1m}(w_{1m}) - f_{2m}(w_{2m}))(w_{2m} - M_2)^+ \mathrm{d}x\mathrm{d}y \tag{6.43}$$

$$+\alpha \int\limits_{\Omega \times \Gamma_2} (Hw_{3m} - w_{2m})(w_{2m} - M_2)^+ \mathrm{d}x\mathrm{d}\gamma_y,$$

$$\frac{1}{2}\frac{d}{dt}\int\limits_{\Omega} |(w_{3m} - M_3)^+|^2 \mathrm{d}x + d_3^0 \int\limits_{\Omega} |\nabla(w_{3m} - M_3)^+|^2)\mathrm{d}x$$

$$\leq -\alpha \int\limits_{\Omega\Gamma_2} (Hw_{3m} - w_{2m})(w_{3m} - M_3)^+ \mathrm{d}x\mathrm{d}\gamma_y \quad \text{a.e. on } [0, T]. \tag{6.44}$$

Here, note that $\mathcal{R}_m(w_{1m}) - \mathcal{R}_m(w_{1m} - (w_{1m} - M_1)^+) \geq 0$. Adding (6.42)–(6.44), we get

$$\frac{1}{2}\frac{d}{dt}\left(\int\limits_{\Omega \times Y_1} (|(w_{1m} - M_1)^+|^2 + |(w_{2m} - M_2)^+|^2)\mathrm{d}x\mathrm{d}y + \int\limits_{\Omega} |(w_{3m} - M_3)^+|^2\mathrm{d}x\right)$$

$$+ \int\limits_{\Omega \times Y_1} \left(d_1^0 |\nabla(w_{1m} - M_1)^+|^2 + d_2^0 |\nabla(w_{2m} - M_2)^+|^2\right)\mathrm{d}x\mathrm{d}y + d_3^0 \int\limits_{\Omega} |\nabla(w_{3m} - M_3)^+|^2\mathrm{d}x$$

$$\leq \int\limits_{\Omega\times Y_1} (-f_{1m}(w_{1m}) + f_{2m}(w_{2m}))((w_{1m} - M_1)^+ - (w_{2m} - M_2)^+)\mathrm{d}x\mathrm{d}y \quad (6.45)$$

$$+\alpha \int\limits_{\Omega\times\Gamma_2} ((Hw_{3m} - w_{2m})(w_{2m} - M_2)^+ + (w_{2m} - Hw_{3m})(w_{3m} - M_3)^+)\mathrm{d}x\mathrm{d}\gamma_y$$

$$\text{a.e. on } [0,T].$$

We estimate the first term on the r.h.s of (6.45) by making use of $f_{1m}(M_1) = f_{2m}(M_2)$ and the Lipschitz continuity of f_{im}, $i = 1, 2$, as follows: We have

$$\int\limits_{\Omega\times Y_1} (-f_{1m}(w_{1m}) + f_{1m}(M_1) - f_{2m}(M_2) + f_{2m}(w_{2m}))(w_{1m} - M_1)^+\mathrm{d}x\mathrm{d}y$$

$$+ \int\limits_{\Omega\times Y_1} (f_{m1}(w_{1m}) - f_{1m}(M_1) + f_{2m}(M_2) - f_{2m}(w_2))(w_{2m} - M_2)^+\mathrm{d}x\mathrm{d}y$$

$$\leq \int\limits_{\Omega\times Y_1} (f_{2m}(w_{2m}) - f_{2m}(M_2))(w_{1m} - M_1)^+\mathrm{d}x\mathrm{d}y$$

$$+ \int\limits_{\Omega\times Y_1} (f_{1m}(w_{1m}) - f_{1m}(M_1))(w_{2m} - M_2)^+\mathrm{d}x\mathrm{d}y$$

$$\leq C \int\limits_{\Omega\times Y_1} (|(w_{2m} - M_2)^+|^2 + |(w_{1m} - M_1)^+|^2)\mathrm{d}x\mathrm{d}y \quad \text{a.e. on } [0,T].$$

We estimate the second term on the r.h.s in (6.45) as follows:

$$\alpha \int\limits_{\Omega\times\Gamma_2} (Hw_{3m} - HM_3 + M_2 - w_{2m})(w_{2m} - M_2)^+\mathrm{d}x\mathrm{d}\gamma_y$$

$$+\alpha \int\limits_{\Omega\times\Gamma_2} (w_{2m} - M_2 + H(M_3 - w_{3m}))(w_{3m} - M_3)^+\mathrm{d}x\mathrm{d}\gamma_y$$

$$\leq \alpha H \int\limits_{\Omega\times\Gamma_2} (w_{m3} - M_3)(w_{2m} - M_2)^+\mathrm{d}x\mathrm{d}\gamma_y - \alpha \int\limits_{\Omega\times\Gamma_2} |(w_{2m} - M_2)^+|^2\mathrm{d}x\mathrm{d}\gamma_y$$

$$+\alpha \int\limits_{\Omega\times\Gamma_2} (w_{2m} - M_2)(w_{3m} - M_3)^+\mathrm{d}x\mathrm{d}\gamma_y - \alpha H \int\limits_{\Omega\times\Gamma_2} |(w_{3m} - M_3)^+|^2\mathrm{d}x\mathrm{d}\gamma_y$$

$$\leq (\alpha H^2 + \alpha) \int\limits_{\Omega\times\Gamma_2} |(w_{3m} - M_3)^+|^2\mathrm{d}x\mathrm{d}\gamma_y \quad \text{a.e. on } [0,T].$$

Now, (6.45) becomes

$$\frac{1}{2}\frac{d}{dt}\left(\int\limits_{\Omega\times Y_1}\left(|(w_{1m}-M_1)^+|^2+|(w_{2m}-M_2)^+|^2\right)dxdy+\int\limits_{\Omega}|(w_{3m}-M_3)^+|^2dx\right)$$

$$+\int\limits_{\Omega\times Y_1}\left(d_1^0|\nabla(w_{1m}-M_1)^+|^2+d_2^0|\nabla(w_{2m}-M_2)^+|^2\right)dxdy$$

$$+d_3^0\int\limits_{\Omega}|\nabla(w_{3m}-M_3)^+|^2dx$$

$$\leq\quad C\int\limits_{\Omega\times Y_1}\left(|(w_{2m}-M_2)^+|^2+|(w_{1m}-M_1)^+|^2\right)dxdy$$

$$+C\int\limits_{\Omega}|(w_{3m}-M_3)^+|^2dx\quad\text{a.e. on }[0,T].$$

Applying Gronwall's inequality, we get for $t\geq 0$

$$\int\limits_{\Omega\times Y_1}(|(w_{1m}(t)-M_1)^+|^2+|(w_{2m}(t)-M_2)^+|^2)dxdy+\int\limits_{\Omega}|(w_{3m}(t)-M_3)^+|^2dx\leq 0.$$

Hence, $w_{1m}\leq M_1,w_{2m}\leq M_2$ a.e. in $\Omega\times Y_1$ and $w_{3m}\leq M_3$ a.e. in Ω for $t\in(0,T)$. To show that w_{5m} is bounded on $\Omega\times\Gamma_1$, we test (6.4) with $(w_{5m}-M_5)^+$

$$\frac{1}{2}\frac{d}{dt}\int\limits_{\Omega\times\Gamma_1}|(w_{5m}-M_5)^+|^2dxd\gamma_y$$

$$=\int\limits_{\Omega\times\Gamma_1}R_m(w_{1m})Q_m(w_{5m})(w_{5m}-M_5)^+dxd\gamma_y\quad\text{a.e. on }[0,T].\,(6.46)$$

We show that r.h.s of (6.46) is less or equal to zero.
If $w_{5m}<M_5$, it is clear that

$$R_m(w_{1m})Q_m(w_{5m})(w_{5m}-M_5)^+=0.\tag{6.47}$$

If $w_{5m}-M_5\geq 0,w_{5m}\geq M_5\geq\beta_{max}$. By our assumption, $Q(\beta)=0$ for $\beta\geq\beta_{max}$. Thus, (6.47) holds.

This shows that $w_{5m}\leq M_5$ a.e on $(0,T)\times\Omega\times\Gamma_1$. Thus we have (ii).

Accordingly, $(w_{1m},w_{2m},w_{3m},w_{5m})$ satisfies the conditions (S1)-(S4) for $m\geq M_0$ by (i) and (ii). Thus we have proved this theorem.

6.4.1 Proof of Theorem 6.1.4

Let $(w_{1j},w_{2j},w_{3j},w_{5j})$, $j=1,2$, be solutions (6.1)-(6.8) satisfying (S1) - (S4). Since all w_{ij}, $i=1,2,3,5$, $j=1,2$, are bounded, $(w_{1j},w_{2j},w_{3j},w_{4j})$ is also a

solution of (6.1)-(6.8) with $f_1 = f_{1m}$, $f_2 = f_{2m}$, $R = R_m$ and $Q = Q_m$ for some positive constant m. Then Proposition 6.4.1 guarantees the uniqueness. This proves the conclusion of Theorem 6.1.4.

Remark 6.4.2. Having in view the proof of Theorem 6.1.4 and the working techniques in Theorem 3, pp. 520-521 in [48] as well as in Theorem 4.1 in [96], we expect that the solution in the sense of the Definition 6.1.2 is stable to changes with respect to the initial data, boundary data, and model parameters.

6.5   Notes and Comments

We presented in this chapter the analysis of the distributed-microstructure model without including any balance equation for moisture. We combined fixed-point arguments together with a Galerkin's scheme to prove the existence of solutions.

Since the processes in porous media are highly influenced by the geometry of the microstructure, it is a difficult to understand and predict their behavior on a macroscopic scale. The distributed-microstructure models are designed to bridge the information on different spatial scales. From the theory of periodic homogenization, it is known for certain situations that the distributed-microstructure model is a good approximation of the (exact) microscopic model provided that the periodicity a is small. Note however that the distributed-microstructure modeling methodology is applicable away from the context of homogenization (periodicity), provided the well-posedness of the involved systems.

Distributed-microstructure models are usually seen in the context of homogenization limit as the scale of inhomogeneity tends to zero. The convergence of the solution of the well-posed microscopic problem provides a proof of existence of solutions to the distributed-microstructure model, see e.g. Chapter 9 in [67]. Here we view the distributed-microstructure model independent of the homogenization context. Our setting is quite general and includes rather general geometries that may arise in applications.

The reaction rate α (entering in (6.3) and (6.13)) can be chosen other than a constant. It can be taken as a monotone graph which is a sub-gradient operator [67]. A similar approach to [45] could be used to prove the existence of the solutions. If we explore the limit $\alpha \to \infty$, the system we consider here converges to the system with boundary condition (6.13) replaced by the corresponding "matched boundary condition". We investigate this limit numerically in Chapter 7, where we refer to as $Bi^M \to 0$ (large mass-transfer Biot number).

There are other techniques to prove existence of these models: Treutler employed the semi-group methods in [135] and Meier applied Banach fixed point arguments in [86].

Numerical experiments show that these systems are not only easy-to-work and but also they do approximate microscopic models very well, see e.g. [50, 86, 88].

Chapter 7

Multiscale Numerical Simulations

In this chapter, we consider the distributed-microstructure system (7.1)–(7.17) derived in Subsection 3.3.2 and present its numerical simulation. This system is posed on two different spatially separated scales. Due to the multiscale nature of the model, we perform computations at macroscopic length scales while taking into account simultaneously also the transport and reactions occurring at small length scales. We perform all the simulations in a one-dimensional two-scale setting. Our main objective is threefold:

- Calculate macroscopic pH profiles and detect the presence of sudden pH drops.

- Approximate the position of the macroscopic corrosion front[1] from gypsum concentration profiles.

- Explore the way in which the macroscopic Biot number[2] Bi^M connects the two reaction-diffusion scenarios: the matched microstructure model and the one with non-equilibrium transfer at water-air interfaces.

This chapter is structured as follows: In Section 7.1, we shed some light on the motivation behind the simulations we perform in this chapter. Section 7.2 contains the one-dimensional two-scale geometry and the two-scale model equations. In Section 7.3, we approximate numerically the profiles of the concentration of hydrogen sulfide gaseous and gypsum. We make use of profiles of gypsum and $H_2S(g)$ to approximate the corrosion front location separating the corroded and the uncorroded parts of concrete and the macroscopic pH, respectively. Section 7.4 is devoted to understanding the role of macroscopic Biot number. We present a two-scale finite difference numerical scheme and guarantee its convergence. We illustrate numerically the behavior of all concentrations profiles and indicate the expected penetration depth *versus* time curve.

---

[1] This is a sharp front separating the corroded and uncorroded parts of the concrete.

[2] Biot numbers are dimensionless quantities mostly used in heat and mass transfer calculations. They quantify the resistance of a surface (thin layer) to heat and/or mass transfer.

The results exhibited in this chapter have been presented in [27, 28]. This work has been carried out in collaboration with V. Chalupecký (Fukuoka), J. Kruschwitz (Kiel) and A. Muntean (Eindhoven). Thanks are due to V. Chalupecký for producing the C-code behind the plots.

7.1   Motivation

The biophysics of the corrosion problem is coupled to the mechanics of the concrete material. In order to be able to tackle these at a later stage (e.g. by including the solid-phase transformations and the evolving ecology of bacteria) and to capture the macroscopic fracture initiation, we focus here on a much simpler setting describing the multiscale transport and reaction of the active chemical species involved in the sulfatation process. The multiscale nature of the model allows us to perform computations at macroscopic length scales that are relevant to practical applications while capturing effects of the processes occurring at a microscopic scale.

All cement-based materials (including concrete) involve a combination of heterogeneous multi-phase material, multiscale chemistry, multiscale transport (flow, diffusion, ionic fluxes, etc.), and multiscale mechanics. Having in view this complexity, such materials are very difficult to describe, to analyze mathematically, and to deal with numerically in an efficient and sufficiently accurate way. We expect that only when the multiscale aspects of such materials are handled properly, a good prediction of the large-time behavior may be obtained. We are interested in simulating numerically the influence of microstructural effects on macroscopic quantities. To achieve our goal, we numerically approximate macroscopic pH profiles using the profiles of H_2SO_4 and the position of the corrosion front using gypsum profiles, and delineate the role of the macroscopic mass-transfer Biot number.

The strength of the chemical attack depends on the ability of the acid to dissociate and on the solubility of its calcium salt. Our interest in the pH scale is due to the fact that high pH and low temperature reduce the release of hydrogen sulfide to the sewer atmosphere as it corresponds to the low growth rate of the *Acidithiobacillus thiooxidans* [74]. It is well-known that the pH of a concrete is approximately 12, and sulfate-producing bacteria can not grow in such a alkaline environment. Experiments show that the drop in pH from 9 to 8 corresponds to the the presence of $H_2S(aq)$ and further reduction to pH$<$ 3 corresponds to situations when the reaction (1.4) has already occurred, see e.g. [93, 145]. In spite of the fact that we do not include all the responsible species in the sulfatation process, we are able to capture numerically a drop in pH which is in the experimental range [93].

The main focus of the Section 7.4 is on the role of two *micro-macro transmission conditions*. We explore numerically the way in which the macroscopic Biot number Bi^M connects the two reaction-diffusion scenarios. We indicate connections between the solution of the distributed-microstructure system (with moderate size of Bi^M) and the solution to the matched-microstructure system (with blowing up size of Bi^M), where Henry's law plays the role of the micro-macro transmission condition. This should give us hints on the intermediate and large-time behavior of the concentrations in particular as well as on the corrosion process in general.

7.2 Geometry. Model equations

First we describe our geometry in which the physical processes are observed and then we present our distributed-microstructure model.

7.2.1 One-dimensional two-scale geometry

Focusing on the already damaged part of the concrete, we consider a homogeneous macroscopic domain $\Omega := (0, L)$ (with $L > 0$) representing the concrete sample in the region where corrosion initiates. The boundary of Ω, say Γ, is
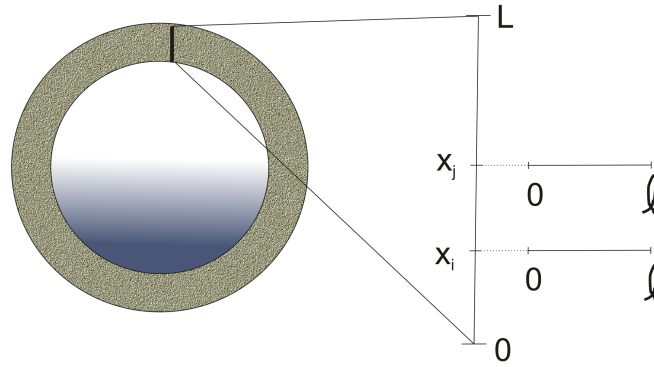

FIGURE 7.1: Cross-section of a concrete pipe and two-scale domain pointing out microstructure at each point.

composed of two disjoint parts $\Gamma^D := \{0\}$ (the inner surface of the pipe) and $\Gamma^N := \{L\}$, the Dirichlet and the Neumann boundaries, respectively. At each point in Ω, we can zoom into a typical microstructure $Y := (0, l)$ (with $l > 0$). Usually, cells (pores) in concrete contain a stationary water film, air and solid fractions in different ratios depending on the local porosity. Generally, we expect that the choice of the microstructure depends on the macroscopic position $x \in \Omega$. Here we assume that the medium Ω is made by periodically repeating the *same* microstructure Y, see Fig. 7.1. Since at the microscopic level, the involved reaction and diffusion processes take place in the pore water, we denote by $Y_1 := (0, \ell), \ell < l < L$ the wet part of the pore and completely neglect the air part of the pores.

7.2.2 Distributed-microstructure model equations

We consider the distributed-microstructure system derived in Subsection 3.3.2, see (3.54)–(3.65). Let $(0, T)$ (with $T > 0$) be the time interval during which we observe the corrosion processes. Here w_1 denotes the concentration of H_2SO_4 in $\Omega \times Y_1$, w_2 the concentration of H_2S aqueous species in $\Omega \times Y_1$, w_3 the concentration of H_2S gaseous species in Ω, w_4 the concentration of the moisture and w_5 is

the *gypsum* concentration on $\Omega \times \{y = \ell\}$. The system contains information from two scales – we expressed this by using the slow variable x (macro) and the fast variable y (micro). ∂_y denotes the partial derivatives only with respect to the variable $y \in Y_1$, while ∂_x represents the Laplacian referring only to the partial derivatives with respect to the variable $x \in \Omega$. Our distributed-microstructure system reads as follows:

$$\beta_1 \partial_t w_1 - \beta_1 \gamma_1 d_1 \partial_y w_1 = -\Phi_1^2 k_1 w_1 + \Phi_2^2 k_2 w_2 \quad \text{in } \Omega \times Y_1 \times (0, T), \qquad (7.1)$$

$$\beta_2 \partial_t w_2 - \beta_2 \gamma_2 d_2 \partial_y w_2 = \Phi_1^2 k_1 w_1 - \Phi_2^2 k_2 w_2 \quad \text{in } \Omega \times Y_1 \times (0, T), \qquad (7.2)$$

$$\partial_t w_3 - d_3 \partial_x w_3 = -Bi^M \left(H w_3 - \frac{\beta_2}{\beta_3} w_2|_{y=0} \right) \quad \text{in } \Omega \times (0, T), \qquad (7.3)$$

$$\beta_4 \partial_t w_4 - \beta_4 \gamma_4 d_4 \partial_y w_4 = k_1 w_1 \quad \text{in } \Omega \times Y_1 \times (0, T), \qquad (7.4)$$

$$\beta_5 \partial_t w_5 = \Phi_3^2 \eta(w_1, w_5) \quad \text{in } \Omega \times \{y = \ell\} \times (0, T). \quad (7.5)$$

The reaction rate η takes the form

$$\eta(\alpha, \beta) = \begin{cases} k_3 \alpha^p [(\beta_{max} - \beta)^q]^+, & \text{if } \alpha \geq 0, \ \beta \geq 0, \\ 0, & \text{otherwise,} \end{cases} \qquad (7.6)$$

with $p, q = 1$. The above system is supplemented with the following initial and boundary conditions

$$\begin{array}{llll}
w_k(x, y, 0) & = w_k^0(x, y) & \text{on } \Omega \times Y_1 \times \{t = 0\}, k \in \{1, 2, 4\}, & (7.7) \\
w_3(x, 0) & = w_3^0(x) & \text{on } \Omega \times \{t = 0\}, & (7.8) \\
w_5(x, y, 0) & = w_5^0(x, y) & \text{on } \Omega \times \{y = \ell\} \times \{t = 0\}, & (7.9) \\
-d_1 \partial_y w_1 & = 0 & \text{on } \Omega \times \{y = 0\} \times (0, T), & (7.10) \\
-d_1 \partial_y w_1 & = \Phi_3^2 \eta(w_1, w_5) & \text{on } \Omega \times \{y = \ell\} \times (0, T), & (7.11) \\
-d_2 \partial_y w_2 & = -Bi^M(\frac{H\beta_3}{\beta_2} w_3 - w_2) & \text{on } \Omega \times \{y = 0\} \times (0, T), & (7.12) \\
-d_2 \partial_y w_2 & = 0 & \text{on } \Omega \times \{y = \ell\} \times (0, T), & (7.13) \\
w_3 & = w_3^D & \text{on } \Gamma^D \times (0, T), & (7.14) \\
-d_3 \partial_x w_3 & = 0 & \text{on } \Gamma^N \times (0, T), & (7.15) \\
-d_4 \partial_y w_4 & = 0 & \text{on } \Omega \times \{y = \ell\} \times (0, T), & (7.16) \\
-d_4 \partial_y w_4 & = 0 & \text{on } \Omega \times \{y = 0\} \times (0, T), & (7.17)
\end{array}$$

where $d_m > 0$, $m \in \{1, 2, 3, 4\}$, are the diffusion coefficients and $k_i, i \in \{1, 2, 3\}$, are functions modeling the rate constants. $\Phi_i^2, i \in \{1, 2, 3\}$ are Thiele-like moduli corresponding to three distinct chemical mechanisms (reactions). They are dimensionless numbers that compare the characteristic time of the fastest transport mechanism (here: the diffusion of H_2S in the gas phase) to the characteristic timescale of the ℓ-th chemical reaction (defined in (3.9) and also see Table 7.2). Bi^M denotes the dimensionless macroscopic Biot number which quantifies the resistance of the interface to mass transfer (defined in (3.2) and also see Table 7.2). $\beta_j, j \in \{1, 2, 4, 5\}$ represents the ratio of the maximum concentration

of the jth species to the maximum bulk $H_2S(g)$ concentration. We take here $\beta_j = 1, j \in \{1, 2, 4, 5\}$. Note that all involved parameters (except for the Henry constant H, diffusion coefficient[3] for $H_2S(g)$ d_3 and Biot number Bi^M) contain microscopic information. The coefficients d_3 and Bi^M are effective ones (see Section 3.2 for the rule to calculating them), while H can be read off from existing macroscopic experimental data. Note that the information at the microscale is connected to the macroscale situation via the right-hand side of (7.3) and via the *micro-macro transmission condition* (7.12). This coupling is a consequence of the different scaling of the diffusion coefficients in formal homogenization procedure, see Subsection 3.3.2 for details.

For pH computations, we decide to leave out the partial differential equation for moisture by assuming that Ω is uniformly wet.

7.3 Capturing changes in macroscopic pH

We use a logarithmic expression to compute the values of a macroscopic pH based on the volume averaged concentration of the sulfuric acid w_1, which is obtained by numerically resolving the distributed-microstructure system defined on two spatial scales. To point out corrosion effects, we evaluate the content of the main sulfatation reaction product (gypsum) inside Ω and numerically show the presence of a kink in the gypsum's concentration profile. The presence of the kink (i.e. loss of regularity) and definition (7.6) make us believe that the reaction front localizes close to kink's position.

7.3.1 Simulations on $H_2S(g)$ and gypsum

First we simulate the profiles of $H_2S(g)$ and gypsum. To extract the position of the corrosion front, we use gypsum profiles. To obtain macroscale pH profiles, we use the concentration of sulfuric acid H_2SO_4 at the microscale. Our numerical scheme is essentially based on the method of lines.

We use a two-scale finite difference discretization in space while in time we employ an implicit higher-order time integrator to find the solution of the non-linear ordinary differential equation system (see (7.21)–(7.23) and (7.24)–(7.26) in Section 7.4). In Table 7.1, we summarize the values of our set of model

d_3	$d_{1,2}$	k_1	k_2	k_3	$\Phi_{1,2}^2$	Φ_3^2	Bi^M	H	β_{max}	w_3^D	L	ℓ	$\gamma_{1,2,4}$
0.864	0.00864	1.48	0.0084	10	1	10^3	86.4	0.3	1	0.011	30	1	1

TABLE 7.1: Parameter values used in the numerical simulations in Section 7.3.

parameters used in the simulations described in this section whereas Table 7.2 contains the definition of the dimensionless parameters. For more details on the dimensional analysis, see Chapter 3.

---

[3]In general, d_3 includes the porosity information. In our case, the porosity is constant.

Bi^M	γ_i	$d_{1,2,3,4}$	$k_{1,2,3}$	$\Phi^2_{1,2,3}$	$\tau^{1,2,3}_{reac}$	τ_{diff}
$\dfrac{b^m_{ref}L}{\varepsilon D}$	$\dfrac{D_i}{D_3}$	$\dfrac{\tilde{d}_{1,2,3,4}}{D^{ref}_{1,2,3,4}}$	$\dfrac{\tilde{k}_{1,2,3}}{K^{ref}_{1,2,3}}$	$\dfrac{\tau_{diff}}{\tau^{1,2,3}_{reac}}$	$\dfrac{U_1}{\eta^{ref}_{1,2,3}}$	$\dfrac{L^2}{D_3}$

TABLE 7.2: Definition of the dimensionless parameters.

Parameter	Units
$d_{1,2,3,4}$	$\text{mm}^2\text{day}^{-1}$
w^D_3	$g\,\text{mm}^{-3}$
H	dimensionless
U_1	$g\,\text{mm}^{-3}$
β_{max}	$g\,\text{mm}^{-2}$
$k_{1,2}$	day^{-1}
k_3	$\text{mm}^{2(p+q-1)}g^{1-p-q}\text{day}^{-1}$

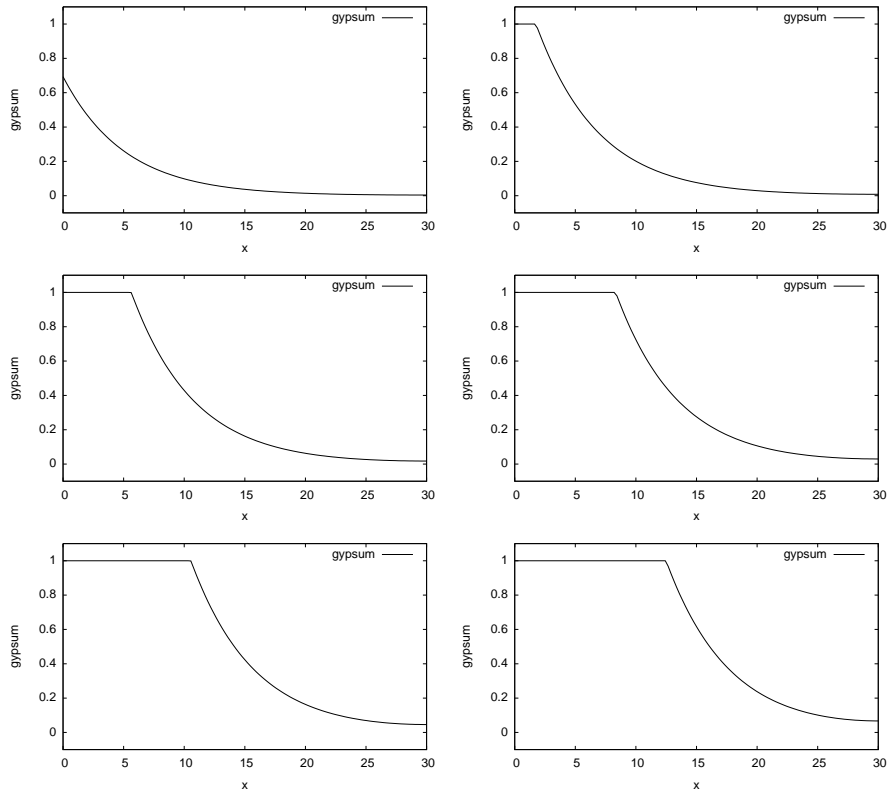TABLE 7.3: Quantities with units.
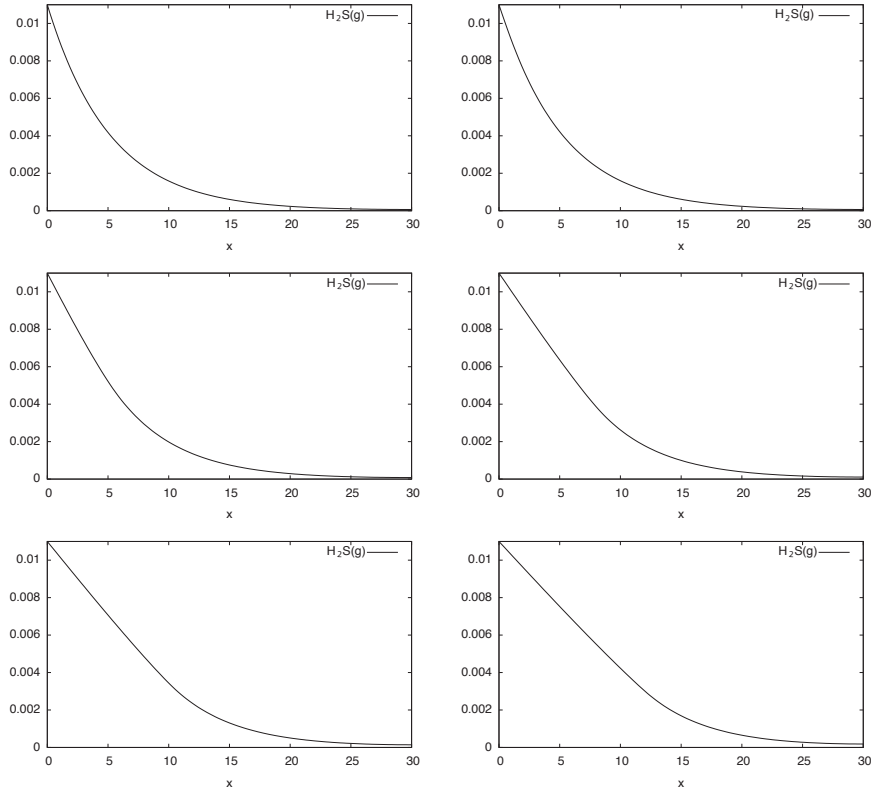
FIGURE 7.2: Time evolution of the concentration of $H_2S(g)$ [g/mm^3] *vs.* penetration depth x [mm] shown at $t \in \{2000, 4000, 8000, 12000, 16000, 20000\}$ [days] in left-right and top-bottom order.

7.3.2 Localization of the free boundary

Fig. 7.2 and Fig. 7.3 show the evolution of $H_2S(g)$ $(w_3(x,t))$ and gypsum $(w_5(x,t))$ in time, respectively. The Dirichlet boundary condition $w_3(0,t) = w_3^D$ models a constant inflow of $H_2S(g)$ at $x = 0$. As the gas diffuses through the porous structure, it enters the water film in the pores, where it undergoes biogenic oxidation to sulfuric acid. Consequently, its concentration decreases with increasing depth. As the system becomes saturated with sulfuric acid and the sulfatation reaction (1.4) converts available $CaCO_3$ into gypsum, the total concentration of $H_2S(g)$ starts to increase (see Fig. 7.2).

FIGURE 7.3: Time evolution of gypsum $[g/mm^2]$ *vs.* penetration depth x [mm] shown at $t \in \{2000, 4000, 8000, 12000, 16000, 20000\}$ [days] in left-right and top-bottom order.

Sulfuric acid reacts at $y = \ell$ and converts the cement paste into gypsum. The concentration profile of gypsum is shown in Fig. 7.3. Although the behavior of w_3 is purely diffusive, we note that a macroscopic gypsum layer is formed around $t = 1500$ and grows in time. Fig. 7.4 indicates that there are two distinct

regions separated by a slowly moving intermediate layer. The left region is the place where the gypsum production has reached saturation (a fixed threshold β_{max} appears cf. (7.6)), while the right region is the place of the ongoing sulfatation reaction (1.4) where the gypsum production has not reached the natural threshold.
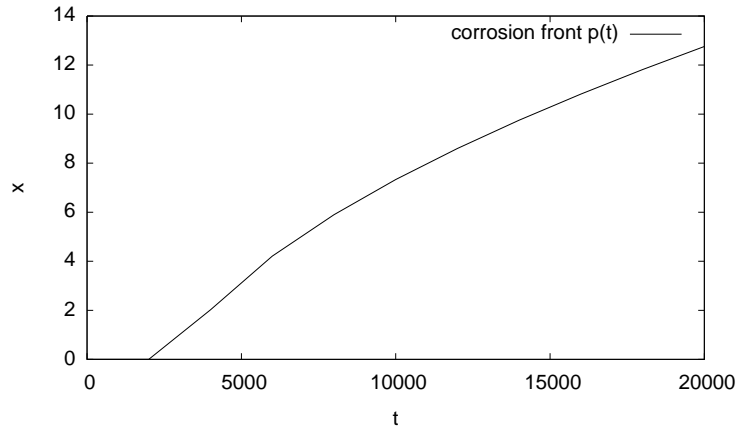

FIGURE 7.4: Position of the corrosion front $p(t)$ [mm] *vs.* time [day]. In about 15 years, we get $p(t) = 5$ mm.

The kink in the gypsum profiles indicates that there is something going on there. Note that the precise position of the front is *a priori unknown* and to capture it simultaneously with the computation of the concentration profiles would require a moving-boundary formulation similar to the one reported in [23]. To avoid a moving-boundary formulation, we extract what happens by plotting the quantity $p(t)$, which we define as

$$p(t) := \{x \in (0, L) \mid w_5(x, t) = \beta_{max} - \delta\}.$$

Here $\delta \in [0, \beta_{max}]$ is a small parameter and β_{max} is the maximum concentration of gypsum produced at the solid-water boundary. Fig. 7.4 shows the graph of $p(t)$, which is our *approximate position of the corrosion front*. We note that as the corroding front advances into the concrete specimen, its rate of growth decreases. This is in agreement with the experimental data, since the hydrogen sulfide gas supplied from the outside environment has to be transported (via diffusion) over larger distances. Having in min the large-time behavior of solutions to two-phase Stefan-like problems (see e.g. [5]), we may think that $p(t)$ is of order of $\mathcal{O}(\sqrt{t})$ for sufficiently large times t. This behavior seems to not hold here for our set of reference parameters. In Fig. 7.4, we see a $a(t - 2000)^{\frac{1}{b}}$−like behavior for the position of the penetrating front, where $a = 0.065$ and $b = 1.3$. In Fig. 7.5, the plot for $\dot{p}(t)$ is shown. It indicates that the rate of change in $p(t)$ is high in the beginning and slows down gradually as expected.
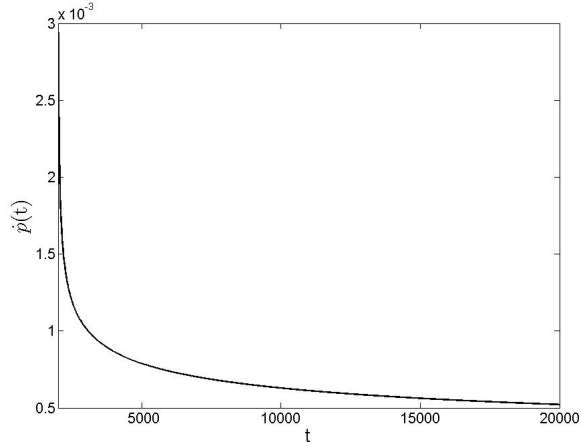
FIGURE 7.5: Plot of the speed $\dot{p}(t)$ [mm/day] of the approximate free boundary position *vs.* time [days].

7.3.3 Macroscopic pH

Now we compute the macroscopic values of pH from the available micro-scale data. This can be viewed as a sort of post-processing of the solution to (7.1)–(7.3) and (7.5)–(7.15).

Typically, the concentration of hydronium ions not bound in water is proportional to the concentration of sulfuric acid. Having this in mind, we extract the macroscale concentration of sulfuric acid at each x by taking the volume average of w_1 over Y_1 and use the following expression for computing macroscopic pH:

$$pH_{\mathrm{mac}}(x,t) = -\log_{10}\left(\frac{k_a}{|Y_1|}\int\limits_{Y_1} w_1(x,y,t)dy, \quad x \in \Omega, t \in (t_0, T)\right), \quad (7.18)$$

where k_a is the activity of hydronium ions and $t_0 > 0$ is the time needed for H_2SO_4 to form. Note that we do not know t_0 *a priori.* (7.18) is an *ad hoc* logarithmic expression to approximate numerically macroscopic pH profiles. If we have in mind the expected regularity of w_1, formula (7.18) is well-defined. Note that (in general, the situation is complex) sulfuric acid is a diprotic acid[4] (with a dissociation constant of 7.0 (at $20°C$)) with two stages of dissociation, where the first stage occurs completely while the dissociation in the second stage can be neglected. The pH of the wastewater is therefore of importance when evaluating the potential hydrogen sulfide emission. After the hydrogen sulfide arrives at the pipe's inner crown and diffuses into the concrete, the oxidation

---

[4]A diprotic acid is an acid that contains within its molecular structure two hydrogen atoms per molecule capable of dissociating (i.e. ionizable) in water.

of hydrogen sulfide becomes biologically-driven as soon as the pH has dropped below approximately 8–9 [115].
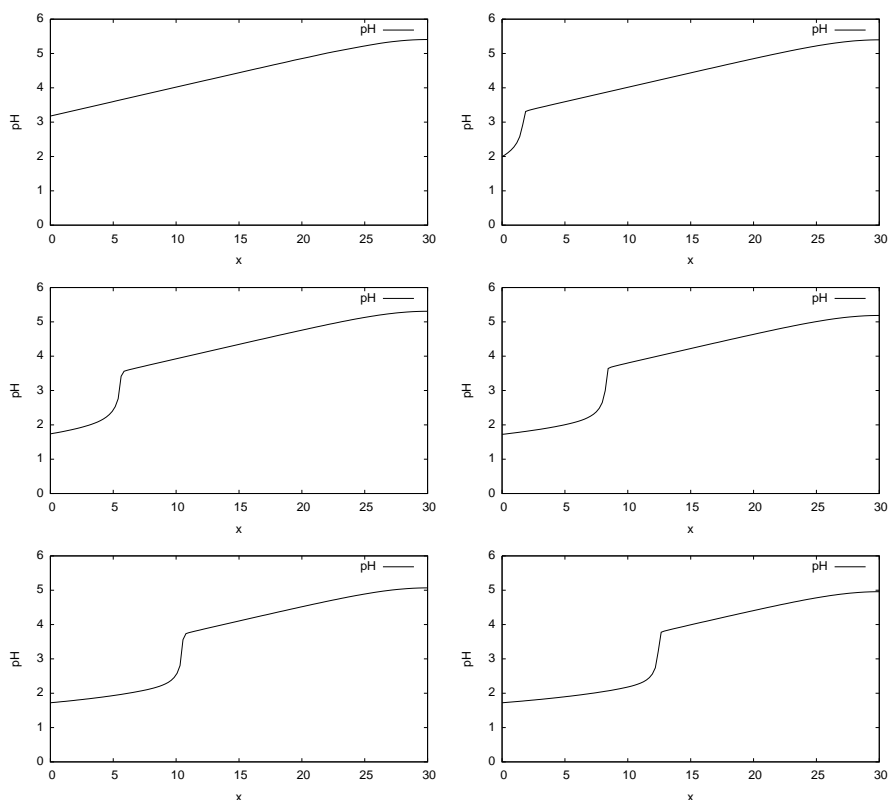

FIGURE 7.6: Time evolution of macro-scale pH profiles computed from micro-scale information shown at $t \in \{2000, 4000, 8000, 12000, 16000, 20000\}$ [days] in left-right and top-bottom order.

The macroscopic pH profile is shown in Fig. 7.6. We can see that in the beginning of the simulation (first graph) with increasing depth, the pH also increases from acidic to more basic values (as expected). Once all the available cement is consumed and converted into gypsum (this happens for the first time at $x = 0$ between the first and second graph in Fig. 7.6 around $t = 1500$), the pH drops rapidly across the corrosion front. This is due to the fact that behind the corrosion front the sulfuric acid is no longer neutralized by the sulfatation reaction (1.4).

7.4 Connecting two multiscale models via Biot numbers

Because of the multiscale nature of the distributed-microstructure model, a natural question arises as to how can one connect the micro and macro information? We numerically explore the way in which the macroscopic Biot number Bi^M (given in Table 7.2) connects two reaction-diffusion scenarios involving at the water-air interface: (i) *micro-macro transmission conditions* and (ii) *matched boundary conditions*. We perform computations at macroscopic length scales that are relevant to practical applications.

We aim to understanding the behavior of the solution to the distributed-microstructure model as the macroscopic mass-transfer Biot number Bi^M (introduced in (3.2)) tends to infinity. We achieve this by comparing the numerical solutions of two systems: one having a *matched boundary condition* and the other having $\mathrm{Bi}^M \to \infty$.

Let us refer to the system (7.1)–(7.17) as problem (P).

Matched-microstructure model

The problem (P) becomes the matched-distributed model if the boundary condition (7.12) is replaced by

$$w_2 = H w_3 \text{ on } \Omega \times \{y = 0\} \times (0, T). \tag{7.19}$$

Actually (7.19) is the well-known Henry's law [47]. This is precisely what we call *matched boundary condition*; see the terminology of Chapter 9 in [67].

We refer to the distributed-microstructure system (7.1)–(7.17) excluding (7.12) and instead including (7.19) as problem $\tilde{P}$.

We show numerically that the solution $(w_1, w_2, w_3, w_4, w_5)$ to problem (P) converges to the solution to the problem $(\tilde{P})$ as

$$\epsilon := \frac{1}{Bi^M} \to 0. \tag{7.20}$$

7.4.1 Numerical scheme for problem (P)

Now we describe a semi-discrete numerical scheme for the problem (P) based on finite-difference discretization in space.

Let $h_x := L/N_x$ and $h_y := \ell/N_y$ be the spatial step sizes, where N_x and N_y are positive integers. Let $\Omega_h := \{x_i := ih_x \in \bar{\Omega} | i = 0, \ldots, N_x\}$ and $Y_h := \{y_j := jh_y \in \bar{Y} | j = 0, \ldots, N_y\}$ be uniform grids of nodes on Ω and Y, respectively. Also, let $\omega_h := \Omega_h \times Y_h$ and $\omega'_h := \Omega_h \times \{y_{N_y}\}$. We define sets of grid functions on Ω_h, ω_h and ω'_h as $\mathcal{G}_h^\Omega := \{u_h | u_h : \Omega_h \to \mathbb{R}\}$, $\mathcal{G}_h^\omega := \{v_h | v_h : \omega_h \to \mathbb{R}\}$ and $\mathcal{G}_h^{\omega'} := \{v_h | v_h : \omega'_h \to \mathbb{R}\}$, respectively, such that $u_i := u_h(x_i)$, $u_h \in \mathcal{G}_h^\Omega \cup \mathcal{G}_h^{\omega'}$ and $v_{ij} := v_h(x_i, y_j)$, $v_h \in \mathcal{G}_h^\omega$. Finally, we define the discrete Laplacian operators as

$\Delta_h u_i := (u_{i-1} - 2u_i + u_{i+1})/h_x^2$, for $u_h \in \mathcal{G}_h^\Omega$, and as $\Delta_{Yh} v_{ij} := (v_{i,j-1} - 2v_{ij} + v_{i,j+1})/h_y^2$, for $v_h \in \mathcal{G}_h^\omega$.

A quintuple $\{w_h^k | k = 1, \ldots, 5\}$ with $w_h^k \in C^1([0,T], \mathcal{G}_h^\omega)$, $k \in \{1,2,4\}$, $w_h^3 \in C^1([0,T], \mathcal{G}_h^\Omega)$, $w_h^5 \in C^1([0,T], \mathcal{G}_h^{\omega'})$ is called a semi-discrete solution of the problem (P), if it satisfies the following system of ordinary differential equations

$$\beta_1 \frac{dw_{ij}^1}{dt} = \beta_1 d_1 \Delta_{yh} w_{ij}^1 - \Phi_1^2 k_1 w_{ij}^1 + \Phi_2^2 k_2 w_{ij}^2, \tag{7.21}$$
$$i = 0, \ldots, N_x, \ j = 0, \ldots, N_y,$$

$$\beta_2 \frac{dw_{ij}^2}{dt} = \beta_2 d_2 \Delta_{yh} w_{ij}^2 + \Phi_1^2 k_1 w_{ij}^1 - \Phi_2^2 k_2 w_{ij}^2, \tag{7.22}$$
$$i = 0, \ldots, N_x, \ j = 0, \ldots, N_y,$$

$$\frac{dw_i^3}{dt} = d_3 \Delta_{xh} w_i^3 - Bi^M \left(H w_i^3 - w_{i,0}^2 \right), \tag{7.23}$$
$$i = 1, \ldots, N_x$$

$$\beta_4 \frac{dw_{ij}^4}{dt} = \beta_4 d_4 \Delta_{yh} w_{ij}^4 + k_1 w_{ij}^1, \tag{7.24}$$
$$i = 0, \ldots, N_x, \ j = 0, \ldots, N_y,$$

$$\beta_5 \frac{dw_i^5}{dt} = \Phi_3^2 \eta \left(w_{i,N_y}^1, w_i^5 \right), \ i = 0, \ldots, N_x, \tag{7.25}$$

for $t > 0$, together with the initial conditions

$$w_h^k(0) \quad = \mathcal{P}_h^k w_{k0}, \ k = 1, \ldots, 5, \tag{7.26}$$

where $\mathcal{P}_h^k$ denotes projection operators that project continuous functions w_{k0} on the corresponding grids.

The values of grid functions on the nodes outside the grids arising in (7.21)-(7.26) are eliminated using centeral difference approximations of the boundary conditions (7.10)-(7.17). Thus, for these values and for the Dirichlet boundary condition we obtain the following relations for $t > 0$

$$w_{i,-1}^1 = w_{i,1}^1, \qquad i = 0, \ldots, N_x, \tag{7.27}$$
$$w_{i,N_y+1}^1 = w_{i,N_y-1}^1 - \frac{2h_y \Phi_3^2}{d_1} \eta \left(w_{i,N_y}^1, w_i^5 \right), \qquad i = 0, \ldots, N_x, \tag{7.28}$$
$$w_{i,-1}^2 = w_{i,1}^2 + \frac{2h_y Bi^M}{d_2} \left(H w_i^3 - w_{i,0}^2 \right), \qquad i = 0, \ldots, N_x, \tag{7.29}$$
$$w_{i,N_y+1}^2 = w_{i,N_y-1}^2, \qquad i = 0, \ldots, N_x, \tag{7.30}$$
$$w_0^3 = w_3^D, \tag{7.31}$$
$$w_{N_x+1}^3 = w_{N_x-1}^3, \tag{7.32}$$
$$w_{i,-1}^4 = w_{i,1}^4, \qquad i = 0, \ldots, N_x, \tag{7.33}$$
$$w_{i,N_y+1}^4 = w_{i,N_y-1}^4, \qquad i = 0, \ldots, N_x. \tag{7.34}$$

k_1	k_2	k_3	$d_{1,2,4}$	d_3	β_{max}	H	Φ_i^2	L	ℓ	γ_i
0.84	7.2	1.0	0.00864	0.864	0.9	2.5	1	10	1	1

TABLE 7.4: Reference set of parameter values used in all numerical experiments presented in Section 7.4.

7.4.2 Numerical results

In this section we present numerical results illustrating the behavior of solutions to the problem (P). The numerical results for the problem (P) were obtained by integrating the initial value problem (7.21)–(7.34) in time by means of the toolbox CVODE [44].

To fix ideas, we consider $\Omega = (0, 10)$ and $Y_1 = (0, 1)$. The computational grid is chosen so that $N_x = N_y = 128$. The relative and absolute tolerance for the CVODE solver is set to the value of 10^{-9}. We assume zero constant initial conditions for $w_h^k(0)$, $k = 2, 4, 5$, while $w_h^1(0) = 0.01$. The value of $w_h^3(0)$ is chosen to be compatible with the Dirichlet boundary condition $w_3^D = 0.011 g/cm^3$. The values of the remaining parameters which are common to all numerical experiments presented in this section are summarized in Table 7.4. We compute the solution until $T = 800$.

7.4.2.1 Rate of convergence of the scheme (7.21)–(7.34) for $h \to 0$

Here we present results of measuring the *experimental order of convergence* of the scheme (7.21)–(7.34) as the spatial size of the computational mesh decreases to zero. As there is no analytical solution available with which we can compare the approximate solution, we use a so-called double-mesh principle: we consider a set of gradually refined meshes whose number of mesh nodes N_x, N_y is chosen so that $N_x = N_y = 2^N$, where $N = 5, \ldots, 9$. Then we measure the convergence by comparing the error of approximate solutions obtained on two successive meshes, i.e., meshes with the spatial step sizes $h := (h_x, h_y)$ and $h/2 := (h_x/2, h_y/2)$.

We define the discrete error at time T as a grid function e_h^k in the following way:

$$(e_h^k)_i := (w_h^k)_i(T) - (w_{h/2}^k)_{2i}(T), \tag{7.35}$$

for $k \in \{3, 5\}$ and

$$(e_h^k)_{ij} := (w_h^k)_{ij}(T) - (w_{h/2}^k)_{2i,2j}(T), \tag{7.36}$$

for $k \in \{1, 2, 4\}$.

To quantify the error, we define the discrete L^2-norms and maximum norms

by

$$\|e_h^k\|_2^2 \quad := \quad \frac{h_x}{2} \sum_{i=0}^{N_x-1} \left((e_i^k)^2 + (e_{i+1}^k)^2 \right), \tag{7.37}$$

$$\|e_h^k\|_\infty \quad := \quad \max_{x_i \in \Omega_h} |e_i^k|, \tag{7.38}$$

for $k \in \{3, 5\}$ and

$$\|e_h^k\|_2^2 \quad := \quad \frac{h_x h_y}{4} \sum_{i=0}^{N_x-1} \sum_{i=0}^{N_y-1} \left((e_{ij}^k)^2 + (e_{i+1,j}^k)^2 + (e_{i,j+1}^k)^2 \right.$$

$$\left. + (e_{i+1,j+1}^k)^2 \right), \tag{7.39}$$

$$\|e_h^k\|_\infty \quad := \quad \max_{x_{ij} \in \mathcal{G}_h^{\omega'}} |e_{ij}^k|, \tag{7.40}$$

for $k \in \{1, 2, 4\}$.

N	32	64	128	256
$\|e_h^1\|_2$	0.01929	0.00533	0.00137	0.00034
EOC_2^1	1.85569	1.96049	1.98988	
$\|e_h^2\|_2$	0.00216	0.00060	0.00015	0.00004
EOC_2^2	1.85466	1.96036	1.98986	
$\|e_h^3\|_2$	0.00009	0.00003	0.00001	0.00000
EOC_2^3	1.80801	1.94844	1.98686	
$\|e_h^4\|_2$	0.98538	0.27633	0.07125	0.01795
EOC_2^4	1.83429	1.95547	1.98865	
$\|e_h^5\|_2$	0.01368	0.00399	0.00104	0.00026
EOC_2^5	1.77918	1.94165	1.98519	

TABLE 7.5: Results of our convergence rate study (measured in the discrete L^2-norm).

Finally, we define the *experimental order of convergence EOC_p^k of w_h^k* as

$$EOC_p^k := \log_2 \left(\frac{\|e_h^k\|_p}{\|e_{h/2}^k\|_p} \right). \tag{7.41}$$

Using these expressions for discrete error and *experimental order of convergence*, we performed the analysis of the rate of convergence for w_h^k, $k = 1, \ldots, 5$. We set $L_x = L_y = 1$ to obtain equal spatial step sizes in both directions and we evolved the solution until $T = 80$.

Also, to minimize the influence of the truncation error from the time integration, we set the relative and absolute tolerance to a stringent value of 10^{-13}. The Biot number Bi^M was set equal to 86.4 and the values of the remaining parameters are given in Table 7.4. The results of the EOC computations are given in Table 7.5 where the error is measured in L^2-norms defined in (7.37) and (7.39), and in Table 7.6 where the error is measured in maximum norms (7.38) and (7.40). In the first row the number of mesh nodes N in one direction is shown (the corresponding spatial step size is thus $h_x = h_y = 1/2^N$). In the following rows, we show the norm of the error function for each w_h^k, $k \in \{1, \ldots, 5\}$ together with the EOC.

N	32	64	128	256
$\|e_h^1\|_\infty$	0.04280	0.01078	0.00269	0.00067
EOC_∞^1	1.98990	2.00096	2.00047	
$\|e_h^2\|_\infty$	0.00417	0.00105	0.00026	0.00007
EOC_∞^2	1.99067	2.00400	2.00091	
$\|e_h^3\|_\infty$	0.00012	0.00003	0.00001	0.00000
EOC_∞^3	1.80827	1.94850	1.98687	
$\|e_h^4\|_\infty$	1.27092	0.35626	0.09185	0.02314
EOC_∞^4	1.83487	1.95564	1.98869	
$\|e_h^5\|_\infty$	0.01411	0.00408	0.00106	0.00027
EOC_∞^5	1.79127	1.94369	1.98563	

TABLE 7.6: Results of our convergence rate study (measured in the discrete maximum norm).

From the obtained results we can conclude that, with very high probability, the scheme converges with second-order accuracy.

7.4.2.2 Illustration of concentration profiles for $\epsilon > 0$

We present several computations to demonstrate the behavior of the system (P) for various values of the parameter ϵ defined by (7.20).

In Fig. 7.8, Fig. 7.7 and Fig. 7.9, the columns show the time evolution of $w_k, k \in \{1, 2, 3, 4, 5\}$ and each row corresponds to one time moment with the top row showing the initial conditions. We plot the functions w_k, $k \in \{1, 2, 4\}$, as functions of y for four fixed values of $x \in X := \{1, 3, 5, 9\}$. The position of these values of x is shown in the third and fifth column as colored vertical dotted lines and the color of each dotted line matches the color of the graph of the functions $w_k(x, \cdot)$, $k \in \{1, 2, 4\}$, $x \in X$, in the first, second and fourth column.
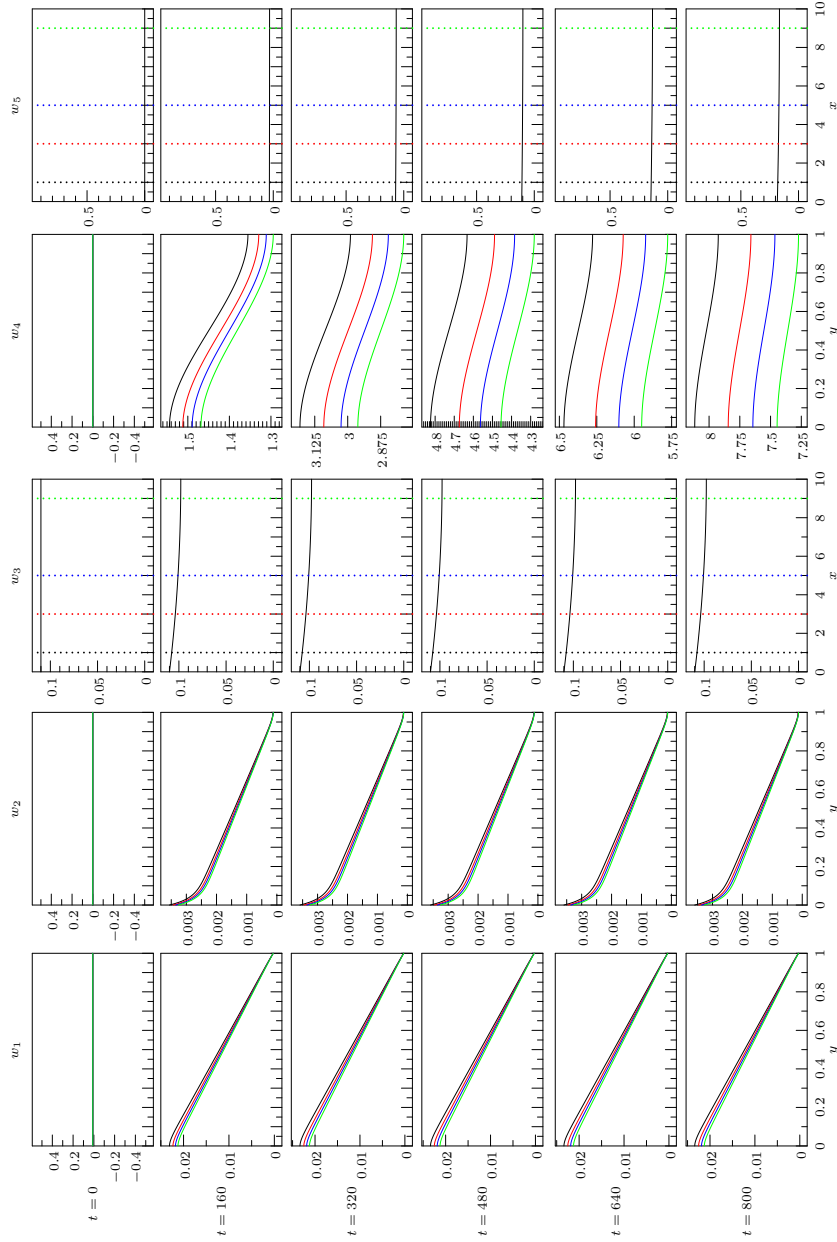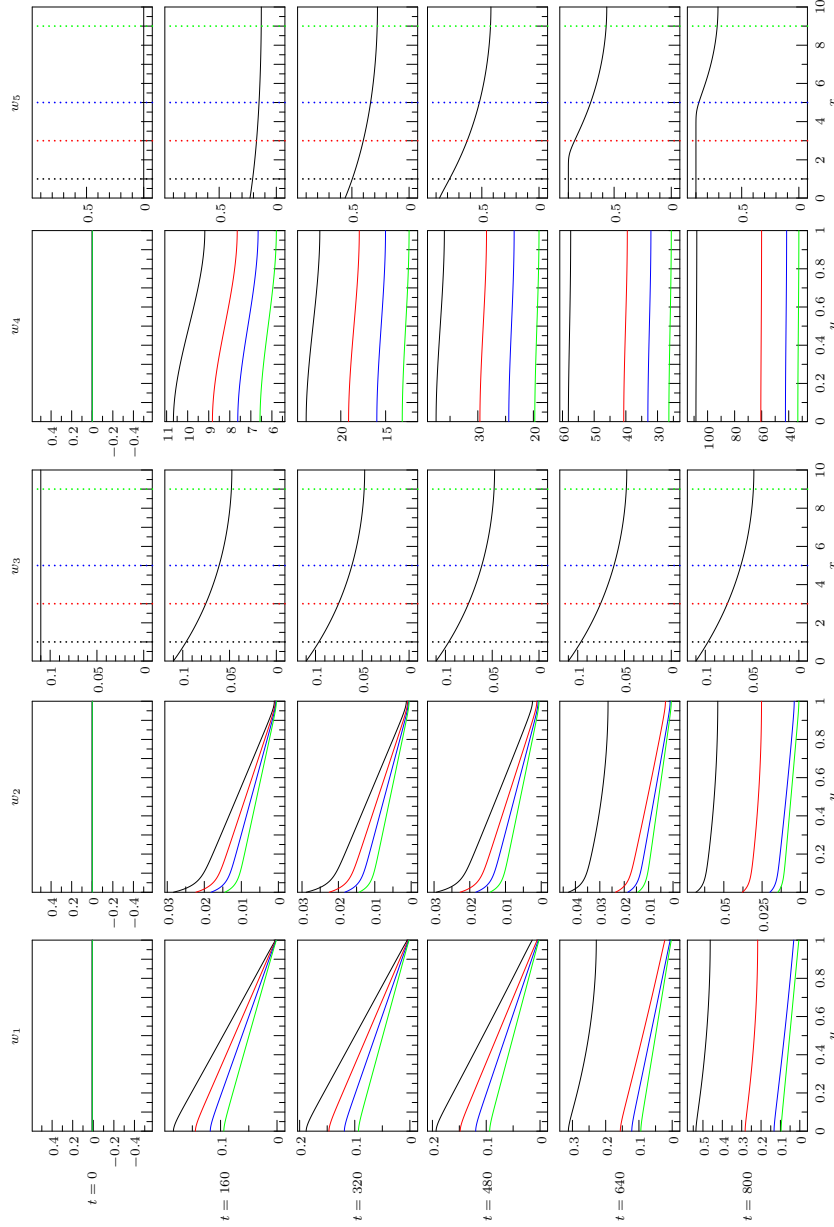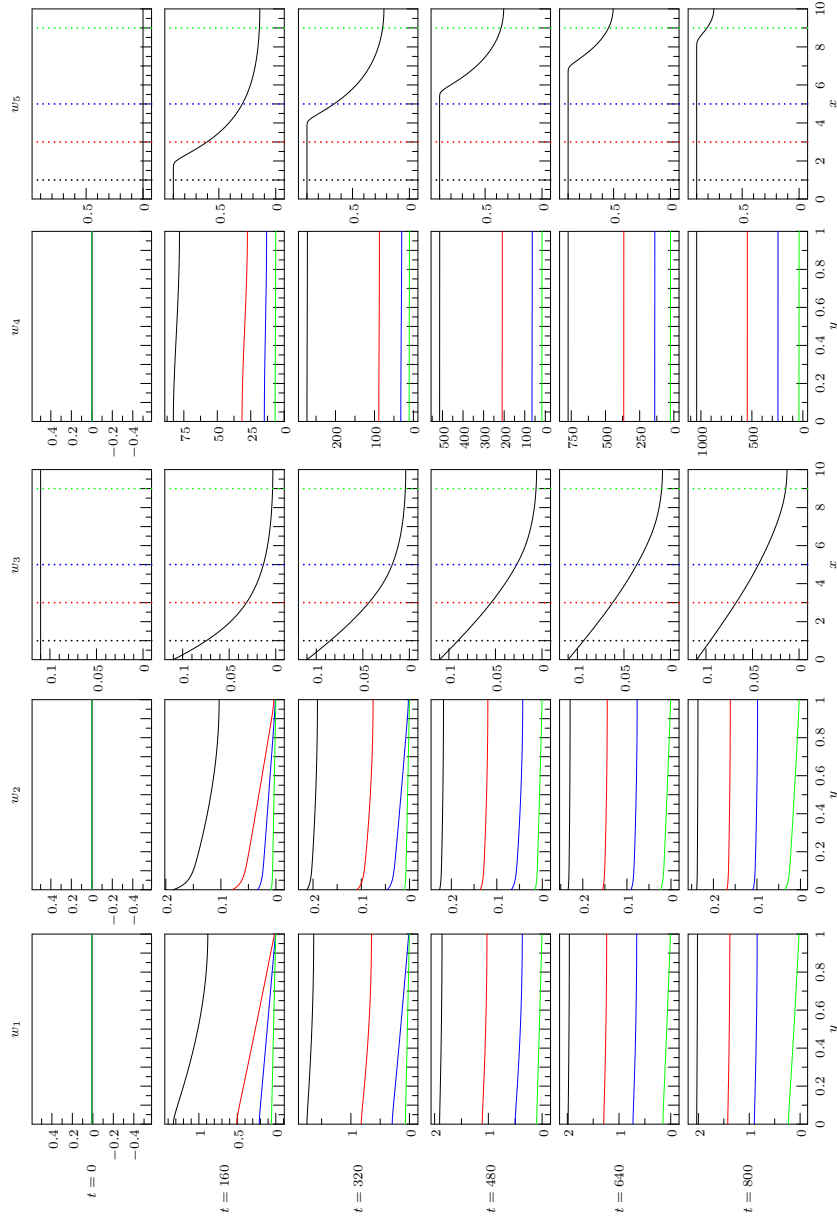
FIGURE 7.7: Plots of the time evolution of the semi-discrete solution to problem (P) computed with the scheme (7.21)-(7.25) for $Bi^M = 0.000864$. The profiles of w_1, w_2, w_3, w_4 [g/mm^3] and w_5 [g/mm^2] are plotted *vs.* x, y [mm] at $t \in \{0, 160, 320, 480, 800\}$ [days].

FIGURE 7.8: Plots of the time evolution of the semi-discrete solution to problem (P) computed with the scheme (7.21)–(7.25) for $Bi^M = 0.00864$. The profiles of w_1, w_2, w_3, w_4 [g/mm^3] and w_5 [g/mm^2] are plotted *vs.* x, y [mm] at $t \in \{0, 160, 320, 480, 800\}$ [days].

FIGURE 7.9: Plots of the time evolution of the semi-discrete solution to problem (P) computed with the scheme (7.21)-(7.25) for $Bi^M = 864$. The profiles of w_1, w_2, w_3, w_4 [g/mm^3] and w_5 [g/mm^2] are plotted $vs.$ x, y [mm] at $t \in \{0, 160, 320, 480, 800\}$ [days].

The result of the first computation is shown in Fig. 7.8, where $Bi^M = 0.00864$ ($\epsilon \approx 115.741$). Starting with the middle column displaying the evolution of w_3, we see that the initially constant concentration of $H_2S(g)$ decreases rapidly as it enters through the water-air interface into the water phase at each pore unsaturated by H_2S. After entering into the water phase, H_2S diffuses and undergoes reaction that converts it into H_2SO_4. This evolution is depicted in the second column. w_2 attains higher values at lower x position (closer to the inner surface of the pipe) similar to the profile of w_3 at $y = 0$.

The concentration of H_2SO_4 is plotted in the first column. At first, w_1 has a nearly linear profile for each fixed x decreasing to almost zero at $y = \ell$. This conversion of concrete into gypsum can be seen in the fifth column. At the beginning, the concrete is fresh and $w_5 = 0$. Increased concentration of w_1 at $y = \ell$ results in growing concentration of w_5. w_5 continues to grow until it reaches a critical value $\beta_{max} = 0.9$.

Once w_5 reaches β_{max}, w_1 does not react with the solid matrix anymore and the boundary condition at $y = \ell$ changes into no-flux condition. At $t = 640$, this change has already taken place at $x = 1$ and is about to take place at $x = 3$. As a consequence, w_1 starts to grow at $x = 1$ gradually approaching a constant value over all Y_1. At $t = 800$, the corrosion front has nearly arrived at $x = 5$: the profiles of w_1 corresponding to $x = 1$ and $x = 3$ have already grown and the one corresponding to $x = 5$ is now starting to grow. The growth of w_1 results in the growth of w_2 which in turn results in a slow growth of w_3. Finally, the fourth column shows the evolution of w_4 (moisture) as a product of reaction decomposing H_2SO_4. As time increases, the corrosion tends to be complete and the system wants to reach a constant steady state.

In Fig. 7.7, we show a computation with a Biot number much lower than in the previous numerical experiment. Consequently, the coupling between the equations for w_3 and w_2 becomes weaker. As a result, w_3 does not decrease as much as in the previous experiment due to a *barrier* for H_2S in the air hindering its entrance into the water phase. Hence w_2 and w_1 attain lower values and their profiles tend to be uniform along the x-axis. Eventually, this leads to a gradual corrosion of the pipe wall simultaneously along the whole domain and we do not observe the same progress of the corroding front as in the previous case (there is nearly no motion of the corrosion front).

Fig. 7.9 shows a computation with a much larger Biot number compared to both previous experiments. Here we used $Bi^M = 864$ ($\epsilon \approx 0.00116$), which means that the boundary condition for w_2 at $y = 0$ is essentially a Dirichlet one. We observe that, in this case, the concentrations of w_2 and w_3 are higher than in the previous numerical experiments. Additionally, the corrosion process seems to be much faster exhibiting a prominent corroding front (observable in the fifth column) advancing into the concrete.

7.4.2.3   Illustration of the convergence scenario as $\epsilon \to 0$

Now we are concerned with the behavior of solutions to (P) as $\epsilon \to 0$. The main result here is that we show numerically that

$$\|Hw_3 - w_2|_{y=0}\|_{L^2(\Omega)} \to 0 \text{ as } \epsilon \to 0,$$

i.e., as $Bi^M \to \infty$. We show this by simply measuring the *experimental order of convergence*. We proceed as follows: We compute solutions of (7.21)–(7.34) at $T = 800$ for gradually increasing values of $Bi^M = 4^i$, $i \in \{1, \ldots, 6\}$. For each choice of ϵ, we measure the quantity $E_\epsilon := \|Hw_h^3(T) - w_h^2(T)|_{\Omega_h}\|_2$ in terms of the discrete L^2-norm; see (7.37). Finally, we define the *experimental order of convergence* of E_ϵ as

$$EOC_{E_\epsilon} := \frac{\log(E_{\epsilon_1}) - \log(E_{\epsilon_2})}{\log(\epsilon_1) - \log(\epsilon_2)}. \tag{7.42}$$

The results shown in Table 7.7 indicate that E_ϵ behaves as $O(\epsilon)$.

$\log_4 Bi^M$	$\left\|Hw_h^3 - w_h^2\|_{\Omega_h}\right\|_2$	EOC_{E_ϵ}
-2	$6.95208 \cdot 10^{-2}$	0.98907
-1	$1.76455 \cdot 10^{-2}$	0.98806
0	$4.48495 \cdot 10^{-3}$	0.99612
1	$1.12728 \cdot 10^{-3}$	0.99896
2	$2.82225 \cdot 10^{-4}$	0.99973
3	$7.05819 \cdot 10^{-5}$	0.99993
4	$1.76471 \cdot 10^{-5}$	0.99998
5	$4.41187 \cdot 10^{-6}$	0.99999
6	$1.10297 \cdot 10^{-6}$	

TABLE 7.7: Experimental order of convergence of E_ϵ as $\epsilon \to 0$.

7.4.3   Convergence of the two-scale finite difference scheme (7.21)–(7.34) as $h \to 0$

To close the chapter, we list the results obtained by V. Chalupecký and A. Muntean in [29], proving that the two-scale finite difference scheme (7.21)–(7.34) converges to the weak solution of (7.1)–(7.3) and (7.5)–(7.15).

Assumption 7.4.1.   1. $d_i > 0, i \in \{1, 2, 3\}$, $Bi^M, H, w_3^D > 0$ are constants.

2. We assume that $\eta(\alpha, \beta) := kR(\alpha)Q(\beta)$ is positive for $\alpha, \beta \geq 0$ and zero otherwise. In addition, η is globally Lipschitz in both arguments. Furthermore, R is taken to be sublinear, i.e., $R(\alpha) \leq C\alpha$ for $\alpha \in \mathcal{R}_+$ and Q is bounded above by the threshold $\beta_{max} > 0$.

3. $w_{10}, w_{20} \in \{L^2(\Omega; H^1(Y_1)) \cap L_+^\infty(\Omega \times Y_1)\}^2$, $w_{30} \in H^2(\Omega) \cap L_+^\infty(\Omega)$, $w_{50} \in H^1(\Omega) \cap L_+^\infty(\Omega)$.

Under the Assumption 7.4.1, the semi-discrete solution to problem (P) was defined as follows:

Definition 7.4.2. We call (w^1, w^2, w^3, w^5) with

$$w_h^1, w_h^2 \in C^1([0,T]; \mathcal{G}_h^\omega), w_h^3 \in C^1([0,T]; \mathcal{G}_h^\Omega) \text{ and } w_h^5 \in C^1([0,T]; \mathcal{G}_h^{\omega'})$$

a semi-discrete solution to problem (P), if it satisfies the system of ordinary differential equations given in (7.21)– (7.23) and (7.25) together with the initial and boundary conditions (7.26)–(7.32).

Proposition 7.4.3. Consider Assumption 7.4.1. There exists a unique semi-discrete solution

$$w_h^1, w_h^2 \in C^1([0,T]; \mathcal{G}_h^\omega), w_h^3 \in C^1([0,T]; \mathcal{G}_h^\Omega) \text{ and } w_h^5 \in C^1([0,T]; \mathcal{G}_h^{\omega'})$$

in the sense of Problem 7.4.2.

For the proof of Proposition 7.4.3, see Proposition 3 in [29].

Theorem 7.4.4. Consider Assumption 7.4.1, there exists a semi-discrete solution $\{w_h^1, w_h^2, w_h^3, w_h^5\}$ for any time $T > 0$ whose interpolate $\{\hat{w}_h^1, \hat{w}_h^2, \hat{w}_h^3, \hat{w}_h^5\}$ converges in $L^2(\Omega \times Y)$, $L^2(\Omega \times Y)$, $L^2(\Omega \times Y)$, $L^2(\Omega \times Y)$ respectively, as $|h| \to 0$ to a weak solution (w_1, w_2, w_3, w_5) to problem (P) in the sense of Definition 7.4.2.

For the proof of the statement, see Theorem 15 in [29].

For the complete implementation details in C of the numerical scheme (7.21)–(7.32), we refer the reader to Chapter 7 in [99].

7.5 Notes and comments

In this chapter, we illustrated numerically the macroscopic pH and gypsum profiles which point out approximate position of the corrosion front. We also showed the behavior of the solution for the distributed-microstructure model for large mass transfer Biot number Bi^M.

Although our model does not include all the responsible species in the sulfatation reaction (e.g. bacteria are missing), yet our pH profiles are in the range seen in the experimental data published in [93, 109]. For instance in [109], it is

stated that the pH of the heavily corroded gypsum layer that is exposed to the H_2S is within the range 2.6 to 2.7. To meet this, it is necessary to incorporate in the model other species involved in the sulfatation of concrete. We expect that the size of the drop of pH will become comparable to the one seen in [109] as soon as the effects of nonlinear moisture transport, bacteria motility, and temperature effects are taken into account in the model equations. The main message here is that we are able to detect and compute a macroscopic pH drop, once the right micro-information is available.

The calculation time is rather long: e.g. to estimate 10 years of corrosion takes a bit more than 2 hours. We expect this to happen due to our choice of the reference parameters in Table 7.1. More numerical studies are needed to check the stability of the solution with respect to initial data and parameters.

We see in Fig. 7.4 penetration of the corrosion front of about 5mm in 15 years. The speed of the front seems to be rather slow compared to what is seen experimentally (i.e. 10–15 mm in about 15 years, see e.g. [92]). In this chapter, we performed simulations for a fixed geometry. In the case of $x-$dependent (locally-periodic) microstructures, efficient direct computations as well as the corresponding error analysis are generally open problems.

A practical question regarding the large-time behavior of the penetrating front $p(t)$ arises at this point. We have seen in Fig. 7.4 that $p(t)$ is of order of $\mathcal{O}(a(t-t_0)^{\frac{1}{b}})$. It is worth checking how do a, p and t_0 depend on the solution and on the choice of parameters (e.g. cement, porosity, transport and reaction coefficients).

It is worth mentioning that there are many multiscale numerical techniques available that could be used to tackle RD systems of the type treated here. We mention here three such approaches:

1. The multiscale finite element method (FEM) developed by Babuška at el, see the monograph [51] for more references.

2. Computations on two-scale FEM spaces [85] / two-scale Galerkin approximations [100, 101]. Kouznetsova *et al.* deal with multiscale computational homogenization – a tool which fits well to computing distributed-microstructure models, see [42, 43, 58, 76].

3. Heterogeneous multiscale methods (HMM) [1, 142]. Since the concrete is highly saturated in the sewerage, it is possible to extend the model by considering the mobility of the water. In this case, convective effects appear and most likely the two-scale finite element scheme based on homogenization provided in [147]/HMM become applicable.

Chapter 8

Conclusions and Outlook

8.1 Conclusions

In the thesis, we use multiscale reaction-diffusion systems to describe corrosion processes induced by the presence of aggressive chemical reactions. We focus here on the concrete sulfatation. The goal was to identify reliable and easy-to-use upscaled models able to forecast the penetration of sulfuric acid into sewer pipes walls estimating in this way the durability of the material. We paid attention to the following aspects:

  (i) Modeling of reaction-induced corrosion [with focus on concrete sulfatation];

 (ii) Multiscale mathematical analysis;

(iii) Multiscale simulation.

The role of (i)-(iii) is to prepare a multiscale methodology to proceed towards comparison with experiments. For modeling of corrosion processes, we took into account balance equations expressing physical processes taking place in the microstructures of partially saturated concrete pipes. We considered two different types of models: On one hand, we looked at pore scale reaction-diffusion systems describing corrosion propagation and applied averaging (homogenization) techniques to scale out the oscillations occurring in space. On other hand, we considered a distributed-microstructure reaction-diffusion system containing information from two scales (micro and macro). The models we discussed in the thesis underline two important features:

- non-equilibrium exchange of H_2S from water to the air phase (and vice versa);

- production of gypsum at microscopic solid-water interfaces.

We modeled the transfer of H_2S by means of Henry's law, while the production of gypsum was incorporated into a non-standard non-linear reaction rate. Our proposed models consist of coupled semilinear partly diffusive reaction-diffusion system posed in a spatially heterogeneous domain. The presence of the spatial heterogeneities urged the need of averaging techniques to approximate the overall

behavior of the microscopic equations with oscillating coefficients. We dwelt on the following mathematical issues:

1. Formal derivation of multiscale corrosion models for locally-periodic domains for two special scalings of the diffusion coefficients;

2. Rigorous derivation of the upscaling of one of the reaction-diffusion models;

3. Construction of corrector estimates for concentrations and their fluxes;

4. Solvability of a distributed-microstructure system incorporating a variational inequality.

We tried as much as possible to deviate from the uniform periodicity assumption by accounting for a class of locally-periodic microstructures. In the latter framework, we considered two particular scalings of the diffusion coefficients. As a next step, we used two-scale asymptotic expansions to expand the solution in powers of the scaling parameter ε. As a result of the two scalings, we obtained two different types of upscaled models (both two-scale or with distributed-microstructure). For the rigorous derivation of the multiscale models posed in uniformly periodic domains, we ensured the well-posedness of the microscopic system of partial differential equations, and then, we obtained ε-independent energy estimates needed to achieve the necessary compactness for subsequences – an essential ingredient to pass to the limit in the microscopic system. The nonlinearity posed at the oscillating boundary made the rigorous averaging procedure challenging. To cope with this difficulty, we combined two averaging techniques: two-scale convergence in the sense of Nguestseng and Allaire and periodic boundary unfolding. Consequently, we derived upscaled equations together with explicit formulae for the effective diffusion coefficients and reaction constants. In order to understand the quality of the upscaling, we asked ourselves: *How good our averaging strategy is?* We addressed this question in terms of corrector estimates for concentrations and their fluxes. We obtained error (corrector) estimates under minimal regularity assumptions on the solutions to the microscopic and macroscopic systems and to the corresponding auxiliary cell problems.

Apart from the homogenization context, we considered a distributed-microstructure reaction-diffusion system. For this, we ensured basic estimates like positivity and L^∞−bounds on the concentrations to the system. Then we proved the global in time existence and uniqueness of a suitable class of positive and bounded solutions. The main ingredients in the proof of the existence part included fixed-point arguments and convergent two-scale Galerkin approximations.

To address practical questions especially concerning the presence of the corrosion front and the large-time behavior of the overall system, we used an *ad hoc* logarithmic expression to approximate numerically macroscopic pH profiles dropping down with the onset of corrosion. We extracted from the gypsum profiles the approximate position of the corrosion front. At this point, our pH results are only of qualitative nature, specially because we have not included

in our models the evolution of bacteria. To get insight into air-liquid mass transfer processes, we studied the role of Bi^{M} – the macroscopic mass transfer Biot number (quantifying the mass-transfer of $H_2S(g)$ at air-liquid interface). We illustrated numerically that Bi^{M} naturally connects two multiscale reaction-diffusion scenarios, i.e., as $\text{Bi}^{\text{M}} \to \infty$ the solution of the two-scale system having the Henry law acting as micro-macro transmission condition converges to the solution of the matched two-scale system (matched-microstructure system).

Due to the complexity of the subject, several modeling, analytical and simulation questions remain open for further investigation. We enumerated selectively a few of them within the frame of the section *Notes and comments* at the end of each chapter of this thesis.

8.2   Open issues

There are a few modeling and mathematical issues that would need further investigation.

8.2.1   Open issues (at the modelling level)

1. To get realistic estimation of corrosion, the presence of bacteria needs to be included in the model, see section 2.1.1 in chapter 2. Perhaps, a Michaelis-Menten type mass-action kinetics could be used to address this issue.

2. Our numerical experiments indicate the presence of a free boundary penetrating the concrete. Having this in mind, it is perhaps possible to consider a free boundary formulation of the corrosion model in a similar way as it was done in [23]. The main difficult question is: What are the correct free-boundary conditions at the corrosion front? Such approach would provide direct information on the location of the corrosion front.

8.2.2   Open issues (at the mathematical level)

1. Rigorous derivation of upscaled systems with locally-periodic distribution of pores is not fully solved. Useful tools are available in the literature, see notes and comments in chapter 4, some others [e.g., a good concept of unfolding operator valid for non-period geometries] are still missing;

2. It would be interesting to study large-time behavior of the concentrations in distributed-microstructure model;

3. The identification of convergence rates (corrector estimates) of microscopic solutions in locally-periodic domains is difficult to handle;

4. Singular limits (fast reaction limit, slow diffusion limit, etc.) may become involved in the context of homogenization [see e.g. [87] by Meier and Muntean]. This topic intuitively connects to the occurrence of boundary layers and is mathematically not fully understood;

5. Relating to point 2 in subsection 8.2.1: The well-posedness of multiscale moving-boundary problems is generally not understood.

8.2.3   Open issues (regarding the validation against durability tests)

Regarding the numerics and the validation of the models presented in the thesis *versus* experiments we mention the following aspects:

1. Efficient multiscale numerical methods for problems involving locally periodic microstructure are needed. In particular, (*a priori* and *a posteriori* control on the multiscale approximations need to be constructed);

2. There is need for two-scale experiments for the calibration of the model and identification of the parameters (like transport coefficient, reaction rates, etc.);

3. Multiscale goal-oriented adaptivity can play a role in the above mentioned issues.

Appendix

Proof of Theorem 4.2.5

In this Appendix, we prove the existence of solutions to problem (4.4)–(4.8). For this, we use a Galerkin approximation and show its convergence in appropriate function spaces. For the sake of simplicity, we drop the superscript ε from the notation of the concentrations and of the domains. We consider a Schauder basis of the form $\{\zeta_k\}_{k \in \mathbb{N}}$, where $\{\zeta_k\}_{k \in \mathbb{N}}$ is a basis of $H^1(\Omega)$ with $\{\zeta_k\}_{k \in \mathbb{N}}$ constituting an orthonormal system with respect to $L^2(\Omega)$-norm. We define the projection operator on the finite dimensional subspaces P^N associated with the bases $\{\zeta_k\}_{k \in \mathbb{N}}$. Projections of φ are defined by

$$(P^N \varphi)(x) = \sum_{k=1}^{N} a_k \zeta_k(x).$$

The choice of the bases $\{\zeta_k\}_{k \in \mathbb{N}}$ is made in such a way that the projection operator P^N is stable with respect to the L^2-norm and H^1-norm. Here we are interested in the finite-dimensional approximations of the functions u_1, u_2, U_3, u_4, u_5, where $U_3 := u_3 - u_3^D$ which are of the form

$$u_1^N(t,x) := \sum_{k}^{N} \alpha_k^N(t) \zeta_k(x), \qquad u_2^N(t,x,y) := \sum_{i,j=1}^{N} \beta_k^N(t) \zeta_k(x),$$

$$U_3^N(t,x) := \sum_{i=1}^{N} \gamma_k^N(t) \zeta_k(x), \qquad u_4^N(t,x) := \sum_{i=1}^{N} \xi_k^N(t) \zeta_k(x)$$

$$u_5^N(t,x) := \sum_{i,j=1}^{N} (t) \mu_k^N \zeta_k(x), \text{ with}$$

$$\lim_{N \to \infty} u_\ell^N(0,x) = u_{\ell 0}(x) \in L^2(\Omega_1), \;\; \ell \in \{1,2,4\},$$

$$\lim_{N \to \infty} U_3^N(0,x) = U_{\ell 0}(x) \in L^2(\Omega_2) \quad \lim_{N \to \infty} u_4^N(0,x) = w_{40}(x) \in L^2(\Gamma_1) \;\; (8.1)$$

where the coefficients $\alpha_k^N, \beta_k^N, \gamma_k^N, \xi_k^N, \mu_k^N, \; k = 1, 2, ..., N$ are determined by the following relations:

$$\int_{\Omega_1} \Big(\partial_t u_1^N(t) \phi_1 + d_1 \nabla u_1^N(t) \nabla \phi_1 + k_1 u_1^N(t) \phi_1 - k_2 u_2^N(t) \phi_1 \Big) dx$$

$$= -\varepsilon \int_{\Gamma_1} \eta(u_1^N(t), u_5^N(t))\phi_1 d\gamma_x, \tag{8.2}$$

$$\int_{\Omega_1} \Big(\partial_t u_2^N(t)\phi_2 + d_2 \nabla u_2^N(t)\nabla_y\phi_2 - k_1 u_1^N(t)\phi_2 + k_2 u_2^N(t)\phi_2 \Big) dx$$

$$= \int_{\Gamma_2} \big(a(U_3^N + u_3^D)(t) - bu_2^N(t) \big)\phi_2 d\gamma_x, \tag{8.3}$$

$$\int_{\Omega_1} \partial_t U_3^N(t)\phi_3 dx + \int_{\Omega_2} d_3 \nabla U_3^N(t)\nabla\phi_3 dx = \int_{\Omega} (\partial_t u_3^D(t) - d_3 \triangle u_3^D(t))\phi_3 dx$$

$$- \int_{\Gamma_2} \big(a(U_3^N + u_3^D)(t) - bu_2^N(t) \big)\phi_3 d\gamma_x, \tag{8.4}$$

$$\int_{\Omega_1} \Big(\partial_t u_4^N(t)\phi_4 + d_4 \nabla u_4^N(t)\nabla\phi_4 - k_1 u_1^N(t)\phi_4 \Big) dx = 0, \tag{8.5}$$

$$\int_{\Omega \times \Gamma_1} \partial_t w_5^N(t)\phi_5 d\gamma_x = \int_{\Gamma_1} \eta(u_1^N(t), w_5^N(t))\phi_5 d\gamma_x, \tag{8.6}$$

for all $\phi_i \in \operatorname{span}\{\zeta_k(x) : k \in \{1, 2, ..., N\}\}, i \in \{1, 2, 3, 4, 5\}$ with

$$\alpha_k^N(0) := \int_{\Omega_1} u_{10}\zeta_k dx, \qquad\qquad \beta_k^N(0) := \int_{\Omega_1} u_{20}\zeta_k dx, \tag{8.7}$$

$$\gamma_k^N(0) := \int_{\Omega_2} (u_{30} - u_3^D(0))\zeta_k dx, \qquad \xi_k^N(0) := \int_{\Omega_1} w_{40}\zeta_k dxdy \tag{8.8}$$

$$\mu_k^N(0) := \int_{\Gamma_1} w_{50}\zeta_k dxd\gamma_y, .$$

Consider $\phi_i = \zeta_k, k \in \{1, 2, ..., N\}, i \in \{1, 2, 3, 4, 5\}$ as a test functions in (8.2)–(8.6), this yields the system of ordinary differential equations

$$\partial_t \alpha_k^N(t) + \sum_{j=1}^{N} (A_j)_k \alpha_k^N(t) = F(\alpha_k^N(t), \beta_k^N(t)) + \varepsilon \tilde{F}(\alpha_k^N(t), \mu_k^N(t)), \tag{8.9}$$

$$\partial_t \beta_k^N(t) + \sum_{j=1}^{N} (B_j)_k \beta_k^N(t) = F(\alpha_k^N(t), \beta_k^N(t)) + \varepsilon G(\beta_k^N(t), \gamma_k^N(t)), \tag{8.10}$$

$$\partial_t \gamma_k^N(t) + \sum_{j=1}^{N} (C_j)_k \gamma_k^N(t) = -\varepsilon G(\beta_k^N(t), \gamma_k^N(t)), \tag{8.11}$$

$$\partial_t \xi_k^N(t) + \sum_{j=1}^{N} (D_j)_k \xi_k^N(t) = \hat{F}(\alpha_k^N(t), \beta_k^N(t)) \tag{8.12}$$

$$\partial_t \mu_k^N(t) = \tilde{F}(\alpha_k^N(t), \mu_k^N(t)), \tag{8.13}$$

where all $j, k = 1, ..., N$, we have

$$(A_j)_k := \int\limits_{\Omega_1} d_1 \nabla \zeta_j \nabla \zeta_k dx, \qquad\qquad (B_j)_k := \int\limits_{\Omega_1} d_2 \nabla \zeta_j \nabla \zeta_k dx,$$

$$(C_j)_k := \int\limits_{\Omega_1} d_3 \nabla \nabla \zeta_j \nabla \zeta_k dx, \qquad\qquad (D_j)_k := \int\limits_{\Omega_1} d_4 \nabla \nabla \zeta_j \nabla \zeta_k dx,$$

$$F_k := \int\limits_{\Omega_1} \Big(- k_1 u_1^N(t) + k_2 u_2^N(t) \Big) \zeta_k dx, \qquad \tilde{F}_k := \int\limits_{\Gamma_1} \eta(w_1^N(t), w_5^N(t)) \zeta_k dx,$$

$$G_k := \alpha \int\limits_{\Gamma_2} \Big((a(U_3^N + u_3^D)(t) - b u_2^N(t)) \Big) \zeta_k d\gamma_x, \qquad \hat{F}_k := \int\limits_{\Omega_1} k_1 w_2^N(t) \zeta_k d\gamma_x.$$

Note that $F, \tilde{F}, G$ and $\hat{F}$ are globally Lipschitz continuous functions. According to the standard existence theory for ordinary differential equations, there exists a unique continuous solution $(\alpha_k^N, \beta_k^N, \gamma_k^N, \xi_k^N, \mu_k^N)$, $k \in \{1, 2, ..., N\}$ satisfying (8.7)–(8.13) for a.e. $0 \le t \le T$. Thus the solution $(u_1^N, u_2^N, U_3^N, u_4^N, u_5^N)$ defined in (8.1) solves (8.2)–(8.6).

Lemma 8.2.1. *Assume (A1)–(A4). There exists sequences such that*

$u_1^N, u_2^N, u_4^N \to u_1, u_2, u_4$ *strongly in* $L^\infty(0, T; L^2(\Omega_1))$ *and* $L^2(0, T; H^1(\Omega_1))$,
$U_3^N \to U_3$ *strongly in* $L^\infty(0, T; L^2(\Omega_2))$ *and* $L^2(0, T; H_0^1(\Omega_2))$,
$u_5^N \to u_5$ *strongly in* $L^\infty(0, T; L^2(\Gamma_1))$,
$\partial_t u_1^N, \partial_t u_2^N, \partial_t u_4^N \to \partial_t u_1, \partial_t u_2, \partial_t u_4$ *weakly in* $L^2((0, T) \times \Omega_1)$,
$\partial_t U_3^N \to \partial_t U_3$ *weakly in* $L^2((0, T) \times \Omega_2)$,
$\partial_t u_5^N \to \partial_t u_5$ *strongly in* $L^2((0, T) \times \Omega \times \Gamma_1)$.

Proof. We show that the sequences $u_1^N, u_2^N, U_3^N, u_4^N, u_5^N$ are Cauchy sequences in spaces given in statement and hence converge strongly. From (8.2), it follows for $N_1 \le N_2$

$$\int\limits_{\Omega_1} (\partial_t u_1^{N_1} - \partial_t u_1^{N_2}) \phi_1 dx + \int\limits_{\Omega_1} d_1 \nabla(u_1^{N_1} - u_1^{N_2}) \nabla \phi_1 dx = -\int\limits_{\Omega_1} (k_1 u_1^{N_1} - k_1 u_1^{N_2}) \phi_1 dx$$

$$+ \int\limits_{\Omega 1} (k_2 u_2^{N_1} - k_2 u_2^{N_2}) \phi_1 dx - \varepsilon \int\limits_{\Gamma_1} \big(\eta(u_1^{N_1}, u_5^{N_1}) - \eta(u_1^{N_2}, u_5^{N_2}) \big) \phi_1 d\gamma_x.$$

We take $\phi_1 = u_1^{N_1} - u_1^{N_2}$ to obtain

$$\frac{1}{2} \partial_t \int\limits_{\Omega_1} |u_1^{N_1} - u_1^{N_2}|^2 dx + \int\limits_{\Omega_1} d_1 |\nabla(u_1^{N_1} - u_1^{N_2})|^2 dx = -\int\limits_{\Omega_1} k_1 (u_1^{N_1} - u_1^{N_2})(u_1^{N_1} - u_1^{N_2}) dx$$

$$+ \int\limits_{\Omega_1} k_2 (u_2^{N_1} - u_2^{N_2})(u_1^{N_1} - u_1^{N_2}) dx - \varepsilon \int\limits_{\Gamma_1} \big(\eta(u_1^{N_1}, u_5^{N_1}) - \eta(u_1^{N_2}, u_5^{N_2}) \big)(u_1^{N_1} - u_1^{N_2}) d\gamma_x \quad (8.14)$$

Similarly, (8.3) leads to ($\phi_2 = u_2^{N_1} - u_2^{N_2}$)

$$\frac{1}{2}\partial_t \int\limits_{\Omega_1} |u_2^{N_1} - u_2^{N_2}|^2 dx + \int\limits_{\Omega_1} d_2 |\nabla(u_2^{N_1} - u_2^{N_2})|^2 dx$$

$$= \int\limits_{\Omega_1} k_1(w_1^{N_1} - 1u_1^{N_2})(u_2^{N_1} - u_2^{N_2})dx - \int\limits_{\Omega_1} k_2(u_2^{N_1} - u_2^{N_2})(u_2^{N_1} - u_2^{N_2})dx$$

$$+ \varepsilon \int\limits_{\Gamma_2} a(u_3^{N_1} - u_3^{N_2})(u_2^{N_1} - u_2^{N_2})d\gamma_x - \varepsilon \int\limits_{\Omega \times \Gamma_2} b|u_2^{N_1} - u_2^{N_2}|^2 dxd\gamma_x. \qquad (8.15)$$

By (8.4), we have

$$\frac{1}{2}\partial_t \int\limits_{\Omega_2} |u_3^{N_1} - u_3^{N_2}|^2 dx + \int\limits_{\Omega_2} d_3 |\nabla(u_3^{N_1} - u_3^{N_2})|^2 dx$$

$$= -\varepsilon \int\limits_{\Gamma_2} a|u_3^{N_1} - u_3^{N_2}|^2 d\gamma_x + \varepsilon \int\limits_{\Gamma_2} b(u_2^{N_1} - u_2^{N_2})(u_3^{N_1} - u_3^{N_2})d\gamma_x. \qquad (8.16)$$

$$\frac{1}{2}\partial_t \int\limits_{\Omega_1} |u_4^{N_1} - u_4^{N_2}|^2 dx + \int\limits_{\Omega_1} d_4 |\nabla(u_4^{N_1} - u_4^{N_2})|^2 dx = \int\limits_{\Omega_1} k_1(w_1^{N_1} - u_1^{N_2})(u_4^{N_1} - u_4^{N_2})dx \quad (8.17)$$

From (8.6), we obtain

$$\frac{1}{2}\partial_t \int\limits_{\Gamma_1} |u_5^{N_1} - u_5^{N_2}|^2 d\gamma_x = \int\limits_{\Gamma_1} \left(\eta(u_1^{N_1}, u_5^{N_1}) - \eta(u_1^{N_2}, u_5^{N_2})\right)(u_1^{N_1} - u_1^{N_2})d\gamma_x. \quad (8.18)$$

Adding up (8.14)–(8.18) and re-arranging terms, we obtain

$$\frac{1}{2}\partial_t E_0(t) + \int\limits_{\Omega_1} \left(d_1^0 |\nabla(u_1^{N_1} - u_1^{N_2})|^2 + d_2^0 |\nabla(u_2^{N_1} - u_2^{N_2})|^2 + d_4^0 |\nabla(u_4^{N_1} - u_4^{N_2})|^2\right)dx$$

$$+ d_3^0 \int\limits_{\Omega} |\nabla(u_3^{N_1} - u_3^{N_2})|^2 dx + \varepsilon \int\limits_{\Gamma_2} b|u_2^{N_1} - u_2^{N_2}|^2 d\gamma_x dx + \varepsilon \int\limits_{\Gamma_2} a|u_3^{N_1} - u_3^{N_2}|^2 d\gamma_x$$

$$\leq (k_1^\infty + k_2^\infty) \int\limits_{\Omega_1} (u_2^{N_1} - u_2^{N_2})(u_1^{N_1} - u_1^{N_2})dx + \varepsilon \int\limits_{\Gamma_2} a(u_3^{N_1} - u_3^{N_2})(u_2^{N_1} - u_2^{N_2})d\gamma_x$$

$$- \varepsilon \int\limits_{\Gamma_1} \left(\eta(u_1^{N_1}, u_5^{N_1}) - \eta(u_1^{N_2}, u_5^{N_2})\right)(u_1^{N_1} - u_1^{N_2})d\gamma_x$$

$$+ \varepsilon \int\limits_{\Gamma_2} b(u_2^{N_1} - u_2^{N_2})(u_3^{N_1} - u_3^{N_2})d\gamma_x + \int\limits_{\Omega_1} k_1(u_1^{N_1} - u_1^{N_2})(u_4^{N_1} - u_4^{N_2})dx$$

$$+ \varepsilon \int\limits_{\Gamma_1} \left(\eta(u_1^{N_1}, u_5^{N_1}) - \eta(u_1^{N_2}, u_5^{N_2})\right)(u_5^{N_1} - u_5^{N_2})d\gamma_x, \qquad (8.19)$$

where

$$
\begin{aligned}
E_0(t) \quad := & \int_{\Omega_1} |u_1^{N_1} - u_1^{N_2}|^2 dx + \int_{\Omega_1} |u_2^{N_1} - u_2^{N_2}|^2 dx + \int_{\Omega_2} |u_3^{N_1} - u_3^{N_2}|^2 dx \\
& + \int_{\Omega_1} |u_4^{N_1} - u_4^{N_2}|^2 dx + \varepsilon \int_{\Gamma_1} |u_5^{N_1} - u_5^{N_2}|^2 d\gamma_x.
\end{aligned}
$$

Using Assumption (4.1.4) to the terms on r.h.s. of (8.19). First term on r.h.s leads to

$$
(k_1^\infty + k_2^\infty) \int_{\Omega_1} (u_2^{N_1} - u_2^{N_2})(u_1^{N_1} - u_1^{N_2}) dx \le C \int_{\Omega_1} \left(|u_1^{N_1} - u_1^{N_2}|^2 + |u_2^{N_1} - u_2^{N_2}|^2 \right) dx,
$$

while second and fourth terms are estimated by using (4.1) as follows:

$$
\begin{aligned}
\varepsilon \int_{\Gamma_2} a(u_3^{N_1} - u_3^{N_2})(u_2^{N_1} - u_2^{N_2}) d\gamma_x \le & \; \varepsilon C \int_{\Gamma_2} \left(|u_2^{N_1} - u_2^{N_2}|^2 + |u_3^{N_1} - u_3^{N_2}|^2 \right) d\gamma_x \\
\le & \; C \int_{\Omega_1} \left(|u_2^{N_1} - u_2^{N_2}|^2 + \varepsilon^2 |\nabla(u_2^{N_1} - u_2^{N_2})|^2 \right) dx \\
& + C \int_{\Omega_2} \left(|u_3^{N_1} - u_3^{N_2}|^2 + \varepsilon^2 |\nabla(u_3^{N_1} - u_3^{N_2})|^2 \right) dx.
\end{aligned}
$$

We estimate fifth term by

$$
\int_{\Omega_1} k_1(u_1^{N_1} - u_1^{N_2})(u_4^{N_1} - u_4^{N_2}) dx \le C \int_{\Omega_1} \left(|u_1^{N_1} - u_1^{N_2}|^2 + |u_4^{N_1} - u_4^{N_2}|^2 \right) dx.
$$

Third term can be estimated as

$$
\begin{aligned}
-\varepsilon \int_{\Gamma_1} \left(\eta(u_1^{N_1}, u_5^{N_1}) - \eta(u_1^{N_2}, u_5^{N_2}) \right)(u_1^{N_1} - u_1^{N_2}) d\gamma_x \\
\le \varepsilon \int_{\Gamma_1} \left(R(u_1^{N_1}) - R(u_1^{N_2}) \right) Q(u_5^{N_1})(u_1^{N_1} - u_1^{N_2}) dx d\gamma_x \\
+ \varepsilon \int_{\Gamma_1} R(u_1^{N_2}) \left(Q(u_5^{N_1}) - Q(u_5^{N_2}) \right)(u_1^{N_1} - u_1^{N_2}) dx d\gamma_x.
\end{aligned}
$$

Using (A3) in Assumption 4.1.4

$$
\begin{aligned}
-\varepsilon \int_{\Gamma_1} \left(\eta(u_1^{N_1}, u_5^{N_1}) - \eta(u_1^{N_2}, u_5^{N_2}) \right)(u_1^{N_1} - u_1^{N_2}) d\gamma_x \\
\le \varepsilon C \int_{\Gamma_1} |u_1^{N_1} - u_1^{N_2}|^2 d\gamma_y + \varepsilon C \int_{\Gamma_1} |u_5^{N_1} - u_5^{N_2}|^2 d\gamma_x \\
\le C \int_{\Omega_1} \left(|u_1^{N_1} - u_1^{N_2}|^2 + \varepsilon^2 |\nabla(u_1^{N_1} - u_1^{N_2})|^2 \right) d\gamma_x + \varepsilon C \int_{\Gamma_1} |u_5^{N_1} - u_5^{N_2}|^2 d\gamma_x,
\end{aligned}
$$

and similarly

$$\varepsilon \int\limits_{\Gamma_1} \big(\eta(u_1^{N_1}, u_5^{N_1}) - \eta(u_1^{N_2}, u_5^{N_2})\big)(u_5^{N_1} - u_5^{N_2})d\gamma_x$$

$$\leq C \int\limits_{\Omega_1} \big(|u_1^{N_1} - u_1^{N_2}|^2 + \varepsilon^2 |\nabla(u_1^{N_1} - u_1^{N_2})|^2\big)d\gamma_x + \varepsilon C \int\limits_{\Gamma_1} |u_5^{N_1} - u_5^{N_2}|^2 d\gamma_x,$$

(8.19) becomes

$$\frac{1}{2}\partial_t E_0(t) + E_1(t) \leq C \int\limits_{\Omega_1} |u_1^{N_1} - u_1^{N_2}|^2 dx + C \int\limits_{\Omega_1} |u_2^{N_1} - u_2^{N_2}|^2 dx$$

$$+ C \int\limits_{\Omega_2} |u_3^{N_1} - u_3^{N_2}|^2 dx + C \int\limits_{\Omega_1} |u_4^{N_1} - u_4^{N_2}|^2 dx + \varepsilon C \int\limits_{\Gamma_1} |u_5^{N_1} - u_5^{N_2}|^2 d\gamma_x$$

$$\leq C E_0(t),$$

where

$$E_1(t) \quad := (d_1^0 - \varepsilon^2 C) \int\limits_{\Omega_1} |\nabla_y(u_1^{N_1} - u_1^{N_2})|^2 dx + (d_2^0 - \varepsilon^2 C) \int\limits_{\Omega_1} |\nabla_y(u_2^{N_1} - u_2^{N_2})|^2 dx$$

$$+ (d_3^0 - \varepsilon^2 C) \int\limits_{\Omega_2} |\nabla_y(u_3^{N_1} - u_3^{N_2})|^2 dx + (d_4^0 - \varepsilon^2 C) \int\limits_{\Omega_1} |\nabla_y(u_4^{N_1} - u_4^{N_2})|^2 dx$$

$$+ \int\limits_{\Gamma_2} b|u_2^{N_1} - u_2^{N_2}|^2 d\gamma_x + \int\limits_{\Gamma_2} b|u_3^{N_1} - u_3^{N_2}|^2 d\gamma_x.$$

Applying Gronwall's inequality, we have

$$E_0(t) + \int\limits_0^t E_1(t)d\tau \leq e^{ct} E_0(0) \leq e^{cT} \Big(\int\limits_{\Omega_1} |u_1^{N_1}(0) - u_1^{N_2}(0)|^2 dx$$

$$+ \int\limits_{\Omega_1} |u_2^{N_1}(0) - u_2^{N_2}(0)|^2 dx + \int\limits_{\Omega_2} |u_3^{N_1}(0) - u_3^{N_2}(0)|^2 dx + \int\limits_{\Omega_1} |u_4^{N_1}(0) - u_4^{N_2}(0)|^2 dx$$

$$+ \varepsilon \int\limits_{\Omega \times Y_1} |u_5^{N_1}(0) - u_5^{N_2}(0)|^2 d\gamma_x \Big) \longrightarrow 0 \quad \text{as } N_1, N_2 \to \infty.$$

For the estimates on the time-derivative of the concentrations, we follow the procedure in the proof of Lemma 4.3.2.

Now, we return to the actual proof of the Theorem 4.2.5. We pass to the limit in (8.2)–(8.6) for $N \to \infty$ using the convergence results obtained in Lemma 8.2.1. For the non-linear function η, we use the Lipschitz continuity and strong convergence to obtain the system (4.4)–(4.8).

It remains to show that $u_i(0) = u_{i0}, i \in \{1, 2, 4, 5\}$. The initial data can be recovered following the same lines given in [52], see page 357.

Bibliography

[1] A. Abdulle and E. Weinan. Finite difference heterogeneous multi-scale method for homogenization problems. *J. Comput. Phys.*, 191:18–39, 2002.

[2] E. Acerbi, V. Chiadò Piat, G. Dal Maso, and D. Percivale. An extension theorem from connected sets, and homogenization in general periodic domains. *Nonlinear Anal. TMA*, 18(5):481–496, 1992.

[3] D. Agreba-Driolett, F. Diele, and R. Natalini. A mathematical model for the SO_2 aggression to calcium carbonate stones: Numerical approximation and asymptotic analysis. *SIAM J. Appl. Math.*, 64(5):1636–1667, 2004.

[4] T. Aiki and A. Muntean. A free-boundary problem for concrete carbonation: Rigorous justification of the $\sqrt{t}$-law of propagation. *Disc. Cont. Dynam. Sys.*, 29(4):1345–1365, 2011.

[5] T. Aiki and A. Muntean. On the uniqueness of a weak solution of the one-dimensional concrete carbonation problem. *Interfaces and Free Boundaries, in press*, 2013.

[6] H. Aleksanyan, H. Shahgholian, and P. Sjölin. Application of Fourier analysis in homogenization and boundary layer. *Arxiv:1205.5210v2*, 2012.

[7] R. Alexandre. Homogenization and $\theta - 2$ convergence. *Proc. Royal. Soc. of Edinburgh*, 127A:441–455, 1997.

[8] G. Allaire. Homogenization and two-scale convergence. *SIAM J. Math. Anal.*, 23(6):1482–1518, 1992.

[9] G. Allaire and C. Conca. Boundary layers in the homogenziation of a spectral problem in fluid–solid structure. *SIAM J. Math. Anal.*, 29(2):343–379, 1998.

[10] G. Allaire, A. Damlamian, and U. Hornung. Two-scale convergence on periodic surfaces and applications. *World Scientific Publishing Co. Pte. Ltd.*, 1995.

[11] G. Astarita. *Mass Transfer with Chemical Reaction.* Elsevier Publishing Company, Amsterdam, 1967.

[12] J.-L. Auriault. Heterogeneous medium: Is an equivalent macroscopic description possible? *Int. J. Eng. Sci*, 29(7):785–795, 1991.

[13] Z.P. Bažant and L.J. Najjar. Nonlinear water diffusion in nonsaturated concrete. *Matériaux et Construction*, 5(1):3–20, 1972.

[14] P.W. Balls and P.S. Liss. Exchange of H_2S between water and air. *Atmospheric Environment*, 17(4):735–742, 1983.

[15] C. Barbarosie and A.-M. Toader. Optimization of bodies with locally periodic microstructure. *Mechanics Adv. Mat. Structures*, 19(4):290–301, 2012.

[16] J. Bear. *Dynamics of Fluids in Porous Media*. Dover Publications Inc., N.Y., 1972.

[17] R.E. Beddoe and H.W. Dorner. Modelling acid attack on concrete: Part 1. The essential mechanisms. *Cement and Concrete Research*, 12:2333–2339, 2005.

[18] R.E. Beddoe and H. Hilbig. Simulation of time dependent degradation of porous materials: Final report on priority program 1122. *Cuvillier Verlag, Göttingen*, pages 275–293, 2009.

[19] A.G. Belyaev, A.L. Pyatnitski, and G.A. Chechkin. Asymptotic behaviour of a solution to a boundary value problem in a perforated domain with oscillating boundary. *Siberian Math. J.*, 39(4):621–644, 1998.

[20] D. Ben-Avraham, M.A. Burschka, and C.R. Doering. Statics and dynamics of a diffusion-limited reaction: anomalous kinetics, noneqnilibrium self-ordering, and a dynamic transition. *J. Stat. Phys.*, 60(5-6):595–728, 1990.

[21] A. Bensoussan, J.-L. Lions, and G.C. Papanicolaou. Boundary layers and homogenization of transport processes. *Publ. Res. Inst. Math. Sci.*, 15(1):53–157, 1979.

[22] A. Bensoussan, J.-L. Lions, and G. Papanicolau. *Asymptotic Analysis for Periodic Structures*. Amsterdam: North-Holland, 1978.

[23] M. Böhm, F. Jahani, J. Devinny, and I.G. Rosen. A moving-boundary system modeling corrosion of sewer pipes. *Appl. Math. Comput.*, 92:247–269, 1998.

[24] M. Böhm and I.G. Rosen. Global weak solutions and uniqueness for a moving boundary problem for a coupled system of quasilinear reaction-diffusion equations arising as a model of chemical corrosion surface, Part 2. *Humbolt University Berlin, Deptt. of Mathematics, Preprint*, 1997.

[25] M. Böhm and I.G. Rosen. Global weak solutions and well-posedness of weak solutions for a moving boundary problem for a coupled system of reaction-diffusion equations arising in the corrosion-modeling of concrete, Part 1. *Humbolt University Berlin, Deptt. of Mathematics, Preprint*, 1997.

[26] M. Briane. Homogenization of a non-periodic material. *J. Math. Pures Appl.*, 73:47–66, 1994.

[27] V. Chalupecký, T. Fatima, J. Kruschwitz, and A. Muntean. Macroscopic corrosion front computations of sulfate attach in sewer pipes based on a micro-macro reaction-diffusion model. *Proc: Multiscale Mathematics: Hierachy of collective phenomena and interrelations between hierachical structures, Kyushu University*, 39:22–31, 2012.

[28] V. Chalupecký, T. Fatima, and A. Muntean. Numerical study of a fast micro-macro mass transfer limit: The case of sulfate attack in sewer pipes. *J. Math-for-Industry*, 2B:171–181, 2010.

[29] V. Chalupecký and A. Muntean. Semi-discrete finite difference multiscale scheme for a concrete corrosion model: *a priori* estimates and convergence. *Japan J. Indus. Appl. Math.*, 29:289–316, 2012.

[30] G. Chechkin and A.L. Piatnitski. Homogenization of boundary-value problem in a locally periodic perforated domain. *Applicable Anal.*, 71(1):215–235, 1999.

[31] G. Chechkin, A.L. Piatnitski, and A.S. Shamaev. *Homogenization Methods and Applications*, volume 234 of Translations of Mathematical Monographs. AMS, Providence, Rhode Island USA, 2007.

[32] G.A. Chechkin and T.P. Chechkina. On homogenization of problems in domains of the "infusorium" type. *J. Math. Sci.*, 120(3):386–407, 2004.

[33] D. Cioranescu, A. Damlamian, P. Donato, G. Griso, and R. Zaki. The periodic unfolding method in domains with holes. *SIAM J. Math. Anal.*, 42(2):718–760, 2012.

[34] D. Cioranescu, A. Damlamian, and G. Griso. Periodic unfolding and homogenization. *SIAM J. Math. Anal.*, 40(4):1585–1620, 2008.

[35] D. Cioranescu and P. Donato. *An Introduction to Homogenization*. Oxford University Press, New York, 1999.

[36] D. Cioranescu, P. Donato, and R. Zaki. Periodic unfolding and Robin problems in perforated domains. *C. R. Acad. Sci. Paris*, Ser. I(342):469–474, 2006.

[37] D. Cioranescu, P. Donato, and R. Zaki. Periodic unfolding method in perforated domains. *Portugaliae Mathematica*, 63:467496,, 2006.

[38] D. Cioranescu, P. Donato, and R. Zaki. Asymptotic behavior of elliptic problems in perforated domains with nonlinear boundary conditions. *Asymptotic Anal.*, 53:209–235, 2007.

[39] D. Cioranescu and J.S.J. Paulin. Homogenization in open sets with holes. *J. Math. Anal. Appl.*, 71:590–607, 1979.

[40] D. Cioranescu and J.S.J. Paulin. *Homogenization of Reticulated Structures.* Springer, New York, 1998.

[41] F. Clarelli, A. Fasano, and R. Natalini. Mathematics and monument conservation: Free boundary models of marble sulfation. *SIAM J. Appl. Math.*, 69(1):149–168, 2008.

[42] E.W.C. Coenen, V.G. Kouznetsova, and M.G.D. Geers. Computational homogenization for heterogeneous thin sheets. *Int. J. Numerical Methods in Engineering*, 83(8-9):1180–1205, 2010.

[43] E.W.C. Coenen, V.G. Kouznetsova, and M.G.D. Geers. Multi-scale continuous-discontinuous framework for computational-homogenization-localization. *J. Mech. Phys. Solids*, 60:1486–1507, 2012.

[44] S.D. Cohen and A.C. Hindmarsh. Cvode, a stiff/nonstiff ode solver in C. *Computers in Phys.*, 10:731–756, 1996.

[45] J.D. Cook and R.E. Showalter. Distributed systems of pde in Hilbert space. *J. Math. Anal. Appl.*, 6:981–994, 1993.

[46] A. Damlamian and K. Petterson. Homogenization of oscillating boundaries. *Discr. Cont. Dyn. Sys.*, 23(1-2):197–219, 2009.

[47] P.V. Danckwerts. *Gas-Liquid Reactions.* McGraw-Hill Book Co., 1970.

[48] R. Dautray and J.-L. Lions. *Mathematical Analysis and Numerical Methods for Science and Technology*, volume 5. Springer-Verlag Berlin-Heidelberg-New York, 2000.

[49] C. Eck. Homogenization of a phase field model for binary mixtures. *Multiscale Model. Simul.*, 3(1):1–27, 2004.

[50] C. Eck. *A Two-Scale Phase Field Model for Liquid-Solid Phase Transitions of Binary Mixtures with Dendritic Microstructure.* Habil. thesis, Naturwissenschaftliche Fakultäten der Universität Erlangen Nürnberg, 2004.

[51] Y. Efendiev and T.Y. Hou. *Multiscale finite element method. In: Theory and Application. Survey and Tutorials in the Applied Mathematiccal Science.* Springer Berlin, 2009.

[52] L.C. Evans. *Partial Differential Equations*, volume 19. AMS, Providence, Rhode Island USA, 1998.

[53] A. Fasano and A. Mikelić. The 3D flow of a liquid through a porous medium with absorbing and swelling granules. *Interface and Free Boundaries*, 4:239–261, 2002.

[54] T. Fatima, N. Arab, E.P. Zemskov, and A. Muntean. Homogenization of a reaction-diffusion system modeling sulfate corrosion in locally-periodic perforated domains. *J. Eng. Math.*, 69(2-3):261–276, 2011.

[55] T. Fatima and A. Muntean. Sulfate attack in sewer pipes: Derivation of a concrete corrosion model via two-scale convergence. *Nonlinear Anal. RWA DOI:10.1016/j.nonrwa.2012.01.019*, 2013.

[56] T. Fatima, A. Muntean, and T. Aiki. Distributed space scales in a semilinear reaction-diffusion system including a parabolic variational inequality: A well-posedness study. *Adv. Math. Sci. Appl.*, 22(1):295–318, 2012.

[57] T. Fatima, A. Muntean, and M. Ptashnyk. Unfolding-based corrector estimates for a reaction-diffusion system predicting concrete corrosion. *Applicable Analysis*, 91(6):1129–1154, 2012.

[58] M.G.D. Geers, V.G. Kouznetsova, and W.A.M. Brekelmans. Multi-scale computational homogenization: Trends and challenges. *J. Comput. Appl. Math.*, 234(7):2175–2182, 2010.

[59] G. Griso. Error estimate and unfolding for periodic homogenization. *Asymptotic Anal.*, 40:269–286, 2004.

[60] G. Griso. Interior error estimate for periodic homogenization. *Comptes Rendus Mathematique*, 340(3):251–254, 2005.

[61] F. R. Guarguaglini and R. Natalini. Fast reaction limit and largetime behavior of solutions to a nonlinear model of sulphation phenomena. *Communications in PDEs*, 32:163–189, 2007.

[62] F.R. Guarguaglini and R. Natalini. Global existence of solutions to a nonlinear model of sulphation phenomena in calcium carbonate stones. *Nonlinear Anal. RWA*, 6:477–494, 2005.

[63] M. Heida. Asymptotic expansion for multiscale problems on non-periodic stochastic geometries. *arXiv:1101.4090v1*, 2011.

[64] M. Heida. An extension of stochastic two-scale convergence and application. *Asymtotic Analysis*, 72:1–30, 2011.

[65] M. Heida. Stochastic homogenization of heat transfer in polycrystals with nonlinear contact conductivities. *Applicable Analysis*, 91(7):1243–1264, 2012.

[66] P.C. Hewlett. *Lea's Chemistry of Cement and Concrete*. Elsevier Butterworth-Heinemenn Linacre House, Jordan Hill, 4th ed. edition, 1998.

[67] U. Hornung. *Homogenization and Porous Media*. Springer-Verlag New York, 1997.

[68] U. Hornung and W. Jäger. Diffusion, convection, adsorption and reaction of chemical in porous media. *J. Diff. Eqs.*, 92:199–225, 1991.

[69] U. Hornung, W. Jäger, and A. Mikelić. Reactive transport through an array of cells with semi-permeable membranes. *RAIRO M2AN*, 28(1):59–94, 1994.

[70] T. Hvitved-Jacobsen and P.H. Nielsen. Sulfur transformations during sewage transport. *Environmental Technologies to Treat Sulfur Pollution : Principles and Engineering. Lens, P.N.L. : Pol, L. H. (Eds.) IWA Publishing, London, UK.*, 2000.

[71] W. Jäger, M. Neuss-Radu, and T.A. Shaposhnikova. Homogenization limit for the diffusion equation with nonlinear flux condition on the boundary of very thin holes periodically distributed in a domain, incase of a critical size. *Doklady Mathematics*, 82(2):736740, 2010.

[72] F. Jahani, J. Devinny, F. Mansfeld, I.G. Rosen, Z. Sun, and C. Wang. Investigations of sulfuric acid corrosion of the concrete, I: Modeling and chemical observations. *J. Environ. Eng.*, 127(7):572–579, July 2001.

[73] F. Jahani, J. Devinny, F. Mansfeld, I.G. Rosen, Z. Sun, and C. Wang. Investigations of sulfuric acid corrosion of the concrete, II: Electrochemical and visual observations. *J. Environ. Eng.*, 127(7):580–584, July 2001.

[74] H.S. Jensen. *Hydrogen sulfide induced concrete corrosion of sewer networks.* PhD thesis, Aalborg University, Denmark, 2009.

[75] H.S. Jensen, P.N.L. Lensb, J.L. Nielsena, K. Bester, A.H. Nielsena, T. Hvitved-Jacobsena, and J. Vollertsena. Growth kinetics of hydrogen sulfide oxidizing bacteria in corroded concrete from sewers. *J. Hazardous Mat.*, 189:685–691, 2011.

[76] V.G. Kouznetsova, M.G.D. Geers, and W.A.M. Brekelmans. Multi-scale second-order computational homogenization of multi-phase materials: a nested finite element solution strategy. *Computer Methods in Appl. Mech. Engin.*, 193(48-51):5525–5550, 2004.

[77] A. Kufner, O. John, and S. Fucik. *Function Spaces.* Nordhoff Publ. and Czechoslovak Academy of Sciences, Prague, 1977.

[78] K. Kumar. *Upscaling of reactive flows.* PhD thesis, Technische Universiteit Eindhoven, The Netherlands, 2012.

[79] K. Kumar, T.L. van Noorden, and I.S. Pop. Effective dispersion equations for reactive flows involving free boundaries at the microscale. *Multi. Model. Simu.*, 9(4):29–58, 2011.

[80] J.-L. Lions. *Quelques méthodes de résolution des problemes aux limites nonlinéaires.* Dunod, Paris, 1969.

[81] J. Marchand, E. Samson, Y. Maltais, R.J. Lee, and S. Sahu. Predicting the performance of concrete structures exposed to chemically aggressive environment-field validation. *Materials and Structures*, 35:623–631, 2002.

[82] V.A. Marchenko and E.Y. Khruslov. *Homogenization of Partial Differential Equations*. Birkhauser Boston Basel Berlin, 2006.

[83] A. Marciniak-Czochra and M. Ptashnyk. Derivation of a macroscopic receptor-based model using homogenization techniques. *SIAM J. Math. Anal.*, 40(1):215–237, 2008.

[84] M.L. Mascarenhas. Homogenization problems in locally periodic perforrated domains. *Proc: International Conference on Asymptotic Methods for Elastic Structures, Hawthorne, USA*, (141-149), 1995.

[85] A.-M. Matache, I. Babuska, and C. Schwab. Generalized p-FEM in homogenization. *Numerische Mathematik*, 86:319–375, 2000.

[86] S.A. Meier. *Two-scale models for reactive transport and evolving microstructures*. PhD thesis, University of Bremen, Bremen, Germany, 2008.

[87] S.A. Meier and A. Muntean. A two-scale reaction-diffusion system with micro-cell reaction concentrated on a free boundary. *Comptes Rendus Mécanique*, 336(6):481–486, 2009.

[88] S.A. Meier, M.A. Peter, A. Muntean, and M. Böhm. Dynamics of the internal reaction layer arising during carbonation of concrete. *Chem. Eng. Sci.*, 62(4):1125–1137, 2007.

[89] S.A. Meier, M.A. Peter, A. Muntean, M. Böhm, and J. Kropp. A two-scale approach to concrete carbonation. *Proceedings First International RILEM Workshop on Integral Service Life Modeling of Concrete Structures, Guimaraes, Portugal*, pages 3–10, 2007.

[90] A. Mikelić, V. Devigne, and C.J. van Duijn. Rigorous upscaling of the reactive flow through a pore, under dominant Peclet and Damköhler numbers. *SIAM J. Math. Anal.*, 38(4):1262–1287 (electronic), 2006.

[91] S. Monsurro. Homogenization of a two-component composite with interfacial thermal barrier. *Adv. Math. Sci. Appl.*, 13(1):43–64, 2003.

[92] J. Monteny, N. de Belie, E. Vincke, W. Verstraete, and L. Taerwe. Chemical and microbiological tests to stimulate acid corrosion of polymer-modified concrete. *Cement and Concrete Research*, 31:1359–1365, 2001.

[93] T. Mori, T. Nonaka, K. Tazaki, M. Koga, Y. Hikosaka, and S. Noda. Interactions of nutrients, moisture and pH on microbial corrosion of concrete sewer pipes. *Water Research*, 26(1):2937, 1992.

[94] W. Müllauer, R. E. Beddoe, and D. Heinz. Sulfate attack on concrete - solution concentration and phase stability. *RILEM Publications SARL*, pages 18–27, 2009.

[95] A. Muntean. *A Moving-Boundary Problem: Modeling, Analysis and Simulation of Concrete Carbonation*. PhD thesis, University of Bremen, Bremen, Germany, 2006.

[96] A. Muntean. Continuity with respect to data and parameters of weak solutions to a Stefan-like problem. *Acta Mathematica Universitatis Comenianae*, LXXVIII(2):205–222, 2009.

[97] A. Muntean. On the interplay between fast reaction and slow diffusion in the concrete carbonation process: a matched-asymptotics approach. *Meccanica*, 44(1):35–46, 2009.

[98] A. Muntean and M Böhm. Interface conditions for fast-reaction fronts in wet porous mineral materials: the case of concrete carbonation. *J. Eng. Math.*, 65(1):89–100, 2009.

[99] A. Muntean and V. Chalupecký. *Homogenization Method and Multiscale Modeling*, volume 34 of Lecture Notes of the Institute for Mathematics for Industry. Kyushu University, Fukuoka, Japan, 2011.

[100] A. Muntean and O. Lakkis. Rate of convergence for a Galerkin scheme approximating a two-scale reaction-diffusion system with nonlinear transmission condition. *RIMS Kokyuroku*, 1693:85–98, 2010.

[101] A. Muntean and M. Neuss-Radu. A multiscale Galerkin approach for a class of nonlinear coupled reaction-diffusion systems in complex media. *J. Math. Anal. Appl.*, 371(2):705–718, 2010.

[102] A. Muntean and T. van Noorden. Corrector estimates for the homogenization of a locally-periodic medium with areas of low and high diffusivity. *CASA-Report 11-29, Eindhoven University of Technology*, 2011.

[103] J.D. Murray. *Mathematical Biology*, volume 19. Spinger-Verlag Berlin, 1990.

[104] M. Neuss-Radu. Some extensions of two-scale convergence. *C. R. Acad. Sci. Paris Sér. I Math*, 332:899–904, 1996.

[105] M. Neuss-Radu, S. Ludwig, and W. Jäger. Multiscale analysis and simulation of a reaction-diffusion problem with transmission conditions. *Nonlinear Anal. RWA*, 11:4572–4585, 2010.

[106] G. Nguestseng. A general convergence result for a functional related to the theory of homogenization. *SIAM J. Math. Anal*, 20:608–623, 1989.

[107] C.V. Nikolopoulos. A mushy region in concrete corrosion. *Appl. Math. Model.*, 34:4012–4030, 2010.

[108] S. Okabe, T. Itoh, K. Sugita, and H. Satoh. Succession of internal sulfur cycles and sulfur oxidizing bacterial communities in microaerophilic wastewater biofilms. *Appl. Environ. Microbiology*, 71(5):2520–2529, 2005.

[109] S. Okabe, M. Odagiri, T. Itoh, and H. Satoh. Succession of sulfur-oxidizing bacterial in the microbial community on corroding concrete in sewer systems. *Appl. Environ. Microbiology*, 73(3):971–980, 2007.

[110] D. Onofrei. The unfolding operator near a hyperplane and its application to the Neumann sieve model. *Adv. Math. Sci. Appl.*, 16(1):239–258, 2006.

[111] D. Onofrei and B. Vernescu. Error estimates for periodic homogenization with non-smooth coefficients. *Asymptotic Analysis*, 54:103–123, 2007.

[112] V.G. Papadakis, C.G. Vayenas, and M.N. Fardis. A reaction engineering approach to the problem of concrete carbonation. *AIChE Journal*, 35:1639–1650, 1989.

[113] C.D. Parker. The corrosion of concrete 1. The isolation of a species of bacterium associated with the corrosion of concrete exposed to atmospheres containing hydrogen sulphide. *Australian J. Experi. Bio. Medi. Sci.*, 23(2):81–90, 1945.

[114] C.D. Parker. The corrosion of concrete 2. The function of thiobacillus-concretivorus (nov-spec) in the corrosion of concrete exposed to atmospheres containing hydrogen sulphide. *J. General Microbiology*, 23(2):91–98, 1945.

[115] C.D. Parker. Species of sulphur bacteria associated with the corrosion of concrete. *Nature*, 153(4039):439–440, 1947.

[116] C.D. Parker and J. Prisk. The oxidation of inorganic compounds of sulphur by various sulphur bacteria. *J. General Microbiology*, 8(3):344–364, 1952.

[117] G.A. Pavliotis and A.M. Stuart. *Multiscale Methods: Averaging and Homogenization*. Springer - Berlin Heidelberg NewYork, 2007.

[118] L. Pel, A.A.J. Ketelaars, O.C.G. Adan, and A.A. van Well. Determination of moisture diffusivity in porous media using scanning neutron radiography. *Int. J. Heat and Mass Transfer*, 36(5):1261–1267, 1993.

[119] L. Pel, K. Kopinga, and H.J.P. Brocken. Moisture transport in porous building materials. *Heron*, 41(2):95–105, 1996.

[120] L.E. Persson, L. Persson, N. Svanstedt, and J. Wyller. *The Homogenization Method*. Chartwell Bratt, Lund, 1993.

[121] M.A. Peter. *Coupled reaction-diffusion systems and evolving microstructure: mathematical modelling and homogenisation.* PhD thesis, University of Bremen, Germany, 2006.

[122] M.A. Peter. Homogenisation of a chemical degradation mechanism inducing an evolving microstructure. *Comptes Rendus Mcanique*, 335(11):679–684, 2007.

[123] M.A. Peter and M. Böhm. Different choices of scaling in homogenization of diffusion and interfacial exchange in a porous medium. *Math. Meth. Appl. Sci.*, 31:1257–1282, 2008.

[124] M.A. Peter and M. Böhm. Multi-scale modelling of chemical degradation mechanisms in porous media with evolving microstructures. *Multiscale Model. Simul.*, 7(4):1643–1668, 2009.

[125] M. Ptashnyk. Two-scale convergence for locally-periodic microstructure and homogenization of plywood structure. *Multiscale Modelling and Simulation (accepted), arXiv:1105.0349*, 2013.

[126] N. Ray, A. Muntean, and P. Knabner. Rigorous homogenization of a Stokes-Nernst-Planck-Poisson problem for various boundary conditions. *J. Math. Anal. Appl.*, 390(1):374–393, 2012.

[127] N. Ray, T. van Noorden, F. Frank, and P. Knabner. Multiscale modeling of colloid and fluid dynamics in porous media including an evolving microstructure. *Transport in Porous Media*, 95(3):669–696, 2012.

[128] R.E. Showalter and D.B. Visarraga. Double-diffusion models from a highly-heterogeneous medium. *J. Math. Anal. Appl.*, 295:191–210, 2004.

[129] H.W. Song, H.J. Lim, V. Saraswathy, and T.H. Kim. A micro-mechanics based corrosion model for predicting the service life of reinforced concrete structures. *Int. J. Electrochem. Sci.*, 2(7):341–354, 2007.

[130] A. Steffens. *Modellierung von Karbonatisierung und Chloridbindung zur numerischen Analyse der Korrosionsgefährdung der Betonbewehrung.* PhD thesis, Institut Statik, Technische Universität Braunschweig, 2000.

[131] H.F.W. Taylor. *Cement Chemistry.* Academic Press London, 1990.

[132] M.E. Taylor. *Partial Differential Equations I : Basic Theory.* Springer New York, 2011.

[133] R. Tixier, B. Mobasher, and M. Asce. Modeling of damage in cement-based materials subjected to external sulfate attack. I: Formulation. *J. Materials Civil Engng.*, 15:305–313, 2003.

[134] R. Tixier, B. Mobasher, and M. Asce. Modeling of damage in cement-based materials subjected to external sulfate attack. II: Comparison with Experiments. *J. Material Civil Engng.*, 15:314–323, 2003.

[135] D. Treutler. *Strong solutions of the matched microstructure model for fluid in fractured porous media.* PhD thesis, University of Hanover, Germany, 2011.

[136] D. Treutler. Well-posedness for a quasilinear generalization of the matched microstructure model. *Nonlinear Anal. RWA*, 13(6):2622–2632, 2012.

[137] K.G. van der Zee, E.H. van Brummelen, I. Akkerman, and R. de Borst. Goal-oriented error estimation and adaptivity for fluid-structure interaction using exact linearized adjoints. *Computer Methods in Appl. Mechanics and Engineering*, 200(37-40):2738–2757, 2011.

[138] K.G. van der Zee, E.H. van Brummelen, and R. de Borst. Goal-oriented error estimation and adaptivity for free-boundary problems: the domain-map linearization approach. *SIAM J. Sci. Comp.*, 32(2):1064–1092, 2010.

[139] T. van Noorden. Crystal precipitation and dissolution in a porous medium: Effective equations and numerical experiments. *Multiscale Model. Simul.*, 7(3):1220–1236, 2009.

[140] T. van Noorden and A. Muntean. Homogenization of a locally-periodic medium with areas of low and high diffusivity. *Eur. J. Appl. Math.*, 22(5):493–516, 2011.

[141] E. Vincke, S. Verstichel, J. Monteny, and W. Verstraete. A new test procedure for biogenic sulfuric acid corrosion of concrete. *Earth Environ. Sci.*, 10(6):421–428, 2000.

[142] E. Weinan and B. Engquist. Heterogeneous multiscale methods. *Communication Math. Sci.*, 1:87–132, 2003.

[143] K. Wilmanski. Porous media at finite strains. The new model with the balance equation for porosity. *Archives of Mechanics*, 48(4):591–628, 1996.

[144] K. Wilmanski. A thermodynamic model of compressible porous materials with the balance equation of porosity. *Transport in Porous Media*, 32:21–47, 1998.

[145] C. Yongsiri, J. Vollertsen, and T. Hvitved-Jacobsen. Effect of temperature on air-water transfer of hydrogen sulfide. *Water Envir. Res.*, 130(1):104–109, 2004.

[146] C. Yongsiri, J. Vollertsen, M. Rasmussen, and T. Hvitved-Jacobsen. Air-water transfer of hydrogen sulfide: An approach for application in sewer networks. *Water Envir. Res.*, 76(81):81–88., 2004.

[147] W. Zhihua and Y. Ningning. Numerical simulation for convection-diffusion problem with periodic micro-structure. *Acta Mathematica Scientia*, 28B(2):236–252, 2008.

[148] V.V. Zhikov and A.L. Pyatniskii. Homogenization of random singular structures and random measures. *Izv. Math.*, 70(1):19–67, 2006.

Summary

Multiscale Reaction-Diffusion System Describing Concrete Corrosion: Modeling and Analysis

This thesis deals with the modeling and multiscale analysis of reaction-diffusion systems describing concrete corrosion processes due to the aggressive chemical reactions occurring in concrete. We develop a mathematical framework that can be useful in forecasting the service life of sewer pipes. We aim at identifying reliable and easy-to-use multiscale models able to forecast the penetration of sulfuric acid into sewer pipes walls.

For modeling of corrosion processes, we take into account balance equations expressing physico-chemical processes that take place in the microstructures (pores) of the partially saturated concrete. We consider two different modeling strategies: (1) we propose microscopic reaction-diffusion systems to delineate the corrosion processes at the pore level and (2) we consider a distributed-microstructure model containing information from two separated spatial scales (micro and macro). All systems of differential equations are semi-linear, weakly coupled, and partially diffusive. Since the precise microstructure of the material is far too complex to be described accurately, we consider two approximations, namely uniformly-periodic and locally-periodic array of microstructures, which are tractable by using averaging mathematical tools.

We use different homogenization techniques to obtain the effective behavior of the microscopically oscillating quantities. For the formal derivation of our multiscale models, we apply the asymptotic expansion method to the microscopic reaction-diffusion systems defined in locally-periodic domains for two special choices of scaling in ε of the diffusion coefficients. We end up with (i) upscaled systems and (ii) distributed-microstructure systems. As far as rigorous derivations are concerned, we apply the notion of two-scale convergence to the PDE system defined in the uniformly periodic domain. To deal with the non-diffusive object, i.e. the ordinary differential equation tracking the damage-by-reaction, we combine the two-scale convergence idea with the periodic-boundary-unfolding technique.

Additionally, we use the periodic unfolding techniques to obtain corrector estimates assessing the quality of the averaging method. These estimates are convergence rates measuring the error contribution produced while approximat-

ing macroscopic solutions by microscopic ones. We derive these estimates under minimal regularity assumptions on the solutions to the microscopic and macroscopic systems, microstructure boundaries, and to the corresponding auxiliary cell problems.

We prove the well-posedness of a distributed-microstructure reaction-diffusion system which includes transport (diffusion) and reaction effects emerging from two separated spatial scales. We perform this analysis by incorporating a variational inequality requiring minimal regularity assumptions on the initial data. We ensure basic estimates like positivity and $L^\infty-$bounds on the solution to the system. Then we prove the global-in-time existence and uniqueness of a suitable class of positive and bounded solutions.

To predict the position of the corrosion front penetrating the concrete, we use our distributed-microstructure model to perform simulations at macroscopic length scales while taking into account transport and reactions occurring at small length scales. Using an *ad hoc* logarithmic expression, we approximate numerically macroscopic pH profiles dropping down with the onset of corrosion. We extract from the gypsum profiles the approximate position of the corrosion front penetrating the uncorroded concrete. We illustrate numerically that as the macroscopic mass-transfer Biot number $\text{Bi}^\text{M} \to \infty$, Bi^M naturally connects two different multiscale reaction-diffusion scenarios: the solution of the distributed-microstructure system having the Henry's law acting as micro-macro transmission condition converges to the solution of the matched distributed-microstructure system.

Nomenclature

x, y, t	macro (slow), micro (fast) and time variable , respectively
Ω	Global domain in three dimensional setting
Y	Single pore in Ω
Y_1	Water-filled part of the pore
Y_2	Air-filled part of the pore
Γ	Boundary of Ω
Γ_1	Solid-water interface in Ω
Γ_2	Water-air interface in Ω
ε	Small scaling parameter
Ω_1	Union of all water-filled parts within Ω
Ω_2	Union of all air-filled parts within Ω
Ω_1^ε	Union of all water-filled parts scaled by ε within Ω
Ω_2^ε	Union of all air-filled parts scaled by ε within Ω
Γ_1^ε	Union of all solid-water interfaces between Ω_1^ε and solid matrix
Γ_2^ε	Union of all air-water interfaces between Ω_1^ε and Ω_1^ε
$k_{1,2}$	$inf_{(0,T)\times\Omega_1^\varepsilon}|k_1^\varepsilon|$
$k_{1,2}^\infty$	$sup_{(0,T)\times\Omega_1^\varepsilon}|k_2^\varepsilon|$
a, b	$inf_{(0,T)\times\Omega^\varepsilon}|a^\varepsilon|, inf_{(0,T)\times\Omega^\varepsilon}|b^\varepsilon|$
a^∞, b^∞	$sup_{(0,T)\times\Omega^\varepsilon}|a^\varepsilon|, sup_{(0,T)\times\Omega^\varepsilon}|b^\varepsilon|$
u_1^ε	Concentration of H_2SO_4 in Ω_1^ε
u_2^ε	Concentration of $H_2S(aq)$ in Ω_1^ε
u_3^ε	Concentration of $H_2S(g)$ in Ω_2^ε
u_4^ε	Concentration of H_2O in Ω_1^ε
u_5^ε	Concentration of gypsum on Γ_1^ε
w_1	Concentration of H_2SO_4 in $\Omega \times Y_1$
w_2	Concentration of $H_2S(aq)$ in $\Omega \times Y_1$
w_3	Concentration of $H_2S(g)$ in Ω_2^ε
w_4	Concentration of H_2O in $\Omega \times Y_1$
w_5	Concentration of gypsum on $\Omega \times \Gamma_1$

Bi^M	Mass-transfer number at the interface
$k_{1,2,3}$	reaction constants
Φ_j^2	Thiele modulus
ω^k	Solution of the cell functions
φ^+	Positive part of the function φ
φ^-	Negative part of the function φ
f_1, f_2	reaction rates in the bulk
η	Reaction rate on the surface
$L_+^\infty(\Omega)$	Space of bounded functions on Ω which are positive as well
$\mathcal{T}_{Y_1}^\varepsilon$	Unfolding operator
$\mathcal{T}_{\Gamma_1}^\varepsilon$	Boundary unfolding operator
ϕ_i	Test functions
$\mathcal{R}$	Primitive of R
$\mathcal{M}_{Y_i}^\varepsilon$	Local average operator
$\mathcal{Q}_{Y_i}^\varepsilon$	Q_1-interpolation of $\mathcal{M}_{Y_i}^\varepsilon$
$\mathcal{U}_{Y_i}^\varepsilon$	Averaging operator
$\mathcal{P}$	Extension operator
Λ	Contraction operator
C	A generic constant independent of ε
$M_{1,2,3,4,5}$	Supremum bounds on the concentrations

List of Publications

1. T. Fatima and A. Muntean. Sulfate attack in sewer pipes: Derivation of a concrete corrosion model via two-scale convergence, *Nonlinear Analysis, Real World Applications DOI:10.1016/j.nonrwa.2012.01.019*, 2013.

2. T. Fatima, A. Muntean and T. Aiki. Distributed space scales in a semilinear reaction-diffusion system including a parabolic variational inequality: A well-posedness study, *Advances in Mathematical Science and Application*, 22(1):295-318, 2012.

3. T. Fatima, A. Muntean and M. Ptashnyk. Unfolding-based corrector estimates for a reaction-diffusion system predicting concrete corrosion, *Applicable Analysis* 91(6): 1129-1154, 2012.

4. T. Fatima, N. Arab, E.P. Zemskov and A. Muntean. Homogenization of a reaction-diffusion system modeling sulfate corrosion in locally-periodic perforated domains, *Journal of Engineering Mathematics* 69(2-3):261-276, 2011.

5. V. Chalupecký, T. Fatima and A. Muntean. Numerical study of a fast micro-macro mass transfer limit: The case of sulfate attack in sewer pipes, *Journal of Math-for-Industry* 2B:171-181, 2010.

6. V. Chalupecký, T. Fatima, J. Kruschwitz and A. Muntean. Macroscopic corrosion front computations of sulfate attach in sewer pipes based on a micro-macro reaction-diffusion model, *Proc. Multiscale Mathematics: Hierarchy of Collective Phenomena and Interrelations between Hierarchical Structures,* Institute of Mathematics for Industry, Kyushu University, 39:22-31, 2012.

Index

Acknowledgements

First of all, I thank Almighty Allah for the completion of this work. I would like to express my gratitude to all those who supported me to reach this point. First of all, I would like to express my appreciation and sincere gratitude to my supervisor Dr. Adrian Muntean and my promotor Prof. Mark A. Peletier for giving me the opportunity to work on the project as well as for their counsel and support. I am grateful for all the things I learnt from them. I am also very thankful to them for facilitating me as a mother. I am particularly indebted to Dr. A. Muntean for introducing me to the fascinating topic of homogenization (multiscale), for his patience and guidance, and for all the interesting and stimulating discussions.

I would like to thank my collaborators, Mariya Ptashnyk (Dundee), Toyohiko Aiki (Tokyo), Nasrin Arab (Regensburg), Vladimír Chalupecký (Fukuoka) and Jens Kruschwitz (Kiel), for inspiring me by their expertises in many ways. I am grateful to Vladimír Chalupecký for the simulations presented in the thesis. I extend my thanks to prof. Sorin I. Pop and Dr. Georg Prokert for their useful advices and interesting discussions.

I want to thank my office mates Oleg, david, Patrick, and Andriy for keeping up the good and positive atmosphere in our office for all these years. I am thankful to my colleagues from CASA from 2008 to 2013 for their help, support and also for creating a nice and friendly working environment. Thanks are due to my colleagues who read the chapters of the thesis during preparation. I would like to thank Kundan Kumar for the interesting discussions about mathematics and life, research topic and for the help when I was in need of. I am greatly thankful to Mirela Darau for helping me with my child during SWI 2011 and snow periods, and for the tasty dinners and discussions. I want to thank our two secretaries Marése and Enna for their taking care of all administrative work.

On the personal level, I would like to thank my family and friends for their love and support. My special regards go to my teachers from whom I learnt even a single word. I have no words for my father (deceased) who influenced my personality more than anybody else, making me able to believe in myself and go where I am now. I would like to express my gratitude and love to my mother, who always believed in me and who was helping me in more ways than I can count. At the end, I would like to thank my husband M. Asif Arif and my lovely son Omer Asif for supporting me during all these years. I dedicate this thesis to my father.

Curriculum Vitae

Tasnim Fatima was born at Kasur in Pakistan on October 17th, 1979. She did her Bachelor as an extramural candidate from the University of the Punjab, Lahore in Pakistan in 1999. In 2001, she finished her M. Sc. in Mathematics at Lahore College for Women University Lahore in Pakistan with distinction. Afterward, she pursued a M. Phil. (Master of Philosophy) degree in Mathematics with the thesis entitled "*Energy-Momentum Distribution: A Crucial Problem in General Relativity*" under the supervision of prof.dr. M. Sharif at University of the Punjab Lahore in 2004.

She served as a part-time lecturer in Mathematics at the Institute of Geology, University of the Punjab, Lahore in Pakistan. In December 2005, she got a permanent job as a lecturer in the Federal Directorate of Education at Islamabad. During school and college, she won many table tennis competitions at different levels. She also played two times national women football championship held in 2006 & 2007 at Islamabad in Pakistan. In November 2008, she started her doctoral research in the Centre for Analysis, Scientific computing and Applications (CASA), department of Mathematics and Computer Science at the Eindhoven University of Technology under the supervision of dr.habil. A. Muntean and prof.dr. M.A. Peletier, the results of which are presented in this thesis.